Protein Mixtures: Interactions and Gelation

Carsten Ersch

Thesis committee

Promotor

Prof. Dr Erik van der Linden
Professor of Physics and Physical Chemistry of Foods
Wageningen University

Co-promotors

Dr Anneke H. Martin
Senior Scientist
TNO, Zeist

Dr Paul Venema
Assistant professor, Physics and Physical Chemistry of Foods
Wageningen University

Other members

Prof. Dr Remko Tuinier, Eindhoven University of Technology
Dr R.Hans Tromp, Utrecht University
Dr Taco Nicolai, Université du Maine, Le Mans, France
Prof. Dr Jasper van der Gucht, Wageningen University

This research was conducted under the auspices of the Graduate School VLAG (Advanced studies in Food Technology, Agrobiotechnology, Nutrition and Health Sciences).

Protein Mixtures:

Interactions and Gelation

Carsten Ersch

Thesis

submitted in fulfilment of the requirements for the degree of doctor
at Wageningen University
by the authority of the Rector Magnificus
Prof. Dr A.P.J. Mol,
in the presence of the
Thesis Committee appointed by the Academic Board
to be defended in public
on Thursday, 27th of August 2015
at 11 a.m. in the Aula.

Carsten Ersch

Protein Mixtures: Interactions and Gelation,

220 pages.

PhD thesis, Wageningen University, Wageningen, NL (2015)

With references, with summary in English

ISBN 978-94-6257-421-2

Für meine Familie

ABSTRACT

Gelation is a ubiquitous process in the preparation of foods. As most foods are multi constituent mixtures, understanding gelation in mixtures is an important goal in food science. Here we presented a systematic investigation on the influence of molecular interactions on the gelation in protein mixtures. Gelatin gels with added globular protein and globular protein gels with added gelatin were analyzed for their gel microstructure and rheological properties. Mixed gels with altered microstructure (compared to single gels) also differed in modulus from single gels. Mixed gels with microstructures similar to single gels were rheologically similar to single gels. Alterations in microstructure were attributed to segregative phase separation between proteins which occurred during gelation. Gelation was treated as a growth process from macromolecule to space spanning network. At conditions where electrostatic interactions were screened the occurrence of phase separation was attributed to the molecular size ratio between gelling and non-gelling proteins before gelation and changes of this size ratio during gelation. Here only mixtures that during gelation passed a region of high compatibility (similar molecular sizes) before entering a region of decreasing solubility phase separated. For applications this implies that whenever the gelling molecule is larger than the non-gelling molecule phase separation during gelation is unlikely while reversely, if the gelling molecules is smaller than the non-gelling molecule phase separation during gelation typically does occur.

CONTENTS

	Description	**Units**
a	Radius of a sphere (or protein) Also the size of random inhomogeneities in SESANS analysis	[nm]
α	Volume ratio of phase I in phase separated solutions	
A'	First coefficient describing non-linear behavior of osmotic pressure data	[mol kg^{-2} m^3]
A''	Second coefficient describing non-linear behavior of osmotic pressure data	[mol kg^{-3} m^6]
A'_A	Apparent coefficient A'	[mol kg^{-2} m^3]
β	Form factor for exponential function in CLSM autocorrelation analysis	
$B'_{i,i}$	Second virial coefficient representing the interaction between polymers of type i	[m^3 mol^{-1}]
$B'_{1,2}$	Second cross virial coefficient representing the interaction between polymers of type 1 and type 2	[m^3 mol^{-1}]
B'_A	Apparent second virial coefficient B'	[m^3 mol^{-1}]
B'_{crit}	Ratio between second cross virial coefficient and second virial coefficients in a mixed system	
B'_{HS}	Second virial coefficient for additive hard spheres	[m^3 mol^{-1}]
C	Scaling constant in percolation model	
c(r)	Radially averaged density correlation function	
c_0	Minimum gelling concentration	[$g_{protein}$ / g_{water}]
c	The polymer molar concentration	[mol m^{-3}]
c_p	Total polymer concentration in solution (= solute mass concentration) Or the polymer concentration based on the total amount of water in the system	[kg / m^3] [$g_{protein}$ / g_{water}]
$c_{p(total)}$	The polymer concentration expressed relative to the total sample weight	[$g_{protein}$ / g_{Sample}]
δ	Depth of the attractive well in square well potential	[k_B T]
δi	Variance of fluctuation intensity	
Δ	Non-additivity parameter in hard sphere model	
e	Charge of an electron	[C]
ε	Depth of the square well in attractive square well potential	[k_B T]
ε_r	Dielectric constant	
Γ	Gamma function	
G(a,b)	Autocorrelation function	

g(a,b)	Scaled autocorrelation function	
G(z)	Normalized dimensionless function in SESANS analysis	
G’	Storage modulus	[Pa]
G'_c	Storage modulus of mixed gels (composites)	[Pa]
G'_G	Storage modulus of the gelatin phase in a phase separated mixed gel	[Pa]
G'_{GP}	Storage modulus of the globular protein phase in a phase separated mixed gel	[Pa]
G”	Loss modulus	[Pa]
H	Hurst Exponent (SESANS)	
I	Ionic strength	[mmol kg^{-1}_{Water}]
$\hat{\imath}$; $\hat{\jmath}$	Unit vectors	
i(x,y)	Intensity of CLSM image with the coordinates x and y in the image matrix	
κ^{-1}	Debije length	[nm]
k_B	Boltzmann constant	[m^2 kg s^{-2} K^{-1}]
K	Modified Bessel Function Or Bulk Modulus	[Pa]
λ	Wavelength	[nm]
λ_B	Bjerrum Length	[nm]
m	Total mass of an ingredient in the sample	[g]
M_w	Weight averaged molecular weight	[kg mol^{-1}]
M_n	Number averaged molecular weight	[kg mol^{-1}]
$M_{n,A}$	Apparent number averaged molecular weight	[kg mol^{-1}]
$\bar{M}_n$	Apparent average molecular weight of a mixed solution from osmometry measurements	[kg mol^{-1}]
M	Stability Matrix	
M, N	Size of matrix for autocorrelation	
n	Number of molecules also molecule number density or Refractive index	[mol] [l^{-1}]
N_A	Avogadro’s number	[mol^{-1}]
N_{Ap}	Numerical aperture	
Φ	Volume fraction	
Π	Osmotic pressure	[Pa]
p	Relative water distribution between the phases in phase separated gels or airy units	
p(r)	Density probability function obtained from autocorrelation of CLSM matrix	

P(z)	Standardized polarization from SESANS measurements	
q	Size ratio between two particles	
ρ	Density of a solution And in CLSM image analysis the density of fluorescent dye	[kg/m³] [1]
$\Delta\rho$	Neutron scattering length density contrast	m^{-2}
r	Radial distance	[nm]
$\vec{r}'; \vec{r}$	Position vectors in spatial autocorrelation	
R	General gas constant	[m^3 Pa K^{-1} mol^{-1}]
Σ_t	Scattering probability (SESANS)	
σ^2	Measure for the distribution of intensity in a CLSM image	
s	Ratio between measured and expected storage modulus in mixed gels	
T	Absolute temperature	[K]
τ	Stickiness parameter in sticky hard sphere model (Baxter model)	
t	Exponent in percolation model	
μ	Chemical potential	
μ_r	Dimensionless radius in extended Baxter model	
U_A	Depth of the adhesive well in extended Baxter model	[k_B T]
V	Total sample volume	[m^3]
w	Weight fraction of polymers or the weight of water inside a phase in a phase separated system	 [g]
w(r)	Potential of mean force	[k_B T]
ξ	Dimensionless parameter in the extended Baxter model or correlation length obtained from image analysis or neutron scattering	[nm]
z	Voxel depth (thickness of slice in CLSM imaging) or spin echo length (SESANS)	[nm] [m]
Z_{eff}	Effective charge of a protein	
$\bar{Z}$	Corrected charge of a protein in extended Baxter Model	
$\langle\ldots\rangle_{x,y}$	Average over all x and y	

OTHER ABBREVIATIONS

	Description
1	Refers to polymer number 1
2	Refers to polymer number 2
β-lac	β – lactoglobulin
BSA	Bovine Serum Albumin
C	Composite (mixed gel)
CLSM	Confocal laser scanning microscope
DMSO	Dimethyl sulfoxide
FITC	Fluorescein isothiocyanate
G	Gelatin
GP	Globular Protein
HA	Hashin approach
HS	Hard Sphere
I	Phase one in phase separated solutions
II	Phase 2 in phase separated solutions
M	Mixed
mM	Millimolality
MOPS	Trivial name for 3-propanesulfonic acid based buffer
pI	Isoelectric point
PS	Phase separated
PS-B	Phase separated bi-continuous microstructure
PS-SE	Phase separated microstructure with spherical enclosures of one phase in another phase
SEC-MALLS	Size exclusion chromatography with multi angle laser light scattering
SESANS	Spin-echo small-angle neutron scattering
SPI	Soy protein isolate
T	Takayanagi approach
w/w	Weight per weight
WPA	Whey protein aggregates
WPI	Whey protein isolate

CHAPTER 1

General Introduction

Gelation is a common phenomenon in foods. Milk turns from liquid to solid during cheese making, marmalade solidifies only after being boiled and left to set and liquid cake batter or eggs solidify once heated. In each of these examples the ingredient (or better molecule) responsible for gelation is different. So are the interactions between the molecules, typically leading to different gelling mechanisms. Over many decades, the different main gelling mechanisms have been identified and studied in detail in food model systems [1-8]. An understanding of the main gelling mechanisms is the foundation for investigations of gelation in increasingly complex systems. This transition from a description of gelation in pure, single molecule systems, to complex, mixed systems is the first step towards a better scientific description of processes as they are occurring in the preparation of everyday foods.

Most foods are complex mixtures of different gelling biopolymers (mainly polysaccharides and proteins). During gelation, these biopolymers are frequently found to partition unevenly throughout the gels. This partitioning during gelation impacts on the texture [9-13] and also the taste [14-17] of foods which can be desirable or undesirable dependent on the application. Çakir et al. [9, 18, 19] showed in their systematic investigation on heat induced whey protein / kappa - carrageenan mixtures how the different spatial arrangement of gels (phase separated gel microstructure) and the resulting rheological properties of mixed gels can be translated into textural changes. Van den Berg et al. [10, 12, 20-22] showed similar relationships using acid induced polysaccharide / whey protein gels indicating that these results are not system specific and can be translated to other biopolymer mixtures. The application of this knowledge to selectively induce or suppress textural or sensorial changes to other gel systems, however, requires a further thorough scientific description of phase separation processes leading to mixed gel microstructure formation during gelation.

Over the last decades an increasing number of studies, focusing especially on polysaccharides / protein mixtures, have reported several connections between microstructural and rheological properties of mixed gels [23-30]. Compared to the large

number of investigations on mixed polysaccharide / protein solutions and gels, relatively few scientific literature is available on mixed protein systems. To understand the gelation of complex foods, however, they are equally important. Especially due to the increasing industrial interest in interchanging protein sources (for ethical, religious, societal or simply product formulation reasons) the scientific understanding of mixed protein systems is becoming increasingly important. In mixed systems proteins can form one synergistic gel [31, 32] or two independent gels [33-38] dependent on whether both proteins have the same or different gelling mechanisms. This significantly differentiates protein mixtures from the mixtures containing polysaccharides where mostly no synergistic networks are formed. Also, protein mixtures differentiate from mixtures containing polysaccharides as they are co-soluble up to high total protein concentrations (no phase separation) which only changes upon e.g. denaturation of proteins, as pointed out in a series of publications by Polyakov et al. [39-41].

This thesis deals with protein mixtures and the gelation of gelatin and globular proteins that form independent gels and only interact non-specifically via e.g. excluded volume or electrostatic interactions. Globular proteins (such as whey proteins and soy proteins) can be gelled by heating them above their denaturation temperature [42]. Gelatin molecules, due to their lack of tertiary structure, do not undergo denaturation at the temperatures where globular proteins do and thus are not incorporated in the globular protein gel network. Gelatin itself forms a gel via the formation of triple helices when cooled below its coil to helix transition temperature [43, 44]. Globular proteins do not have the required amino acid sequence to form these triple helixes and do not participate in the gelatin network. The globular protein / gelatin mixture is therefore a good model system to study the development of a protein gel structure in the presence of secondary proteins. Combinations of gelatin with globular protein mixtures such as whey protein concentrate [34-36, 45], soy protein isolate (shown in chapter 6 [46]), whey protein isolate [47], aggregated whey proteins [48], mixtures of different milk proteins [49] or egg white protein [37, 38] have already been shown to lead to a large range of rheological behavior and related microstructures, which is important in the development of foods with targeted textural properties. However, an investigation of the mechanisms leading to this large range in microstructural and rheological properties in these systems is still missing.

The aim of this thesis is to understand the importance of different molecular properties on the processes leading to the microstructural arrangements and the final rheological properties in mixed globular protein / gelatin gels. By combining different types of gelatins and different globular proteins it is possible to selectively change either their molecular interaction (e.g. attraction or repulsion) and / or the molecular size ratio between gelatins and globular proteins. This allows to study the effect of interactions and molecular size

ratios on the compatibility of gelatins and globular proteins in solution (at equilibrium condition) and during gelation of either one of the two proteins.

Even though this thesis exclusively describes globular protein / gelatin mixed systems, the developed approaches and presented theory are proposed to be universal and therefore directly translatable to other mixed biopolymer systems.

Structure formation in mixed biopolymer gels

Mixed protein gels can be classified in several ways. One is according to Brownsey and Morris (1987) [50] who distinguished type I and type II networks, dependent on whether one (I) or both (II) of the biopolymers form a gel. Lipatov et al. (2007) [51] categorized mixed gels dependent on whether they arise simultaneously (both biopolymers gel at the same time) or sequentially (one biopolymer gels after the other). Another commonly used classification is based on the gel microstructure (one phase or phase separated) where the latter one can be further divided into bi-continuous gels and gels with spherical enclosures in a continuous matrix.

A combination of the classification according to Brownsey and Morris (1987) and Lipatov et al. (2007) is shown in Figure 1.1. The starting situation is a homogeneous solution where both biopolymers are mixed on a molecular level. Mixed biopolymer gels formed from a solution where biopolymers show any degree of phase separation in this initial step (in solution before gelation) are excluded from this thesis. For these mixtures the properties of the mixed gels depend on the degree of phase separation before gelation, which in return depends on the location of the system in the phase diagram, the kinetics of phase separation and the effort spent on keeping the solutions in a mixed state [52-55] and therefore poses experimental difficulties regarding reproducibility. When starting from a homogeneous situation, as considered in this thesis, only the gelation itself and interactions between biopolymers during gelation are the important parameters that determine the properties of the final mixed gels.

Starting from a homogeneous mixed solution, simultaneous gelation (route (1) in Figure 1.1) can occur if both biopolymers are triggered to gel at the same time. For mixed protein gels, where both proteins exhibit the same gelling mechanism, this typically results in a gel structure where both proteins form one gel network. This is a common phenomenon especially in mixtures containing different types of globular proteins, which, upon heat induced gelation, interact to form one network consisting out of both proteins [32]. Simultaneous gelation can also occur in systems where both gel networks arise in parallel, which allows the simultaneous formation of two separate networks. In both situations the complex interplay between interactions among biopolymers and intermediate aggregates

and the gel formation kinetics of the two gels determine the final gel morphology and gel properties.

Sequential formation of gels (routes (2) and (3) in Figure 1.1), as considered in this thesis, requires proteins to have independent gelling mechanisms. For the special case where the gelling protein forms its gel network without being disturbed by the second protein, routes (2) and (3) can lead to identical final mixed gels. However, in most cases the presence of a non-gelling protein (or other biopolymer) will affect the gelation and final protein gel properties in steps (2.1) or (3.1) and the two routes need to be considered separately. From an experimental point of view, sequentially formed gels allow a separate analysis of the two gelation steps which simplifies their investigation. The sequential formation allows one to separately control the gel formation (e.g. kinetically or by varying external conditions) of each constituent which increases the number of possible gel structures and gel properties. Most, if not all, globular protein / gelatin mixed gels, have separate gelling mechanisms and therefore form sequentially. Here routes (2) and (3) lead to gels that are different in their rheological and microstructural properties as shown earlier for the gelatin type B / whey protein mixture [34-36, 47].

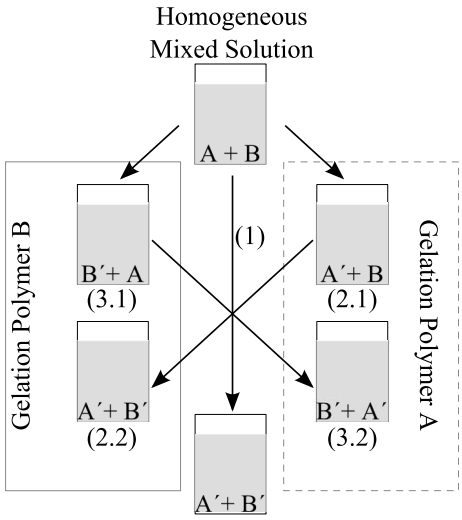

Figure 1.1 Possible routes for gelation in binary mixed systems. Starting point is a homogeneous mixed solution of polymers A and B that can be gelled simultaneously (route 1) or independently (gelled state indicated by A' or B') via routes 2 or 3 (with intermediate steps 2.1 and 2.2 or 3.1 and 3.2 respectively)

Phase behavior and gel microstructure

Another important characteristic of mixed gels is the microstructural arrangements of the polymers inside the mixed gel. Molecules can either stay mixed on a molecular scale throughout the gelation process or show some degree of phase separation [51]. Biopolymer gel networks that stay mixed on a molecular level throughout the gelation process are rare and only phase separated microstructures will be considered here. The possible microstructures for phase separated biopolymer mixtures are schematically shown in Figure 1.2. Figure 1.2A is a two-dimensional representation of a bi-continuous network where both phases (shown in white and black) are continuous throughout the whole system. The second microscopic organization of biopolymers in phase separated systems are spherical enclosures of one phase in a continuous matrix of the second phase (shown schematically in Figure 1.2B).

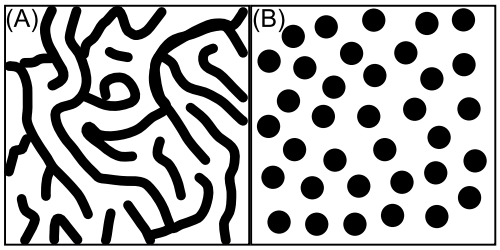

Figure 1.2 Schematic two-dimensional representation of possible gel microstructures in phase separated mixed gels. (A) bi-continuous and (B) spherical enclosures in a continuous gel matrix

The microstructure of a mixed gel depends on the composition of the mixture (location in the phase diagram) and for how long phase separation proceeds before it is arrested by gelation. An example of a phase diagram is shown in Figure 1.3A. Especially the location of the binodal, which separates the one phase region (below the binodal) from the region where phase separation is possible (above the binodal), is important for mixed systems. Homogeneously mixed solutions which are the starting point for mixed protein gels considered in this thesis, are located below the binodal, where no phase separation occurs. During gelation, however, the co-solubility of the two polymers can change, which, in a simplified way, can be understood as a shift of the binodal (and also spinodal) closer to the axis of the phase diagram [39, 56]. Figure 1.3B visualizes schematically the change in the location of the binodal as a function of gelation. As shown by the arrow in Figure 1.3B mixtures can change from the one phase region to the metastable or unstable region of the phase diagram during gelation and therefore show phase separation.

Whether a sample enters the unstable or metastable region during gelation is often not determinable but has a large effect on the final gel structure of the mixture. In the

unstable region (above the spinodal) phase separation occurs via spinodal decomposition leading to a bi-continuous microstructure (Figure 1.2A). Spherical enclosures of one phase in a continuous phase of a second phase (microstructure in Figure 1.2B) are typical for samples located in the metastable region of the phase diagram (location between binodal and spinodal) or for the late stage of phase separation of samples that initially showed a bi-continuous microstructure [57-59]. The final microstructure in the gel is thus determined by an interplay between phase separation during gelation and the arrest of the system due to the formation of a space spanning network.

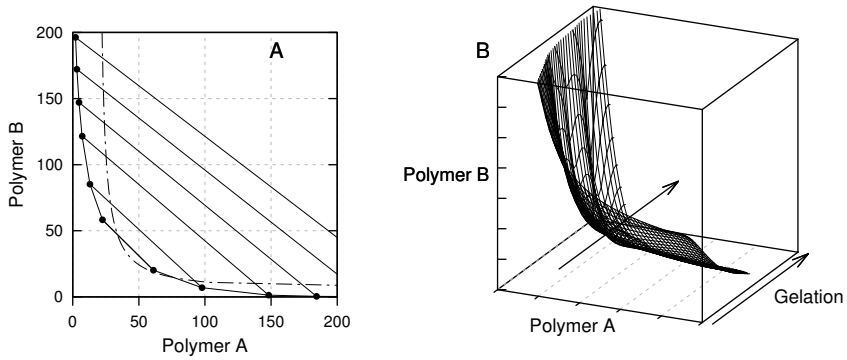

Figure 1.3 Graph A: Typical phase diagram containing binodal (solid curve), spinodal (dashed line) and tie lines (solid lines). Graph B: Schematic phase diagram of binary mixture of polymer A and polymer B during gelation. Arrow indicates location of sample with constant composition during gelation.

Outline of the thesis

Figure 1.4 shows a general scheme for the preparation of a mixed biopolymer gel. The first step involves the preparation of an aqueous solution for both proteins separately. In a second step, a mixed solution is prepared by mixing the two protein solutions. The third step is the gelation where a distinction is made whether component A or B forms a gel and whether only one or both biopolymers are gelled. This thesis follows closely this general scheme with the goal of understanding stepwise the evolution of mixed systems from a single protein solution towards a mixed gel.

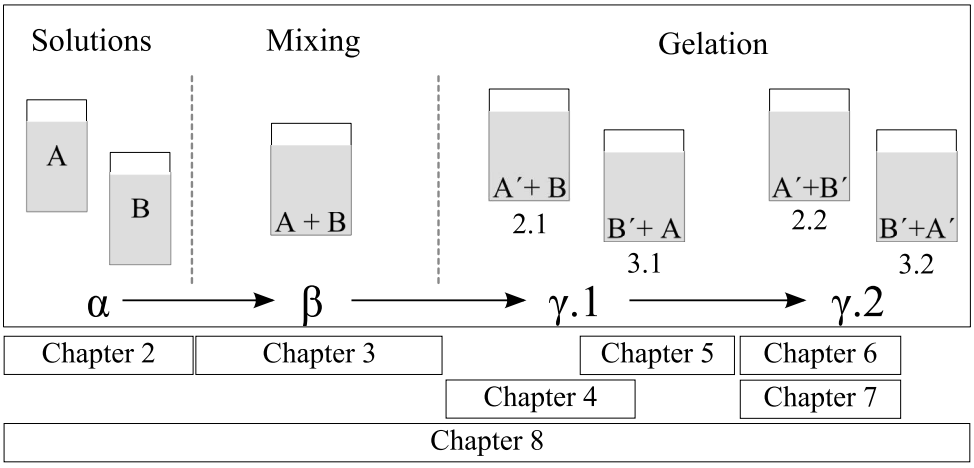

Figure 1.4 General flowchart of preparation for mixed biopolymer gels. Two types of biopolymers are indicated with A and B and their gelled form using A' and B'. Step α: preparation of stock solution. Step β: mixing of stock solutions. Step γ.1: gelation of either one of the biopolymers. Step γ.2: Gelation of the secondary biopolymer in the presence of a gel network. The systems in step γ are additionally labelled according Figure 1.1 using the steps 2.1, 3.1 and final gel structures 2.2 and 3.2.

Chapter 2 introduces membrane osmometry as a tool to characterize proteins in solutions in terms of molecular size and molecular interactions (second virial coefficient B') at neutral pH and varying solvent conditions (ionic strength). Molecular weights and B' are compared to literature values and theories dealing with molecular interactions.

Chapter 3 extends this characterization to mixed systems by quantifying the interactions between two different proteins in aqueous mixtures. Many biopolymer mixtures show phase separation at this stage. Proteins on the other hand are well known for their high compatibility (no phase separation) and this chapter therefore focuses especially on the absence of liquid – liquid phase separation in protein mixtures compared to protein / polysaccharide mixtures.

Chapter 4 concentrates on the gelation of gelatin in the presence of secondary, non-gelled (globular) proteins. The occurrence or absence of phase separation during gelatin gelation is explained based on the molecular interactions and molecular size obtained in chapters 2 and 3. Phase separation is linked to rheological changes and a general approach towards predicting whether mixed systems show phase separation during gelatin gelation is given based on the protein size ratios.

Chapter 5 focuses on the heat induced gelation of globular proteins in the presence of different types of non-gelled gelatin. Similar to chapter 4 the molecular size ratio between proteins is used to explain the occurrence of phase separation and the related rheological changes of mixed gels compared to single globular protein gels. A distinction between the gelatin gels with added globular proteins and globular protein gels with added gelatin is made and related to their gelation mechanisms.

Chapter 6 demonstrates that gelatin is able to form a gel inside the initially formed globular protein gels on the example of soy protein isolate / gelatin mixtures. Fracture properties (fracture stress and strain) of these mixed gels are related to the fracture of the individual gel networks where the stronger of the two networks determines the fracture of the mixed gel. Fracture properties are compared to literature via a texture map to demonstrate the relevance of using mixed protein gels to obtain foods with desired textural properties.

Chapter 7 deals with the applicability of different theories relating the modulus of mixed gels to the gel microstructure and rheological properties of the respective individual gels. Using data from the preceding chapters discrepancies in the applicability of these models to especially globular protein gels are discussed and possible reasons for these inconsistencies are given.

Chapter 8 discusses results across the different chapters and places the current work in a wider context of the available scientific literature before giving an outlook on the possible next steps in mixed biopolymer gel research.

References

1. Clark, A.H., S.B. Ross-Murphy, and S.K.T.N.B. Ubbink, *CHAPTER 1 - Biopolymer Network Assembly: Measurement and Theory*, in *Modern Biopolymer Science*. 2009, Academic Press: San Diego. p. 1-27.
2. Linden, E.v.d. and E.A. Foegeding, *CHAPTER 2 - Gelation: Principles, Models and Applications to Proteins*, in *Modern Biopolymer Science*. 2009, Academic Press: San Diego. p. 29-91.
3. Bremer, L.G.B., *Fractal aggregation in relation to formation and properties of particle gels*. 1992, PhD Thesis Wageningen University.
4. Axelos, M.A.V. and M. Kolb, *Crosslinked biopolymers: Experimental evidence for scalar percolation theory.* Physical Review Letters, 1990. **64**(12): p. 1457-1460.
5. Dickinson, E., *Simple statistical thermodynamic model of the heteroaggregation and gelation of dispersions and emulsions.* Journal of Colloid and Interface Science, 2011. **356**(1): p. 196-202.
6. Dickinson, E., *On gelation kinetics in a system of particles with both weak and strong interactions.* Journal of the Chemical Society, Faraday Transactions, 1997. **93**(1): p. 111-114.
7. Dickinson, E., *On flocculation and gelation in concentrated particulate systems containing added polymer.* Journal of the Chemical Society, Faraday Transactions, 1995. **91**(24): p. 4413-4417.
8. Walstra, P., *Physical Chemistry of Foods*. 2003: Marcel Dekker.
9. Çakır, E., C.R. Daubert, M.A. Drake, C.J. Vinyard, G. Essick, and E.A. Foegeding, *The effect of microstructure on the sensory perception and textural characteristics of whey protein/κ-carrageenan mixed gels.* Food Hydrocolloids, 2012. **26**(1): p. 33-43.
10. van den Berg, L., A.L. Carolas, T. van Vliet, E. van der Linden, M.A.J.S. van Boekel, and F. van de Velde, *Energy storage controls crumbly perception in whey proteins/polysaccharide mixed gels.* Food Hydrocolloids, 2008. **22**(7): p. 1404-1417.
11. van den Berg, L., T. van Vliet, E. van der Linden, M.A.J.S. van Boekel, and F. van de Velde, *Breakdown properties and sensory perception of whey proteins/polysaccharide mixed gels as a function of microstructure.* Food Hydrocolloids, 2007. **21**(5–6): p. 961-976.
12. van den Berg, L., T. van Vliet, E. van der Linden, M.A.J.S. van Boekel, and F. van de Velde, *Serum release: The hidden quality in fracturing composites.* Food Hydrocolloids, 2007. **21**(3): p. 420-432.
13. van den Berg, L., *Texture of food gels explained by combining structure and large deformation properties*. Physics and Physical Chemistry of Foods. 2008: PhD Thesis - Wageningen University.

14. Mosca, A.C., *Designing food structures to enhance sensory responses*, in *Product Design and Quality Management*. 2012, Wageningen University.
15. Mosca, A.C., J.A. Rocha, G. Sala, F. van de Velde, and M. Stieger, *Inhomogeneous distribution of fat enhances the perception of fat-related sensory attributes in gelled foods.* Food Hydrocolloids, 2012. **27**(2): p. 448-455.
16. Mosca, A.C., F. van de Velde, J.H.F. Bult, M.A.J.S. van Boekel, and M. Stieger, *Effect of gel texture and sucrose spatial distribution on sweetness perception.* LWT - Food Science and Technology, 2012. **46**(1): p. 183-188.
17. Mosca, A.C., F.v.d. Velde, J.H.F. Bult, M.A.J.S. van Boekel, and M. Stieger, *Enhancement of sweetness intensity in gels by inhomogeneous distribution of sucrose.* Food Quality and Preference, 2010. **21**(7): p. 837-842.
18. Çakir, E. and E.A. Foegeding, *Combining protein micro-phase separation and protein-polysaccharide segregative phase separation to produce gel structures.* Food Hydrocolloids, 2011. **25**(6): p. 1538-1546.
19. Çakır, E., S.A. Khan, and E.A. Foegeding, *The effect of pH on gel structures produced using protein–polysaccharide phase separation and network inversion.* International Dairy Journal, 2012. **27**(1–2): p. 99-102.
20. van den Berg, L., Y. Rosenberg, M.A.J.S. van Boekel, M. Rosenberg, and F. van de Velde, *Microstructural features of composite whey protein/polysaccharide gels characterized at different length scales.* Food Hydrocolloids, 2009. **23**(5): p. 1288-1298.
21. van den Berg, L., T. van Vliet, E. van der Linden, M.A.J.S. van Boekel, and F. van de Velde, *Breakdown properties and sensory perception of whey proteins/polysaccharide mixed gels as a function of microstructure.* Food Hydrocolloids, 2007. **21**(5-6): p. 961-976.
22. Van Den Berg, L., T. Van Vliet, E. Van Der Linden, M.A.J.S. Van Boekel, and F. Van De Velde, *Physical properties giving the sensory perception of whey proteins/polysaccharide gels.* Food Biophysics, 2008. **3**(2): p. 198-206.
23. Almrhag, O., P. George, A. Bannikova, L. Katopo, D. Chaudhary, and S. Kasapis, *Investigation on the phase behaviour of gelatin/agarose mixture in an environment of reduced solvent quality.* Food Chemistry, 2013. **136**(2): p. 835-842.
24. de Jong, S. and F. van de Velde, *Charge density of polysaccharide controls microstructure and large deformation properties of mixed gels.* Food Hydrocolloids, 2007. **21**(7): p. 1172-1187.
25. Gaaloul, S., S.L. Turgeon, and M. Corredig, *Phase behavior of whey protein aggregates/κ-carrageenan mixtures: Experiment and theory.* Food Biophysics, 2010. **5**(2): p. 103-113.

26. Ould Eleya, M.M. and S.L. Turgeon, *Rheology of κ-carrageenan and β-lactoglobulin mixed gels.* Food Hydrocolloids, 2000. **14**(1): p. 29-40.
27. Pires Vilela, J.A., Â.L.F. Cavallieri, and R. Lopes da Cunha, *The influence of gelation rate on the physical properties/structure of salt-induced gels of soy protein isolate-gellan gum.* Food Hydrocolloids, 2011. **25**(7): p. 1710-1718.
28. Quiroga, C.C. and B. Bergenståhl, *Rheological behavior of amylopectin and β-lactoglobulin phase-segregated aqueous system.* Carbohydrate Polymers, 2008. **74**(3): p. 358-365.
29. Shrinivas, P., S. Kasapis, and T. Tongdang, *Morphology and mechanical properties of bicontinuous gels of agarose and gelatin and the effect of added lipid phase.* Langmuir, 2009. **25**(15): p. 8763-8773.
30. Tobin, J.T., S.M. Fitzsimons, V. Chaurin, A.L. Kelly, and M.A. Fenelon, *Thermodynamic incompatibility between denatured whey protein and konjac glucomannan.* Food Hydrocolloids, 2012. **27**(1): p. 201-207.
31. Kasapis, S. and S.L. Tay, *Morphology of Molecular Soy Protein Fractions in Binary Composite Gels†.* Langmuir, 2009. **25**(15): p. 8538-8547.
32. Comfort, S. and N.K. Howell, *Gelation properties of soya and whey protein isolate mixtures.* Food Hydrocolloids, 2002. **16**(6): p. 661-672.
33. Chronakis, I.S. and S. Kasapis, *Structural properties of single and mixed milk/soya protein systems.* Food Hydrocolloids, 1993. **7**(6): p. 459-478.
34. Walkenström, P. and A.-M. Hermansson, *Mixed gels of fine-stranded and particulate networks of gelatin and whey proteins.* Food Hydrocolloids, 1994. **8**(6): p. 589-607.
35. Walkenström, P. and A.-M. Hermansson, *Fine-stranded mixed gels of whey proteins and gelatin.* Food Hydrocolloids, 1996. **10**(1): p. 51-62.
36. Walkenström, P. and A.-M. Hermansson, *High-pressure treated mixed gels of gelatin and whey proteins.* Food Hydrocolloids, 1997. **11**(2): p. 195-208.
37. Ziegler, G.R., *Microstructure of mixed gelatin-egg white gels: Impact on rheology and application to microparticulation.* Biotechnology Progress, 1991. **7**(3): p. 283-287.
38. Ziegler, G.R. and S.S.H. Rizvi, *Predicting the Dynamic Elastic Modulus of Mixed Gelatin-Egg White Gels.* Journal of Food Science, 1989. **54**(2): p. 430-436.
39. Polyakov, V.I., V.Y. Grinberg, and V.B. Tolstoguzov, *Thermodynamic incompatibility of proteins.* Food Hydrocolloids, 1997. **11**(2): p. 171-180.
40. Polyakov, V.I., O.K. Kireyeva, V. Grinberg, and V.B. Tolstoguzov, *Thermodynamic compatibility of proteins in aqueous media. Part. I. Phase diagrams of some water--protein A--protein B systems.* Die Nahrung, 1985. **29**(2): p. 153-160.
41. Polyakov, V.I., I.A. Popello, V. Grinberg, and V.B. Tolstoguzov, *Thermodynamic compatibility of proteins in aqueous media. Part 2. The effect of some physicochemical*

factors on thermodynamic compatibility of casein and soybean globulin fraction. Die Nahrung, 1985. **29**(4): p. 323-333.

42. Gosal, W.S. and S.B. Ross-Murphy, *Globular protein gelation.* Current Opinion in Colloid and Interface Science, 2000. **5**(3-4): p. 188-194.
43. Joly-Duhamel, C., D. Hellio, A. Ajdari, and M. Djabourov, *All gelatin networks: 2. The master curve for elasticity.* Langmuir, 2002. **18**(19): p. 7158-7166.
44. Djabourov, M., J. Leblond, and P. Papon, *Gelation of aqueous gelatin solutions. I. Structural investigation.* J. Phys. France, 1988. **49**(2): p. 319-332.
45. Brink, J., M. Langton, M. Stading, and A.-M. Hermansson, *Simultaneous analysis of the structural and mechanical changes during large deformation of whey protein isolate/gelatin gels at the macro and micro levels.* Food Hydrocolloids, 2007. **21**(3): p. 409-419.
46. Ersch, C., I. ter Laak, E. van der Linden, P. Venema, and A.H. Martin, *Modulating fracture properties of mixed protein systems.* Food Hydrocolloids, 2014. **44**: p. 59-65.
47. Devi, A.F., R. Buckow, Y. Hemar, and S. Kasapis, *Modification of the structural and rheological properties of whey protein/gelatin mixtures through high pressure processing.* Food Chemistry, 2014. **156**(0): p. 243-249.
48. Fitzsimons, S.M., D.M. Mulvihill, and E.R. Morris, *Segregative interactions between gelatin and polymerised whey protein.* Food Hydrocolloids, 2008. **22**(3): p. 485-491.
49. Pang, Z., H. Deeth, P. Sopade, R. Sharma, and N. Bansal, *Rheology, texture and microstructure of gelatin gels with and without milk proteins.* Food Hydrocolloids, 2014. **35**: p. 483-493.
50. Brownsey, G. and V. Morris, *Mixed and filled gels: models for foods*, in *Food Structure: Creation and Evaluation*. 1987, Elsevier. p. 7-23.
51. Lipatov, Y. and T. Alekseeva, *Phase-Separated Interpenetrating Polymer Networks*. 2007, Springer Berlin Heidelberg. p. 1-227.
52. Leng, X.J. and S.L. Turgeon, *Study of the shear effects on the mixture of whey protein/polysaccharides—2: Application of flow models in the study of the shear effects on WPI/polysaccharide system.* Food Hydrocolloids, 2007. **21**(7): p. 1014-1021.
53. Ould Eleya, M.M., X.J. Leng, and S.L. Turgeon, *Shear effects on the rheology of β-lactoglobulin/β-carrageenan mixed gels.* Food Hydrocolloids, 2006. **20**(6): p. 946-951.
54. Turgeon, S.L., M. Beaulieu, C. Schmitt, and C. Sanchez, *Protein–polysaccharide interactions: phase-ordering kinetics, thermodynamic and structural aspects.* Current Opinion in Colloid & Interface Science, 2003. **8**(4–5): p. 401-414.
55. Wolf, B., R. Scirocco, W.J. Frith, and I.T. Norton, *Shear-induced anisotropic microstructure in phase-separated biopolymer mixtures.* Food Hydrocolloids, 2000. **14**(3): p. 217-225.

56. Matalanis, A., O.G. Jones, and D.J. McClements, *Structured biopolymer-based delivery systems for encapsulation, protection, and release of lipophilic compounds.* Food Hydrocolloids, 2011. **25**(8): p. 1865-1880.
57. Poesio, P., G. Cominardi, A.M. Lezzi, R. Mauri, and G.P. Beretta, *Effects of quenching rate and viscosity on spinodal decomposition.* Physical Review E - Statistical, Nonlinear, and Soft Matter Physics, 2006. **74**(1).
58. Sarkar, S. and B. Bagchi, *Inherent structures of phase-separating binary mixtures: Nucleation, spinodal decomposition, and pattern formation.* Physical Review E - Statistical, Nonlinear, and Soft Matter Physics, 2011. **83**(3).
59. Herzig, E.M., K.A. White, A.B. Schofield, W.C.K. Poon, and P.S. Clegg, *Bicontinuous emulsions stabilized solely by colloidal particles.* Nature Materials, 2007. **6**(12): p. 966-971.

CHAPTER 2

Interactions in Protein Mixtures. Part I: Second virial coefficients from osmometry[1]

ABSTRACT

The interaction of proteins (β-lactoglobulin, Bovine Serum Albumin (BSA), gelatins and whey protein isolate (WPI)) in solution was quantified by measuring their second virial coefficient using membrane osmometry. At neutral pH below 20 - 40 mM ionic strength, electrostatic repulsion dominated the interaction. At higher ionic strength, BSA, WPI and whey protein aggregates (WPA) were well approximated as hard spheres. On the other hand β-lactoglobulin behaved as an adhesive hard sphere for which the stickiness parameter τ (known from the Baxter model for sticky hard spheres) and depth and width of the adhesive part of the interaction potential were calculated.

[1] This chapter is based on: Ersch, C., Meijvogel, L. M. L., van der Linden, E., Martin, A. H., & Venema, P. (2015). Interactions in protein Mixtures. Part I: Second Virial Coefficients from Osmometry. *Food Hydrocolloids* (Accepted).

GRAPHICAL ABSTRACT

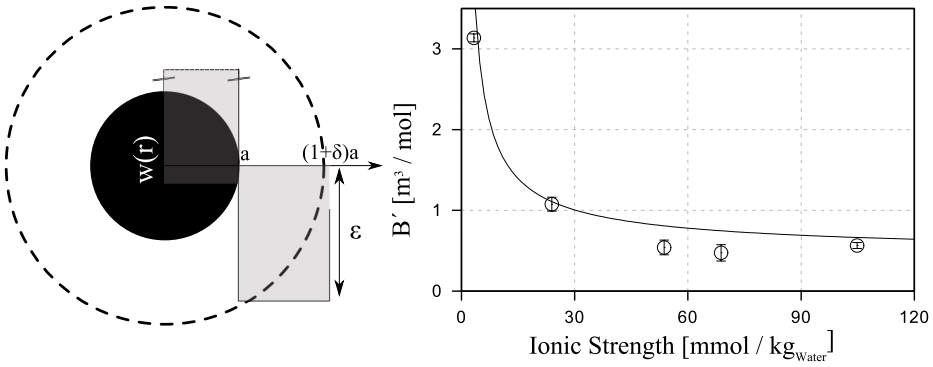

KEYWORDS

Second virial coefficient, molecular interactions, osmometry, protein interaction

Introduction

The interactions between proteins play an important role in many physical phenomena like protein crystallization, aggregation, solubility and phase separation. For the understanding of these phenomena it is important to know their mutual interactions, which are typically expressed in terms of the second virial coefficient [1]. The second virial coefficient *B'* has been directly linked to the crystallization behavior of single and purified protein solutions, which was found to solely occur within a narrow range called 'crystallization slot' [2-8]. Here most experimental data are available for BSA and lysozyme at conditions typically needed to crystallize them [3, 5-7, 9-15]. However, in areas other than protein crystallization, experimental data on second virial coefficients are rare. Only few studies have been published, including β-lactoglobulin at the isoelectric point [16] or uncharged polymers such as dextran [17] and PEG [18-20].

In mixtures of different polymers, their mutual interaction is characterized by their second cross virial coefficient. Also here only a limited number of studies have been published. Measurements of the second cross virial coefficient for the lysozyme / ovalbumin mixture were used to explain the absence of aggregation [21]. Second cross virial coefficients failed to predict the phase behavior of β-lactoglobulin / dextran [17] and PEG / lysozyme [17, 22] mixtures indicating that their phase behavior is not well described by two particle interactions. In other systems, however, second virial coefficients were successfully used to predict the phase behavior for e.g. different PEG mixtures and for mixtures of proteins and polysaccharides [19, 20, 23]. The success of all these investigations largely depends to which extent one is able to measure the virial coefficients accurately. This was addressed by Simonet et al. (2002) in their study of a guar gum / dextran mixture using static light scattering, a frequently used technique for measuring virial coefficients [3-5, 8, 24-28]. Virial coefficients can also be determined using various chromatography methods [2, 14, 22] or membrane osmometry [2, 16, 17, 21, 29, 30].

We have chosen to use membrane osmometry for our study as it provides one of the most direct ways to measure virial coefficients. Virial coefficients can be obtained directly from measurement data by a simple and straight forward fitting procedure. The measurements are relatively fast (approximately 20 minutes per measurement series) and highly reproducible as long as the necessary precautions are taken to control solvent conditions, something that will be addressed in the Material and Methods section. One of the specific advantages of membrane osmometry is that the measured quantities are number averaged, which makes this method insensitive to dust in the samples, often a problem in light scattering.

In the first part of this thesis we aim to quantify the interaction between proteins in terms of second virial coefficients and aim to link these coefficients to the molecular properties and phase behavior. The results are reported in two separate parts. This chapter focuses on the interaction and phase behavior in simple systems and the subsequent chapter 3 on more complex, i.e. mixed, systems. For simple systems we have chosen to study bovine serum albumin (BSA), β-lactoglobulin (β-lac) and dextran because these molecules are well described in literature and often used in applications. Furthermore, we studied whey protein isolate (WPI) and two types of gelatin, relevant proteins in food. To our knowledge no experimental data on the second virial coefficient of these proteins have been published before. Determination of the second virial coefficient under different solvent conditions will contribute towards a better understanding of the behavior of these proteins. This approach has been proven to be fruitful earlier in a limited number of studies, where the gelation of caseinates [31] and the aggregate formation of β-lactoglobulin [32] was studied.

Theory

The virial expansion for the osmotic pressure up to the first three terms is given by [33]

$$\Pi = RTc_p\left(\frac{1}{M_n} + A'c_p + A"c_p^2\right) \qquad 2.1$$

Where c_p denotes the solute mass concentration [kg m^{-3}], R is the gas constant, T the absolute temperature and M_n the solute molecular weight [kg mol^{-1}]. Here the first term describes ideal behavior and is known as the Van 't Hoff's law [33, 34]. Deviations from ideal behavior are expressed by the coefficients A' [mol kg^{-2} m^3] and A'' [mol kg^{-3} m^6]. The coefficient A' is usually expressed in terms of a so-called second virial coefficient defined by B' [m³ mol^{-1}] as

$$B' = A'M_n^2 \qquad 2.2$$

The second virial coefficient B' reflects the pair-wise interaction of two molecules and is directly related to the potential of mean force between them [11, 16, 35] via

$$B' = 2\pi N_A \int \left(1 - e^{-\frac{w(r)}{k_B T}}\right) r^2\, dr \qquad 2.3$$

where r is the distance from the center of the particle, N_A is Avogadro's number, k_B the Boltzmann constant, and $w(r)$ the interaction potential of mean force. We note that the third virial coefficient plays a role once three particle interaction occur (at higher concentrations) [2]. While the interaction is typically only expressed in terms of second virial coefficients, the importance of higher virial coefficients should not be under estimated especially when dealing with more concentrated systems [9, 30, 36-39].

In principle, one would like to determine $w(r)$ using equation 2.3 from a sufficiently large data set for B'. However, apart from the issue how to deal with the dependence of the interaction on pH and ionic strength, this route poses a so-called inversion problem that only has a unique solution when the potential is monotonic, something that is physically not expected. An alternative approach is to postulate the interaction potential.

In general, the potential can be written as

$$\frac{w(r)}{k_B T} = w(r)_{Hard\ Sphere} - w(r)_{attraction} + w(r)_{repulsion} \qquad 2.4$$

To a first approximation, proteins can be modelled as hard spheres (HS) for which the interaction potential is shown in Figure 2.1.1 and given by

$$w(r)_{HS} = \begin{cases} 0, & r > a \\ \infty, & r \leq a \end{cases} \qquad 2.5$$

where *a* denotes the radius of a sphere. Using this potential in equation 2.1 leads to

$$B'_{HS} = \frac{16\pi N_A}{3} a^3 \qquad 2.6$$

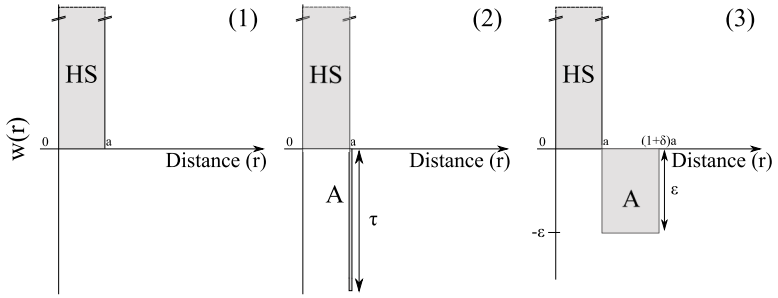

Figure 2.1 Interaction potentials for hard spheres (HS) (1), sticky hard spheres with an infinitely thin attractive well (Baxter model) (2) and hard spheres with an attractive square well potential (3). The particle radius is given by *a*, the attractive well is indicated by (A), characterized by its depth *ε* (τ in Baxter model) and width *δ*

The simplest extension of the hard sphere model is the addition of a square attractive well. One way to include this attractive part is the Baxter model (Figure 2.1.2) [40] commonly known as the "adhesive hard sphere model". It describes the adhesiveness by using a parameter τ, which is related to the depth of the attractive well in the interaction potential while its width is regarded to be infinitely small [41, 42].

Using the Baxter model it is possible to derive the following expression for the osmotic pressure [38, 43]:

$$\frac{\Pi}{RTn} = \frac{1 + \phi + \phi^2}{(1-\phi)^3} - \phi\lambda\left(\frac{18(2+\phi) - \phi\lambda^2}{36(1-\phi)^3}\right) \qquad 2.7$$

where ϕ is the hard sphere volume fraction of the solute and *n* the solute molar density. It is noted that the first term in equation 2.7 corresponds to the pressure of a hard sphere fluid (a result from the scale particle theory) [44, 45].

The second term in equation 2.7 accounts for the attractive part of the potential and its parameter λ is given by

$$\lambda = 6\left[\left(1-\tau+\frac{\tau}{\phi}\right)-\left[\left(1-\tau+\frac{\tau}{\phi}\right)^2-\frac{1}{6}\left(1+\frac{2}{\phi}\right)\right]^{\frac{1}{2}}\right] \qquad 2.8$$

The parameter τ can also be obtained from the second virial coefficient using

$$B' = B'_{HS}\left(1-\frac{1}{4\tau}\right) \qquad 2.9$$

In order to arrive at a more realistic description of the interaction potential, including both repulsive and attractive contributions, Prinsen et al. (2004) have proposed an optimized Baxter model, which gives a crude approximation of the second virial coefficient as a function of ionic strength (equation 2.10). It has been successfully applied to lysozyme [38] and gives, in contrast to the Baxter model, information about the depth (U_A) and width (δ) of the attractive well. The relation they proposed reads

$$\frac{B'}{B'_{HS}} = 1+\frac{3\xi}{2\mu_r}-\frac{3}{2}e^{-\xi}\delta e^{U_A} \qquad 2.10$$

where μ_r is the dimensionless radius ($\mu_r = \kappa a$ / 2), with κ^{-1} [nm] the Debije length as given by

$$\kappa^{-1} = \frac{1}{\sqrt{8\pi\lambda_B N_A I}} \qquad 2.11$$

with $\lambda_B = e^2 / \varepsilon_r k_B T$ the Bjerrum length, e the charge of an electron, ε_r the dielectric constant of the continuous phase and I the ionic strength given by

$$I = \frac{1}{2}\sum_i c_i z_i^2 \qquad 2.12$$

where c is the molar concentration and z the charge number of ion i. The parameter ξ in equation 2.10 is a dimensionless parameter defined by

$$\xi = \frac{\lambda_B}{a}\left(\frac{\bar{Z}}{1+\mu}\right)^2 \qquad 2.13$$

where $\bar{Z} = Z_{eff} - 1$ with Z_{eff} the effective charge of the protein.

As an alternative to the Baxter model the attractive square well in the interaction potential can also be approximated as having a depth (ε) and a width (δ) for which the potential is shown in Figure 2.1.3 and given by

$$w(r) = \begin{cases} 0, & r > (1+\delta)a \\ -\varepsilon, & a < r < (1+\delta)a \\ \infty, & r \leq a \end{cases} \qquad 2.14$$

The second virial coefficient can in this case be expressed in terms of the parameters δ and ε given by

$$B' = \frac{16\pi}{3}a^3\left[1 - \left(e^{\varepsilon/k_BT} - 1\right)(\delta^3 + 3\delta^2 + 3\delta)\right] \qquad 2.15$$

Material and Methods

Materials

β-lactoglobulin (β-lac) lyophilized powder, dextran (dextran from Leuconostoc spp. M_r ~100 kDa) and Bovine Serum Albumin (BSA) lyophilized powder were purchased from Sigma Aldrich (Steinheim, Germany). Whey Protein Isolate (WPI, 94% protein content determined by Kjeldal) was purchased from Davisco Foods international Inc. (Le Sueur, USA, MN). Gelatins type A (90% protein, bloom strength 290 and pI ~8) and type B (88% protein, bloom strength 260, pI 5; all values determined by manufacturer) were kindly provided by Rousselot BVBA (Gent, Belgium). Ingredients except dextran were used without further purification. All other chemicals were of analytical grade and purchased from Sigma Aldrich (Steinheim, Germany).

Dialysis

Dialysis was performed to remove low molecular weight fragments from dextran samples. Dextran was dissolved in deionized water (Merck Millipore, Darmstadt, Germany) at a concentration of 0.8% w/w and stirred for > 2 hours until dissolved. The sample was placed in dialysis tubes with a cut-off of 12 to 14 kDa (Spectra Pore, Spectrum Laboratories INC, Los Angeles, USA) and dialyzed against an excess of water at 4 °C. Dialysis was performed for 3 days and dialysis water exchanged twice a day. After dialysis, dextran was freeze dried and then stored at 4°C until further use. For size exclusion chromatography analysis, the same procedure was used for one aliquot of WPI solutions. For SEC analysis of gelatins, gelatin solutions were dialyzed at 40°C. Samples for SEC analysis were not freeze dried and analyzed within a day after finishing dialysis.

Sample preparation

Solutions were prepared in MOPS buffer (20 mM, pH 6.8) which was prepared using deionized water (18 MΩ cm). The ionic strength of the MOPS buffer was adjusted using NaCl. MOPS buffers were degassed using a vacuum pump. WPI, dextran, β-lactoglobulin and BSA solutions were prepared by dissolving the powders in the MOPS buffer at the desired ionic strength and stirring at room temperature until all powder was dissolved. Gelatin solutions were prepared in the same way but stirred at 60 °C for 1 hour to dissolve gelatin granules. Solutions were then stored at 4 °C overnight. All sample handling from this point onwards was performed at 40 °C. The pH was re-adjusted (adjustment only needed for gelatin containing samples) to pH 6.8 using NaOH.

For whey protein aggregate (WPA) preparation WPI was dissolved in MOPS buffer without added salt. Due to pH adjustment the ionic strength of this buffer was around 3

mmolal. WPA were prepared by heating the WPI solution for 30 min at 95 °C in a water bath. WPA were prepared at 1%, 2%, 4% and 6% w/w protein content. Samples prepared at 1% and 2% were concentrated to 6% using an amicon stirred cell equipped with a 10 kDa membrane (Merck Millipore, Darmstadt, Germany). The protein content of these samples was then determined by Kjeldahl (N-factor 6.25). For WPA measurements at higher ionic strength, NaCl was added to the aggregate solution after cooling to room temperature.

For osmometry measurements, dilution series were prepared using MOPS buffer (tempered to 40°C) to ensure constant ionic strength. The polymer concentrations for each sample were chosen such that the osmotic pressure was between 10^2 and 10^5 Pa. This was typically the case for concentrations between 0.2% and 4% w/w for all samples. For gelatins and dextran it was checked that the concentrations were below their critical overlap concentrations. Dilutions were performed on a weight basis using an analytical scale and sample concentrations re-calculated accordingly. For interpretation of osmometry measurements in terms of equation 2.1, the concentration has to be expressed in mass per volume. To convert concentrations from weight per weight basis to mass per volume it is not correct to assume that all samples have identical densities. For this reason, the density (mass per volume) of each sample was calculated separately using

$$\rho_{S(I,c)} = \rho_{B(I)}\left(1 - \Phi_p\right) + \rho_p \Phi_p \qquad 2.16$$

where $\rho_{S(I,C)}$ is the density of the solution at a given polymer concentration c and ionic strength I. Here $\rho_{B(I)}$ is the density of the corresponding buffer, ρ_p the density of the polymer and Φ_p the polymer volume fraction. The buffer density was measured using a densiometer (DMA 5000, Anton Paar GMBH, Graz, Austria) and found to be linear with increasing ionic strength (results not shown).

The volume fraction of the polymer was determined using

$$\Phi_p = \frac{1}{\rho_p} c_p \, \rho_{B(I)} \qquad 2.17$$

where c_p is the polymer concentration in $g_{Polymer}$ / g_{water}. The density (mass per volume) of protein (1350 kg / m³) was taken from literature [46]. For dextran the density was determined using measurements of a dilution series of dextran resulting in a density of 1452 kg / m³. Calculations were checked with density measurements of protein solutions and a good agreement between measured and predicted values was found (results not shown).

Size exclusion chromatography (SEC - MALLS)

Size exclusion chromatography (Agilent technologies, 1200 series, Amstelveen, Netherlands) with two columns in series (TSK gel G6000 PWXL + TSK gel G3000 PWXL) was performed at 60 °C and a constant flowrate of 0.5 ml / min. Samples were filtered (0.22 µm) before analysis. As running buffer, a 10 mM phosphate buffer having a pH of 6.8 and 125 mM $NaNO_3$ + 0.02% NaN_3 was used. Multi angle laser light scattering (MALLS) was performed using a Wyatt Dawn Heleos II. Data was fitted using a first order fit (ZIMM model) between 35 and 153°.

Osmotic pressure measurements

A 090 membrane osmometer from Gonotec GmbH (Berlin, Germany) was used. Measurements were performed at 40 °C using a 10 kDa cellulosetriacetate membrane which was purchased from the manufacturer of the osmometer. For each measurement, the osmometer was filled freshly with the same buffer as used for sample preparation and dilution. Calibration was performed as described by the manufacturer and calibration constant did not vary significantly between measurements.

The equipment was left to equilibrate before each measurement for 1 hour to obtain a stable baseline (stable ± 5 Pa) which was only obtained after rigorous degassing of the buffer in the reference chamber. For each sample, a dilution series was injected from low to high polymer content. After injection equilibrium pressure (pressure change < 1 Pa / 10 sec) was typically obtained within 30 sec. Longer equilibration times were observed for samples where either small molecular weight fractions could pass the membrane or differences in ionic strength between the sample and the reference solutions existed. Measurement series where this was observed were excluded from this publication. Each sample was injected three times and the value from the final injection recorded as suggested by the manufacturer. Data below 100 Pa were excluded from data analysis. Osmotic pressure data were fitted to equation 2.1 using linear least square regression (MS Excel 2010). The data for the osmotic pressure was fitted taking into account the first two terms of equation 2.1. The coefficient *A''* was only included in the fit when this term significantly contributed ($p < 0.05$). This was only the case for a limited number of measurements. The raw osmometry data and the fitting parameters are available in the Supporting Information as distributed with the publication related to this chapter.

Standard errors for osmometry results are expressed as uncertainly in fitting parameters from regression. Double measurements have shown very good reproducibility which resulted in experimental errors smaller than the fitting errors.

Results and discussion

Pure polymer systems

Figure 2.2 shows the experimental data for the reduced osmotic pressure (i.e. $\Pi / c_p RT$) for Bovine Serum Albumin (BSA) and β-lactoglobulin (β-lac) at low and medium ionic strength. The reduced osmotic pressure was fitted using equation 2.1 which allowed the determination of the molecular weight and *A'*. The difference in y-axis intercept, corresponding to $1/M_n$, reflects the difference in molecular mass for BSA and β-lac. This is also observed at different ionic strengths (cf. Figure 2.3A). The slopes of the lines in Figure 2.2 representing *A'* in equation 2.1 are presented in Figure 2.3B. For both proteins an increase in ionic strength yields a decrease in *A'*. For β-lac a change from a positive to a negative value of *A'* was observed when the ionic strength changed from 3 to 70 mM. This indicates a change from a repulsive to an attractive interaction at increasing higher ionic strength.

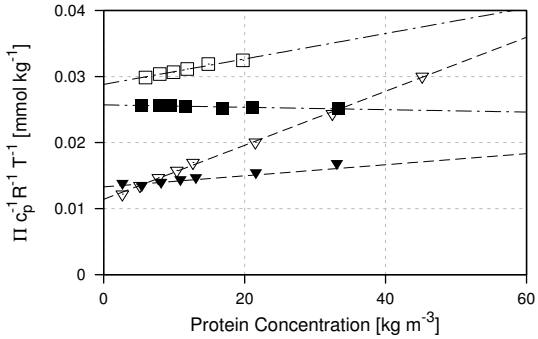

Figure 2.2 Reduced osmotic pressure for BSA (▼▽) and β-lac (■□) at an ionic strength of 3 mM (open symbols) and 70 mM (closed symbols). Lines are first order fits of equation 2.1 to the data.

Figure 2.3 shows the molecular weight and *A'*, for BSA, β-lac and dextran, as a function of ionic strength. Figure 2.4 contains the corresponding size exclusion chromatography (SEC) results for the same material. Dextran had a nominal molecular weight of 100 kDa according to the supplier. The average molecular weight from SEC was 210 kDa with a large polydispersity (Figure 2.4 M_w/M_n ~ 4) similar to values reported in literature [47]. Both values are significantly above the values obtained by osmometry (40 kDa). The peak maximum of the size distribution from SEC, however, is around 40 kDa which is close to the molecular weight obtained by osmometry. Differences between measurements are results from differences in the measurement principles applied. While in light scattering larger aggregates dominate the measurements due to their volume averaged nature, osmometry results are number averaged and therefore typically show lower M_n values.

The M_n of BSA obtained from osmometry is around 80 kDa independent of ionic strength. The BSA monomer has a nominal molecular weight of 66 kg / mol [48] which is also the value obtained from light scattering for the BSA monomers (peak at 37.5 min, Figure 2.4). Osmometry measurements reflect an average over all molecules, and, as SEC results indicated the presence of slightly larger aggregates, the osmometry results yield a slightly larger molecular weight than that of the single BSA molecule.

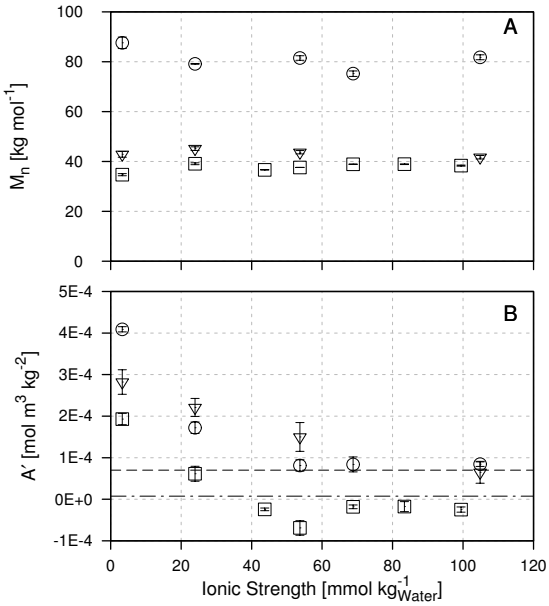

Figure 2.3 Molecular weight (graph A) and *A'* (i.e. B'/M_n^2, with *B'* the second virial coefficient) (graph B) as determined from osmometry for dextran (▽), BSA (O) and beta lactoglobulin (□) as a function of ionic strength. The coefficient *A'* expected for hard sphere interaction for BSA (dashed) and β-lac (dash-dotted) in graph B are calculated using equation 2.6 and literature values for protein radii as presented in the text.

The monomer of β-lac has a nominal molecular weight of 18.3 kg / mol [49]. SEC analysis showed an average molecular weight of 35.1 kg / mol (β-lac dimer) and the presence of a small number of aggregated protein (peak around 28 min, Figure 2.4). In line with this the average M_n from osmometry is slightly above the molecular weight of the dimer. Osmometry results indicate that below an ionic strength of 50 mM this dimerization is slightly more shifted towards the monomer. Above 50 mM however, a constant value of 39 kDa indicates complete dimerization of β-lac. This is in line with earlier published

researches on the dimerization and oligomerization of β-lac [32, 49-51] which is known to vary with salt concentration [32, 51].

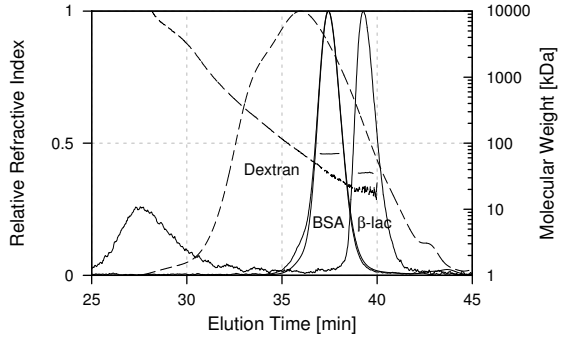

Figure 2.4 Molecular weight distribution from SEC for dextran (dashed), BSA (standard and material used for osmometry) and β-lactoglobulin from SEC

For dextran, as for the proteins, increasing ionic strength leads to a decrease in the second virial coefficient. For dextran, the shape of the curve in Figure 2.3 is significantly different than for the proteins. While the proteins show an initial decrease in *A'* and a plateau value at higher ionic strength, the *A'* of dextran decreases over the whole range of ionic strengths. This is most likely caused by a change in solvent quality, since dextran is an uncharged polymer, making electrostatic contributions to the interaction negligible [17, 52].

A' values for BSA are comparable to literature values (Table 2.1). For β-lac values are slightly higher than values obtained at the isoelectric point [16] but no direct comparison to literature is possible. *A'* values decrease with increasing ionic strength and level off above 20 – 40 mM for both proteins. For the ease of wording, this will be referred to as plateau value of *A'* in the subsequent paragraphs.

Table 2.1 Literature values for virial coefficients and molecular weight from osmometry

Protein	pH	Conditions	M_n [kDa]	A' [mol m³ kg^{-2}]	A" [mol m^{6} kg^{-3}]	Ref
BSA	5.6	0.1 M KCl	63.00	9.20E-05	--	[12]
	7.6		101.00	1.71E-04	--	
	5.4	0.15 M $(NH_4)_2SO_4$	80.2	4.00E-05	--	[13]
	7.4		70.1	6.02E-06	--	
	6	1 M $(NH_4)_2SO_4$		8.39E-06	6.07E-07	[10]
	7			2.09E-05	9.26E-07	
	8			8.69E-06	5.87E-07	
	7.4	0.15 M NaCl	--	1.79E-04	--	[37]
β-lac	7.4	1 M NaCl	57.2	-1.64E-05	1.25E-06	[53]
	5.18	0.03 M NaCl	36.4	-2.43E-04	3.81E-06	[16]
		0.18 M NaCl	34.0	-1.55E-04	8.26E-06	
		1.0 M NaCl	38.7	-7.35E-05	--	
Dextran	5.18	0.03 M NaCl	347.00	3.00E-04		[17]

The experimental value of *A'* at high ionic strength for BSA lies close to the theoretical value for a hard sphere with a radius 3.35 nm, the size of the BSA monomer [54]. Similar hard sphere behavior has been reported earlier for BSA at high ionic strength, over a wide pH range [10]. Increased repulsion between proteins at decreasing ionic strength *(I)* has been discussed in terms of electrostatic double layers [32, 55, 56]. Figure 2.5 shows experimental values and theoretical predictions for the second virial coefficient *B'* for BSA. The theoretical predictions have been calculated by using for the radius the hard sphere radius increased by the Debije length. While this calculation is only the simplest possible approximation of a complex molecular interaction it suggests that the reduction of *B'* at increasing ionic strength is closely related to the screening of the electrostatic interactions and the decrease of the Debije length.

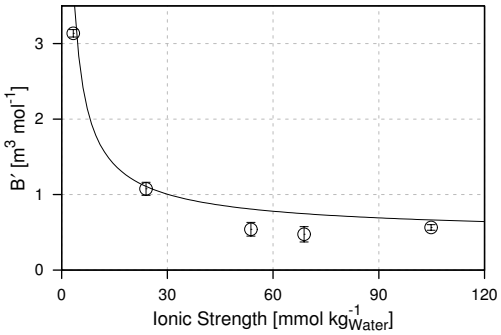

Figure 2.5 Second virial coefficient B' for BSA (O) at different ionic strengths, the line was calculated via equation 2.6 using an effective radius of the protein given by $a + \kappa^{-1}$, where a = 3 nm and κ^{-1} the Debije length.

Now going back to the case of β-lactoglobulin, Figure 2.3, we also observe a decrease in the second virial coefficient at increasing ionic strength. As for BSA this can be attributed to a decrease of the Debije length, κ^{-1}. At ionic strength *I* above 40 mM, and pH 6.8, the negative value for the second virial coefficient indicates that an attractive pair interaction exists between β-lac molecules, mainly present in the form of dimers. Negative second virial coefficients for β-lac have been reported for pH's close to the isoelectric point (Table 2.1, [16]). Negative *B'* values also have been determined for lysozyme and sodium caseinate at similar solvent conditions [2, 36].

To account for the measured attraction (negative *B'*) between β-lac molecules the hard sphere approximation as used for BSA needs to be extended. The simplest extension is the addition of an attractive square well potential to the interaction potential as shown in Figure 2.1.3. For an attractive well width (δ) equal to the Debije length we obtained a depth (ε) of 0.6 k_BT. Additionally we have used the adhesive hard sphere model (Baxter

model) and determined the stickiness parameter τ (a measure for the adhesiveness) via equation 2.7. In this route the parameter τ is obtained directly from osmotic pressure data at low volume fractions. We also have determined τ from our second virial coefficient data using equation 2.9 (results shown in Table 2.2). The two methods give comparable values for τ. Following the route of Prinsen et al. (2004) we have also determined the parameter δe^{UA} (equation 2.10) which gives an estimation of the depth (U_A = 2.97 k_BT) and width (δ = 0.0647 σ/2) of the attractive potential well. Values are within the range of expected values [42]. In order to fit our data we find an effective surface charge of -3e.

Values for τ have been used to predict liquid - liquid phase separation in protein solutions. For example, for β-lactoglobulin [43] liquid-liquid phase separation was observed at the iso-electric point at low ionic strength. For the Baxter model, liquid – liquid phase separation is predicted for $\tau < 0.113$. Indeed, Parker et al. (2005) finds that the β-lactoglobulin system phase separates at $\tau = 0.11$ and remains one phase at $\tau = 0.24$. In our systems $\tau > 0.113$ (cf. Table 2.2), implying that no phase separation is expected. Indeed we did not observe phase separation, nor has it been reported.

Using literature values of the second virial coefficient for β-lac [16] we determined τ at the isoelectric point ($\tau = 0.066$ for I = 180 mM and $\tau = 0.056$ for I = 30 mM). These τ values would predict phase separation at both conditions. However, this is not what is observed experimentally (see published phase diagram [43]). A possible reason for this discrepancy is that τ is volume fraction dependent, as already put forward by Prinsen et al. (2004). This volume dependency is caused by contributions of the higher virial coefficients to τ when determined at higher volume fractions. In the interpretation of τ this should be included. When obtained experimentally at low volume fractions (or via the second virial coefficient) τ is in general not sufficient to predict phase separation unless the second virial coefficient is dominating the phase separation. This value, however, is a direct measure of the molecular two particle interaction (“stickiness”). When obtained at higher volume fractions on the other hand τ can possibly be used to predict phase separation but cannot be used to derive information on the particle-particle interactions.

Table 2.2 τ parameter for β-lactoglobulin obtained via different routes using hard sphere radius = 2 nm, U_A = 2.97, δ = 0.0647 and $\overline{Z}$=-3

Ionic Strength [mmol / kg_{water}]	M_n [kDa]	B' [m^3 / mol]	τ [38]	τ [43]	μ_r	ξ
3.29	34.71	0.232			0.364	0.708
23.93	39.09	0.094			0.982	0.336
43.71	36.63	-0.033	0.178	0.189	1.327	0.243
53.69	37.61	-0.098	0.113	0.131	1.471	0.216
68.79	38.89	-0.027	0.186	0.199	1.665	0.186
83.36	38.91	-0.027	0.188	0.200	1.832	0.164
99.44	38.34	-0.036	0.172	0.188	2.001	0.146

Crude protein systems

Besides being able to measure the molecular weight of relatively pure systems, osmometry has the advantage that it is strictly number based. This method is therefore suitable for crude systems that may contain small numbers of larger aggregates besides monomeric proteins. If the crude systems consists of differently sized molecules one determines the number averaged molecular weight and interaction. As these results summarize a large number of different molecules and aggregates they will be referred to as apparent molecular weight, $M_{n,A}$, and apparent second virial coefficient, B'_A and according coefficient A'_A, related to one another by equation 2.2.

Figure 2.6 shows the $M_{n,A}$ and A'_A of WPI and gelatin together with the results for β-lac and BSA. The quality of these data as obtained from membrane osmometry depends on the assumption that the used membrane is impermeable to all molecules. For crude systems it is important to verify this. Figure 2.7 shows the SEC elution profiles of our protein mixtures before and after excessive dialysis. Dialysis was performed with a membrane having a nominal cut-off of 12 - 14 kDa which is slightly above the 10 kDa cut-off as used in osmometry measurements. The good agreement between both elution profiles for WPI and gelatin shows that no material was able to move through the membrane.

In Figure 2.6 the $M_{n,A}$ for both gelatins scatters around 80 kDa with no clear trend over ionic strength. This value for the apparent molecular weight is significantly below the peak maxima and average molecular weights as obtained from SEC-MALLS (Figure 2.7), which were 150 kDa and 145 kDa for gelatin A and B, respectively. These differences are

however still reasonable because of the uncertainty in the SEC-MALLS analysis due to the width of the elution peak.

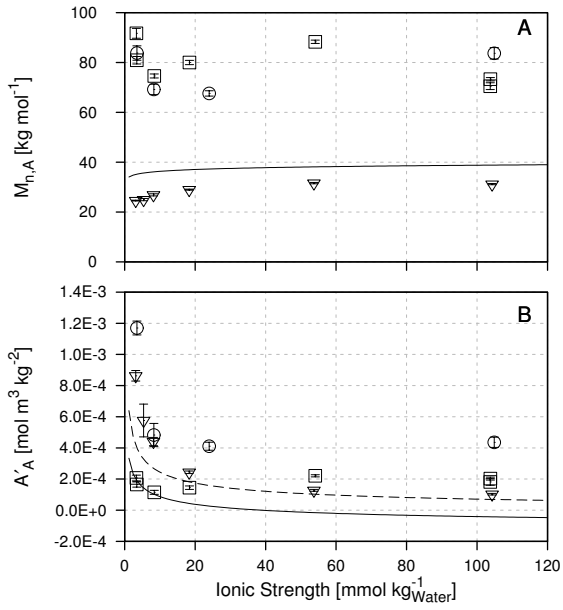

Figure 2.6 Apparent molecular weight $M_{n,A}$ (graph A) and apparent coefficient A'_A (graph B) from osmometry as a function of ionic strength at pH 6.8 and 40 °C for WPI (▽), gelatin type A (□) and gelatin type B (O). Lines show interpolated values for pure BSA (dashed line) and β-lac (solid line) from Figure 2.3.

WPI is a complex mixture of different proteins which makes it difficult to compare its average molecular weight to literature values. It contains mainly β-lac (50%; 18-36 kDa), α-lac (20%; 14 kDa) , immunoglobulins (10%; 100-200 kDa) and BSA (6%; 69 kDa) (percentages in w/w)[49, 57-59]. SEC-MALLS analysis (Figure 2.7) also indicated the presence of larger aggregates. In fact, WPI contains aggregates from a few µm as found in SEC to tenths of µm as shown in the CLSM image in Figure 2.7. In osmometry, however, these aggregates hardly contribute since the results are number averaged. The fact that one measures a number average also explains why the apparent molecular weight $M_{n,A}$ of WPI is significantly below that of β-lac, since in WPI especially α-lac is present in large numbers. The molecular weight of WPI increases with increasing ionic strength from 25 kDa at low ionic strength to 31 kDa above 40 mM. WPI measurements were performed at similar total protein concentrations as the measurements for pure β-lac. In WPI

measurements, the β-lac therefore was present only at 50% of the concentration used in pure β-lac measurements. With the monomer / dimer equilibrium shifting towards the monomer at low ionic strength and low protein concentration it can be expected that in WPI measurements at low ionic strength relatively more monomeric β-lac is present. With increasing ionic strength the equilibrium shifts towards the β-lac dimer which is suggested to be the main cause for the increase of $M_{n,A}$ upon increasing ionic strength.

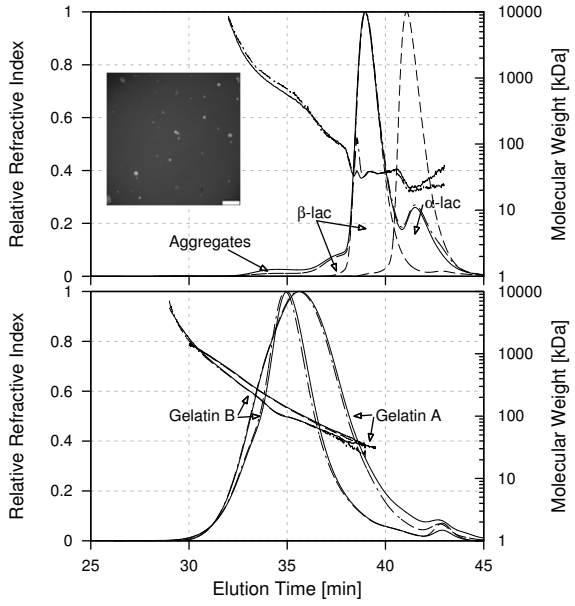

Figure 2.7 Molecular weight and relative refractive index as a function of elution time of WPI (graph A) and gelatins (graph B) as obtained from SEC-MALLS. Graph A: WPI before dialysis (solid line) and after dialysis (interrupted line), β-lac and α-lac standards are shown for reference (dashed lines); Graph B: gelatins as labelled in the graph before (solid line) and after dialyzing (interrupted line). Image in graph A shows a CLSM image of a WPI solution (scale bar 100µm)

The apparent coefficient A'_A of WPI and gelatin B have a similar behavior as a function of ionic strength as for BSA, which was attributed to the screening of the electrostatic double layer. At pH 6.8, i.e. above the isoelectric points (pI) of WPI and gelatin B (WPI pI = 4.8-5.2 [59], gelatin B pI = 5 [60]), the proteins WPI and gelatin B carry significant amounts of negative charge, similar to BSA. Gelatin A at pH 6.8 (pI 8 [60]) is only weakly positively charged and its apparent second coefficient A'_A was found to be independent of ionic strength. Therefore electrostatic repulsion is assumed to be negligible in the interaction

between gelatin A molecules at neutral pH. This was in line with our experimental results within the range of measured ionic strength. Assuming that we may approximate proteins as hard spheres, an effective protein radius of 2.2 nm was obtained from plateau values of A'_A for WPI. For gelatin this value is larger with 4.5 nm for type A and 6 nm for type B. Our values are typically lower than the ones reported in literature [61, 62].

Figure 2.8 presents the apparent molecular weight $M_{n,A}$ together with the apparent second virial coefficient B'_A for whey protein aggregates (WPA) at varying ionic strength. WPA were prepared at fixed solvent conditions (pH 6.8, 3 mM ionic strength) at increasing protein concentration, leading at sufficiently high protein concentration, to protein aggregates with constant internal structure and increasing radius [32]. The effective aggregate radius as calculated from the virial coefficient at high ionic strength is shown in Figure 2.8A. The effective aggregate radius and molecular weight both increase with increasing protein concentration. Their values are significantly smaller than values reported [63, 64].

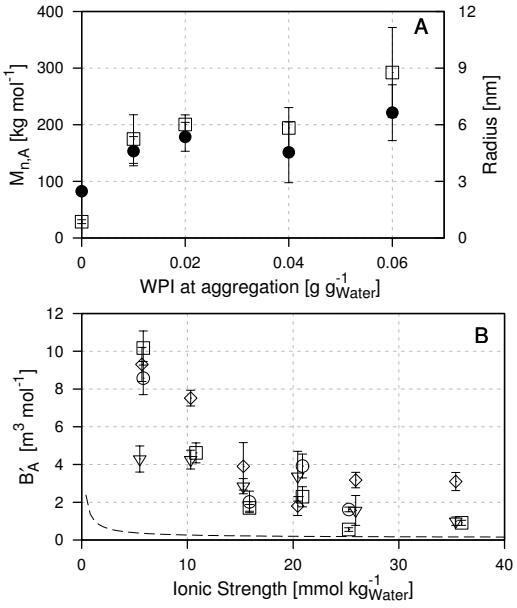

Figure 2.8. Graph A: Apparent molecular weight (□) and WPA radius (●) calculated from the apparent second virial coefficient B'_A at high ionic strength. The value of $M_{n,A}$ and radius at zero concentration WPI corresponds to native WPI. Graph B: apparent second virial coefficient (B'_A) for WPI (dashed line) and WPI aggregates prepared at 1% (□), 2% (O), 4% (▽) and 6% (◊) protein concentration.

For both WPA and WPI the apparent second virial coefficient B_A' is positive and decreases with increasing ionic strength. The values of B_A' increase with increasing aggregate size and are larger than B_A' as obtained for WPI. Results indicate no significant difference between the dependency of B_A' versus ionic strength for whey proteins versus whey protein aggregates. This suggests that the interaction between WPA is similar to the interaction between WPI molecules; a hard sphere interaction with a radius equal to the hard sphere radius plus the Debije length.

Conclusion

Osmometry was successfully used to determine the molecular weights of various protein and a dextran sample. The number averaged molecular weight results obtained from the osmotic pressure measurements were systematically below volume averaged values reported in literature. This difference is attributed to the different measurement principles. Number averaged values are especially useful for direct incorporation in thermodynamic theories.

For the proteins BSA and WPI, and whey protein aggregates (WPA), the behavior of the second virial coefficient as a function of ionic strength suggests that they can be modelled as hard spheres with a radius equal to the hard sphere radius plus the Debije length. Once the electrostatic double layer was screened, simple hard body interaction described their interactions well. For the protein β-lac we found that for our solvent conditions it was well described as a sticky hard sphere, where the depth and width of the attractive well in the interaction potential were determined.

To our knowledge this is the first systematic investigation of second virial coefficients for food relevant proteins at conditions frequently used for applications. Especially for those conditions where proteins have been shown to behave as hard spheres, application of these results to explain their behavior via well described theories for colloidal systems should now be feasible. The next steps will be towards describing the phase behavior of mixed systems based on the virial coefficients. Here, a special interest lies in whether for mixed systems it is possible to predict their phase behavior based on two particle interaction (second virial coefficient), which we will report on in chapter 3.

Supporting Information

Second virial coefficients in table format and raw data of osmotic pressure measurements are published as supporting material with the publication connected to this chapter.

Acknowledgements

We would like to thank Guido Staring from NIZO Food Research B.V. for performing the SEC MALLS measurements.

References

1. Tolstoguzov, V., *Some thermodynamic considerations in food formulation.* Food Hydrocolloids, 2003. **17**(1): p. 1-23.
2. Ahamed, T., M. Ottens, G.W.K. van Dedem, and L.A.M. van der Wielen, *Design of self-interaction chromatography as an analytical tool for predicting protein phase behavior.* Journal of Chromatography A, 2005. **1089**(1–2): p. 111-124.
3. Bonneté, F., S. Finet, and A. Tardieu, *Second virial coefficient: Variations with lysozyme crystallization conditions.* Journal of Crystal Growth 1999. **196**(2-4): p. 403-414.
4. Ducruix, A., J.P. Guilloteau, M. Riès-Kautta, and A. Tardieu, *Protein interactions as seen by solution X-ray scattering prior to crystallogenesis.* Journal of Crystal Growth, 1996. **168**(1-4): p. 28-39.
5. Guo, B., S. Kao, H. McDonald, A. Asanov, L.L. Combs, and W. William Wilson, *Correlation of second virial coefficients and solubilities useful in protein crystal growth.* Journal of Crystal Growth, 1999. **196**(2–4): p. 424-433.
6. Mehta, C.M., E.T. White, and J.D. Litster, *Correlation of second virial coefficient with solubility for proteins in salt solutions.* Biotechnology Progress, 2012. **28**(1): p. 163-170.
7. Wanka, J. and W. Peukert, *Optimized Production of Protein Crystals: From 1D Crystallization Slot towards 2D Supersaturation B22 Diagram.* Chemical Engineering & Technology, 2011. **34**(4): p. 510-516.
8. Wilson, W., *Light scattering as a diagnostic for protein crystal growth—A practical approach.* Journal of Structural Biology, 2003. **142**(1): p. 56-65.
9. Vilker, V.L., C.K. Colton, and K.A. Smith, *The osmotic pressure of concentrated protein solutions: Effect of concentration and ph in saline solutions of bovine serum albumin.* Journal of Colloid and Interface Science, 1981. **79**(2): p. 548-566.
10. Moon, Y.U., R.A. Curtis, C.O. Anderson, H.W. Blanch, and J.M. Prausnitz, *Protein-protein interactions in aqueous ammonium sulfate solutions. Lysozyme and bovine serum albumin (BSA).* Journal of Solution Chemistry, 2000. **29**(8): p. 699-717.
11. Moon, Y.U., C.O. Anderson, H.W. Blanch, and J.M. Prausnitz, *Osmotic pressures and second virial coefficients for aqueous saline solutions of lysozyme.* Fluid Phase Equilibria, 2000. **168**(2): p. 229-239.

12. Park, Y. and G. Choi, *Effects of pH, salt type, and ionic strength on the second virial coefficients of aqueous bovine serum albumin solutions.* Korean Journal of Chemical Engineering, 2009. **26**(1): p. 193-198.
13. Lu, Y., D.-J. Chen, G.-K. Wang, and C.-L. Yan, *Study of Interactions of Bovine Serum Albumin in Aqueous (NH4)2SO4 Solution at 25 °C by Osmotic Pressure Measurements.* Journal of Chemical & Engineering Data, 2009. **54**(7): p. 1975-1980.
14. Le Brun, V., W. Friess, T. Schultz-Fademrecht, S. Muehlau, and P. Garidel, *Lysozyme-lysozyme self-interactions as assessed by the osmotic second virial coefficient: Impact for physical protein stabilization.* Biotechnology Journal, 2009. **4**(9): p. 1305-1319.
15. Kulkarni, A.M., A.P. Chatterjee, K.S. Schweizer, and C.F. Zukoski, *Effects of polyethylene glycol on protein interactions.* The Journal of Chemical Physics, 2000. **113**(21): p. 9863-9873.
16. Schaink, H.M. and J.A.M. Smit, *Determination of the osmotic second virial coefficient and the dimerization of β-lactoglobulin in aqueous solutions with added salt at the isoelectric point.* Physical Chemistry Chemical Physics, 2000. **2**(7): p. 1537-1541.
17. Schaink, H.M. and J.A.M. Smit, *Protein–polysaccharide interactions: The determination of the osmotic second virial coefficients in aqueous solutions of β-lactoglobulin and dextran.* Food Hydrocolloids, 2007. **21**(8): p. 1389-1396.
18. Hasse, H., H.P. Kany, R. Tintinger, and G. Maurer, *Osmotic Virial Coefficients of Aqueous Poly(ethylene glycol) from Laser-Light Scattering and Isopiestic Measurements.* Macromolecules, 1995. **28**(10): p. 3540-3552.
19. Edmond, E. and A.G. Ogston, *An approach to the study of phase separation in ternary aqueous systems.* Biochemical Journal, 1968. **109**(4): p. 569-576.
20. Kang, C.H. and S.I. Sandler, *Phase behavior of aqueous two-polymer systems.* Fluid Phase Equilibria, 1987. **38**(3): p. 245-272.
21. McCarty, B.W. and E.T. Adams Jr, *Osmotic pressure measurements of ovalbumin and lysozyme mixtures.* Biophysical Chemistry, 1987. **28**(2): p. 149-159.
22. Bloustine, J.D., *Experimental Investigations into Interactions and Collective Behavior in Protein/Polymer Mixtures and Granular Rods*, in *The Faculty of the Graduate School of Arts and Sicences*. 2005, Brandeis University. p. 120.
23. Semenova, M.G. and L.B. Savilova, *The role of biopolymer structure in interactions between unlike biopolymers in aqueous medium.* Food Hydrocolloids, 1998. **12**(1): p. 65-75.
24. Rosenbaum, D., P.C. Zamora, and C.F. Zukoski, *Phase Behavior of Small Attractive Colloidal Particles.* Physical Review Letters, 1996. **76**(1): p. 150-153.

25. Muschol, M. and F. Rosenberger, *Interactions in undersaturated and supersaturated lysozyme solutions: Static and dynamic light scattering results.* The Journal of Chemical Physics, 1995. **103**(24): p. 10424-10432.
26. Rosenbaum, D.F., A. Kulkarni, S. Ramakrishnan, and C.F. Zukoski, *Protein interactions and phase behavior: Sensitivity to the form of the pair potential.* The Journal of Chemical Physics, 1999. **111**(21): p. 9882-9890.
27. Velev, O.D., E.W. Kaler, and A.M. Lenhoff, *Protein Interactions in Solution Characterized by Light and Neutron Scattering: Comparison of Lysozyme and Chymotrypsinogen.* Biophysical Journal, 1998. **75**(6): p. 2682-2697.
28. Malo de Molina, P., M.-S. Appavou, and M. Gradzielski, *Oil-in-water microemulsion droplets of TDMAO/decane interconnected by the telechelic C18-EO150-C18: clustering and network formation.* Soft Matter, 2014. **10**(28): p. 5072-5084.
29. Mc Bride, D.W. and V.G.J. Rodgers, *Obtaining protein solvent accessible surface area when structural data is unavailable using osmotic pressure.* AIChE Journal, 2012. **58**(4): p. 1012-1017.
30. Yousef, M.A., R. Datta, and V.G.J. Rodgers, *Understanding Nonidealities of the Osmotic Pressure of Concentrated Bovine Serum Albumin.* Journal of Colloid and Interface Science, 1998. **207**(2): p. 273-282.
31. Ruis, H.G.M., *Structure-rheology relations in sodium caseinate containing systems*, in *Physics and Physical Chemistry of Foods*. 2007, Wageningen University. p. 121.
32. Baussay, K., C.L. Bon, T. Nicolai, D. Durand, and J.-P. Busnel, *Influence of the ionic strength on the heat-induced aggregation of the globular protein β-lactoglobulin at pH 7.* International Journal of Biological Macromolecules, 2004. **34**(1–2): p. 21-28.
33. Yamakawa, H., *Modern Theory of Polymer Solutions*, in *Harper's chemistry series*. 2001, Harper & Row
34. Bahl, B.S., G.D. Tuli, and A. Bahl, *Essentials of Physical Chemistry*. 2000: S. Chand Limited.
35. McMillan, W.G. and J.E. Mayer, *The Statistical Thermodynamics of Multicomponent Systems.* The Journal of Chemical Physics, 1945. **13**(7): p. 276-305.
36. Yousef, M.A., R. Datta, and V.G.J. Rodgers, *Confirmation of Free Solvent Model Assumptions in Predicting the Osmotic Pressure of Concentrated Globular Proteins.* Journal of Colloid and Interface Science, 2001. **243**(2): p. 321-325.
37. Yousef, M.A., R. Datta, and V.G.J. Rodgers, *Model of osmotic pressure for high concentrated binary protein solutions.* AIChE Journal, 2002. **48**(4): p. 913-917.
38. Prinsen, P. and T. Odijk, *Optimized Baxter model of protein solutions: electrostatics versus adhesion.* J Chem Phys, 2004. **121**(13): p. 6525-37.

39. Petsev, D.N., X. Wu, O. Galkin, and P.G. Vekilov, *Thermodynamic Functions of Concentrated Protein Solutions from Phase Equilibria.* The Journal of Physical Chemistry B, 2003. **107**(16): p. 3921-3926.
40. Baxter, R.J., *Percus–Yevick Equation for Hard Spheres with Surface Adhesion.* The Journal of Chemical Physics, 1968. **49**(6): p. 2770-2774.
41. de Kruif, K.G., M.A.M. Hoffmann, M.E. van Marle, P.J.J.M. van Mil, S.P.F.M. Roefs, M. Verheul, and N. Zoon, *Gelation of proteins from milk.* Faraday Discussions, 1995. **101**(0): p. 185-200.
42. Mezzenga, R. and P. Fischer, *The self-assembly, aggregation and phase transitions of food protein systems in one, two and three dimensions.* Reports on Progress in Physics 2013. **76**(4).
43. Parker, R., T.R. Noel, G.J. Brownsey, K. Laos, and S.G. Ring, *The Nonequilibrium Phase and Glass Transition Behavior of β-Lactoglobulin.* Biophysical Journal, 2005. **89**(2): p. 1227-1236.
44. Reiss, H., H.L. Frisch, and J.L. Lebowitz, *Statistical mechanics of rigid spheres.* The Journal of Chemical Physics 1959. **31**(2): p. 369-380.
45. Lekkerkerker, H.N.W. and R. Tuinier, *Colloids and the Depletion Interaction*. Lecture Notes in Physics 2011: Springer Science+Business Media B.V.
46. Fischer, H., I. Polikarpov, and A.F. Craievich, *Average protein density is a molecular-weight-dependent function.* Protein Science, 2004. **13**(10): p. 2825-2828.
47. Edelman, M.W., R.H. Tromp, and E. van der Linden, *Phase-separation-induced fractionation in molar mass in aqueous mixtures of gelatin and dextran.* Physical Review E - Statistical, Nonlinear, and Soft Matter Physics, 2003. **67**(2 1): p. 214041-2140411.
48. El Kadi, N., N. Taulier, J.Y. Le Huérou, M. Gindre, W. Urbach, I. Nwigwe, P.C. Kahn, and M. Waks, *Unfolding and Refolding of Bovine Serum Albumin at Acid pH: Ultrasound and Structural Studies.* Biophysical Journal, 2006. **91**(9): p. 3397-3404.
49. Verheul, M., J.S. Pedersen, S.P.F.M. Roefs, and K.G. de Kruif, *Association behavior of native β-lactoglobulin.* Biopolymers, 1999. **49**(1): p. 11-20.
50. Butré, C.I., P.A. Wierenga, and H. Gruppen, *Effects of Ionic Strength on the Enzymatic Hydrolysis of Diluted and Concentrated Whey Protein Isolate.* Journal of Agricultural and Food Chemistry, 2012. **60**(22): p. 5644-5651.
51. Renard, D., J. Lefebvre, M.C.A. Griffin, and W.G. Griffin, *Effects of pH and salt environment on the association of β-lactoglobulin revealed by intrinsic fluorescence studies.* International Journal of Biological Macromolecules, 1998. **22**(1): p. 41-49.

52. Doublier, J.L., C. Garnier, D. Renard, and C. Sanchez, *Protein-polysaccharide interactions.* Current Opinion in Colloid and Interface Science, 2000. **5**(3-4): p. 202-214.
53. Wu, J. and J.M. Prausnitz, *Osmotic pressures of aqueous bovine serum albumin solutions at high ionic strength.* Fluid Phase Equilibria, 1999. **155**(1): p. 139-154.
54. Barbosa, L.R.S., M.G. Ortore, F. Spinozzi, P. Mariani, S. Bernstorff, and R. Itri, *The importance of protein-protein interactions on the pH-induced conformational changes of bovine serum albumin: A small-angle x-ray scattering study.* Biophysical Journal, 2010. **98**(1): p. 147-157.
55. Walstra, P., *Physical Chemistry of Foods*. 2003: Marcel Dekker.
56. Moreira, L.A., M. Boström, B.W. Ninham, E.C. Biscaia, and F.W. Tavares, *Effect of the ion-protein dispersion interactions on the protein-surface and protein-protein interactions.* Journal of the Brazilian Chemical Society, 2007. **18**: p. 223-230.
57. Wang, T. and J.A. Lucey, *Use of Multi-Angle Laser Light Scattering and Size-Exclusion Chromatography to Characterize the Molecular Weight and Types of Aggregates Present in Commercial Whey Protein Products.* Journal of Dairy Science, 2003. **86**(10): p. 3090-3101.
58. Ramos, Ó.L., J.O. Pereira, S.I. Silva, M.M. Amorim, J.C. Fernandes, J.A. Lopes-da-Silva, M.E. Pintado, and F.X. Malcata, *Effect of composition of commercial whey protein preparations upon gelation at various pH values.* Food Research International, 2012. **48**(2): p. 681-689.
59. Zydney, A.L., *Protein Separations Using Membrane Filtration: New Opportunities for Whey Fractionation.* International Dairy Journal, 1998. **8**(3): p. 243-250.
60. Mohanty, B. and H.B. Bohidar, *Systematic of Alcohol-Induced Simple Coacervation in Aqueous Gelatin Solutions.* Biomacromolecules, 2003. **4**(4): p. 1080-1086.
61. Eagland, D., G. Pilling, and R.G. Wheeler, *Studies of the collagen fold formation and gelation in solutions of a monodisperse [small alpha] gelatin.* Faraday Discussions of the Chemical Society, 1974. **57**(0): p. 181-200.
62. Herning, T., M. Djabourov, J. Leblond, and G. Takerkart, *Conformation of gelatin chains in aqueous solutions: 2. A quasi-elastic light scattering study.* Polymer, 1991. **32**(17): p. 3211-3217.
63. de la Fuente, M.A., Y. Hemar, and H. Singh, *Influence of κ-carrageenan on the aggregation behaviour of proteins in heated whey protein isolate solutions.* Food Chemistry, 2004. **86**(1): p. 1-9.
64. de Kruif, K.G. and R. Tuinier, *Whey protein aggregates and their interaction with exo-polysaccharides.* International Journal of Food Science and Technology, 1999. **34**(5-6): p. 487-492.

CHAPTER 3

Interactions in Protein Mixtures. Part II: A virial approach to predict phase behavior[2]

ABSTRACT

A virial theory was used to relate molecular interactions (in terms of second virial coefficients, B') and molecular size ratios to liquid – liquid phase separation. Application of the virial theory to binary hard sphere mixtures (additive and non-additive) confirmed the applicability of this simple approach towards predicting phase behavior based on two-particle interactions. Experimentally, second cross virial coefficients were obtained for dextran / gelatin, whey protein isolate (WPI) / gelatin mixtures and whey protein aggregate (WPA) / gelatin mixtures using membrane osmometry at varying ionic strength. From this, solvent conditions where interactions between proteins are dominated by electrostatics and solvent conditions where interactions are dominated by hard body interactions could be determined. Using experimentally obtained second virial coefficients, the liquid – liquid phase separation for gelatin / dextran mixtures was successfully predicted. Second cross virial coefficients for gelatin / whey protein isolate and for gelatin / whey protein aggregates could be related to the absence of phase separation in these mixtures. This could be related to a similar size of the proteins and their non – additive behavior at conditions where they mainly interact via hard body interactions.

[2] This chapter is based on: Ersch, C., van der Linden, E., Martin, A. H., & Venema, P. (2015). Interactions in Protein Mixtures. Part II: A Virial Approach to Predict Phase Behavior. *Food Hydrocolloids* (Accepted).

GRAPHICAL ABSTRACT

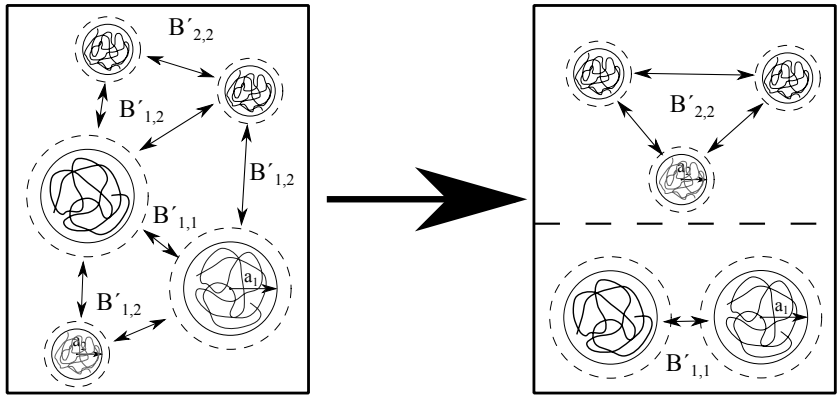

KEYWORDS

Liquid – liquid phase separation, virial coefficient, protein interaction, particle interaction, second virial coefficient, second cross virial coefficient

Introduction

Proteins are present in many biological systems whose macroscopic appearance can be typically described by the interactions between proteins [1]. The interactions can be quantified in terms of the second virial coefficient, taking into account interactions between pairs of proteins. However, experimental data on the second virial coefficient for proteins are scarce in literature.

Second virial coefficients for proteins have been mainly obtained in connection with the crystallization behavior of lysozyme and Bovine Serum Albumin [2-12]. Other proteins are only studied sporadically and within a limited range of solvent conditions [13-17]. The molecular interactions between polymers of different kind (including proteins) have received even less attention. The interaction between different polymers is quantified in terms of the so-called second cross virial coefficient. Studies here mostly focus on model biopolymer solutions and their phase behavior. Using a virial theory, Edmond et al. (1968) [16] successfully predicted the phase behavior of PEG mixtures. A similar approach was followed by Kang et al. (1987) [17] for dextran / PEG mixtures and by Semenova et al. (1998) [18] describing the phase separation of several protein / polysaccharide mixtures. Schaink et al. (2007) [14] showed for β-lactoglobulin / dextran mixtures that a virial theory only including the second virial coefficient underestimates the critical concentrations above which phase separation can be expected. In line with this result Bloustine et al. (2005) [19] also observe that in order to describe the phase behavior of PEG / lysozyme mixtures it was important to include higher virial coefficients.

Apart from using (second) virial coefficients to describe phase separation in polymer mixtures, they are also valuable to describe other processes. Virial coefficients have been used for the explanation of caseinate gelation [20], the coacervation of ovalbumin and lysozyme [21] and the aggregate formation of β-lactoglobulin [22]. Nevertheless, the total number of investigations including virial coefficients to describe protein (or more general biopolymer) interactions is limited.

Experimentally, the second virial coefficient can be obtained using different scattering techniques [10, 11, 23-29], sedimentation experiments [16] or membrane osmometry [13, 14, 21, 30-32]. We have decided to use membrane osmometry because of its direct measurement of the osmotic pressure, and because the measured values are number-averaged and therefore insensitive to sample impurities, like dust. In chapter 2 we have determined the molecular weight and molecular interactions for a variety of proteins and crude protein mixtures. These results were used to estimate the strength of the adhesive interactions between β-lactoglobulin molecules, which turned out to be well-described as

adhesive hard spheres. Bovine Serum Albumin, whey protein isolate (WPI) and two types of gelatins were found to interact mainly via hard body interactions at higher ionic strengths, while at lower ionic strengths electrostatic repulsion (additional to hard body interaction) contributes more and more to their total interaction.

In this chapter we focus on the pair interaction between proteins at solvent conditions often found in foods (neutral pH and low to intermediate salt concentrations). Because in many foods proteins are frequently present in their aggregated form we also include whey protein aggregates prepared by a pre-heating step of the native protein. Compared to whey protein in the native state, whey protein aggregates are reported to cause phase separation in protein mixtures at lower concentrations [34-36]. We aim to present the experimental results in such a way that they can be directly used in other studies involving protein mixtures.

The theory section of this chapter is divided in three parts. Part 1 presents the route how second cross virial coefficients can be obtained from osmometry measurements. Part 2 focuses on predicting liquid – liquid phase separation based on two-particle interactions via the virial expansion approach. In the third part we then apply this approach to predict liquid – liquid phase separation in binary hard sphere mixtures. In the experimental part we then apply the theory to predict phase separation in gelatin / dextran mixtures and explain the absence of phase separation in different gelatin / whey protein mixtures.

Theory

Polymer interactions

The interaction between polymers can be described by their so called interaction potential of mean force. This means that an average over all solvent molecules has taken place (the behavior of solvent molecules has been integrated out). For thermodynamic considerations the interaction potential is typically expressed in terms of the second virial coefficient where the relation between the two is given via the McMillan-Mayer theory [37]

$$B' = 2\pi N_A \int \left(1 - e^{-\frac{w(r)}{k_B T}}\right) r^2 \, dr \qquad 3.1$$

with B' the second virial coefficient, N_A Avogadro's number, $w(r)$ the interaction potential of mean force, r the radial distance and k_BT the thermal energy, with k_B the Boltzmann constant and T the absolute temperature. In this expression $w(r)$ is assumed to be isotropic. Experimental determination of virial coefficients can be performed using osmotic pressure measurements. The relationship between osmotic pressure Π [Pa] and polymer weight concentration c_p [kg m^{-3}] can be written for single polymer solutions as:

$$\Pi = RTc_p\left(\frac{1}{M_n} + A'c + A"c^2\right) \qquad 3.2$$

Here R is the gas constant and M_n the molecular weight. The first term represents the Van 't Hoff law and A' [mol m^3 kg^{-2}] and A'' [mol m^6 kg^{-3}] are coefficients describing the deviation from ideal behavior. These coefficients are directly related to the second and third virial coefficient, B' and B'', respectively. For the second virial coefficient this relationship is given by:

$$B' = A'M_n^2 \qquad 3.3$$

To account for the interaction between different types of polymers in mixtures, equation 3.2 can be extended including pair-wise particle interactions as

$$\frac{\Pi}{c_p RT} = \frac{1}{\overline{M}_n} + c_p\left[A'_{1,1}\, w_1^2 + A'_{2,2} w_2^2 + 2w_1 w_2 A'_{1,2}\right] \qquad 3.4$$

Here (Π / c_pRT) is the so-called reduced osmotic pressure and c_p the total polymer weight concentration [kg m^{-3}]. $A'_{1,1}$ is the interaction coefficient for polymer 1, $A'_{2,2}$ the interaction coefficient for polymer 2 and $A'_{1,2}$ the cross interaction coefficient

representing the particle-particle interaction between polymer 1 and polymer 2. The weight fractions w_1, w_2 for polymer 1 and 2 are defined by

$$w_1 = \frac{c_{p,1}}{c_{p,1} + c_{p,2}} \qquad w_2 = \frac{c_{p,2}}{c_{p,1} + c_{p,2}} \qquad 3.5$$

$$w_1 + w_2 = 1 \qquad c_{p,1} + c_{p,2} = c_p$$

where $c_{p,1}$ and $c_{p,2}$ are the weight concentrations of polymer 1 and 2 respectively and c_p the total polymer concentration. $1/\bar{M}_n$ in equation 3.2 is defined by

$$\frac{1}{\bar{M}_n} = \frac{w_1}{M_{w,1}} + \frac{w_2}{M_{w,2}} \qquad 3.6$$

Using equation 3.2 the cross interaction coefficient ($A'_{1,2}$) can be obtained from osmotic pressure measurements if the coefficients $A'_{1,2}$, $A'_{2,2}$ and molecular masses $M_{n,1}$, $M_{n,2}$ of both polymers were determined in separate measurements. The coefficients can then be related to the second virial coefficients via a generalized version of equation 3.3 given by

$$B'_{i,j} = A'_{i,j} M_{n,i} M_{n,j} \qquad 3.7$$

with $i = 1,2$ and $j = 1,2$ referring to the two polymers. Ideally, one would like to determine the interaction potential from the virial coefficients by measuring the second virial coefficient as a function of e.g. pH, T or ionic strength and inverting equation 3.1. In case of a gas this can be done using different temperatures. However, in case of a protein this route is less practical and, in general, the inversion is anyway only possible if the interaction potential $w(r)$ is monotonic, something which is not expected [38]. Another route to compare experimental values for the second virial coefficients to theory would be to postulate the interaction potential $w(r)$ and evaluate equation 3.1. However, this requires detailed knowledge of a number of molecular and solution parameters which are not known for the crude polymer sources we study here.

We will therefore analyze the experimentally obtained second virial coefficients in terms of a simple hard sphere (HS) model for which the interaction potential is given by

$$w(r)_{HS} = \begin{cases} 0, & r > a \\ \infty, & r \leq a \end{cases} \qquad 3.8$$

and the second virial coefficient (*B'1,1* or *B'2,2*) as

$$B'_{1,1} = \frac{16\pi N_A}{3}(a)^3 \qquad 3.9$$

where *a* is the radius of the sphere (protein). The interaction potential for the second cross coefficient is given by

$$w(r)_{HS\,1,2} = \begin{cases} 0, & r > (a_1 + a_2)/2 \\ \infty, & r \leq (a_1 + a_2)/2 \end{cases} \qquad 3.10$$

where a_1 and a_2 refer to the radii of spheres 1 and 2, respectively, as shown in Figure 3.1. The second cross virial coefficient for a mixture of binary additive hard spheres can be calculated from the hard sphere potential $w(r)_{HS\,1,2}$ which reads

$$B'_{1,2} = \frac{16\pi N_A}{3}\left(\frac{a_1 + a_2}{2}\right)^3 \qquad 3.11$$

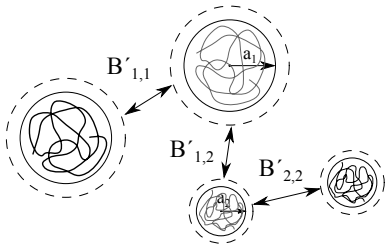

Figure 3.1 Mixture of two types of spheres with the radii (*a*) and second virial coefficients (*B'*) indicated.

Phase diagrams based on two particle interaction

To obtain phase diagrams we follow the virial expansion approach originally forwarded by McMillan and Mayer (1945) [37]. Second virial coefficients as obtained from osmometry can be directly used in this approach without conversions or additional assumptions. To determine the phase diagram, one uses the fact that in thermodynamic equilibrium (at the binodal) the chemical potential of each component and the osmotic pressure in both phases are equal [14]:

$$\frac{\Pi^I}{RT} = \frac{\Pi^{II}}{RT}$$
$$\frac{{\mu_i}^I}{RT} = \frac{{\mu_i}^{II}}{RT} \qquad 3.12$$

Where the two phases are denoted by I and II, μ_i denotes the chemical potential of component *i = 1,2* and *Π* denotes the osmotic pressure. Within the McMillan-Mayer theory the potential of mean force is introduced, where the contribution of the solvent molecules is integrated out and as a result the chemical potential of the solvent does not have to be considered anymore. The chemical potential of a polymer in a dilute solution can be expressed in terms of the second virial coefficients and polymer molar concentration using [39, 40]

$$\mu_i = \mu_i^0 - RT\left(ln\, c_i + 2B'_{i,i}c_i + 2\sum_{\substack{j=1,\\ j\neq i}}^{2} B'_{i,j}c_j\right) \qquad 3.13$$

Where *i* = 1,2 refers to polymers 1 and 2 respectively, μ_i^0 the standard state chemical potential, *c* the molar concentration in [mol m^{-3}] and *B'* the second virial coefficient in [m³ mol^{-1}].

From equation 3.4 and equation 3.13 it is possible to evaluate equations 3.12 which for two polymers in solution are explicitly given by:

$$c_1^I + c_2^I + B'_{1,1}{c_1^I}^2 + B'_{1,2}c_1^I c_2^I + B'_{2,2}{c_2^I}^2 = c_1^{II} + c_2^{II} + B'_{1,1}{c_1^{II}}^2 + B'_{1,2}c_1^{II}c_2^{II} + B'_{2,2}{c_2^{II}}^2$$
$$ln(c_1^I) + 2B'_{1,1}c_1^I + 2B'_{1,2}c_2^I = ln(c_1^{II}) + 2B'_{1,1}c_1^{II} + 2B'_{1,2}c_2^{II} \qquad 3.14$$
$$ln(c_2^I) + 2B'_{1,2}c_1^I + 2B'_{2,2}c_2^I = ln(c_2^{II}) + 2B'_{1,2}c_1^{II} + 2B'_{2,2}c_2^{II}$$

The resulting system of three equations with four unknowns (c_1^I, c_2^I, c_1^{II}, c_2^{II}) can be evaluated iteratively by choosing a value for either one of the four unknowns and calculate the other three. Alternatively, this can be expressed as a set of five equations with five unknowns when taking the conservation of mass into consideration, as is shown in the appendix to this chapter. Equations 3.14 can be used to calculate the location of the binodal. The binodal is the line in a phase diagram that separates the one phase region from the two phase region (for an example of a phase diagram we refer to Figure 3.6). In the region close to the binodal (but still below the spinodal), mixtures are metastable or can phase separate via nucleation and growth. The spinodal can be determined using the determinant of the stability matrix of the system (equation 3.15) [41]. The spinodal separates the metastable region of the phase diagram (area between binodal and spinodal) from the unstable region (area above the spinodal). Binodal and spinodal coincide at the critical point (equation 3.20) which is defined as the point with the lowest total polymer concentration that shows phase separation.

$$Det(M_1) = 0 \qquad 3.15$$

Here M_1 is the stability matrix of the partial derivatives of the chemical potential for the two polymers relative to their number density [42, 43], given by:

$$M_1 = \begin{bmatrix} \frac{\partial \mu_1}{\partial n_1} & \frac{\partial \mu_1}{\partial n_2} \\ \frac{\partial \mu_2}{\partial n_1} & \frac{\partial \mu_2}{\partial n_2} \end{bmatrix} \qquad 3.16$$

By substituting this into equation 3.15 we arrive at

$$Det(M_1) = \left(\frac{\partial \mu_1}{\partial n_1}\right)\left(\frac{\partial \mu_2}{\partial n_2}\right) - \left(\frac{\partial \mu_1}{\partial n_2}\right)\left(\frac{\partial \mu_1}{\partial n_2}\right) = 0 \qquad 3.17$$

Evaluating equation 3.17 leads to the following equation for the spinodal

$$4\left(B'_{1,1}B'_{2,2} - B'^2_{1,2}\right)c_1c_2 + 2B'_{2,2}c_2 + 2B'_{1,1}c_1 + 1 = 0 \qquad 3.18$$

which can be rewritten as

$$c_2 = \frac{-\left(1 + 2B'_{1,1}c_1\right)}{4\left(B'_{1,1}B'_{2,2} - B'^2_{1,2}\right)c_1 + 2B_{2,2}} \qquad 3.19$$

The critical point of the mixture can be found by applying the following two conditions [41]

$$Det(M_1) = 0$$
$$Det(M_2) = 0 \qquad 3.20$$

where the matrix M_2 can be obtained by replacing any of the row vectors of M_1 by

$$\left[\frac{\partial(Det(M_1))}{\partial n_1} \quad \frac{\partial(Det(M_1))}{\partial n_2}\right] \qquad 3.21$$

Following this route, a set of two equations (derivation details given in appendix) are obtained (equations 3.22) that must be solved numerically to obtain the molar concentration of polymer 1 (c_1) and polymer 2 (c_2) at the critical point.

$$4\left(B'_{1,1}B'_{2,2} - B'^{2}_{1,2}\right)c_1c_2 + 2B'_{1,1}c_1 + 2B'_{2,2}c_2 + 1 = 0$$
$$\left(2B'_{1,2}c_2\right)\left(1 + 2B'_{2,2}c_2\right) - \left(1 + 2B'_{1,1}c_1\right)^2 = 0 \qquad 3.22$$

For a two-polymer system for which the second virial coefficients are known, equations 3.14 to 3.22 allow the construction of a phase diagram without any adjustable parameters. To estimate whether in certain situations phase separation is predicted by this approach we use equation 3.18. For a system with positive second virial coefficients (mainly repulsive interactions), equation 3.18 only has a solution if $\left(B'_{1,2}\right)^2$ is at least larger than the product of $B'_{1,1}B'_{2,2}$. We define the parameter B'_{crit} as

$$B'_{crit} = \frac{\left(B'_{1,2}\right)^2}{B'_{1,1}B'_{2,2}} \qquad 3.23$$

For $B'_{crit} > 1$ a system can in principle show phase separation while for $B'_{crit} < 1$ this is not possible. Whether a liquid – liquid phase separation does occur, however, also depends on the total solute concentration which needs to be considered separately. This will be discussed in the subsequent paragraphs.

Phase separation in hard sphere systems

The approach described in the previous section can be used to determine the phase diagram of mixed systems where the second virial coefficients ($B'_{1,1}$, $B'_{2,2}$ and $B'_{1,2}$) are known. These can be obtained experimentally as will be discussed at a later stage. To illustrate the features of this virial theory we first consider a binary hard sphere mixture where two-particle interactions (and therefore second virial coefficients) typically describe the phase behavior of binary hard sphere systems well [44, 45]. The hard sphere model has been proven valuable to understand the phase behavior of systems containing monodisperse colloidal particles. The hard sphere approximation also applies to binary mixtures of hard spheres and polymers as long as the polymers are not much larger than the colloids [46]. An overview of theoretical and experimental results regarding hard sphere systems can be found in the relevant literature [46, 47].

Hard sphere interactions are typically modelled as either additive or non-additive [48, 49]. For so called additive hard spheres the interaction between similar spheres ($B'_{1,1}$ and $B'_{2,2}$), as well as the interaction between two different spheres ($B'_{1,2}$), are solely due to their excluded volume (equation 3.11). Non-additivity accounts for deviations of the interactions between both species ($B'_{1,2}$) relative to the value expected for the additive case, which when introduced in equation 3.11 yields

$$B'_{1,2} = \frac{16\pi N_A}{3}\left(\frac{a_1 + a_2}{2}(1+\Delta)\right)^3 \qquad 3.24$$

where Δ (≥ -1) is defined as the non-additivity parameter. The parameter Δ in equation 3.24 is the simplest possible way to account for a non-ideal behavior where the physical reasons behind non-ideal behavior are not known. For Δ = 0 equation 3.24 reduces to equation 3.11 which represents the additive hard sphere case. In binary hard sphere mixtures phase separation is based on the depletion of the smaller particles away from the larger particles. Because in hard sphere mixtures all second virial coefficients can be calculated using equation 3.24 we can use the route outlined in the previous section to predict phase behavior. Alternatively one could use depletion theory [46] to derive the interaction potential and from the interaction potential the second virial coefficient.

Phase separation via depletion in binary hard sphere mixtures depends on the size ratio q of the two spheres:

$$q = \frac{a_1}{a_2} \qquad 3.25$$

Where a_1 and a_2 are the radii of the two spheres.

For binary additive hard sphere mixtures B_{crit} (see equation 3.23) can be expressed in terms of q by

$$B_{crit} = \frac{\left(B'_{1,2}\right)^2}{B_{1,1}B_{2,2}} = \frac{(1+q)^6}{64q^3} \qquad 3.26$$

Figure 3.2 shows the behavior of B_{crit} as a function of the size ratio q together with the total critical volume fraction (obtained from equations 3.22 with $\Phi_{c,i} = B'_{i,i}c_i/4$ where i = 1,2 refers to spheres 1 and 2 respectively). The critical volume fraction Φ_{crit} is defined as the total volume fraction of spheres at the critical point ($\Phi_{crit} = \Phi_{c,1} + \Phi_{c,2}$ with $\Phi_{c,1}$ and $\Phi_{c,2}$ the volume fractions of particle 1 and 2 at the critical point). Because the hard spheres only differ in size, Figure 3.2 is symmetrical around q = 1. At q = 1 where the spheres are equally sized we have B_{crit} = 1, indicating the absence of liquid - liquid phase separation. Since spheres only interact via their excluded volume, the q = 1 case corresponds to a system consisting of monodisperse hard spheres. Here indeed, no liquid – liquid phase transition was predicted, but only a liquid – solid phase transition [47]. For unequally sized hard spheres where $q \neq 1$ we find that $B_{crit} > 1$, indicating the possibility of liquid – liquid phase separation at sufficiently high volume fraction. The critical volume fraction (Φ_{crit}) needed for a liquid – liquid phase transition is around Φ_{crit} = 0.3 for either $q << 1$ or $q >> 1$. The critical volume fraction Φ_{crit} seems to show two shallow minima close to q = 10 and q = 0.1 and diverges when approaching q = 1.

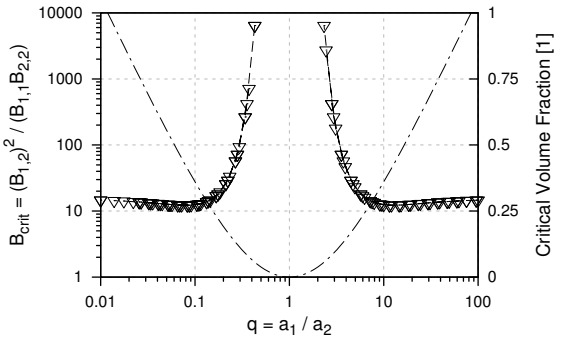

Figure 3.2 Behavior of B_{crit} (indicated by interrupted line, left vertical axis) and the critical volume fraction Φ_{crit} (▽, right vertical axis) as a function of sphere size ratio q.

Until now we have only considered additive hard spheres. In practice most systems show non-additivity, which changes their phase behavior [48]. We have determined the location of the critical point for binary hard sphere systems with varying non-additivity (Δ) over a range of size ratios q (from 10^{-3} to 10^{3}), which is shown in Figure 3.3. The q values for the case Δ = 0.2 are shown on a separate axis inside the plotting area in Figure 3.3. The

graph is symmetrical relative to the line $\Phi_{c,1} = \Phi_{c,2}$ where the points for $q < 1$ lie above and those for $q > 1$ lie below this diagonal line. The q-values for other Δ values change similarly where $q = 1$ lies on the line $\Phi_{c,1} = \Phi_{c,2}$.

For $\Delta < 0$ the range of q-values where no phase separation is found widens (larger diagonal distance between the line $\Phi_{c,1} = \Phi_{c,2}$ and the critical point values). The condition $\Delta < 0$ corresponds to a decrease in second cross virial coefficient compared to the purely additive case. The larger q-range where no phase separation is found (gap between diagonal and critical points) is a good measure for a higher compatibility of binary hard spheres in this case ($\Delta < 0$).

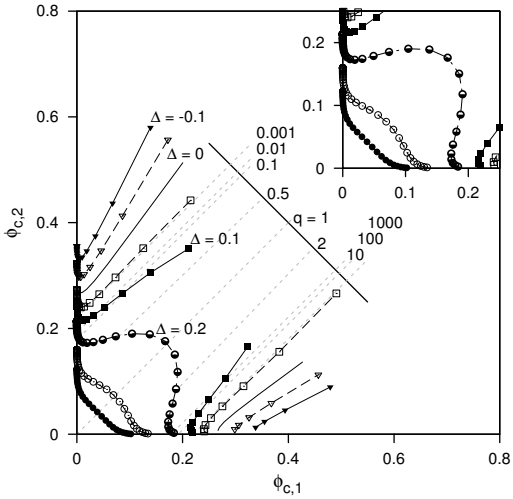

Figure 3.3 Location of the critical point (equations 3.22) for binary mixtures of additive and non-additive hard spheres at varying q-values (10^{-3} to 10^{3}). Axis show the volume fraction of particles at the critical point ($\Phi_{c,1}$ and $\Phi_{c,2}$). The inset is an enlarged view at low volume fractions. Solid line without points represents additive hard spheres with Δ = 0 at varying size ratio q. Binary hard sphere systems with a negative non-additivity parameter Δ are indicated with triangles (▼ for Δ = -0.1 and ▽ for Δ = -0.05). Binary hard sphere systems with a positive non – additivity parameter Δ are indicated by squares and dots (Δ = 0.05 (□), Δ = 0.1 (■), Δ = 0.2 (◒), Δ = 0.4 (○) and Δ = 0.6 (●)). The change in q for Δ = 0.2 is indicated by an additional axis in the graph area. For other Δ values q changes correspondingly.

With increasing positive Δ the location of the critical point shifts to lower volume fraction at given q-values (indicated by dashed lines with labelled q-values). Above Δ = 0.2, phase separation is also observed at q – values closer to 1 (closer to the diagonal). Both observations show the decreasing compatibility of hard spheres with increasing Δ which leads to phase separation at lower volume fraction and lower q-values. Δ > 0 corresponds

to a situation with increased repulsion compared to the additive hard sphere case. It corresponds to cases such as electrostatic repulsion between the two different types of hard spheres or non-spherical shapes which are both known to reduce compatibility of colloidal particles.

Results show that the virial expansion theory including up to the second virial coefficients is capable to predict phase separation in binary hard sphere mixtures. Results are comparable to approaches such as e.g. Monte Carlo simulations of non-additive hard spheres where e.g. $\Delta \approx 0.2$ as critical non-additivity factor for liquid – liquid phase separation has been obtained (at q = 1) [50, 51]. Figure 3.4 shows the phase diagrams for systems with $q = 1$ at different non-additivity parameters. At $\Delta = 0.2$ liquid – liquid phase separation is in fact predicted at reasonably low total volume fraction ($\Phi_{crit} \sim 0.4$) for phase separation to be observable in practice. Of course, since we do not consider possible solid-liquid phase separation in this model, the liquid-liquid phase separation might be meta-stable relative to the liquid-solid transition.

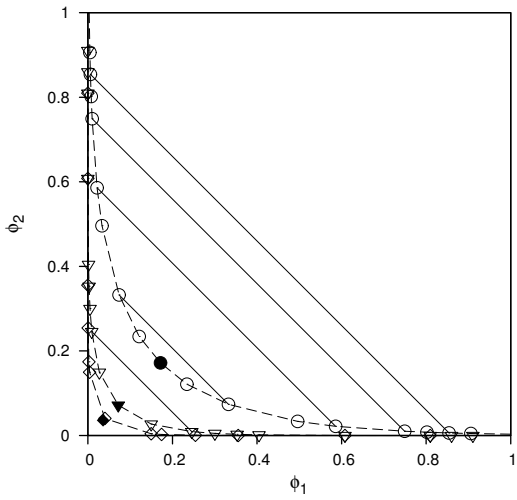

Figure 3.4 Calculated binodals (dashed lines) and critical points (filled dots (●)) for equally sized binary hard sphere mixtures ($q = 1$) as a function of the particle volume fraction Φ_1 and Φ_2 at varying non-additivity $\Delta = 0.2$ (○), $\Delta = 0.4$ (▽) and $\Delta = 0.6$ (◇). Some of the tie lines are indicated by solid lines.

Material and Methods

Materials used in this chapter have been described and characterized in detail in chapter 2 which also contains more details about the osmometry measurements. Whey protein isolate (WPI) was purchased from Davisco Foods international Inc. (Le Sueur, MN, USA). Gelatin samples were provided by Rousselot BVBA (Gent, Belgium). Dextran (Dextran from Leuconostoc spp. M_r ~100 kDa) was obtained from Sigma Aldrich (Steinheim, Germany). All materials except dextran were used without further purification. Dextran was dialyzed and freeze dried before use to remove low molecular weight fractions (details see Material and Methods section in chapter 2).

Whey protein aggregates (WPA) were prepared by heating a 4% or 6% w/w WPI solution (20 mM MOPS buffer pH 6.8 with an ionic strength of 3 mM) at 95 °C for 30 minutes which lead to differently sized aggregates (characterized in chapter 2). The aggregate solutions were then adjusted to the desired ionic strength for the measurement and from this point onwards treated identically to the protein stock solutions. The protein or dextran stock solutions were prepared by initially dissolving proteins or dextran in MOPS buffer (20 mM pH 6.8) at the desired ionic strength (adjusted by adding NaCl). Ionic strength (I) was calculated using

$$I = \frac{1}{2}\sum_i c_i {z_1}^2 \qquad 3.27$$

where *c* is the concentration of ion *i* in mol / kg_{water} and *z* the corresponding charge.

Gelatin stock solutions were heated for 1 hour at 60 °C until dissolved. WPI and dextran stock solutions were stirred at room temperature until dissolved. Stock solutions were then stored at 4 °C overnight. Before sample preparation stock solutions were heated to 40 °C. Stock solutions were then mixed to obtain samples with different polymer ratios. From these samples a dilution series was prepared using MOPS buffer with the desired ionic strength. In this way samples inside one dilution series were identical in their ionic strength and polymer ratio while differing in total polymer concentration. Measurements were performed at polymer concentrations between 0.2% and 4% w/w so that the osmotic pressure was between 10^2 and 10^5 Pa.

Osmometry measurements were performed at 40 °C using a 090 membrane osmometer from Gonotec GmbH (Berlin, Germany) equipped with a 10 kDa cellulose-triacetate membrane. To calculate the second cross virial coefficient ($B'_{1,2}$), osmotic pressure data for different polymer ratios were fitted simultaneously to equation 3.4 (truncated after the second coefficient) using one $A'_{1,2}$ value for all polymer ratios. The average molecular

weight ($\overline{M}_w$) was used as a variable in these fitting procedures to allow a comparison thereof with the expected value as calculated via equation 3.6. All calculations were performed in MsExcel 2010 with the exception of solving the set of equations 3.14 to 3.22 which was performed using MatLab® 2013a.

To obtain phase diagrams, samples were prepared in 96 well plates (200 µl per well). The complete range of experimentally accessible concentrations was obtained by first mixing stock solutions in different mixing ratios and then diluting these samples further. Phase separation was detected by visually analyzing the sample for changes in turbidity. Visual observation was shown to be more accurate than the measurement of transmission which was influenced by the unavoidable formation of small, highly stable air bubbles on top of the samples during pipetting.

Results and Discussion

Gelatin A / Dextran model system

The reduced osmotic pressure of gelatin type A / dextran mixtures at three different polymer ratios is shown in Figure 3.5A. The value for the cross coefficient $A'_{1,2}$ and the apparent average molecular weight $\bar{M}_n$ was obtained by fitting the reduced osmotic pressure to equation 3.4. The coefficients $A'_{1,1}$ and $A'_{2,2}$ and the molecular weights $M_{n,1}$ and $M_{n,2}$ were obtained from osmometry measurements of the single components of the mixture ($w_1 = 1$ or $w_2 = 1$) as determined in chapter 2. One single value for $A'_{1,2}$ gave a good fit for all three polymer ratios. Figure 3.5B shows the apparent average molecular weight ($\bar{M}_n$) (black dots) as obtained by fitting the experimental results to equation 3.4, together with the value of $\bar{M}_n$ as determined from equation 3.6 (open circles). Given the good correspondence in Figure 3.5B between the two sets of data points, it can be concluded that aggregation or dissociation of the biopolymers did not occur upon mixing.

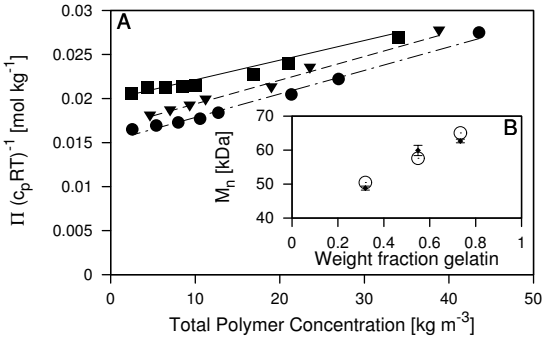

Figure 3.5 Graph A: Reduced osmotic pressure of dextran / gelatin type A mixtures at three different weight fractions (gelatin weight fraction 0.31 ■, 0.54 ▼ and 0.73 ●) at ionic strength 100 mM as a function of total polymer weight concentration. The lines are fits to the data using equation 3.4. Graph B: Experimental results for the average molecular weight $\bar{M}_n$ values (indicated by black dot with error bars) and theoretically expected values via equation 3.6 (O) as a function of the weight fraction of gelatin in the mixture.

Gelatin and dextran are well-known for their liquid-liquid phase separation at relatively low concentrations [52-54]. It is therefore expected that the phase separation can be described using the earlier described virial theory where only pairwise interactions are considered. Figure 3.6 shows the phase diagram for a gelatin type A / dextran mixture obtained at 40 °C. The phase diagram was calculated using equations 3.14 to 3.22 and the second virial coefficients from osmometry (Table 3.1). The phase diagram shows the binodal, spinodal, the critical point and the tie lines. The experimental data is also included and was obtained earlier by Edelman et al. (2003) [52]. Given the proximity of

the calculated and experimental data we conclude that the above virial theory is capable to predict the liquid-liquid phase transitions for this system.

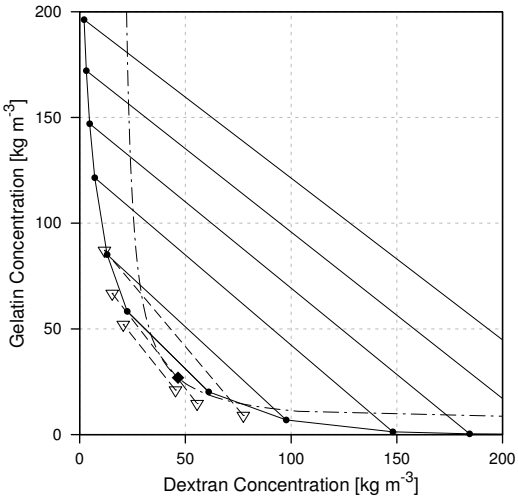

Figure 3.6 Calculated phase diagram of dextran / gelatin type A at 40 °C with the binodal including the tie lines (solid curve and lines), spinodal (interrupted line) and critical point (◆). Second virial coefficients are $B'_{1,1(Gelatin)}$ = 1.28 m³ / mol, $B'_{2,2(Dextran)}$ = 0.12 m³ / mol and $B'_{1,2}$ = 1.27 m³ / mol, molecular weights are given in Table 3.1. Experimental data (▽) was obtained from Edelman et al. (2003) [52]

Gelatin / WPI

We have also determined the second cross virial coefficient ($B'_{1,2}$) for WPI / gelatin type A and type B mixtures. The results are listed in Table 3.1. The molecular weights M_n and second virial coefficients ($B'_{1,1}$ and $B'_{2,2}$) for WPI and gelatin (type A and type B) had already been obtained in chapter 2. For gelatins the molecular weight was found independent of ionic strength. For WPI a slight increase in molecular weight with increasing ionic strength was observed and attributed to the dimerization of β-lactoglobulin. Table 3.1 also contains the effective radii for WPI and gelatin. Radii were obtained from second virial coefficients at high ionic strength where electrostatics are screened as determined in chapter 2. For WPI and gelatin type B the second virial coefficient $B'_{1,1}$ decreases with increasing ionic strength which is based on the reduction of electrostatic repulsion due to the screening of the electrostatic double layer. For gelatin type A on the other hand the second virial coefficient B' is independent of ionic strength. Measurement conditions are close to the isoelectric point of gelatin type A where the contribution of the electrostatic interaction is minimal. Since we measured the behavior of

the second virial coefficients and molecular weights as a function of ionic strength, we are also able to determine the second cross virial coefficients as a function of ionic strength. Results are shown in Table 3.1 and Figure 3.7A and B.

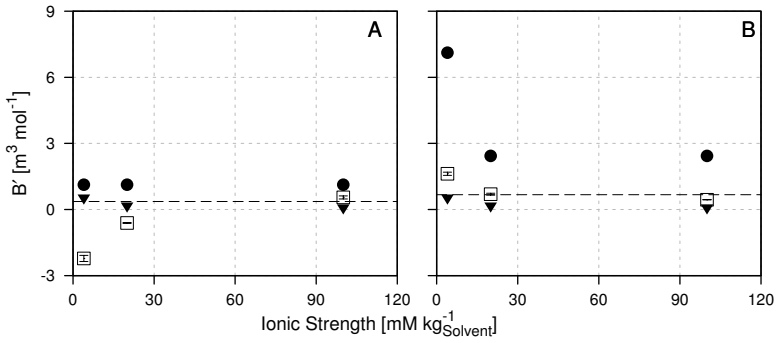

Figure 3.7 Graph A: Second virial coefficients for WPI (▼), gelatin type A (●) and their cross second virial coefficient $B'_{1,2}$ (□). Graph B: Second virial coefficients for WPI (▼), gelatin type B (●) and their cross second virial coefficient $B'_{1,2}$ (□). Dashed line (-----) represents the expected second cross virial coefficient of WPI and gelatins if they would behave as additive hard spheres (equation 3.11).

For WPI / gelatin A the second cross virial coefficient $B'_{1,2}$ is negative at low ionic strength, indicating a net attraction between the molecules. This net attraction stems from the fact that the molecules have opposite charges, as the pH of the solvent lies in between the isoelectric point of WPI and gelatin A. To estimate the strength of this attraction we have used a hard sphere model with an attractive square well potential as shown in Figure 3.8. With the width (δ) of the attractive well estimated in the order of magnitude of the Debije length (κ^{-1}) the square well depth (ε) can be calculated for the measured (negative) second cross virial coefficients. For WPI / gelatin type A at low ionic strength this leads to $\varepsilon < 0.6\ k_B T$. This attraction is not sufficient to form stable aggregates (in the form of complex coacervates). This result is supported by a good overlay between measured and predicted $\bar{M}_n$ values shown in Figure 3.9 and macroscopic observations that showed no changes in turbidity of these solutions. Addition of small amounts of salt reduced the attractive interaction between WPI and gelatin A. At an ionic strength of 100 mM the cross second virial coefficient $B'_{1,2}$ lies above the value expected for hard body interactions (cf. equation 3.11) of these proteins (Figure 3.7A).

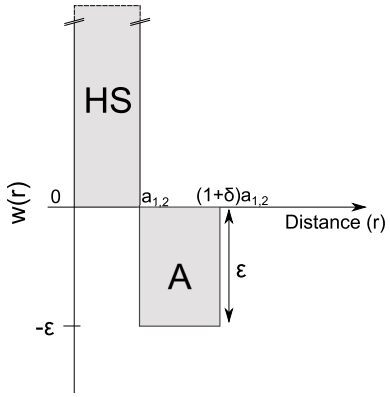

Figure 3.8 Hard sphere potential (HS) with attractive square well potential (A) for the two particle interaction. The additive radius is given by $\alpha_{1,2} = (\alpha_1+\alpha_2)/2$ where 1 and 2 refer to gelatin A and WPI

In the other mixed system (WPI / gelatin B) both proteins are negatively charged at the used solvent conditions. This is also reflected in their second cross virial coefficient $B'_{1,2}$ which is positive and lies between the values of the second virial coefficients $B'_{1,1}$ and $B'_{2,2}$ of the single systems (Figure 3.7B). The second cross virial coefficient ($B'_{1,2}$) decreases with increasing ionic strength with a similar trend as the one observed for the second virial coefficients $B'_{1,1}$ and $B'_{2,2}$.

Although the interactions between WPI and gelatin A and WPI / gelatin B (characterized by the second cross virial coefficient $B'_{1,2}$) have different signs (positive (repulsive) for gelatin B and negative (attractive) for gelatin A) in both cases increasing the ionic strength leads to a decrease in their magnitude. This behavior has been attributed in chapter 2 to the suppression of the electrostatic double layer in single protein systems. It suggests that also the interaction between WPI and gelatins are dominated by the electrostatic interactions at low ionic strength. At higher ionic strength, the $B'_{1,2}$ are close to those expected from the hard body interaction (represented by the dashed lines in Figure 3.7A and B).

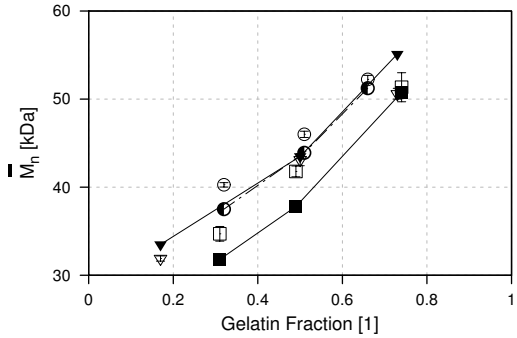

Figure 3.9 Experimental results for the average molecular weight $\bar{M}_n$ values (indicated by the open symbols) of WPI / gelatin mixtures as a function of the weight fraction of gelatin. The average molecular weight $\bar{M}_n$ was determined at an ionic strength of 3 mM (□), 20 mM (O) and 100 mM (▽). The values for the expected average molecular weight $\bar{M}_n$ as obtained from equation 3.6 are included in the graph (closed symbols with lines).

With second virial coefficients $B'_{1,1}$ and $B'_{2,2}$ and the second cross virial coefficient $B'_{1,2}$ determined for the mixed protein systems we now investigate the possible liquid – liquid phase separation in these mixtures. For mixtures where proteins only show repulsive interactions (positive second virial coefficients $B_{1,1}$, $B'_{2,2}$ and $B'_{1,2}$) phase separation can occur when B_{crit} > 1. For systems where either one of the second virial coefficients is negative this criterion is not sufficient. For WPI / gelatin A at low ionic strength where the cross virial coefficient is negative we have used equations 3.22 directly to determine whether liquid – liquid phase separation can be predicted. For the systems at 4 mM and 24 mM ionic strength there is no solution to equations 3.22 that is physically realistic, i.e. no phase separation is predicted using the above described route.

For mixtures with positive second cross virial coefficients B_{crit} is given in Table 3.1. Only for two of the measured mixtures B_{crit} was found larger than 1. The predicted critical protein concentration for WPI / gelatin type A at 100 mM ionic strength ($c_{p,WPI}$ = 130 kg / m³ and $c_{p,gelatin\ A}$ = 129 kg / m³) and WPI / gelatin B at 24 mM ionic strength ($c_{p,WPI}$ = 406 kg / m^3 and $c_{p,gelatin\ B}$ = 1072 kg / m^3) are outside the experimentally accessible concentration range, where the mixtures become too viscous to handle. From our results we conclude that no phase separation for gelatin (type A or type B) / WPI mixtures is observed, and that it also is not predicted by the described virial route within the experimentally accessible protein concentration ranges.

Table 3.1 Molecular weight M_n, second virial coefficients $B'_{1,1}$ and $B'_{2,2}$ in 20 mM MOPS buffer at pH 6.8 from chapter 2 together with the second cross virial coefficients $B'_{1,2}$ for different gelatin (A or B)/ WPI and a gelatin A / dextran mixture; (standard deviations determined from uncertainty in fit and only shown for data obtained in this chapter). Definition of symbols: ionic strength (I) ; B'_{crit} is obtained using measurement values for $B'_{1,2}$, $B'_{2,2}$ and $B'_{1,2}$ and equation 3.23; a_1 and a_2 are the number averaged molecular radii of protein 1 and 2 as given in chapter 2; q is the molecular size ratio given by equation 3.25; B_{crit} HS: the B_{crit} value expected for the protein 1 / protein 2 pair with only hard sphere interaction (using the given q value and equation 3.26).

Protein 1	**Gelatin A**			**Gelatin B**			**Gelatin A**
Protein 2	WPI						Dextran
I [mmol/kg$_{Water}$]	4	24	104	4	24	104	100
M_{n1} [kDa]	80	80	80	78	78	78	80
M_{n2} [kDa]	25	30	30	25	30	30	43
B'_{11} [m³/mol]	1.13	1.13	1.13	7.12	2.43	2.43	1.28
B'_{22} [m³/mol]	0.54	0.18	0.09	0.54	0.18	0.09	0.12
B'_{12} [m³/mol]	-2.22 ±0.14	-0.61 ±0.02	0.55 ±0.07	1.62 ±0.07	0.70 ±0.04	0.45 ±0.01	1.27 ±0.04
$B_{crit\ HS}$ [1]		1.4			1.8		1.1
B_{crit} [1]	--	--	2.81	0.69	1.11	0.87	10.48
a_1 [nm]	4.5	4.5	4.5	6	6	6	4.5
a_2 [nm]	2.2	2.2	2.2	2.2	2.2	2.2	3
q [1]	0.5	0.5	0.5	0.4	0.4	0.4	0.7

Comparison protein / protein and protein / polysaccharide systems

There is a large difference between the critical phase separation concentration of gelatin A / dextran (70 kg / m³) and gelatin / WPI mixtures (> 250 kg / m³). This poses the question for the reasons behind this difference. When comparing the second virial coefficients $B'_{1,1}$ and $B'_{2,2}$ and the radius for WPI and dextran molecules, no large differences could be observed (Table 3.1). The differences in phase behavior must therefore be attributed to the difference in the cross interaction (second cross virial coefficient $B'_{1,2}$).

We have added to Table 3.1 the B_{crit} value as it would be expected from the hard body interaction (called $B_{crit\ HS}$) which relates to the additive hard sphere situation based on the molecular size of the proteins. For gelatin / WPI mixtures the measured B_{crit} is always below this value expected for hard spheres. Within the non-additive hard sphere model this would correspond to a slightly negative non-additivity parameter Δ for WPI / gelatin mixtures. For the dextran / gelatin A mixture the measured B_{crit} is about 10 times above $B_{crit\ HS}$ which corresponds to a strongly positive non-additivity parameter ($\Delta \approx 1.7$). Non-additivity can be related to several properties such as e.g. chemical incompatibility or non-spherical shape and the exact source thereof cannot be answered using only information on the second virial coefficients. However, we can conclude that the difference in phase behavior between dextran / gelatin and WPI / gelatin mixtures can be attributed to their difference in the second cross-virial coefficient $B'_{1,2}$.

Gelatin A / Whey protein aggregates

Aggregation of proteins has been reported to significantly increase their incompatibility with other proteins and also polysaccharides [34, 35]. While it seems reasonable to assume that this is mainly based on the larger excluded volume of aggregates compared to single proteins it might also be due to changes in the particle – particle interaction. We have measured the cross second virial coefficients of gelatin A with whey protein aggregates (abbreviated as WPA) of varying size. These aggregates were obtained by varying the WPI protein concentration during aggregation. Aggregates prepared at identical conditions are expected to have similar internal and surface properties, and similar shape, and mainly vary in their size. Their interactions with other components are therefore assumed to be dependent on size only. The results are shown in Table 3.2 and Figure 3.10.

Table 3.2 Molecular weight M_n, second virial coefficient ; $B'_{1,1}$ and $B'_{2,2}$ (from chapter 2) together with the interaction coefficients for different gelatin / whey protein aggregate (WPA) mixtures; (standard deviations determined from uncertainty in fit) Definition of symbols: Ionic strength (I); a_1 and a_2 are the number averaged molecular radii of protein 1 and 2 as given in chapter 2; q the molecular size ratio given by equation 3.25; $B'_{1,2\ HS}$: the $B'_{1,2}$ value expected for the protein 1 / protein 2 pair with only hard sphere interaction (using the given q value and equation 3.26)

Protein 1	**Gelatin A**	**Gelatin A**	**Gelatin A**	**Gelatin A**	**Gelatin A**
Protein 2	WPA 6%	WPA 6%	WPA 6%	WPA 4%	WPA 4%
I [mmol/kg$_{water}$]	4	29	104	4	29
M_{n1} [kDa]	80				
M_{n2} [kDa]	292			194	
$B'_{1,1}$ [m³ mol^{-1}]	1.13				
$B'_{2,2}$ [m³ mol^{-1}]	9.39	3.16	0.62	4.23	1.51
$B'_{1,2}$ [m³ mol^{-1}]	-1.76 ±0.11	-0.48 ±0.14	0.01 ±0.003	-2.07 ±0.56	-0.36 ±0.09
$B'_{1,2\ HS}$ [m³ mol$_{-1}$]	2.23			0.89	
a_1 [nm]	4.5				
a_2 [nm]	7.6			4.4	
q	1.69			0.98	

Table 3.2 and Figure 3.10 also contain the number averaged molecular weight and the second virial coefficients for WPA from chapter 2. In comparison to WPI (Table 3.1) the molecular weight and second virial coefficient $B'_{1,1}$ of WPA increased more than 10 fold (see Figure 3.10B). As a result, the size ratio q with regard to gelatin type A also changed. For WPI the molecular weight and second virial coefficient $B'_{1,1}$ was below that of gelatin A. For WPA the molecular weight and second virial coefficients $B'_{1,1}$ are higher than those obtained for gelatin type A.

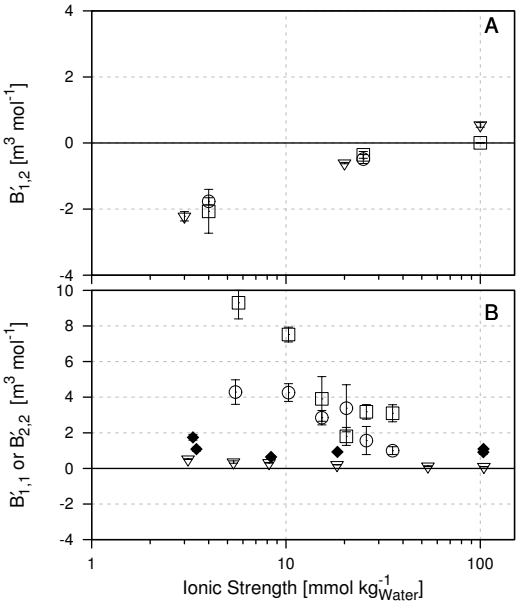

Figure 3.10 Graph A: Cross second virial coefficient ($B'_{1,2}$) for gelatin A / WPI (▽) and gelatin A / WPA (prepared at 4 % (○) or 6% (□) protein content) as a function of ionic strength. Graph B: Second virial coefficients ($B'_{1,1}$ or $B'_{2,2}$) for single systems from chapter 2 for WPI (▽), gelatin A (◆) and WPA prepared at 6% (□) and 4% (○) protein content

The experimentally obtained second cross virial coefficient $B'_{1,2}$ between WPA and gelatin A are shown in Table 3.2. At low ionic strength, a negative $B'_{1,2}$ was found for the gelatin A / WPA interaction. With increasing ionic strength the attraction reduces and at an ionic strength of 100 mM the second cross virial coefficient was close to zero (see Figure 3.10A). This behavior was likewise found for WPI / gelatin A mixtures which is also shown in Figure 3.10A. At low ionic strength the $B'_{1,2}$ values for WPI and WPA are identical. Here the molecular interactions appear to be dominated by the electrostatic

attraction. The contribution of the hard sphere repulsion to the second cross virial coefficient seems negligible as no difference was observed between the differently sized WPI and WPA. At an ionic strength of 100 mM the contribution of electrostatic interactions to $B'_{1,2}$ to the attraction is significantly reduced. For WPA / gelatin A the measured $B'_{1,2}$ value at 100 mM ionic strength is slightly positive but below the value expected from the molecular size of WPA and gelatin A. Expressed in terms of the non-additive hard sphere model this would correspond to a negative non-additivity parameter Δ suggesting high co-solubility of gelatin A and WPA.

The phase diagram for WPA / gelatin A mixtures at 100 mM is shown in Figure 3.11. No phase separation was observed over the whole range of experimentally accessible protein concentrations which is in line with the high co-solubility predicted by the negative non-additivity parameter Δ.

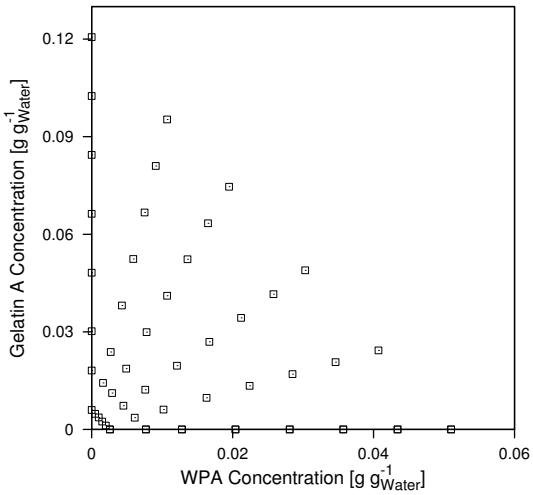

Figure 3.11 Phase diagram of gelatin A / WPA determined at 40 °C, where gelatin A is still liquid. The symbols (□) indicate the prepared samples. All samples remained clear and no sign of phase separation could be observed.

Conclusion

We have shown that using the virial expansion approach up to the second virial coefficient allows the prediction of a liquid – liquid phase separation for binary hard sphere mixtures. For the theoretical case of additive and non-additive hard sphere mixtures this approach was successfully applied to identify the possibility of phase separation as a function of the particle size ratio (q) and non-additivity parameter (Δ).

The considerations for the non-additive hard sphere model could also be used to explain the presence (gelatin / dextran) or absence of phase separation in mixed protein systems. Using experimental results for the second virial coefficients ($B'_{1,1}$, $B'_{2,2}$ and $B'_{1,2}$) the phase diagram of dextran / gelatin could be successfully predicted. The occurrence of phase separation was attributed to the non-additivity of the biopolymers. For protein / protein mixtures their high compatibility could be attributed to their similar sizes (q close to 1) and to the fact that second cross virial coefficients remained typically below those for additive hard spheres. The values for second cross virial coefficients remained low even after aggregation of one of the proteins (WPI), explaining the remaining high compatibility of the protein aggregates with the other protein.

Supporting Information

Numeric data of virial coefficients and raw osmotic pressure data are published in the supporting information of the publication related to this chapter.

Acknowledgements

We would like to thank Lennart L.C. Meijvogel for the help with the osmometry measurements.

References

1. Tolstoguzov, V., *Some thermodynamic considerations in food formulation.* Food Hydrocolloids, 2003. **17**(1): p. 1-23.
2. Wanka, J. and W. Peukert, *Optimized Production of Protein Crystals: From 1D Crystallization Slot towards 2D Supersaturation B22 Diagram.* Chemical Engineering & Technology, 2011. **34**(4): p. 510-516.
3. Vilker, V.L., C.K. Colton, and K.A. Smith, *The osmotic pressure of concentrated protein solutions: Effect of concentration and ph in saline solutions of bovine serum albumin.* Journal of Colloid and Interface Science, 1981. **79**(2): p. 548-566.
4. Moon, Y.U., R.A. Curtis, C.O. Anderson, H.W. Blanch, and J.M. Prausnitz, *Protein-protein interactions in aqueous ammonium sulfate solutions. Lysozyme and bovine serum albumin (BSA).* Journal of Solution Chemistry, 2000. **29**(8): p. 699-717.
5. Moon, Y.U., C.O. Anderson, H.W. Blanch, and J.M. Prausnitz, *Osmotic pressures and second virial coefficients for aqueous saline solutions of lysozyme.* Fluid Phase Equilibria, 2000. **168**(2): p. 229-239.
6. Park, Y. and G. Choi, *Effects of pH, salt type, and ionic strength on the second virial coefficients of aqueous bovine serum albumin solutions.* Korean Journal of Chemical Engineering, 2009. **26**(1): p. 193-198.
7. Lu, Y., D.-J. Chen, G.-K. Wang, and C.-L. Yan, *Study of Interactions of Bovine Serum Albumin in Aqueous (NH4)2SO4 Solution at 25 °C by Osmotic Pressure Measurements.* Journal of Chemical & Engineering Data, 2009. **54**(7): p. 1975-1980.
8. Le Brun, V., W. Friess, T. Schultz-Fademrecht, S. Muehlau, and P. Garidel, *Lysozyme-lysozyme self-interactions as assessed by the osmotic second virial coefficient: Impact for physical protein stabilization.* Biotechnology Journal, 2009. **4**(9): p. 1305-1319.
9. Mehta, C.M., E.T. White, and J.D. Litster, *Correlation of second virial coefficient with solubility for proteins in salt solutions.* Biotechnology Progress, 2012. **28**(1): p. 163-170.
10. Bonneté, F., S. Finet, and A. Tardieu, *Second virial coefficient: Variations with lysozyme crystallization conditions.* Journal of Crystal Growth 1999. **196**(2-4): p. 403-414.
11. Guo, B., S. Kao, H. McDonald, A. Asanov, L.L. Combs, and W. William Wilson, *Correlation of second virial coefficients and solubilities useful in protein crystal growth.* Journal of Crystal Growth, 1999. **196**(2–4): p. 424-433.
12. Kulkarni, A.M., A.P. Chatterjee, K.S. Schweizer, and C.F. Zukoski, *Effects of polyethylene glycol on protein interactions.* The Journal of Chemical Physics, 2000. **113**(21): p. 9863-9873.

13. Schaink, H.M. and J.A.M. Smit, *Determination of the osmotic second virial coefficient and the dimerization of β-lactoglobulin in aqueous solutions with added salt at the isoelectric point.* Physical Chemistry Chemical Physics, 2000. **2**(7): p. 1537-1541.
14. Schaink, H.M. and J.A.M. Smit, *Protein–polysaccharide interactions: The determination of the osmotic second virial coefficients in aqueous solutions of β-lactoglobulin and dextran.* Food Hydrocolloids, 2007. **21**(8): p. 1389-1396.
15. Hasse, H., H.P. Kany, R. Tintinger, and G. Maurer, *Osmotic Virial Coefficients of Aqueous Poly(ethylene glycol) from Laser-Light Scattering and Isopiestic Measurements.* Macromolecules, 1995. **28**(10): p. 3540-3552.
16. Edmond, E. and A.G. Ogston, *An approach to the study of phase separation in ternary aqueous systems.* Biochemical Journal, 1968. **109**(4): p. 569-576.
17. Kang, C.H. and S.I. Sandler, *Phase behavior of aqueous two-polymer systems.* Fluid Phase Equilibria, 1987. **38**(3): p. 245-272.
18. Semenova, M.G. and L.B. Savilova, *The role of biopolymer structure in interactions between unlike biopolymers in aqueous medium.* Food Hydrocolloids, 1998. **12**(1): p. 65-75.
19. Bloustine, J.D., *Experimental Investigations into Interactions and Collective Behavior in Protein/Polymer Mixtures and Granular Rods*, in *The Faculty of the Graduate School of Arts and Sicences*. 2005, Brandeis University. p. 120.
20. Ruis, H.G.M., *Structure-rheology relations in sodium caseinate containing systems*, in *Physics and Physical Chemistry of Foods*. 2007, Wageningen University. p. 121.
21. McCarty, B.W. and E.T. Adams Jr, *Osmotic pressure measurements of ovalbumin and lysozyme mixtures.* Biophysical Chemistry, 1987. **28**(2): p. 149-159.
22. Baussay, K., C.L. Bon, T. Nicolai, D. Durand, and J.-P. Busnel, *Influence of the ionic strength on the heat-induced aggregation of the globular protein β-lactoglobulin at pH 7.* International Journal of Biological Macromolecules, 2004. **34**(1–2): p. 21-28.
23. Wilson, W., *Light scattering as a diagnostic for protein crystal growth—A practical approach.* Journal of Structural Biology, 2003. **142**(1): p. 56-65.
24. Rosenbaum, D., P.C. Zamora, and C.F. Zukoski, *Phase Behavior of Small Attractive Colloidal Particles.* Physical Review Letters, 1996. **76**(1): p. 150-153.
25. Muschol, M. and F. Rosenberger, *Interactions in undersaturated and supersaturated lysozyme solutions: Static and dynamic light scattering results.* The Journal of Chemical Physics, 1995. **103**(24): p. 10424-10432.
26. Rosenbaum, D.F., A. Kulkarni, S. Ramakrishnan, and C.F. Zukoski, *Protein interactions and phase behavior: Sensitivity to the form of the pair potential.* The Journal of Chemical Physics, 1999. **111**(21): p. 9882-9890.

27. Ducruix, A., J.P. Guilloteau, M. Riès-Kautta, and A. Tardieu, *Protein interactions as seen by solution X-ray scattering prior to crystallogenesis.* Journal of Crystal Growth, 1996. **168**(1-4): p. 28-39.
28. Velev, O.D., E.W. Kaler, and A.M. Lenhoff, *Protein Interactions in Solution Characterized by Light and Neutron Scattering: Comparison of Lysozyme and Chymotrypsinogen.* Biophysical Journal, 1998. **75**(6): p. 2682-2697.
29. Malo de Molina, P., M.-S. Appavou, and M. Gradzielski, *Oil-in-water microemulsion droplets of TDMAO/decane interconnected by the telechelic C18-EO150-C18: clustering and network formation.* Soft Matter, 2014. **10**(28): p. 5072-5084.
30. Ahamed, T., M. Ottens, G.W.K. van Dedem, and L.A.M. van der Wielen, *Design of self-interaction chromatography as an analytical tool for predicting protein phase behavior.* Journal of Chromatography A, 2005. **1089**(1–2): p. 111-124.
31. Mc Bride, D.W. and V.G.J. Rodgers, *Obtaining protein solvent accessible surface area when structural data is unavailable using osmotic pressure.* AIChE Journal, 2012. **58**(4): p. 1012-1017.
32. Yousef, M.A., R. Datta, and V.G.J. Rodgers, *Understanding Nonidealities of the Osmotic Pressure of Concentrated Bovine Serum Albumin.* Journal of Colloid and Interface Science, 1998. **207**(2): p. 273-282.
33. Ersch, C., L.M. Meijvogel, E. van der Linden, A.H. Martin, and P. Venema, *Interactions in protein Mixtures. Part I: Second Virial Coefficients from Osmometry.* Food Hydrocolloids, 2015. **(Submitted)**
34. Polyakov, V.I., V.Y. Grinberg, and V.B. Tolstoguzov, *Thermodynamic incompatibility of proteins.* Food Hydrocolloids, 1997. **11**(2): p. 171-180.
35. Fitzsimons, S.M., D.M. Mulvihill, and E.R. Morris, *Segregative interactions between gelatin and polymerised whey protein.* Food Hydrocolloids, 2008. **22**(3): p. 485-491.
36. Tuinier, R., J.K.G. Dhont, and C.G. De Kruif, *Depletion-induced phase separation of aggregated whey protein colloids by an exocellular polysaccharide.* Langmuir, 2000. **16**(4): p. 1497-1507.
37. McMillan, W.G. and J.E. Mayer, *The Statistical Thermodynamics of Multicomponent Systems.* The Journal of Chemical Physics, 1945. **13**(7): p. 276-305.
38. Keller, J.B. and B. Zumino, *Determination of Intermolecular Potentials from Thermodynamic Data and the Law of Corresponding States.* The Journal of Chemical Physics, 1959. **30**(5): p. 1351-1353.
39. Simonet, F., C. Garnier, and J.L. Doublier, *Description of the thermodynamic incompatibility of the guar–dextran aqueous two-phase system by light scattering.* Carbohydrate Polymers, 2002. **47**(4): p. 313-321.

40. Antonov, Y.A., J. Lefebvre, and J.-L. Doublier, *On the one-phase state of aqueous protein-uncharged polymer systems: Casein-guar gum system.* Journal of Applied Polymer Science, 1999. **71**(3): p. 471-482.
41. Ermakova, A. and V.I. Anikeev, *Calculation of spinodal line and critical point of a mixture.* Theoretical Foundations of Chemical Engineering 2000. **34**(1): p. 51-58.
42. Gibbs, J.W., H.A. Bumstead, and R.G. Van Name, *Scientific Papers of J. Willard Gibbs ...: Thermodynamics*. 1906: Longmans, Green and Company.
43. Gibbs, J.W., H.A. Bumstead, and R.G. Van Name, *Scientific Papers of J. Willard Gibbs*. 1906: Longmans, Green and Company.
44. Dijkstra, M., R. van Roij, and R. Evans, *Phase diagram of highly asymmetric binary hard-sphere mixtures.* Physical Review E, 1999. **59**(5): p. 5744-5771.
45. Bolhuis, P.G., E.J. Meijer, and A.A. Louis, *Colloid-Polymer Mixtures in the Protein Limit.* Physical Review Letters, 2003. **90**(6): p. 068304.
46. Lekkerkerker, H.N.W. and R. Tuinier, *Colloids and the Depletion Interaction*. Lecture Notes in Physics 2011: Springer Science+Business Media B.V.
47. Barrio, C. and J.R. Solana, *Binary mixtures of additive hard spheres. Simulations and theories*, in *Lecture Notes in Physics*. 2008. p. 133-182.
48. Hopkins, P. and M. Schmidt, *Binary non-additive hard sphere mixtures: Fluid demixing, asymptotic decay of correlations and free fluid interfaces.* Theoretical Foundations of Chemical Engineering 2010. **22**(32).
49. Sillrén, P. and J.-P. Hansen, *On the critical non-additivity driving segregation of asymmetric binary hard sphere fluids.* Molecular Physics, 2010. **108**(1): p. 97-104.
50. Tenne, R. and E. Bergmann, *Scaled particle theory for nonadditive hard spheres: Solutions for general positive nonadditivity.* Physical Review A, 1978. **17**(6): p. 2036-2045.
51. Jagannathan, K. and A. Yethiraj, *Monte Carlo simulations for the phase behavior of symmetric nonadditive hard sphere mixtures.* The Journal of Chemical Physics, 2003. **118**(17): p. 7907-7911.
52. Edelman, M.W., R.H. Tromp, and E. van der Linden, *Phase-separation-induced fractionation in molar mass in aqueous mixtures of gelatin and dextran.* Physical Review E - Statistical, Nonlinear, and Soft Matter Physics, 2003. **67**(2 1): p. 214041-2140411.
53. Edelman, M.W., E. Van der Linden, E. De Hoog, and R.H. Tromp, *Compatibility of gelatin and dextran in aqueous solution.* Biomacromolecules, 2001. **2**(4): p. 1148-1154.

54. Edelman, M.W., E. Van Der Linden, and R.H. Tromp, *Phase separation of aqueous mixtures of poly(ethylene oxide) and dextran.* Macromolecules, 2003. **36**(20): p. 7783-7790.

Appendix to Chapter 3

Binodal

In the theory section we have discussed that the set of equations (equations 3.14) with four unknowns (c_1^I,c_2^I , c_1^{II}, c_2^{II}) can be solved iteratively by choosing one of the three variables and computing the other three. Here we would like to extend this set of equations to obtain 5 equations with 5 unknowns. Using this set of equations has the advantage that it uses the polymer concentration of the two polymers as input parameters which in an experimental setup are known.

We start from the conservation of mass in the system

$$n = {n_1}^I + {n_1}^{II} + {n_2}^I + {n_2}^{II} \qquad 3.28$$

Where *n* is the number of molecules, subscripts refer to polymers 1 and 2 and roman numbers to the two phases. Since also the volume of the system does not change we can write

$$V = V^I + V^{II} \qquad 3.29$$

With the concentration of the two components in the two phases given by

$${c_1}^I = \frac{{n_1}^I}{V^I} \qquad {c_1}^{II} = \frac{{n_1}^{II}}{V^{II}} \qquad {c_2}^I = \frac{{n_2}^I}{V^I} \qquad {c_2}^{II} = \frac{{n_2}^{II}}{V^{II}} \qquad 3.30$$

The total polymer concentration can be expressed by

$$c = c_1 + c_2 = \frac{n_1 + n_2}{V} = \frac{{n_1}^I + {n_1}^{II} + {n_2}^I + {n_2}^{II}}{V^I + V^{II}} \qquad 3.31$$

Which can be simplified

$$c = \frac{{n_1}^I}{V^I + V^{II}} + \frac{{n_1}^{II}}{V^I + V^{II}} + \frac{{n_2}^I}{V^I + V^{II}} + \frac{{n_2}^{II}}{V^I + V^{II}} = \frac{V^I}{V^I + V^{II}}\left(\frac{{n_1}^I + {n_2}^I}{V^I}\right) + \frac{V^{II}}{V^I + V^{II}}\left(\frac{{n_1}^{II} + {n_2}^{II}}{V^{II}}\right) \qquad 3.32$$

Finally leading to

$$c = c_1 + c_2 = \frac{V^I}{V^I + V^{II}}({c_1}^I + {c_2}^I) + \frac{V^{II}}{V^I + V^{II}}({c_1}^{II} + {c_2}^{II}) \qquad 3.33$$

By defining α as the volume fraction of phase I

$$\alpha = \frac{V^I}{V^I + V^{II}} \qquad 3.34$$

We arrive at

$$c = c_1 + c_2 = \alpha({c_1}^I + {c_2}^I) + (1-\alpha)({c_1}^{II} + {c_2}^{II}) \qquad 3.35$$

Which leads to

$$\begin{aligned} \alpha {c_1}^I + (1-\alpha){c_1}^{II} &= c_1 \\ \alpha {c_2}^I + (1-\alpha){c_2}^{II} &= c_2 \end{aligned} \qquad 3.36$$

Equations 3.36 together with 3.14 form a set of 5 equations with 5 unknowns. As input parameters the virial coefficients ($B'_{1,1}$, $B'_{2,2}$ and $B'_{1,2}$) and the individual polymer concentrations (c_1 and c_2) are needed. As an additional output from the optimization procedure one obtains the volume ratio α. For a set of polymers for which the virial coefficients are known this approach can be used to predict directly experimental results for the cases where the polymer concentrations are known and the ratio of the phases is easily measured.

Spinodal and critical point

We start with the condition that a mixture at the critical point fulfills equations 3.20 as given in the theory section by

$$\begin{aligned} Det(M_1) &= 0 \\ Det(M_2) &= 0 \end{aligned} \qquad 3.20$$

Where M_1 is a matrix with the partial derivates of the chemical potential for the two polymers relative to their number density given by equation 3.16 in the theory section

$$M_1 = \begin{bmatrix} \frac{\partial \mu_1}{\partial n_1} & \frac{\partial \mu_1}{\partial n_2} \\ \frac{\partial \mu_2}{\partial n_1} & \frac{\partial \mu_2}{\partial n_2} \end{bmatrix} \qquad 3.16$$

Which leads to

$$M_1 = \begin{bmatrix} \frac{1}{n_1} + \frac{2B_{1,1}}{V} & \frac{2B_{1,2}}{V} \\ \frac{2B_{1,2}}{V} & \frac{1}{n_2} + \frac{2B_{2,2}}{V} \end{bmatrix} \qquad 3.37$$

and

$$Det(M_1) = \left(\frac{1}{n_1} + \frac{2B_{1,1}}{V}\right)\left(\frac{1}{n_2} + \frac{2B_{2,2}}{V}\right) - \frac{2B_{1,2}}{V}\frac{2B_{1,2}}{V} \qquad 3.38$$

This can be further simplified and re-written in terms of the second virial coefficient and molar concentrations

$$\begin{aligned} Det(M_1) &= \left(\frac{1}{n_1} + \frac{2B_{1,1}}{V}\right)\left(\frac{1}{n_2} + \frac{2B_{2,2}}{V}\right) - \frac{4B_{1,2}^2}{V^2} = 0 \\ Det(M_1) &= \left(\frac{1}{c_1} + 2B_{1,1}\right)\left(\frac{1}{c_2} + 2B_{2,2}\right) - 4B_{1,2}^2 c_1 c_2 = 0 \\ Det(M_1) &= \left(1 + 2B_{1,1}c_1\right)\left(1 + 2B_{2,2}c_2\right) - 4B_{1,2}^2 = 0 \\ Det(M_1) &= 4\left(B_{1,1}B_{2,2} - B_{1,2}^2\right)c_1 c_2 + 2B_{1,1}c_1 + 2B_{2,2}c_2 + 1 = 0 \end{aligned} \qquad 3.39$$

Equation 3.39 can be used directly to obtain the location of the spinodal as outlined in the theory section. The matrix M_2 in equation 3.20 can be obtained by replacing any of the row vectors of M_1 by

$$\begin{bmatrix} \frac{\partial(Det(M_1))}{\partial n_1} & \frac{\partial(Det(M_1))}{\partial n_2} \end{bmatrix} \qquad 3.40$$

Where

$$\begin{aligned} \frac{\partial(Det(M_1))}{\partial n_1} &= -\left(\frac{1}{n_1^2}\right)\left(\frac{1}{n_2} + \frac{2B_{2,2}}{V}\right) \\ \frac{\partial(Det(M_1))}{\partial n_2} &= -\left(\frac{1}{n_2^2}\right)\left(\frac{1}{n_1} + \frac{2B_{1,1}}{V}\right) \end{aligned} \qquad 3.41$$

We here replace the second row in M_1 which leads to

$$M_2 = \begin{bmatrix} \frac{1}{n_1} + \frac{2B_{1,1}}{V} & \frac{2B_{1,2}}{V} \\ -\left(\frac{1}{n_1^2}\right)\left(\frac{1}{n_2} + \frac{2B_{2,2}}{V}\right) & -\left(\frac{1}{n_2^2}\right)\left(\frac{1}{n_1} + \frac{2B_{1,1}}{V}\right) \end{bmatrix} \qquad 3.42$$

and allows to evaluate the second equation in 3.20 which then can be formulated in terms of the second virial coefficients and molar concentrations via

$$Det(M_2) = -\frac{1}{n_2^2}\left(\frac{1}{n_1} + \frac{2B_{1,1}}{V}\right)^2 + \frac{1}{n_1^2}\left(\frac{1}{n_2} + \frac{2B_{2,2}}{V}\right)\left(\frac{2B_{1,2}}{V}\right) = 0$$

$$Det(M_2) = -\frac{1}{c_2^2}\left(\frac{1}{c_1} + 2B_{1,1}\right)^2 + \frac{1}{c_1^2}\left(\frac{1}{c_2} + 2B_{2,2}\right)2B_{1,2} = 0 \qquad 3.43$$

$$Det(M_2) = -\left(1 + 2B_{1,1}c_1\right)^2 + \left(1 + 2B_{2,2}c_2\right)2B_{1,2}c_2 = 0$$

$$Det(M_2) = \left(2B_{1,2}c_2\right)\left(1 + 2B_{2,2}c_2\right) - \left(1 + 2B_{1,1}c_1\right)^2 = 0$$

Which leads to a solution for equation 3.20 given by

$$Det(M_1) = 4\left(B_{1,1}B_{2,2} - B_{1,2}^2\right)c_1c_2 + 2B_{1,1}c_1 + 2B_{2,2}c_2 + 1 = 0$$

$$Det(M_2) = \left(2B_{1,2}c_2\right)\left(1 + 2B_{2,2}c_2\right) - \left(1 + 2B_{1,1}c_1\right)^2 = 0 \qquad 3.44$$

Here, c_1 and c_2 are the molar concentrations of polymer 1 and polymer 2 at the critical point that can be obtained by numerically solving equations 3.44.

CHAPTER 4

The microstructure and rheology of homogeneous and phase separated gelatin gels[3]

ABSTRACT

The gelation of gelatin in mixtures of gelatin (type A or type B) and globular proteins (Whey Protein Isolate (WPI), Whey Protein Aggregates (WPA) and Soy Protein Isolate (SPI)) was studied with a focus on their phase separation during gelation. Confocal laser scanning microscopy, visual observations and rheology were used to link the changes on a microscopic scale to macroscopic gel properties (visual appearance and gel stiffness).

An increase in storage modulus G' compared to single gelatin gels was observed for protein mixtures containing gelatin and SPI or gelatin and WPA. This could be related to segregative phase separation between proteins during gelatin gelation as detected by CLSM and visual observations. In protein mixtures without phase separation (gelatin / WPI mixtures) the storage modulus G' of the gels was the same as in pure gelatin gels. Since all protein mixtures were prepared at an ionic strength of 150 mM, where the electrostatic interactions were screened, the occurrence of phase separation was attributed to the excluded volume interaction between gelatins and globular proteins.

[3] This chapter is based on: Ersch, C., Linden, E. v. d., Venema, P., & Martin, A. H. (2015). The microstructure and rheology of homogeneous and phase separated gelatin gels. *(Submitted)*.

GRAPHICAL ABSTRACT

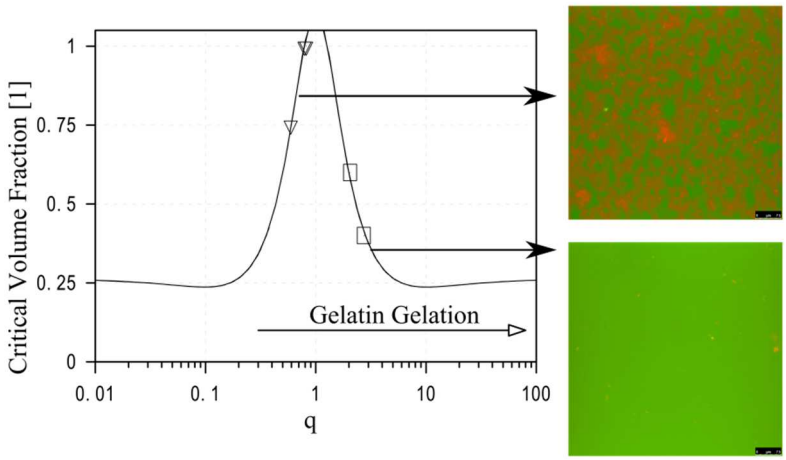

KEYWORDS

Gelatin gels, mixed gels, globular proteins, rheology, molecular size ratio, gel microstructure

Introduction

Many foods are complex multi-component mixtures of biopolymers, for example polysaccharides and proteins. Thermodynamic incompatibility, leading to phase separation, is a common phenomenon in these mixtures. In foods phase separation has a significant impact on the texture [1-5] but also taste [6-9] which can be either desirable or undesirable depending on the application. Understanding the mechanism underlying phase separation is crucial to prevent it or to use it consciously to develop products with desired properties.

Thermodynamic incompatibility leading to phase separation of biopolymers in solutions has been researched over many decades theoretically [10-13] and experimentally [14-20]. Combinations of these approaches have led to an increased understanding of driving forces behind phase separation such as e.g. depletion interactions and electrostatic interactions. These mechanisms, however, are only directly applicable for systems in solution. One example where it is typically difficult to apply these theories are biopolymer mixtures where gelation of one of the biopolymers occurs. Gelation is kinetically controlled and often combined with additional effects such as changes in solubility of the molecules or irregular shapes of the intermediate aggregates, which add complexity to the system and complicate its scientific description.

In foods the main categories of biopolymers are polysaccharides and proteins. In contrast to polysaccharide / protein mixtures [21-30], mixed gels containing two different proteins [31-38] have been given less attention in literature. Gelation in protein systems can be induced via different routes such as the reduction of the electrostatic repulsion between proteins (induced by pH change or addition of salts) or protein aggregation induced by denaturation, typically caused by heating. Many proteins share the same gelation mechanisms, which allows them to form synergistic networks, for example heat induced soy protein / whey protein isolate gels [39]. For protein mixtures where no specific interactions occur between different proteins during gelation, separate protein networks can be formed [32, 34-38] as will be discussed in more detail in chapter 6 and 7. One such system that has gained special interest over the last years is the mixture of gelatin with globular proteins. Here the globular proteins can form a gel via heat induced gelation or by applying pressure. Gelatin gels are formed when cooling the system below the helix to coil transition temperature [31, 34, 36]. In the gelatin / globular protein mixtures the two independent gelation mechanisms allow for a sequential gelation of the two protein species, i.e. the formation of globular protein gels in the presence of (non-gelling) gelatin [34, 35, 37, 38] or gelatin gelation in the presence of non-gelled or already gelled globular protein [32, 33, 36].

Here we have chosen to study gelatin / globular protein mixtures at conditions where only gelatin forms a gel. At the chosen solvent conditions (pH 7, 150 mM NaCl) globular proteins do not participate in the gel network and only influence the gel formation via non-specific interactions between gelatins and globular proteins. Earlier work on gelatin / globular protein mixtures has shown that at neutral pH 7, above the helix to coil transition temperature, gelatin (type B) is compatible (no phase separation occurs) with native and aggregated whey protein isolate and other milk proteins [31-33]. In these studies also the microstructure and rheological response of gelatin gels were not affected by the presence of native whey proteins [32, 33]. The presence of aggregated whey proteins or larger protein clusters (e.g. casein micelles) on the other hand led to phase separation during gelation and to changes in the rheological response of mixed gelatin gels [32, 33]. In this study we aim to further investigate the phase behaviour and rheological response (storage modulus) of globular protein / gelatin mixed systems during gelatin gelation at neutral pH. Different mixed systems were investigated containing either gelatin type A (isoelectric point pI = 8, M_n = 80 kDa[4]) or gelatin type B (pI = 5, M_n = 80 kDa[4]) which were mixed with whey protein isolate (WPI, pI ~ 5, M_n = 30 kDa[4]), soy protein isolate (SPI, pI ≈ 4.8, M_w glycinin = 360 kDa, β-conglycinin ~150 kDa [40]) or whey protein aggregates (pI ~5, M_n ≈ 290 kDa[4]). In combining these globular proteins with gelatin type A or B, the effect of molecular interactions (pH above the isoelectric point of both proteins or in between the isoelectric points) and different size ratios on the phase separation during gelatin gelation could be analyzed.

[4] determined in chapter 2

Material and Methods

Material

Defatted soy flour was obtained from Cargill containing ~50% w/w protein (Kjeldahl) and native soy protein isolate (SPI) was extracted using isoelectric precipitation as described in chapter 6 and reference [41]. Whey protein isolate (WPI) (product name BIPRO, 94% w/w protein) was purchased from Davisco Foods International Inc. (Le Sueur, USA, MN). Pork skin gelatin type A and type B were generously provided by Rousselot BVBA (Ghent, Belgium) having a nominal bloom strength of 290 and 260 (determined by manufacturer) and a protein content of 89.6 and 88.8 % w/w (Kjeldahl), respectively. The isoelectric point of gelatin A was around pH 8 and for gelatin B at pH 5 (determined by isoelectric focusing and QC-RLT by the manufacturer). Both gelatins had only negligible amounts of salts present (determined by ICP-AES). All other chemicals were purchased from Sigma Aldrich (Steinheim, Germany). They were of analytical grade and used without any further purification. Experiments were performed using deionized water (Merck Millipore, Darmstadt, Germany; 18.2 MΩ cm).

Sample preparation

Protein stock solutions containing WPI were prepared by dissolving protein powder in deionized water (Merck Millipore, Darmstadt, Germany) containing 150 mM NaCl at pH 7. Stock solutions were stirred at room temperature (WPI) or 60 °C (gelatins) for several hours until dissolved and subsequently stored overnight at 4 °C. Sample preparation was performed at 40 °C by diluting stock solutions with deionized water containing 150 mM NaCl to the different protein concentrations (0 – 20% w/w) at different protein ratios. Mixtures with soy protein isolate (SPI) contained 300 mM NaCl and the preparation of these samples is described in detail in chapter 6.

Whey protein aggregates (WPA) were prepared as described in chapter 2 by heating a 6% w/w WPI solution (prepared in deionized, ionic strength adjusted to 3 mM with NaCl) at 95 °C for 30 minutes. After cooling to room temperature WPA were used in the same way as WPI solutions to prepare samples.

Small deformation rheology

Samples were added in a liquid state (40 °C) to the rheometer (Anton Paar MC502, Graz, Austria) equipped with a sand-blasted cup-bob geometry (CC17). Samples were covered with paraffin oil to avoid evaporation and afterwards equilibrated at 40 °C for 10 minutes before starting the measurement. Measurements were performed at a strain of 0.5% and a frequency of 1 Hz while cooling samples from 40 °C to 15 °C at a constant rate of 5 °C/min. The storage modulus G' was recorded after 15 min at 15 °C.

Covalent labelling of gelatin

Gelatin was dissolved at 0.5% w/w in 100 mM carbonate buffer at pH 9.1. The solution was heated to 60 °C until gelatin dissolved completely and subsequently cooled to room temperature. FITC was dissolved in Dimethyl sulfoxide (DMSO) at 4 mg / ml and slowly added to the gelatin solution to a final concentration of 4 mg FITC per gram protein. The solution was stirred at room temperature in the dark for 6 hours and then dialyzed against an excess of deionized water for 3 days. The water against which the sample was dialyzed was refreshed 6 times and the samples were subsequently freeze dried. The freeze dried, FITC labelled protein was stored at 4 °C in the dark. Samples containing FITC labelled gelatin were prepared identically to the ones without covalent labelling and still gelled when cooled and melted when heated.

Confocal Laser Scanning Microscopy (CLSM)

For non-covalent staining of the protein 0.001% w/w Rhodamine B was added to the samples for CLSM. Before analysis samples were heated to 40 °C and transferred into CLSM cuvettes (Gene Frame® 125 µl, obtained from Thermo Scientific) which were sealed with a cover glass. Cuvettes were placed with the cover glass on top of a peltier element and tempered at 40 °C for 10 min. They were then cooled from 40 °C to 15 °C at 5 °C / min and kept at 15 °C for 30 min. Afterwards they were stored at 4 °C until analyzed.

CLSM images were taken using a Leica DMI6000 (Wetzlar, Germany). Imaging was performed ~5 µm from the cover glass which during sample preparation was in touch with the peltier element. Imaging was performed in the sequential mode. Rhodamine B was excited at 561 nm and the signal acquired between 570 nm and 790 nm, FITC was excited at 488 nm and the signal acquired between 500 nm and 570 nm. Images were acquired using a scanning speed of 400 Hz and two frames were average for each image. Imaging was performed at 1024 x 1024 measurement points. Several images at different magnifications and different locations in the samples were taken and shown images represent the structure found throughout the samples.

Phase diagrams

Mixtures of gelatin (type A and B) and WPA were prepared in 96 well plates. Sample preparation was done at 40 °C. Well plates were tempered at 40 °C for 1 hour after finalizing sample preparation and then placed in a water bath at 20 °C overnight. After this cooling period the occurrence of turbidity was analyzed visually.

Results and discussion

Phase behavior

Prior to gelation, protein mixtures were prepared at 40 °C where changes in visual appearance (mainly turbidity) of the solutions give an indication of possible changes occurring upon mixing. For the WPI / gelatin type A or type B mixed solutions no changes in macroscopic appearance were observed when mixing the stock solutions at 40 °C. At all studied protein concentration and ratios, the mixed protein solutions were clear with a color similar to that of WPI solutions, indicating that no phase separation occurred. These visual observations are also in line with results from osmometry where no phase separation was found for these mixed solutions in chapter 3. The same results (clear solutions upon mixing at any protein ratio and concentration) were observed for whey protein aggregates (WPA) / gelatin type A and gelatin type B solutions.

For aqueous mixtures of soy protein isolate (SPI) / gelatin A, macroscopic observations of turbidity were hindered by the high turbidity of the SPI stock solution itself. Visually, however, SPI / gelatin type A mixtures had the same turbidity as SPI. To confirm that no phase separation occurred in these mixtures, CLSM imaging was performed at 40 °C. As an example, Figure 4.1 displays images for a sample containing 6% SPI and 2% (all w/w) gelatin type A. The right image shows the SPI signal, the left image the gelatin signal and the center image an overlay of the two (details regarding the channels will be provided later). SPI solutions contained protein aggregates (spots with higher intensity) which explained the high turbidity of the SPI stock solution (see also image for pure SPI samples in Figure 4.2). In between these aggregates soy proteins were evenly distributed throughout the sample. Also gelatin was found to homogeneously distribute throughout the samples with a lower concentration (intensity) at locations where the SPI aggregates were found. These images, typical for all SPI / gelatin type A mixtures, indicate no sign of phase separation (also compare with images showing phase separation after cooling in Figure 4.2). Thus, also the SPI / gelatin type A mixed solutions can be considered to be homogeneous at 40 °C, that is, above the helix to coil transition temperature of gelatin.

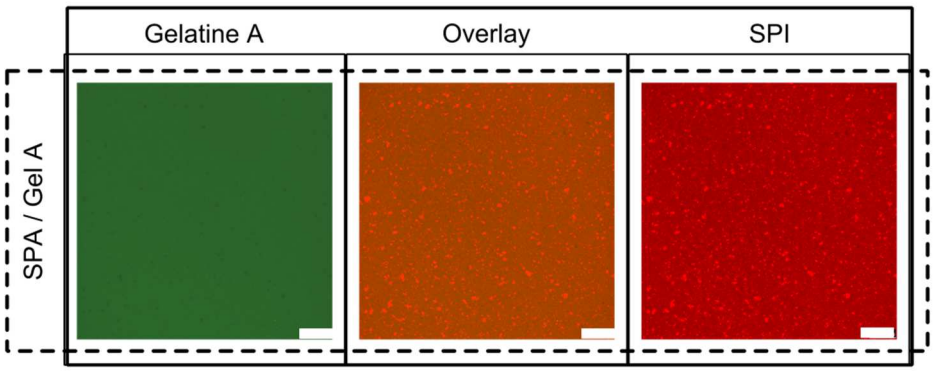

Figure 4.1 CLSM images of a sample containing 6% SPI and 2% gelatin type A at 40 °C. Left image: Gelatin channel. Middle image: overlay. Right image: SPI channel as explained in the text. Scale-bar represents 25 µm

In the next step, the phase behavior and microstructure of these systems after gelatin gelation was investigated. The microstructure of gelatin gels (type A and type B) with added WPI or SPI is shown in Figure 4.2. The first column shows CLSM images of either a WPI or a SPI solution in the absence of gelatin (0% gelatin). Besides the soluble protein, non-soluble protein aggregates were also found in these samples. These samples were stained non–covalently using Rhodamine B. This fluorescent probe has a higher affinity for the hydrophobic areas of proteins than for the water phase. The fluorescence intensity (here shown as red colour) can be attributed to the concentration of WPI or either SPI. In mixed gelatin / globular protein (SPI, WPA or WPI) systems, Rhodamine B was found to have significantly higher affinity for the globular protein than to gelatin as also reported for other fluorescent dyes [42]. This can be attributed to the absence of pronounced hydrophobic areas in the gelatin molecule. Intensity in the Rhodamine B channel in mixed systems can therefore be attributed to the location of globular proteins. To furthermore allow the independent visualization of both proteins, gelatin was labelled covalently with FITC. The signal from the FITC channel is shown in green in Figure 4.2.

In gelatin A gels with added WPI both proteins were homogeneously distributed, indicated by the even intensity distribution of both channels (colours). Also macroscopically no changes in sample turbidity were observed during the gelation. Gels containing 2% gelatin B and 6% WPI were homogeneous in their microstructure. At 6% gelatin B and 6% WPI, domains enriched in WPI (and depleted in gelatin) were observed. These domains could also be observed macroscopically by a slight change in sample opaqueness which had also been described earlier for this system [32]. Macroscopically, however, the sample stayed translucent which indicates that the total number, total volume and total amount of protein in these domains is relatively low.

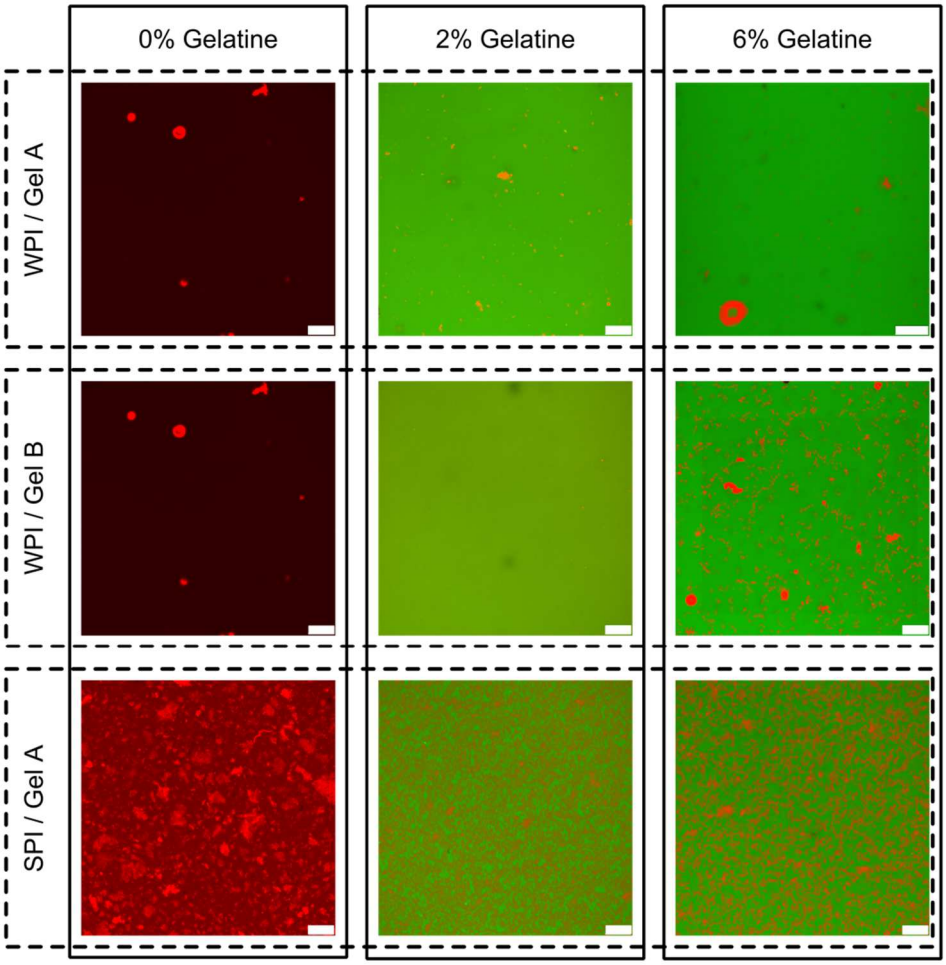

Figure 4.2 CLSM images of mixtures (pH 7, 150 mM NaCl) containing 6% WPI or SPI and 0%, 2% or 6% gelatin (type A or B) at room temperature where gelatin was gelled. Gelatins were labelled covalently with FITC (shown in green), the location of WPI or SPI in the samples is shown in red as discussed in the text. Scale-bar represents 25µm.

In the gelatin A gels with added SPI two distinct phases could be observed on a microscopic scale (Figure 4.2, third row), one enriched in gelatin and the other enriched in SPI. The phase separation of the two proteins could also be observed macroscopically where the mixed gelatin type A / SPI gels increased in opaqueness upon the gelation of gelatin (upon cooling).

In addition to WPI and SPI, gelatin type A and B were also mixed with whey protein aggregates (WPA). It is known that phase separation occurs in the WPA / gelatin B mixture

during gelatin gelation [32]. For WPA / gelatin type A and type B mixtures, a phase diagram was constructed based on turbidity / visual observations (see Figure 4.3).

Most WPA / gelatin type B mixtures (Figure 4.3B) showed a strong increase in opaqueness upon cooling from 40 °C to 20 °C. Only at low total protein concentration the solutions stayed clear. The critical point for phase separation (mixture with lowest total protein concentration where phase separation was found) lies around 0.008 $g_{protein}$ / g_{water} WPI and 0.01 $g_{protein}$ / g_{water} gelatin B. Phase separation was observed for all samples prepared above these protein concentrations.

For WPA / gelatin type A mixtures (Figure 4.3A), phase separation was mainly observed at high WPA concentration and low gelatin concentration. The unstable region of the phase diagram for WPA / gelatin A mixtures (region where phase separation is expected i.e. the binodal) is located close to the WPA axis and does not have the typical shape as expected for phase diagrams at thermodynamic equilibrium. The asymmetric phase diagram in Figure 4.3A for WPA / gelatin A is likely to be caused by the faster gelling of gelatin at higher gelatin concentration, thereby hindering phase separation to occur.

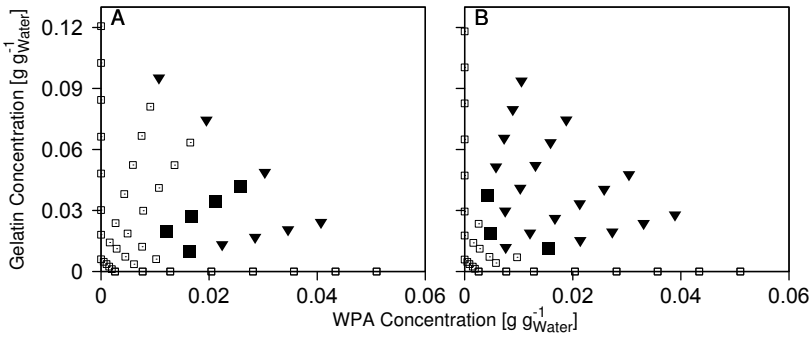

Figure 4.3 Phase diagram of gelatin (graph A: type A and graph B: type B) / whey protein aggregate mixed gels at 150 mM ionic strength and pH 7. Samples are marked according to their turbidity, clear (□), slightly turbid (■) or highly turbid (▼) at 20 °C.

As pointed out in chapter 3 the interaction of WPA and gelatin (type A and B) at the used solvent conditions (pH 7, 150 mM NaCl) is well described by their hard body interaction and the average molecular weight of both gelatin types is comparable. Here the main difference between gelatin type A and type B is their size distribution (see figure 2.7). Gelatin type B contains relatively more high molecular weight gelatins which is suggested to be the reason for the differences in the observed phase behaviour in mixed systems containing whey protein aggregates.

Figure 4.4 shows the microstructure of two phase separated gels at 3% WPA and 6% gelatin (type A or type B). The gelatin signal (green) and WPA signal (red) are shown separately and an overlay of the two signals is shown in the middle column. The intensity of the signals in Figure 4.4 is proportional to the concentration of either gelatin or WPA. The separate images for the two channels show that each protein is concentrated in one phase and depleted from the other as typical for segregative phase separation. There is a 4-fold difference in the length scale at which phase separation can be observed (or the domain size). This length scale is larger for WPA / gelatin type B mixtures than for WPA / gelatin type A mixtures. This relates to location deeper in the unstable region of the phase diagram of WPA / gelatin type B mixtures compared to WPA / gelatin A mixtures as when considering the phase diagram in Figure 4.3.

In conclusion, we find that during gelation two mixed systems (WPI / gelatin type A and WPI / gelatin type B) showed no phase separation. The other three mixed systems (WPA / gelatin type A, WPA / gelatin type B and SPI / gelatin type A) showed segregative phase separation.

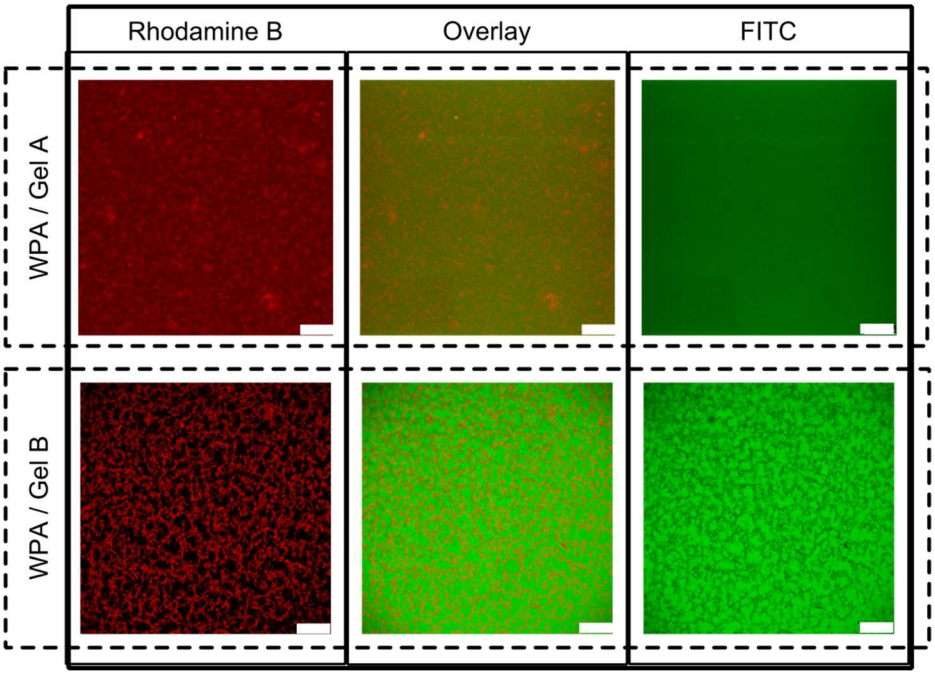

Figure 4.4 CLSM images of 3% WPA / 6% gelatin (type A top, type B bottom row) at pH 7 and 150 mM NaCl after cooling and gelatin gelation. Scale bar for top row is 25 µm and for bottom row 100 µm. Gelatin was covalently labelled with FITC, the FITC signal (gelatin location) is shown in the right column (green). The red colour corresponds to Rhodamine signal (WPA, left column); The middle column is an overlay of the two channels.

Rheology

The gelation of single gelatin and mixed gelatin gels containing added globular proteins was followed during cooling from 40 °C to 15 °C. The storage modulus (G') and loss modulus (G") at 15 °C is plotted as a function of the gelatin concentration in Figure 4.5. Figure 4.5A1 and Figure 4.5B1 show the G' and G" respectively for single gelatin type A and type B gels. The G' increases exponentially with increasing gelatin concentration. For gelatin A and gelatin B similar G' and G" values were obtained. The measured G' data were fitted for both gelatin types separately to equation 4.1 as earlier described [43].

$$G' = C\left(c_p - c_0\right)^t \qquad 4.1$$

with G' the storage modulus, C and t scaling constants, c_0 the minimal gelling concentration and c_p the protein weight concentration. The protein weight concentrations are expressed relative to the total weight of water rather than the total sample weight as defined by:

$$c_p = \frac{m_{protein}}{m_{water}} \qquad 4.2$$

with $m_{protein}$ the total mass of protein and m_{water} the total mass of water in the sample. Good fits between model and experimental G' data with fitting parameters similar to literature values (t = 1.94, c_0 = 0.7% [43, 44]) were obtained for both gelatin A and B as shown in Figure 4.5A1.

The G' and G" of gelatin gels with added globular proteins is shown in Figure 4.5A2 and Figure 4.5B2 respectively. The expected G' and G" values for single gelatin gels are shown as lines. The G" values of mixed gels are significantly above those found for gelatin gels. This can be attributed to the increased viscosity of the solutions (the continuous liquid phase in the pores of the gelatin gel) with added protein. SPI has the highest viscosity as a single protein solution and hence shows the largest effect on the G" in mixed gels while WPI containing samples only slightly increase in G".

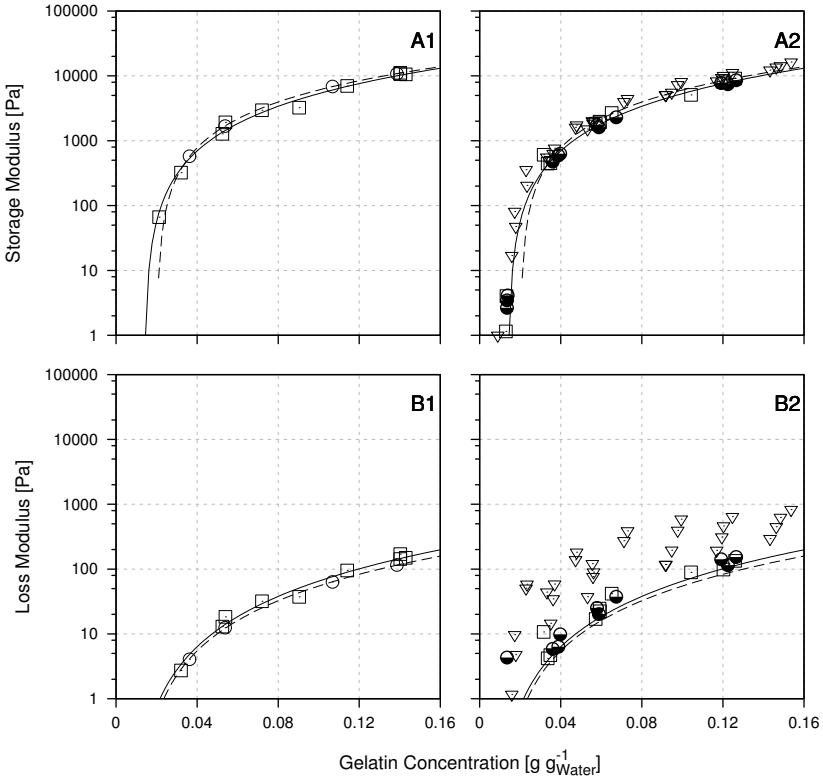

Figure 4.5 Storage and loss modulus of single (graphs 1) and mixed (graphs 2) gelatin gels at 15 °C. Graph A1: Storage modulus G' for gelatin type A (☐ and solid Line) and gelatin type B (○ and dashed line). Symbols are measured values and lines are fits to equation 4.1. Graph B1: Loss modulus G'' for gelatin type A (☐ and solid Line) and gelatin type B (○ and dashed line). Symbols are measured values and lines are drawn to guide the eye. Graph A2: G' for mixed gelatin gels as a function of gelatin concentration. Curves represent pure gelatins as shown in graph A1. Symbols refer to WPI (ranging from 6% to 18%) / gelatin type B (☐), WPI (6% to 18%) / gelatin type A (◒) and SPI (2% to 12%) / gelatin type A (▽) mixed gels. Graph B2: G" for mixed gelatin gels as in graph A2. All concentrations are given in w / w.

The G' of the mixed gelatin gels is close to that of the single gelatin gels. Only for samples with added SPI a slight increase in G' can be observed. To investigate this effect in more detail we scale the results of the elastic modulus of the mixtures $G'_{mixture}$ by the elastic modulus of the gelatin $G'_{gelatin}$ as predicted by equation 4.1. In this way the data can be displayed independent of the gelatin concentration. We define a new parameter *s* as:

$$s \equiv \frac{G'_{mixture}}{G'_{gelatin}} \qquad 4.3$$

In the ideal case where gelatin forms a gel independent of the presence of other proteins, $s = 1$. If $s > 1$ this indicates increased G' values compared to the pure gelatin gel and for $s < 1$ the opposite situation holds. Figure 4.6 shows the ratio *s* for mixed gelatin / globular protein gels. For WPI / gelatin (type A and type B) mixtures $s \approx 1$ independent of the amount of added WPI. These rheological observations are in line with the microstructural analysis and macroscopic observations where gelatin (type A or B) / WPI gels did not show phase separation.

For the phase separated mixtures of gelatin type A with SPI or WPA we find that $s > 1$ and increases with increasing SPI or WPA concentration. This can be linked to the earlier described phase separation. The condition s > 1 indicates that gelatin gelled at an increased effective concentration as caused by the local segregative phase separation where each protein is confined in its own volume, i.e. increasing its local concentration. This can be directly related to the microstructure for these mixed gels as shown in Figure 4.2 and Figure 4.4 which show one phase enriched in gelatin.

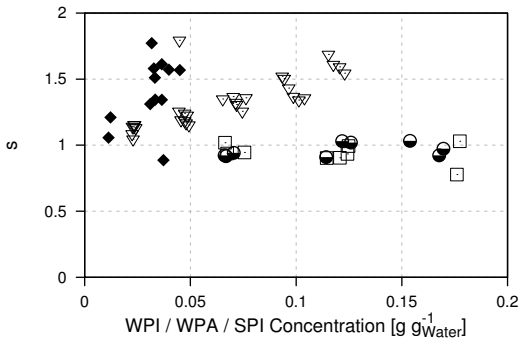

Figure 4.6 The *s* value (equation 4.3) for mixed gelatin / globular protein gels at 15 °C at varying gelatin concentration (5% to 15 % w/w) as a function of globular protein concentration (WPI, WPA or SPI). Symbols represent measurement points for WPI / gelatin type B (□), WPI / gelatin type A (◒), WPA / gelatin type A (◆) and SPI / gelatin type A (▽)

Influence of size

Phase separation during gelation could be linked to an increase in storage modulus G' as observed for WPA / gelatin type A, WPA / gelatin type B and SPI / gelatin type A. On the other hand WPI / gelatin type A or type B mixtures showed no phase separation upon gelation and no increase in G'. All protein mixtures in this study were prepared at an ionic strength of 150 mM at pH 7. In chapter 3 we have shown that at neutral pH and ionic strength > 100 mM gelatins (type A and B), WPI and WPA can be modelled as hard spheres. An important parameter influencing the phase separation in binary hard sphere mixtures is the size ratio *q* defined by

$$q = \frac{a_G}{a_{GP}} \qquad 4.4$$

where a_G is the effective radius of the gelatin molecules and a_{GP} the effective radius of the globular proteins. The size ratio *q* for the different mixtures included in this publication is given in Table 4.1.

Table 4.1 Characteristic size (radius, *a*; molecular weight M_w or M_n and *q* from equation 4.4) for gelatin / globular protein mixtures at 40 °C in solution before gelation. Values taken from chapter 2 are number averaged and indicated using †. Values taken from other literature (*[41] ⁺[40]) are volume averaged.

Gelatin	Gelatin B	Gelatin A	Gelatin A	Gelatin A	Gelatin B
M_n [kg / mol]	80†	80†	80†	80†	80†
a_G [nm]	6†	4.5†	4.5†	4.5†	6†
Globular Protein	WPI	WPI	SPI	WPA	WPA
M_w or M_n [kDa]	32†	32†	180-360⁺	290†	290†
a_{GP} [nm]	2.2†	2.2†	5.5*	7.6†	7.6†
$q = \frac{a_G}{a_{GP}}$	2.7	2	0.8	0.6	0.8
Phase separation after gelation	No		Yes		

As outlined in chapter 3 the phase diagram for binary hard sphere systems can be determined using a virial approach. One characteristic point in the phase diagram indicating the overall miscibility of the two components is the critical point. It is defined as the point with the lowest total concentration where phase separation occurs and is shown in Figure 4.7 as a function of *q*. The volume fraction at the critical point Φ_c summarizes the location of the binodal for a large number of different sample in the simplest way. Lower Φ_c values indicate a location of the binodal closer to the axis (at lower total protein concentration) and increasing Φ_c correspond to a higher miscibility of the two proteins (binodal at higher protein concentration). The region around q = 1 is characterized by a high miscibility of the protein mixture. The miscibility decreases rapidly in the range between q = 1 to q = 10 (or q = 1 to q = 0.1) and afterwards remains almost constant around a volume fraction of 0.3. The *q*-values and corresponding critical volume fraction for the mixed gelatin / globular protein systems were added to Figure 4.7. Upon gelation, q will increase as a result of the increasing characteristic excluded volume of the gelatin due to triple helix formation.

The two mixtures with q > 1 (WPI / gelatin type A or type B) did not show phase separation upon gelation. In contrast, the three mixtures with q < 1 (WPA / gelatin type A or type B and SPI / gelatin type A) phase separated during gelation. Interestingly, these three mixtures passing q = 1 (region of high miscibility), show phase separation during gelation. The two mixtures where no phase separation occurs do not cross this point q = 1. First passing a region of increasing miscibility followed by passing a region of decreasing miscibility during gelation seems to facilitate phase separation.

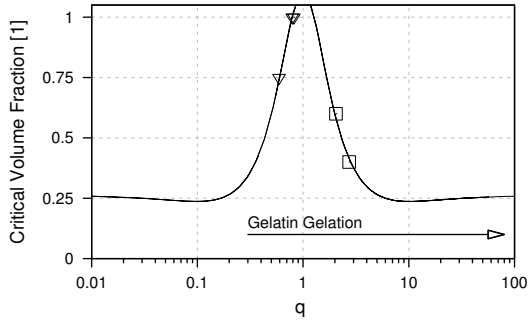

Figure 4.7 The critical volume fraction (total volume fraction of hard spheres at critical point in phase diagram) as a function of *q* (size ratio between spheres, detailed explanation on calculations given in chapter 3). Data points show values from this research for mixed gelatin / globular protein systems that show phase separation (▽) and those that do not show phase separation (□).

Conclusion

At salt conditions where electrostatic interactions between proteins are screened, phase separation occurred during gelatin gelation in mixtures of gelatin (type A or type B) and globular proteins (SPI or WPA) dependent on their molecular size ratios. Phase separation during gelation was observed as increased opaqueness of the samples which could be attributed to segregative phase separation and changes in the gel microstructure of mixed gelatin gels. These microstructural changes were directly related to increased gel stiffness.

The q value (size ratio between the different proteins) was put forward as a good indicator whether microstructural and rheological changes are expected in a mixed gelatin / secondary (globular) protein gel. Mixtures where the molecular size ratios cross the value $q = 1$ during gelation showed phase separation upon gelation. Our results are based on observations of five different gelatin / globular protein mixtures which suggests that this behavior is not system specific. In chapter 5, we will additionally show that crossing $q = 1$ also induced similar changes during the gelation of globular proteins in the presence of gelatin, which is the next step towards a generalization of this effect.

References

1. Çakır, E., C.R. Daubert, M.A. Drake, C.J. Vinyard, G. Essick, and E.A. Foegeding, *The effect of microstructure on the sensory perception and textural characteristics of whey protein/κ-carrageenan mixed gels.* Food Hydrocolloids, 2012. **26**(1): p. 33-43.
2. van den Berg, L., A.L. Carolas, T. van Vliet, E. van der Linden, M.A.J.S. van Boekel, and F. van de Velde, *Energy storage controls crumbly perception in whey proteins/polysaccharide mixed gels.* Food Hydrocolloids, 2008. **22**(7): p. 1404-1417.
3. van den Berg, L., T. van Vliet, E. van der Linden, M.A.J.S. van Boekel, and F. van de Velde, *Breakdown properties and sensory perception of whey proteins/polysaccharide mixed gels as a function of microstructure.* Food Hydrocolloids, 2007. **21**(5–6): p. 961-976.
4. van den Berg, L., T. van Vliet, E. van der Linden, M.A.J.S. van Boekel, and F. van de Velde, *Serum release: The hidden quality in fracturing composites.* Food Hydrocolloids, 2007. **21**(3): p. 420-432.
5. van den Berg, L., *Texture of food gels explained by combining structure and large deformation properties*. Physics and Physical Chemistry of Foods. 2008: PhD Thesis - Wageningen University.
6. Mosca, A.C., *Designing food structures to enhance sensory responses*, in *Product Design and Quality Management*. 2012, Wageningen University.
7. Mosca, A.C., J.A. Rocha, G. Sala, F. van de Velde, and M. Stieger, *Inhomogeneous distribution of fat enhances the perception of fat-related sensory attributes in gelled foods.* Food Hydrocolloids, 2012. **27**(2): p. 448-455.
8. Mosca, A.C., F. van de Velde, J.H.F. Bult, M.A.J.S. van Boekel, and M. Stieger, *Effect of gel texture and sucrose spatial distribution on sweetness perception.* LWT - Food Science and Technology, 2012. **46**(1): p. 183-188.
9. Mosca, A.C., F.v.d. Velde, J.H.F. Bult, M.A.J.S. van Boekel, and M. Stieger, *Enhancement of sweetness intensity in gels by inhomogeneous distribution of sucrose.* Food Quality and Preference, 2010. **21**(7): p. 837-842.
10. Prinsen, P. and T. Odijk, *Optimized Baxter model of protein solutions: electrostatics versus adhesion.* J Chem Phys, 2004. **121**(13): p. 6525-37.
11. McMillan, W.G. and J.E. Mayer, *The Statistical Thermodynamics of Multicomponent Systems.* The Journal of Chemical Physics, 1945. **13**(7): p. 276-305.
12. Rosenbaum, D.F., A. Kulkarni, S. Ramakrishnan, and C.F. Zukoski, *Protein interactions and phase behavior: Sensitivity to the form of the pair potential.* The Journal of Chemical Physics, 1999. **111**(21): p. 9882-9890.

13. Sarkar, S. and B. Bagchi, *Inherent structures of phase-separating binary mixtures: Nucleation, spinodal decomposition, and pattern formation.* Physical Review E - Statistical, Nonlinear, and Soft Matter Physics, 2011. **83**(3).
14. Polyakov, V.I., V.Y. Grinberg, and V.B. Tolstoguzov, *Application of phase-volume-ratio method for determining the phase diagram of water-casein-soybean globulins system.* Polymer Bulletin, 1980. **2**(11): p. 757-760.
15. Polyakov, V.I., O.K. Kireyeva, V. Grinberg, and V.B. Tolstoguzov, *Thermodynamic compatibility of proteins in aqueous media. Part. I. Phase diagrams of some water--protein A--protein B systems.* Die Nahrung, 1985. **29**(2): p. 153-160.
16. Polyakov, V.I., I.A. Popello, V. Grinberg, and V.B. Tolstoguzov, *Thermodynamic compatibility of proteins in aqueous media. Part 2. The effect of some physicochemical factors on thermodynamic compatibility of casein and soybean globulin fraction.* Die Nahrung, 1985. **29**(4): p. 323-333.
17. Polyakov, V.I., I.A. Popello, V. Grinberg, and V.B. Tolstoguzov, *Thermodynamic compatibility of proteins in aqueous media. Part 3. Studies on the role of intermolecular interactions in the thermodynamics of compatibility of proteins according to the data of dilution enthalpies.* Die Nahrung, 1986. **30**(1): p. 81-88.
18. Edelman, M.W., R.H. Tromp, and E. van der Linden, *Phase-separation-induced fractionation in molar mass in aqueous mixtures of gelatin and dextran.* Physical Review E - Statistical, Nonlinear, and Soft Matter Physics, 2003. **67**(2 1): p. 214041-2140411.
19. Edelman, M.W., E. Van der Linden, E. De Hoog, and R.H. Tromp, *Compatibility of gelatin and dextran in aqueous solution.* Biomacromolecules, 2001. **2**(4): p. 1148-1154.
20. Edelman, M.W., E. Van Der Linden, and R.H. Tromp, *Phase separation of aqueous mixtures of poly(ethylene oxide) and dextran.* Macromolecules, 2003. **36**(20): p. 7783-7790.
21. Almrhag, O., P. George, A. Bannikova, L. Katopo, D. Chaudhary, and S. Kasapis, *Investigation on the phase behaviour of gelatin/agarose mixture in an environment of reduced solvent quality.* Food Chemistry, 2013. **136**(2): p. 835-842.
22. Altay, F. and S. Gunasekaran, *Gelling properties of gelatin–xanthan gum systems with high levels of co-solutes.* Journal of Food Engineering, 2013. **118**(3): p. 289-295.
23. Anderson, V.J. and R.A.L. Jones, *The influence of gelation on the mechanism of phase separation of a biopolymer mixture.* Polymer, 2001. **42**(23): p. 9601-9610.
24. Baussay, K., D. Durand, and T. Nicolai, *Coupling between polysaccharide gelation and micro-phase separation of globular protein clusters.* Journal of Colloid and Interface Science, 2006. **304**(2): p. 335-341.

25. Çakir, E. and E.A. Foegeding, *Combining protein micro-phase separation and protein-polysaccharide segregative phase separation to produce gel structures.* Food Hydrocolloids, 2011. **25**(6): p. 1538-1546.
26. Cavallieri, A.L.F., N.A.V. Fialho, and R.L. Cunha, *Sodium caseinate and κ-carrageenan interactions in acid gels: Effect of polysaccharide dissolution temperature and sucrose addition.* International Journal of Food Properties, 2011. **14**(2): p. 251-263.
27. de Jong, S. and F. van de Velde, *Charge density of polysaccharide controls microstructure and large deformation properties of mixed gels.* Food Hydrocolloids, 2007. **21**(7): p. 1172-1187.
28. Lorén, N. and A.-M. Hermansson, *Phase separation and gel formation in kinetically trapped gelatin/maltodextrin gels.* International Journal of Biological Macromolecules, 2000. **27**(4): p. 249-262.
29. Picone, C.S.F. and R.L. da Cunha, *Interactions between milk proteins and gellan gum in acidified gels.* Food Hydrocolloids, 2010. **24**(5): p. 502-511.
30. Nono, M., D. Durand, and T. Nicolai, *Rheology and structure of mixtures of ι-carrageenan and sodium caseinate.* Food Hydrocolloids, 2012. **27**(1): p. 235-241.
31. Devi, A.F., R. Buckow, Y. Hemar, and S. Kasapis, *Modification of the structural and rheological properties of whey protein/gelatin mixtures through high pressure processing.* Food Chemistry, 2014. **156**(0): p. 243-249.
32. Fitzsimons, S.M., D.M. Mulvihill, and E.R. Morris, *Segregative interactions between gelatin and polymerised whey protein.* Food Hydrocolloids, 2008. **22**(3): p. 485-491.
33. Pang, Z., H. Deeth, P. Sopade, R. Sharma, and N. Bansal, *Rheology, texture and microstructure of gelatin gels with and without milk proteins.* Food Hydrocolloids, 2014. **35**: p. 483-493.
34. Walkenström, P. and A.-M. Hermansson, *Mixed gels of fine-stranded and particulate networks of gelatin and whey proteins.* Food Hydrocolloids, 1994. **8**(6): p. 589-607.
35. Walkenström, P. and A.-M. Hermansson, *Fine-stranded mixed gels of whey proteins and gelatin.* Food Hydrocolloids, 1996. **10**(1): p. 51-62.
36. Walkenström, P. and A.-M. Hermansson, *High-pressure treated mixed gels of gelatin and whey proteins.* Food Hydrocolloids, 1997. **11**(2): p. 195-208.
37. Ziegler, G.R., *Microstructure of mixed gelatin-egg white gels: Impact on rheology and application to microparticulation.* Biotechnology Progress, 1991. **7**(3): p. 283-287.
38. Ziegler, G.R. and S.S.H. Rizvi, *Predicting the Dynamic Elastic Modulus of Mixed Gelatin-Egg White Gels.* Journal of Food Science, 1989. **54**(2): p. 430-436.
39. Comfort, S. and N.K. Howell, *Gelation properties of soya and whey protein isolate mixtures.* Food Hydrocolloids, 2002. **16**(6): p. 661-672.

40. Renkema, J.M.S., *Formation, Structure and Rheological Properites of Soy Protein Gels*. Physics and Physical Chemistry of Foods. 2001: PhD Thesis - Wageningen University.
41. Urbonaite, V., H.H.J. de Jongh, E.v.d. Linden, and L. Pouvreau, *The origin of water loss from soy protein gels.* Journal of Agriculture and Food Chemistry, 2014. **62**(30): p. 7550-7558.
42. Devi, A.F., L.H. Liu, Y. Hemar, R. Buckow, and S. Kasapis, *Effect of high pressure processing on rheological and structural properties of milk-gelatin mixtures.* Food Chemistry, 2013. **141**(2): p. 1328-1334.
43. van der Linden, E. and L.M.C. Sagis, *Isotropic Force Percolation in Protein Gels.* Langmuir, 2001. **17**(19): p. 5821-5824.
44. van der Linden, E. and A. Parker, *Elasticity Due to Semiflexible Protein Assemblies near the Critical Gel Concentration and Beyond.* Langmuir, 2005. **21**(21): p. 9792-9794.

CHAPTER 5

Microstructure and rheology of globular protein gels in the presence of gelatin[5]

ABSTRACT

The microstructure and rheological response of globular protein gels (whey protein isolate (WPI) and soy protein isolate (SPI)) in the presence of gelatin (type A, type B and hydrolyzed gelatin type A) was investigated. Microstructural information was obtained using a combination of confocal laser scanning microscopy (CLSM) and spin echo small-angle neutron scattering (SESANS). Addition of gelatin led to a coarsening of the globular protein gel structure and to a reduction in storage modulus of globular protein gels. The presence of hydrolyzed gelatin on the other hand did not induce these changes in the globular protein gels. Results were obtained at conditions where proteins only interact via hard body interactions, where the ratio of molecular sizes (q) was concluded to be the most important determinant for the occurrence or absence of rheological and microstructural changes in globular protein gels prepared in the presence of gelatin.

[5] This Chapter is based on: Ersch, C., Meinders, M. B. J., Bouwman, W. G., Nieuwland, M., Linden, E. v. d., Venema, P., & Martin, A. H. (2015). Microstructure and rheology of globular protein gels in the presence of gelatin. (Submitted).

GRAPHICAL ABSTRACT

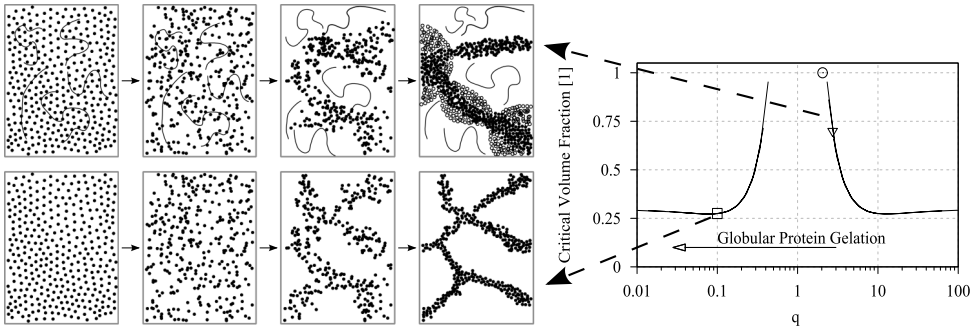

KEYWORDS

Mixed protein gel, gel microstructure, rheological response, CLSM image analysis, SESANS, whey protein isolate, soy protein isolate, gelatin, hard body interactions

Introduction

Gelation is a ubiquitous phenomenon in foods where the molecules responsible for gelation are normally proteins or polysaccharides. Gelation requires molecules to associate into a space spanning network which one observes macroscopically as a transition from a liquid to a semi-solid state. In single component systems the mechanisms that lead to association of molecules, and ultimately gelation, are important to understand gelation of foods. Such mechanisms may for example be protein denaturation, reduction of electrostatic repulsion or formation of junction zones between molecules [1-5]. In case where two types of biopolymers (e.g. proteins and polysaccharides but also different types of proteins or different types of polysaccharides) are present during gelation these molecules may interact before and during gelation, thereby influencing the final properties of the gel network. Understanding the changes in the interactions between biopolymers in solution and during gelation is a challenging task, but essential to understand the sequential events leading to the formation of mixed gels.

For most food relevant biopolymers and their mixtures, quantitative information on the molecular interaction, the molecular dimension and their conformational changes during gelation is not available in literature. Therefore, most research on mixed biopolymer gels focuses on the properties of the final gels. The related scientific literature contains multiple examples of the rheological responses and microstructures of mixed polysaccharide / protein systems [6-21] or mixed protein systems [22-37]. For protein / polysaccharide mixtures also relationships between the microstructural arrangements of biopolymers, rheological properties and the texture [6, 38-41] or taste [42-45] have been investigated. Even though it is likely that these relationships also hold for mixed protein systems this has not yet been established. The next step to use these structure / sensory relationships to selectively develop foods with desired sensorial properties is to study the underlying mechanisms leading to structural and rheological changes in mixed gels due to the presence of secondary biopolymers.

Here we study the influence of molecular interactions and molecular size on the microstructure and rheology for gelatin / globular protein mixed systems. In these systems both proteins are in principle able to form a gel. Dependent on whether gelatin or globular proteins are gelled first, different microstructures and rheological responses have been obtained [33-37, 46]. In these mixed protein systems segregative phase separation has been reported to lead to an increase of the storage modulus of the mixtures relative to the single gels as shown by Fitzsimons et al. (2008) [26], Pang et al. (2014) [28] and in chapter 4 of this thesis. The occurrence of this phase separation during gelatin gelation occurred whenever the globular proteins had a larger effective radius (from spherical

equivalent of the measured excluded volume of the proteins) than the effective radius of gelatin molecules as we discussed in detail in chapter 4. Globular proteins with a smaller effective radius than gelatin did not lead to phase separation or rheological changes, compared to the single gelatin gels. In mixtures where globular proteins were gelled before gelatin gelation, mixed gels were found to have bi-continuous microstructures [33, 34, 36, 37]. This bi-continuous microstructure resulted in a gradual change in fracture properties making them interesting candidates for gradually changing textural properties of gels which will be discussed in more detail in chapter 6. This effect is especially interesting since it was observed for mixtures of gelatin with whey protein concentrate [33, 34], egg white [36, 37] and soy protein isolate (see chapter 6), suggesting a generic mechanism.

Here we study mixed gelatin / globular protein gels with a focus on the gelation of the globular protein. We concentrate on the formation, microstructure and rheology of the globular protein gel in the first stage of the sequential gelation of both proteins. Rheological properties of the globular protein gels were studied above the helix to coil transition temperature of gelatin where gelatin had no elastic response (gelatin solutions behave purely viscous). The microstructure of the globular protein gels was probed using spin echo small-angle neutron scattering (SESANS) and confocal laser scanning microscopy (CLSM) image analysis using covalently labelled gelatin. Mixed gels of globular whey proteins (isoelectric point (pI) ~ 5, M_n = 30 kDa[6]) or globular soy proteins (pI ~ 4.8, M_w glycinin = 360 kDa, β-conglycinin ~150 kDa [47]) mixed with gelatin type A (pI = 8, M_n = 80 kDa[6]), type B (pI = 5, M_n 80 = kDa[6]) or gelatin type A hydrolysate were investigated. By combining these globular proteins with the different gelatin types, their molecular size ratio and molecular interactions were varied.

[6] Determined in chapter 2

Material and Methods

Materials

Soy protein isolate (SPI) was extracted using isoelectric precipitation from defatted soy flour as described earlier [48]. Whey protein isolate (WPI) was purchased from Davisco Foods International Inc. (Le Sueur, USA, MN) product name BIPRO (94 % protein determined by Kjeldahl). Commercially available gelatin (type A and type B) were provided from Rousselot BVBA (Ghent, Belgium). Type A (from porcine skin) had a bloom strength of 290, an isoelectric point (pI) around 8 and a protein content of 89.6% w/w. Type B (from bovine bones) a bloom strength of 260, pI of around 5 and a protein content of 88.8% w/w. A detailed characterization of these research materials is given in chapter 2. Peptan 5000, hydrolyzed gelatin type A was also obtained from Rousselot BVBA (Ghent, Belgium). Other chemicals such as acids and bases used for pH adjustments were of analytical grade and purchased from Sigma Aldrich (Steinheim, Germany).

Sample preparation

Sample preparation was performed as described in chapter 4. In short, stock solutions of proteins were prepared with deionized water (Merck Millipore, Darmstadt, Germany ,18.2 MΩ cm) at pH 7 and constant ionic strength (150 mM for WPI containing samples and 300 mM for SPI containing samples). Stock solutions were mixed to prepare samples with different protein concentration and protein ratios. Sample handling was done at 40 °C where gelatin solutions were in the liquid state.

Small Deformation Rheology

Samples were measured in a rheometer (Anton Paar MC502) using a sand-blasted cup-bob geometry (CC17). They were added in the liquid state (heated for 30 min to 40 °C) and covered with paraffin oil to avoid evaporation. Measurements were performed at a strain of 0.5% and a frequency of 1 Hz. Samples were heated inside the equipment from 40 °C to 95 °C at 5 °C/min and afterwards kept at 95 °C for 1 hour.

Spin echo small-angle neutron scattering (SESANS)

In SESANS samples deuterium oxide (D_2O) was used instead of deionized water for sample preparation and WPI solutions were filtered using a syringe filter with a 1.2 µm cut-off (Sartorius Minisart®). Samples were heated inside the SESANS cuvettes (path length 1 cm) for 30 minutes at 95 °C and subsequently cooled down to room temperature at which temperature the SESANS measurements were performed if not stated otherwise. SESANS measurement were performed at the reactor institute at Delft University of

Technology (the Netherlands) using the setup described by Rekveldt et al. [49]. For the data analysis we use routes described by Andersson et al. [50] which will be outlined in short below.

From the SESANS measurements the normalized polarization *P(z)* (normalized by the empty beam) is given by

$$P(z) = e^{\Sigma_t[G(z)-1]} \qquad 5.1$$

with *z* the spin echo length, Σ_t the scattering power (which indicates the average number of times a neutron scatters while transversing the sample) and *G(z)* a normalized dimensionless function which contains information about the microstructure of the sample. In this study we have used the self-affine random density distribution model to describe *G(z)* which is given by:

$$G(z) = \frac{2}{\Gamma\left(H+\frac{1}{2}\right)}\left(\frac{z}{2a}\right)^{\left(H+\frac{1}{2}\right)} K_{H+\frac{1}{2}}\left(\frac{2}{a}\right) \qquad 5.2$$

where *a* is a measure for the size of the random inhomogeneity in the system. *Γ* is the gamma function, *H* the Hurst exponent (related to the fractal dimension of the systems) and *K* the modified Bessel function. Protein gels are well described as a two phase system with one phase being the protein phase and the other the solvent phase (often called gel pores). For these systems the scattering power Σ_t is given by:

$$\Sigma_t = \lambda^2 t(\Delta\rho)^2 \xi \Phi(1-\Phi) \qquad 5.3$$

with λ the wavelength (0.203 nm), *t* the path length (1 cm), *Φ* the volume fraction of one of the phases, $\Delta\rho$ the neutron scattering length density contrast between the protein and the solvent phase ($\Delta\rho = \rho_{D2O} - \rho_{protein}$ with ρ_{D2O} = 6.38 10^{14} m^{-2} and $\rho_{protein}$ = 3 10^{14} m^{-2} [51]) and ξ the correlation length of the system which is related to the size of the random inhomogeneity via:

$$\xi = 2\pi^{1/2} a \ \frac{\Gamma\left(H+{}^{1}/_{2}\right)}{\Gamma(H)} \qquad 5.4$$

Confocal Laser Scanning Microscopy (CLSM)

Gels were prepared by adding the liquid sample (at 40 °C) to hermetically sealed cuvettes (Gene Frame® 125 µl, obtained from Thermo Scientific) and heating these cuvettes on a Peltier element with the same heating / cooling profile as used for small deformation rheology. After 1 hour at 95 °C the samples were cooled at 5 °C / min to 15 °C and kept at 4 °C until analyzed. Globular proteins were stained using 0.001% w/w Rhodamine B. In some samples gelatin was covalently labelled with Fluorescein Isothiocyanate (FITC). The labelling procedure was given in the Material and Methods section of chapter 4. Imaging was performed using a Leica DMI6000 microscope (Wetzlar, Germany) at room temperature. Images were taken at a sample depth of 5 µm from the cover glass which was in contact with the Peltier element during heating at several randomly chosen locations in the sample and different magnifications. Measurements were performed at 1024 x 1024 measurement points (pixels) at a scanning rate of 400 Hz and two frames were averaged. The sequential mode was used, FITC was excited at 488 nm (measurement between 500 and 570 nm) and Rhodamine B was excited at 561 nm (measurement between 570 and 790 nm).

Image analysis

To obtain quantitative structural information from the CLSM images the spatial autocorrelation function was determined. The spatial autocorrelation function *G(a,b)* of a (digitized) image (2 dimensional, (2D) matrix) with *M* x *N* pixels in the *x*, *y* - plane is defined by [52]

$$G(a,b) = \sum_{x}^{M}\sum_{y}^{N} i(x,y)i(x+a,y+b) = MN < i(x,y)i(x+a,y+b) >_{x,y} \qquad 5.5$$

where *i(x,y)* is the intensity value of a pixel with coordinates (*x,y*) in the image and $<\ldots>_{x,y}$ represents the average over all *x* and *y* values. The autocorrelation function *G(a,b)* is normalized by the average intensity of an image as the average is influenced by acquisition factors which are not part of the structure of interest [53]. The scaled intensity or fluctuation of intensity can be written as

$$\delta i(a,b) = \frac{i(x,y) - < i(x,y) >}{< i(x,y) >} \qquad 5.6$$

which in case of the autocorrelation function leads to the following expression for the scaled auto correlation function *g(a,b)*:

$$g(a,b) =< \delta i(x,y)\delta i(x+a,y+b) >= \frac{< i(x,y)i(x+a,y+b) >}{< i(x,y) >^2} - 1$$
$$= \frac{\frac{1}{NM}\sum_x^M \sum_y^N i(x,y)i(x+a,y+b)}{\left(\frac{1}{NM}\sum_x^M \sum_y^N i(x,y)\right)^2} - 1 \qquad 5.7$$

The intensity fluctuation $\delta i(x,y)$ in a voxel is linearly related to the concentration of fluorescent dyes and, therefore also the protein concentration [54]. The autocorrelation function is therefore related to the density correlation function of the fluorescent dye and the stained sample structures given by [55]:

$$c(r) = \frac{\langle \rho(\vec{r}')\rho(\vec{r}'+\vec{r})\rangle}{\langle \rho(\vec{r}')\rangle^2} = g(a,b) + 1 \qquad 5.8$$

with $\rho(\vec{r}')$ the density of fluorescent molecules at position $\vec{r}$ where $\vec{r}' = x\hat{\imath} + y\hat{\jmath}$ and $\vec{r} = a\hat{\imath} + b\hat{\jmath}$ are the position vectors and $\hat{\imath}$ and $\hat{\jmath}$ unit vectors in the *x* and *y* direction, respectively. For isotropic systems, $\rho(\vec{r}) = \rho(r)$, with $\vec{r} = |\vec{r}|$. Therefore, equation 5.8 can be radially averaged leading to the radial density autocorrelation function $c(r)$.

$$c(r) = g(r) + 1 = \langle g(a,b)\rangle_{a^2+b^2=r^2} + 1 \qquad 5.9$$

For non-crystalline species, the density $\rho(r)$ is uncorrelated at large distances leading to:

$$\lim_{r\to\infty} c(r) = \frac{\langle \rho(\vec{r})\rangle \langle \rho(\vec{r})\rangle}{\langle \rho(\vec{r})\rangle^2} = 1 \qquad 5.10$$

The value of the normalized autocorrelation function $c(r)$ at $r = 0$ equals the variance of the fluctuation intensity δi and is a measure of how much of the total intensity is concentrated in areas with higher intensity relatively to the average intensity of the image. This value (also referred to as σ^2) has been used in literature as a measure for the coarseness of gels [54, 56] and can be calculated directly from the image using

$$\lim_{r\to 0} c(r) = \sigma^2 = \langle \delta i^2 - \langle \delta i\rangle^2\rangle = \left(\frac{\sqrt{\frac{1}{NM}\sum_x^N \sum_y^M [i(x,y) - \langle i\rangle]^2}}{\langle i\rangle}\right)^2 \qquad 5.11$$

Using these two conditions at $r = 0$ and $r \to \infty$, the density auto-correlation function $c(r)$ can be expressed as the normalized density auto-correlation function $p(r)$:

$$p(r) = \frac{c(r) - 1}{\sigma^2} \qquad 5.12$$

For ease of reading we will refer to this function *p(r)* simply as correlation function. The characteristic parameters of this function such as the zero crossing, first minimum and maximum describe different properties of the observed system. In a system with only one type of structures this curve is typically well described by a stretched exponential decay such as [52-54]:

$$p(r) = e^{-\left(\frac{r}{\xi}\right)^{\beta}} \qquad 5.13$$

with ξ the correlation length of the structure and β a form factor.

The image analysis was performed using MatLab® (R2013a Version8.1.0.604; MathWorks Inc.). The autocorrelation function was calculated using the standard routine in the DipImage library (Version 2.5.1; Quantitative Imaging Group, Delft University of Technology). For each image a background image was subtracted before analysis. Background images were obtained from images using a Gaussian filter with a sigma value much larger than the observed structures. This procedure was found not to change results for images with a homogeneous intensity distribution while being able to correct for errors introduced by the CLSM optics (e.g. dark corners) where present.

Size Exclusion Chromatography – Multi Angle Laser Light Scattering

Size exclusion chromatography with multi angle laser light scattering (SEC-MALLS, Agilent technologies, 1200 series) was performed using three columns in series (TSK gel G5000 PWxl + TSK gel G3000 PWxl + TSK gel G2500 PWxl). The columns were heated to 60 °C and separation performed at a constant flow of 0.5 ml / min using 10 mM phosphate buffer at pH 6.8 with 125 mM $NaNO_3$ and 0.02% NaN_3. The MALLS data (acquired using Wyatt Dawn Heleos II) was fitted using a first order Zimm model (using the software Astra 6).

Results and discussion

Rheological characterization

Single and mixed protein systems were characterized for their rheological response at 95 °C. Figure 5.1 shows the storage modulus (G') and loss modulus (G") of single whey protein isolate (WPI) and single soy protein isolate (SPI) gels as a function of protein concentration. The storage modulus G' of WPI and SPI was fitted using equation 7.10 with an earlier described procedure [57].

$$G' = C\left(c_p - c_0\right)^t \qquad 5.14$$

Here C and t are constants, c_p the protein concentration (in $g_{protein}$ / g_{water}) and c_0 a minimum gelling protein concentration. For WPI a good description of the data over a large protein concentration range was found. Also for SPI equation 5.14 describes the behavior of G' well within the range of measured protein concentrations even though the concentration range was limited by the minimum gelling concentration (~ 0.04 $g_{protein}$ / g_{water}) and the concentration of the SPI stock solution obtained from the isolation procedure (~ 0.11 $g_{protein}$ / g_{water}).

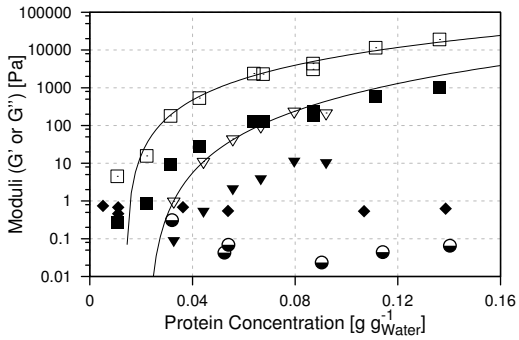

Figure 5.1 Storage modulus G' (▽,□) and loss modulus G'' (▼,■) for single SPI (▽,▼) and single WPI (□,■) gels after 1 hour at 95 °C. Curves were fitted using equation 7.10. Gelatin type A (◒) and type B (◆) showed a purely viscous response and only the loss moduli are shown.

We would like to stress that the model underlying equation 5.14 is a percolation model, but that we use equation 5.14 only semi-empirically. Percolation theory assumes the network to arise throughout the gelation process in a spatially random manner [5] which is strictly spoken not true for WPI or SPI gels. Globular proteins, especially in the presence of salt, exhibit an entrance into a two - phase region during the gelation process, and the protein system shows micro-phase separation, resulting in a system with protein rich and

protein poor phases [58]. The latter we refer to as pores. One therefore should not interpret the fitting parameters such as critical parameters and exponents in our case.

For pure gelatin no elastic response was observed at 95 °C, this is in line with its coil conformation at this temperature. Therefore, also in a mixed globular protein / gelatin system, the measured G' values can be attributed solely to the globular protein gels (WPI or SPI). The concentration of globular proteins in the mixed gels is known. Using this globular protein concentration and equation 5.15 it is possible to calculate an expected G' value (denoted by G'_{GP}, where *GP* stands for globular protein) for a mixed SPI or WPI gel. This G'_{GP} is based on the assumption that the presence of gelatin does not change the storage modulus, and that the protein concentration is based on the actual available water in the sample rather than total sample weight. This definition has already been used in the preceding chapters and the importance of the definition of protein concentration in mixed gels will be discussed in more detail in chapter 8.

The measured storage modulus ($G'_{measured}$) and theoretical G'_{GP} for WPI gels at three different whey protein concentrations as a function of gelatin type A concentration are shown in Figure 5.2. At low gelatin concentration no differences between the measured and theoretical storage modulus were observed. With increasing gelatin concentration $G'_{measured}$ values are below the theoretical G'_{GP} for single WPI gels. This behavior is opposite to the increase in G' upon the addition of (non-gelling) globular proteins to gelatin gels as observed in chapter 4 which will be addressed later on in this chapter.

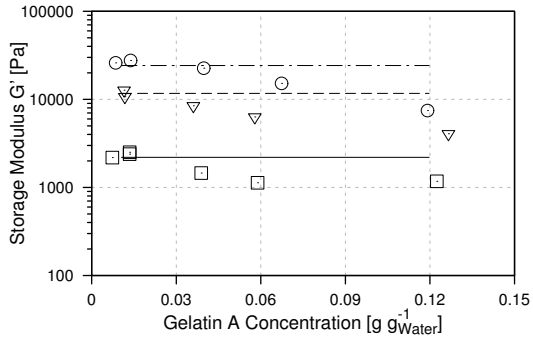

Figure 5.2 Measured storage modulus ($G'_{measured}$) for mixed gels after 1 hour at 95 °C containing 0.06 (□), 0.12 (▽) or 0.16 (○) $g_{protein}$ / g_{water} WPI with added gelatin A. Horizontal lines indicate G'_{GP} which is the storage modulus expected for pure WPI gels without added gelatin.

To express the disparity between $G'_{measured}$ and G'_{GP} we use ratio *s* as introduced in chapter 4 given by

$$s \equiv \frac{G'_{measured}}{G'_{GP}} \qquad 5.15$$

Figure 5.3 shows the ratio *s* for mixed SPI / gelatin type A, WPI / gelatin type A, WPI / gelatin type B and WPI / hydrolyzed gelatin type A gels as a function of gelatin concentration. The ratio *s* of SPI and WPI gels decreases with increasing gelatin type A concentration. We note that for WPI and SPI the *s* values follow the same curve, even though there is a difference of 2 orders of magnitude in absolute value of the storage modulus between these systems (cf. Figure 5.1). Also the ratio *s* for mixed WPI gels with added gelatin type B decreases with increasing gelatin concentration. The decrease in *s* occurs at lower gelatin concentration for gelatin type B compared to gelatin type A. For both gelatin types *s* levels off to *s* = 0.2 at high gelatin concentrations.

Figure 5.3 also shows the ratio *s* of WPI gels prepared in the presence of hydrolyzed gelatin type A. Here *s* > 1 for all measured gelatin and WPI concentrations (performed in the range between 0.02 to 0.12 $g_{protein}$ / g_{water} hydrolyzed gelatin type A and 0.05 to 0.20 $g_{protein}$ / g_{water} WPI). The *s* > 1 indicates that these mixed gels showed an increased storage modulus compared to the one expected for the single WPI gel at identical WPI concentration (corrected for the availability of the water). Increased values compared to the pure WPI gels are most probably due to a high affinity of hydrolyzed gelatin to water which might reduce the availability of water to WPI.

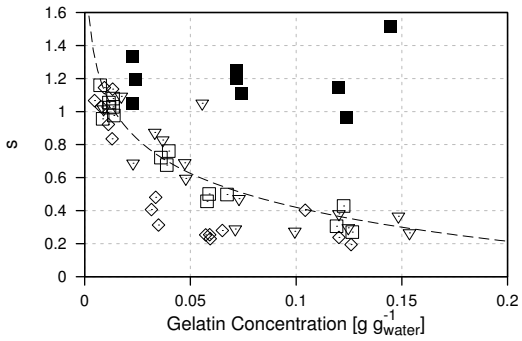

Figure 5.3 Ratio *s* (equation 5.15) for the gels from the different protein mixtures for gels containing WPI / gelatin A (□), SPI / gelatin A (▽) and WPI / gelatin B (◇) (all open symbols) and gels containing WPI / hydrolyzed gelatin type A (■). Dashed line is meant as a guide the eye.

Gel microstructure of single gels

To relate the rheological properties to the microstructure of mixed gels we performed neutron scattering (SESANS) and image analysis on CLSM images for single and mixed gels. Figure 5.4 shows CLSM images of single WPI gels at three different protein concentrations. The images show typical gel structures consisting of a connected network of aggregated protein. These aggregates are typically referred to as building-blocks which on a certain length scale, connect to form a space spanning network [5]. For protein gels, the size of the building blocks is an important parameter in their characterization. The building block size can be determined from the first minima of the radial density correlation function *p(r)* (equation 5.12) which is shown in Figure 5.5A. This minimum represents the distance from any location with high WPI concentration (high intensity) towards the lowest intensity (background) [59, 60]. The other characteristic property related to the size of the building blocks is the correlation length ξ which was obtained by fitting equation 5.13 to *p(r)* as indicated by the solid lines in Figure 5.5A.

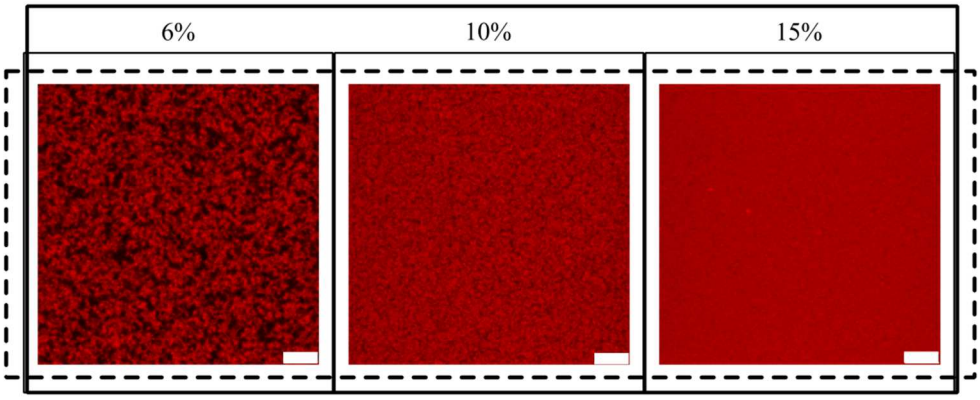

Figure 5.4 CLSM images of single WPI gels at 6%, 10% and 15% w/w protein concentrations (scale bar 7.5 µm).

An additionally important property for gel structures is the way how the aggregates are arranged. This is described by two parameters. First, the typical distance between aggregates, given by the first maximum of the correlation function where the probability to find another building block is highest. Secondly, their arrangement also determines the size of the gel pores, typically defined as the region depleted of protein between the gel building blocks. With the pores having a significantly lower intensity (lower protein concentration) than the protein gel, their size can be extracted from the width of the minimum in the density correlation function *p(r)*. Here it was defined as the distance between the first and second zero crossing of the density correlation function. For a better visible example of the negative peak and first maxima please see Figure 5.8.

The last parameter of interest when analyzing protein gels is the structure within the gel building blocks. Despite the fact that the range of length scales probed by CLSM is not sufficient to extract a fractal dimension of the building blocks [54], the slope of *p(r)* can be used to compare different structures. This can be done by determining the linear region of *p(r)* over the relative distance (radial distance / size of building blocks). The density is also represented in the parameter β of equation 5.13. For β = 2 this equation corresponds to a Gaussian model which would be expected for a 2D projection of a sphere with homogeneous internal structure, β values above 2 are expected for disks. Lower values can have various reasons, one being a non-homogeneous intensity (protein) distribution or an irregular shape of the aggregates.

Table 5.1 summarizes the different parameters obtained from image analysis for single WPI gels at three protein concentrations. With increasing protein concentration the size of the gel building blocks decreases (correlation length and diameter) so does the distance between them and the pore size. These changes are typically summarized in the term "denser protein network" which can also be observed in the images in Figure 5.4.

Figure 5.5 shows the density correlation function from CLSM image analysis and the normalized polarization from SESANS measurements for single WPI gels. While for the analysis of the CLSM images one assumes isotropy to extract information of the 3D gel structure from a 2D projection, SESANS directly probes a relatively large 3D sample volume (approx. 1000 mm^3). The results therefore represent an average over a large number of gel building blocks which makes this technique an interesting addition to the image analysis.

With increasing WPI concentration the initial slope of the normalized polarization versus spin echo length curve changes. The initial slope in this graph represents the volume fraction of WPI inside the gel building blocks. A steeper slope at increasing protein concentration (from 0.06 to 0.15 $g_{protein}$ / g_{water} WPI) reflects the increased volume fraction (higher protein density) of WPI inside the gel building blocks. Additionally, the observed decrease in total scattering (higher plateau value of normalized polarization at high spin echo length) with increasing WPI concentration suggests a decrease in the size of the typical gel building blocks.

To quantify these changes, we have fitted the data in Figure 5.5B to equation 5.1. The obtained results are shown in Table 5.1 together with the results from CLSM. With increasing WPI concentration the size of the random inhomogeneity (a) and the correlation length of the system (ξ) decrease and the Hurst exponent increases. Low Hurst exponent at low protein concentrations indicate an open structure where protein is non-homogeneously distributed. At increasing WPI concentration the Hurst exponent is closer

to 0.5 which indicates that the protein is more homogeneously distributed inside the sample (on the length scale probed by SESANS) which is in line with the visual observations of the CLSM images as shown in Figure 5.4. The correlation length obtained from SESANS are in agreement with results obtained from CLSM. The agreement between the two techniques validates the obtained results from each separate technique and indicates that each of the techniques can be used to obtain structural characteristics of protein gels. More than that, both techniques are complementary and together allowed a full characterization of the WPI gel structures (as shown in Table 5.1) over the length scale 30 nm to several cm which in this research serves as a basis for the analysis of the gel structures in mixed gels.

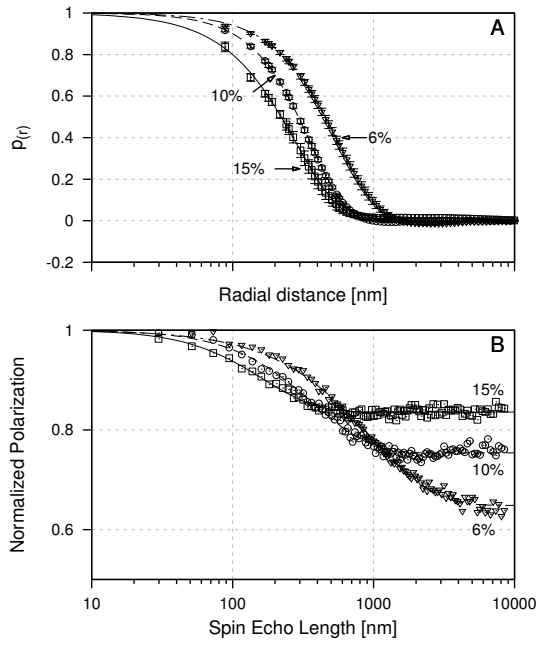

Figure 5.5 Density correlation and normalized polarization function for WPI gels containing 0.06 (▽), 0.10 (○) and 0.15 (□) $g_{protein}$ / g_{water} . CLSM images of these samples are shown in Figure 5.4. Graph A: Average density correlation from image analysis. Graph B: Normalized polarization from SESANS. Lines show fits used for data analysis for CLSM image analysis (equation 5.13) and SESANS (equation 5.1)

Table 5.1 Characteristic values describing the WPI gel structure obtained from CLSM image analysis and SESANS analysis for single WPI gels at three different protein concentrations. Standard deviations are given for values where several independent measurements were taken.

	Parameter	Source	Interpretation	Unit	6%	10%	15%
CLSM	Correlation length (ξ)	Equation 5.13	Characteristic length scale of areas with high fluorescent densities	nm	569.5 ±18.7	360.6 ±5.7	285.9 ±21.9
	Diameter of gel building blocks	First minima from equation 5.12	The diameter of the spherical equivalent of the gel building blocks as visible in CLSM images	nm	2377 ±418	1368 ±79.2	1343 ±384
	Gel pore size	Width negative peak from equation 5.12	The diameter of a spherical equivalent of the gel pores (protein depleted areas).	nm	6856 ± 168	2794 ± 600	--
	Building block distance	First maxima from equation 5.12	Typical distance between two gel building blocks, center to center	nm	4346 ±1985	1878 ±111	1804 ±270
	Exponent β	Equation 5.13	Arrangement of protein inside gel building blocks (related to structure)	--	1.61 ±0.08	1.76 ±0.01	1.43 ±0.04
SESANS	Scattering power (Σ_t)	Equation 5.1	Average how often a neutron scatters when passing the sample		0.43	0.28	0.18
	Size of (intermediate) gel building blocks (a)	Equation 5.2	Size of random inhomogeneity in sample	nm	1055.2	309.6	116.4
	Hurst exponent (H)	Equation 5.2	Related to fractal dimension of gel	--	0.069	0.29	0.45
	Correlation Length (ξ)	Equation 5.4	Sample specific typical length scale	nm	420.9	381.3	216.1

Gel microstructure of mixed gels

Figure 5.6 shows CLSM images of mixed gel structures where globular proteins (WPI or SPI) were gelled in the presence or absence of gelatin. The first column of Figure 5.6 shows single globular protein gels (made of only WPI or SPI). The second and third columns show mixed gels where the globular protein was gelled in the presence of 0.02 or 0.06 $g_{protein}$ / g_{water} gelatin or gelatin hydrolysate. Gelatin was labelled covalently using FITC, while in addition the total protein was labelled non-covalently using Rhodamine B. Throughout the experiments, it was observed that Rhodamine B had a significantly lower affinity for gelatin compared to globular proteins. This is based on the absence of hydrophobic patches in gelatin needed for Rhodamine to bind as already argued in chapter 4 and elsewhere for other systems [61]. In the analysis of mixed gels, this difference can be used to differentiate between the two proteins. The Rhodamine B signal will therefore be used to identify the location of WPI or SPI and the signal from FITC to identify the location of gelatin. For gelatin hydrolysates FITC labelling was not used because this would increase their molecular mass by more than 10%. For these samples only the Rhodamine B signal (WPI) is shown.

Upon the addition of gelatin type A the gel structure of the globular proteins (SPI and WPI shown in red in Figure 5.6) changes and a more pronounced phase separation is observed. With increasing gelatin A concentration the globular proteins become more and more concentrated in their phase and gelatin A is mainly found in the globular protein depleted phase (the globular protein gel pores). Analysis of images at other magnifications (results not shown) showed that at all protein concentrations and protein mixing ratios both phases were continuous throughout the entire sample volume. A similar result was found for the WPI / gelatin type B mixed gels. Comparison of the microstructural data to rheological results showed that the increase in gel coarseness is accompanied by a decrease in G' of the mixed gels. This effect, however, seems independent of the absolute length scale (size) of the phase separated domains as WPI / gelatin A and SPI / gelatin A have similar rheological behavior but differently sized phase separated domains. Figure 5.6 also contains CLSM images of WPI gels prepared in the presence of gelatin type A hydrolysates. Here the microstructure was similar to that of the pure WPI gel and no enhanced phase separation could be observed. The presence of gelatin hydrolysate had no significant effect on the microstructure of the WPI gels which is in line with the observation that the storage moduli of the WPI gels were not decreased by the addition of hydrolysates.

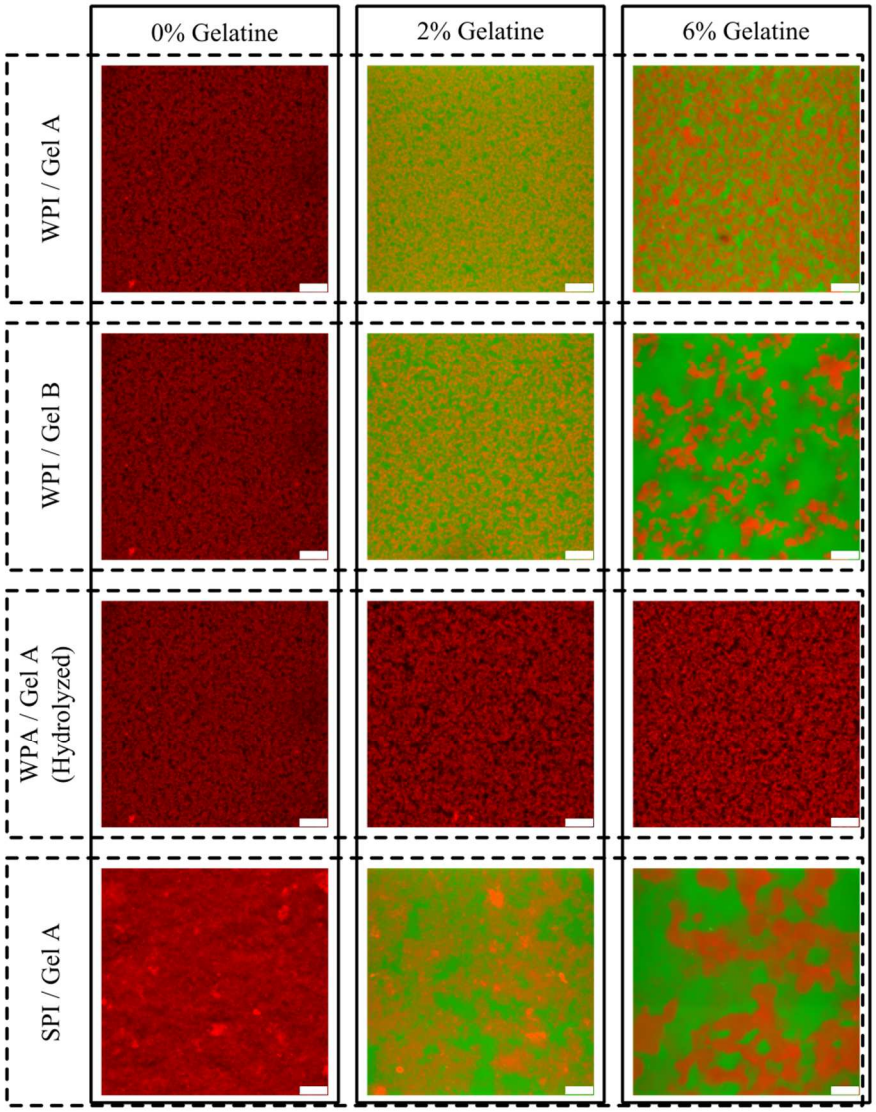

Figure 5.6 CLSM images of single and mixed globular protein (WPI or SPI) at room temperature after being heated to 95 °C. All gels contain 0.06 $g_{protein}$ / g_{water} globular protein (WPI / SPI). The location of globular proteins is shown in red and gelatin in green (details given in text). The first column contains reference images of globular protein gels without added gelatin. Within each row gelatin concentration increases from 0 to 0.02 and 0.06 $g_{protein}$ / g_{water} gelatin. Scalebars are 7.5 µm

For mixed systems the fluorescent signals in CLSM for WPI (Rhodamine B) and gelatin (FITC) were acquired separately. For visualization purposes this allows to display them in different colors as shown in Figure 5.6. For image analysis this additionally permits the analysis of the spatial arrangement of each protein, or better each channel, separately. As

an example, Figure 5.7 shows an overlay and CLSM images of the two channels separately for a sample containing 0.06 $g_{protein}$ / g_{water} WPI and 0.02 $g_{protein}$ / g_{water} gelatin type B. The images of the separate channels show that areas high in WPI concentration are low concentrated in gelatin and the other way round. The two images are in fact negative images of each other which is a direct indication of segregative phase separation between the two proteins. For image analysis this means that one image can be transferred into the other by inversion. Inversion (as all linear modifications of the intensity values) of an image before autocorrelation has no effect on the results from autocorrelation [52]. Thus for phase separated systems as those shown in Figure 5.7 no differences between the results from image analysis for the two channels are expected.

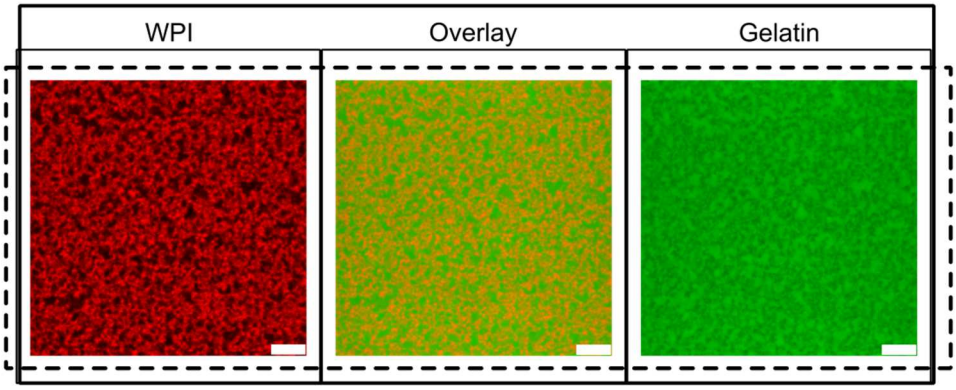

Figure 5.7 CLSM images from the Rhodamine channel (WPI), the FITC channel (gelatin B) and an overlay of a sample containing 0.06 $g_{protein}$ / g_{water} WPI and 0.02 $g_{protein}$ / g_{water} gelatin type B (scale-bar 7.5 µm)

Figure 5.8A shows the density correlation function for single and mixed WPI gels at constant WPI concentration. As expected the density correlation functions from the two channels overlay. The shift of the correlation functions for gels with added gelatin to higher length scales indicates an increase in the correlation lengths of the systems which is more pronounced for gelatin type B compared to type A mixed gels. Figure 5.8B shows the first minima (location thereof in autocorrelation function indicated with an arrow in Figure 5.8A, representing the diameter of gel building blocks) of the density correlation function *p(r)* for a number of mixed gels. As expected also here no significant difference between the results from the two channels was obtained. The same result was found when comparing the other gel characteristics such as e.g. correlation lengths or distance between aggregates (results not shown). It is thus sufficient to analyze one of the channels in mixed systems to obtain the characteristic parameters such as e.g. gel building block size in mixed gels. In the following we will therefore only discuss the results obtained from non-covalently staining proteins with Rhodamine B.

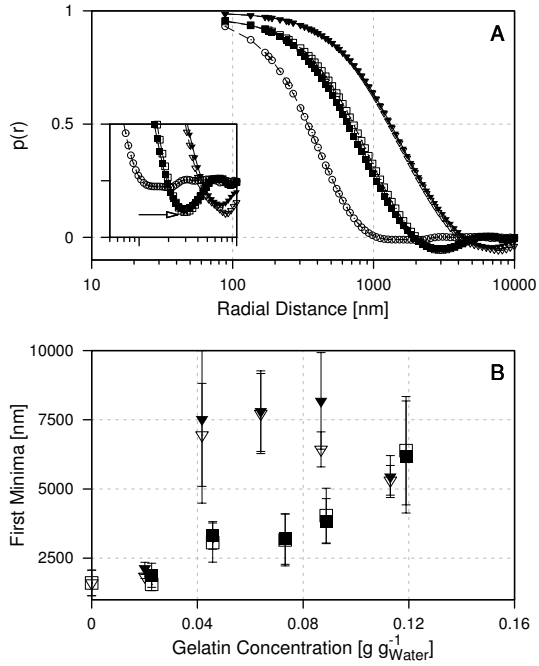

Figure 5.8 Graph A: Separate density correlation functions from the Rhodamine channel (WPI, open symbols) and FITC channel (gelatin, closed symbols) for gels containing 0.06 $g_{protein}$ / g_{water} WPI and no gelatin (reference, ○) and mixed gels containing 0.06 $g_{protein}$ / g_{water} WPI and 0.06 $g_{protein}$ / g_{water} gelatin type A (□) or type B (▽). Insert shows magnification of the area containing first minima (indicated by arrow). Graph B: First minima corresponding to typical building block diameter obtained from image analysis of CLSM images for mixed gels containing 0.06 $g_{protein}$ / g_{water} WPI and varying concentration of gelatin type A (□,■) or gelatin type B (▽,▼). Results from Rhodamine channel (WPI) are shown with open symbols and from FITC channel (gelatin) with closed symbols.

Figure 5.9 displays the average size of the gel building blocks for WPI gels prepared in the presence of gelatin type A (Figure 5.9A1), gelatin type B (Figure 5.9B1) or hydrolyzed gelatin type A (Figure 5.9A2). For WPI / gelatin type A at 0.06 $g_{protein}$ / g_{water} WPI a constant increase of the gel building block size over the whole range of analyzed gelatin concentrations was observed. The same result was found at 0.1 $g_{protein}$ / g_{water} WPI and increasing gelatin type A concentration even though here the effect was less pronounced. The presence of hydrolyzed gelatin type A (Figure 5.9A2) on the other hand did not have an influence on the size of the gel building blocks of WPI. At both analyzed WPI concentrations (0.06 and 0.1 $g_{protein}$ / g_{water}) the building blocks has a size around 1.6 µm independent of the concentration of hydrolyzed gelatin type A. The building block size of WPI gels formed in the presence of gelatin type B (Figure 5.9B1) increased strongly at low

gelatin type B concentrations (< 0.05 $g_{protein}$ / g_{water}). At 0.06 $g_{protein}$ / g_{water} WPI the gel building block size showed a maximum around 0.06 $g_{protein}$ / g_{water} gelatin while at 0.1 $g_{protein}$ / g_{water} WPI it increased over the whole range of analyzed gelatin type B concentrations. Parallel to the building block sizes also the correlation length, the distances between the gel domains and the sizes of the gel pores increased for the WPI / gelatin A and the WPI / gelatin B mixed gels (results not shown). For gel structures one typically summarizes these changes with the term “increasing gel coarseness” which will be used from this point onwards for the ease of reading.

In comparison, gelatin type B had a more pronounced effect on the gel coarseness than gelatin type A at comparable concentrations. This is similar to the effect of the change in G’ of the WPI gels (see Figure 5.3). In chapter 2 and 3 we presented a detailed characterization of these research materials in terms of their molecular sizes, their molecular interactions and also on the interaction of gelatin with native and aggregated whey protein. At solvent conditions as those used here (pH 7, ionic strength 150 mM) gelatin and whey protein (as well as whey protein aggregates) were shown to interact mainly via hard body interactions. Also, the number averaged molecular weight of gelatin type A and type B were comparable. The differences between gelatin type A and type B are most probably due to the presence of relatively more higher molecular weight fractions in gelatin type B than gelatin type A (see Figure 5.14) which can lead to an enhanced phase separation between aggregates of WPI and gelatin during gelation. We will discuss the relationship between the (molecular) size of proteins, changes in size during gelation and the effect on phase separated microstructures further on.

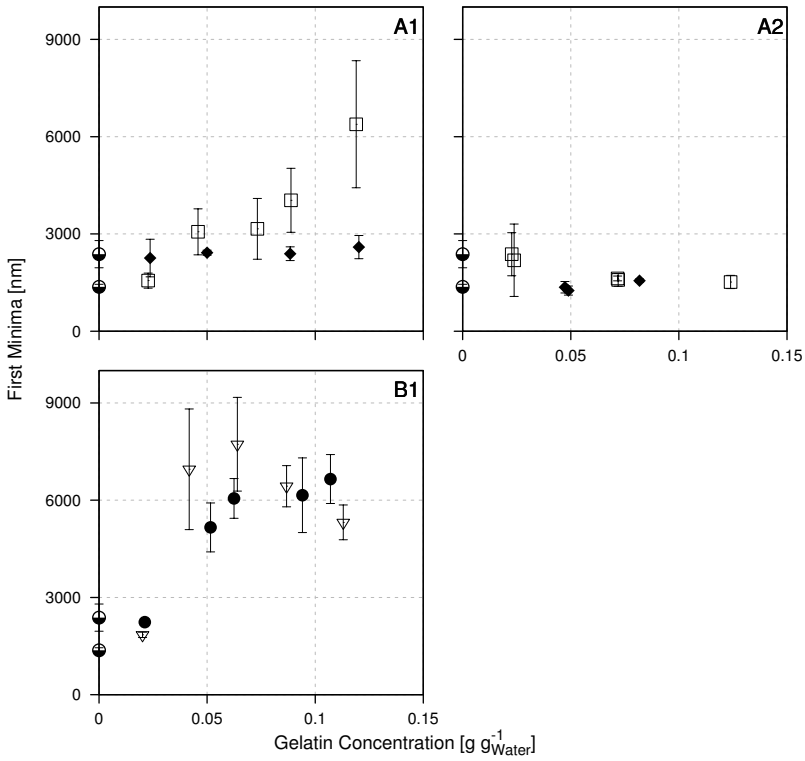

Figure 5.9 Size of the gel building blocks (first minimum in *p(r)* from image analysis) for gels containing 0.06 $g_{protein}$ / g_{water} (open symbols) or 0.1 g / g_{water} (closed symbols) WPI and different gelatin. A1: gelatin type A; A2: hydrolyzed gelatin type A; B1: gelatin type B; symbols at zero gelatin (◒) represent pure WPI gels containing 0.06 and 0.1 g / g_{water} WPI

To further analyze the differences in WPI gel network structures formed in the presence of gelatin type A or hydrolyzed gelatin type A we have performed SESANS measurements on these mixed WPI gels. The length scale over which SESANS is able to detect structural elements is in the range 20 nm to several µm. The length scale of gelatin gels is typically one order of magnitude lower [62]. For SESANS measurements, it is therefore expected that the presence of gelatin does not influence the scattering obtained from the WPI gel. To test this we analyzed a mixed protein gel containing 0.06 $g_{protein}$ / g_{water} WPI and 0.1 $g_{protein}$ / g_{water} gelatin type A at room temperature and at 40 °C. Figure 5.10 shows the

normalized polarization versus spin echo length results at both temperatures. The formation of an ordered structure (gel at room temperature) from a liquid (at 40 °C) where molecules are randomly distributed would significantly change the scattering results if the obtained structures were within the probed length scale of SESANS. No differences between the two measurements could be observed demonstrating that gelatin indeed forms a gel below the length scale probed by SESANS. The gelatin gel can therefore be assumed to be "invisible" in SESANS measurements. However, the presence of gelatin is expected to reduce the neutron scattering length density contrast between the WPI and the solvent phase (gelatin is located in the solvent). Accordingly we observed a decrease in the total scattering of mixed gels compared to the single WPI gels (higher normalized polarization at high spin echo length values in Figure 5.10 compared to Figure 5.5) upon gelatin addition.

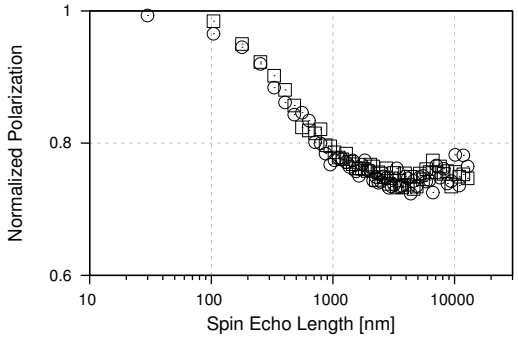

Figure 5.10 Normalized polarization *P(z)* versus spin echo length from SESANS at 40 °C (○) and at room temperature (□) for a sample containing 0.06 $g_{protein}$ / g_{water} WPI and 0.1 $g_{protein}$ / g_{water} gelatin type A.

In conclusion, the scattering signal from SESANS in mixed protein gels can be attributed to the structure of the WPI gel when keeping in mind the effect that gelatin has on the scattering length density contrast between WPI and the solvent phase.

Figure 5.11 shows the normalized polarization for WPI gels prepared in the presence of gelatin type A (Figure 5.11A) or hydrolyzed gelatin type A (Figure 5.11B). For WPI gels prepared in the presence of 0.04 $g_{protein}$ / g_{water} gelatin type A the scattering intensity (normalized polarization value at high spin echo length) is below that expected for the pure WPI gel at this concentration. As discussed before, addition of gelatin is expected to lead to a lower total scattering (higher values for normalized polarization). However, the scattering intensity is also related to the size of the typical building blocks. CLSM results showed an increase in the size of the gel building blocks for WPI gels with added gelatin (see Figure 5.9) which leads to a higher scattering intensity. For the sample containing 0.04 $g_{protein}$ / g_{water} gelatin type A the increase in size seems to have a stronger effect on

the scattering intensity than the decrease in neutron scattering contrast. At higher gelatin concentration (0.07 $g_{protein}$ / g_{water}) the decreasing scattering contrast and increasing building block sizes balanced each other out and the measured scattering intensity was close to that of the pure WPI gel. For mixed WPI gels containing hydrolyzed gelatin type A (Figure 5.11B) a decrease in scattering intensity was observed for both tested concentrations of hydrolyzed gelatin. This suggests that no large changes in the typical size of the building blocks occurred, as also concluded from the results of CLSM. The decrease in scattering intensity indicates that gelatin reduced the contrast between the WPI gel and the (gelatin containing) solvent, as expected.

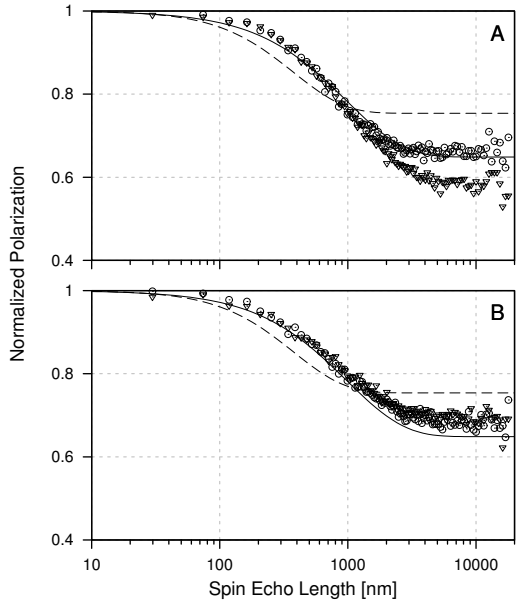

Figure 5.11 Normalized polarization versus spin echo length from SESANS measurements of mixed samples containing 0.06 $g_{protein}$ / g_{water} WPI and 0.04 (▽) or 0.07 (○) $g_{protein}$ / g_{water} gelatin type A (graph A) or hydrolyzed gelatin type A (graph B). Lines represent behavior of pure data (from Figure 5.5B) containing 0.06 $g_{protein}$ / g_{water} (solid line) or 0.1 $g_{protein}$ / g_{water} WPI (dashed line)

Besides this information about the changes in the size of the gel building blocks SESANS also allows an estimation of the density of the primary building blocks via the initial slope of the normalized polarization over spin echo length curve [50]. For pure WPI gels this slope increased with increasing protein concentration (cf. Figure 5.5). The curves of the pure WPI gel prepared at 0.06 $g_{protein}$ / g_{water} WPI and the mixed gels containing the same

WPI concentration overlay in the range between 50 to approximately 1000 nm. As a comparison, the curve for a single WPI gel prepared at 0.1 $g_{protein}$ / g_{water} WPI is shown in Figure 5.11. The initial slope is significantly steeper for the single gel prepared at 0.1 $g_{protein}$ / g_{water} WPI compared to single and mixed gels prepared at 0.06 $g_{protein}$ / g_{water}. This suggests that on a length scale below 1 µm gel building blocks of mixed WPI gels have similar structures to single WPI gels prepared at the same nominal protein concentration (0.06 $g_{protein}$ / g_{water} WPI). At higher length scales, however, mixed gels containing gelatin type A vary in their gel structure from pure WPI gels (discussed before in CLSM analysis). In the SESANS measurements these changes were observable in the obtained Hurst exponent (equation 5.2, related to the fractal dimension) for mixed systems. The Hurst exponent of pure WPI gels and WPI gels with added hydrolyzed gelatin A were close to 0 while those for WPI gels with added gelatin type A were close to 0.4. Although it is questionable whether one should analyze WPI gels or phase separated mixed gels in terms of fractals [2, 58], these changes in the Hurst exponent suggest a different spatial arrangement of proteins in the mixed WPI gels compared to pure WPI gels., in line with the results from CLSM.

Effect of gelatin size on the formation of WPI gels

So far we have been able to strongly suggest a relationship between microstructural changes in globular protein gels and their rheological response. The relationship originates from segregative phase separation between gelatin and WPI during gelation (see e.g. Figure 5.8). This segregative phase separation leads to a confinement of both proteins in their separate phases, where each phase is depleted of the other protein. In the presence of hydrolyzed gelatin A such segregative phase separation and according changes in the gel microstructure and related rheological response, were not observed.

In order to address the different effects of gelatin versus hydrolyzed gelatin on the network structure of globular protein gels, we will first discuss the gelation in pure globular protein (WPI) systems. Heat induced gelation of WPI reflects a complex interplay between aggregation of whey proteins and a concomitant phase separation between these aggregated proteins and the water phase. The process is schematically shown in four steps in Figure 5.12A. In the initial step of gelation a homogeneous protein solution (Figure 5.12A.1) is heated above the denaturation temperature of whey proteins leading to the formation of primary aggregates [63] (Figure 5.12A.2). These aggregates are only stable once they are above a certain size which is typically around 30 to 100 nm dependent on multiple factors such as solvent conditions and gelation kinetics [64, 65]. At the solvent conditions used in this study (pH 7, 150 mM NaCl), aggregates separate from

the solvent phase (referred to as micro-phase separation [58]) as shown in Figure 5.12A.3. This is suggested to occur via spinodal decomposition [66] which is arrested in an early stage by the interconnection of the gel building blocks inside the WPI rich phase (Figure 5.12A.4). This implies a formation of a bi-continuous structure of WPI rich (gel) and solvent rich (gel pores) phases. This microstructure (see also Figure 5.6) is typical for globular protein gels at conditions where electrostatic repulsion is screened [58] (which was the case in this study).

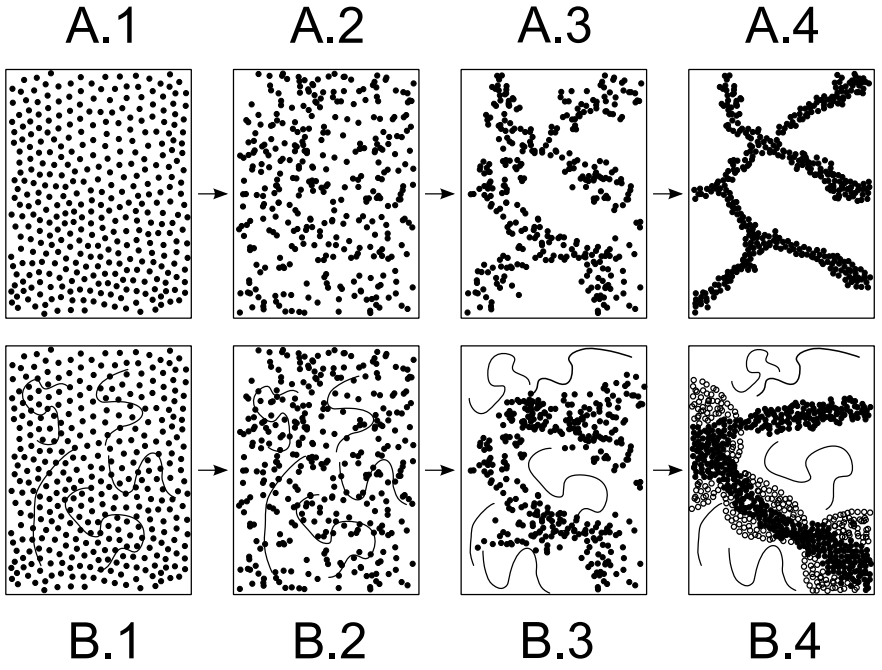

Figure 5.12 Schematic representation of gelation for pure WPI gels (row A) and WPI gels with added gelatin (row B). WPI is represented by black spheres and gelatin as a linear polymer. In scheme B.4 closed spheres represent situation at low total protein concentration and open circles indicate changes upon increasing the total protein concentration.

The proposed effect how the presence of gelatin impacts the WPI gel formation is shown in Figure 5.12B. As for the single WPI gels the initial stage is a homogeneously mixed solution containing WPI and gelatin (Figure 5.12B.1). Upon heat induced denaturation of whey proteins these start to aggregate (Figure 5.12B.2) while gelatin molecules stay soluble and do not participate in this aggregation. SESANS results suggested that the density of the primary aggregates in mixed gels is identical to that for pure WPI gels (see initial slope in Figure 5.11). This suggests that the primary aggregates (and possibly also secondary, as SESANS indicated changes only above 1 μm) were formed

while the system was still completely mixed and thus WPI at its original concentration (which in the case of SESANS measurements was 0.06 $g_{protein}$ / g_{water}).

During further aggregation, the size of the intermediate gel building blocks (or whey protein aggregates) increases. Since the size of the gelatin molecules stays constant the formation of even larger WPI aggregates changes the size ratio between globular protein (aggregates) and gelatin

This size ratio (q) is an important parameter in determining whether mixed systems phase separate or stay mixed and can be expressed by:

$$q = \frac{a_G}{a_{GP}} \qquad 5.16$$

where a_G is the effective radius of the gelatin molecules and a_{GP} the effective radius of the globular proteins (or their aggregates during gelation). As discussed in chapter 2 and chapter 3 gelatin and WPI or whey protein aggregates are well approximated as having mainly hard body interactions at neutral pH and ionic strength > 100 mM. The phase behavior of such systems as a function of the size ratio q can be approximated using a virial approach. Figure 5.13 shows the theoretical critical volume fraction as a function of q for a binary hard sphere mixture. The critical volume fraction in Figure 5.13 represents the point in a phase diagram with the lowest total particle (or here protein) volume fraction where phase separation is expected (critical point in a phase diagram). Around q = 1 binary mixed systems show a high co-solubility which decreases with increasing and decreasing q-values. The q-values of the mixed WPI / gelatin type A and type B and WPI / hydrolyzed gelatin type A before gelation occurs are added to Figure 5.13. The q-values were based on the effective molecular size of the globular proteins and gelatin from chapters 2 and 3. For hydrolyzed gelatin the size was estimated based on SEC results shown in Figure 5.14 which also indicates the reverse size ratio between WPI and gelatin compared to WPI and hydrolyzed gelatin. The arrow indicates the proposed change in q during the gelation of globular proteins (formation of larger globular protein aggregates).

The two mixtures where the presence of gelatin altered the globular protein microstructure are characterized by q > 1 while for the WPI / hydrolyzed gelatin A sample q << 1, where the microstructure of the mixture was equal to that of the pure globular protein gel. Samples where the globular protein microstructure was altered crossed the point q = 1 and subsequently a region with decreasing co-solubility (higher possibility for phase separation) during globular protein gelation. It is proposed that this passing of a region with high co-solubility and subsequent passing a region with reducing co-solubility signifies phase separation during globular protein gelation. If this phase separation occurs

deeper into the 2-phase region, an increase in gel coarseness is expected (increase in size of gel domains, distance between gel domains and gel pores), as schematically shown in Figure 5.12B.4.

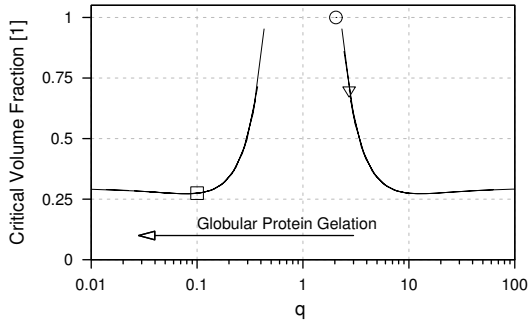

Figure 5.13 Critical volume fraction calculated for hard sphere systems as a function of the particle size ratio *q*. The location of WPI / gelatin A (○) and WPI / gelatin B (▽) systems where increased phase separation was observed and the WPI / hydrolyzed gelatin A where the microstructure of WPI was similar to that of pure WPI (□) are indicated in the graph. The arrow indicates the direction the size ratio *q* changes upon gelation of WPI. Graph re-printed from chapter 3.

We have arrived at the same conclusion when investigating gelatin gelation in the presence of globular proteins in chapter 4. This suggests this effect to be general for these mixed gel systems. Yet, when comparing the effects of phase separation on the rheological response of mixed gelatin gels from chapter 4 with that of globular protein / gelatin gels presented in this chapter, the effects seem contradictory. Phase separation due to the presence of (non-gelling) secondary proteins led to an increase in G' for mixed gelatin gels while in globular protein gels the storage modulus decreases upon the occurrence of (increased) phase separation. These differences are most likely based on different gelling mechanisms. Gelatin exhibits isotropic gelation and for a mixed gelatin gel, phase separation will mainly have an impact on the water distribution and therefore respective concentrations of the gelatin, but to a lower degree on the gel structure. The globular protein gels in the current study, however, were prepared at conditions where electrostatic interactions are screened and where their gelation mechanism includes micro-phase separation. The presence of gelatin in this systems mainly altered the structure of the already phase separated, bi-continuous globular protein gel but did not lead to a gelation of WPI at simply increased protein concentration.

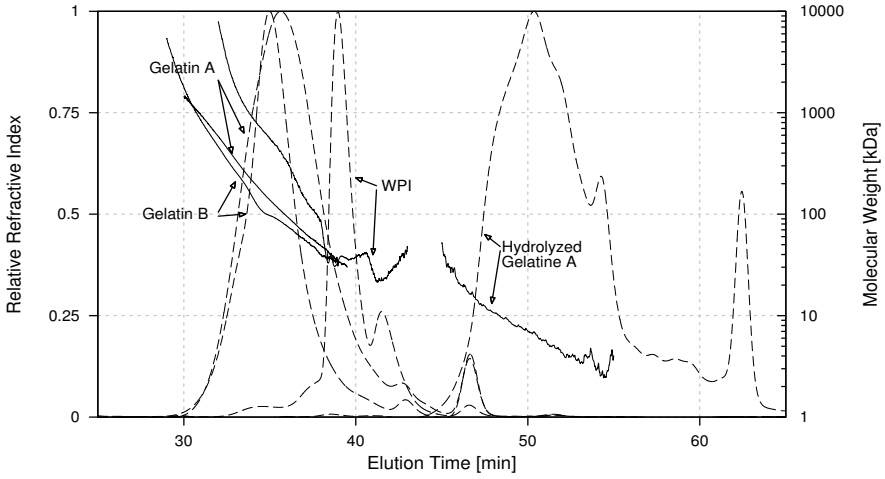

Figure 5.14 SEC-MALLS elution profile containing the relative refractive index (dashed lines, left vertical axis) and molecular weight from light scattering (solid lines, right vertical axis) for WPI, gelatin type A and type B taken from chapter 2 and hydrolyzed gelatin type A as indicated in the graph.

Conclusion

Rheological methods together with microstructural analysis using CSLM and SESANS was shown to selectively probe the structure of WPI gels (or more general globular protein gels) in the presence of gelatin. This allowed the stepwise analysis of the formation of mixed globular protein / gelatin gels. We focused on the first step of the sequential gelling step of globular protein / gelatin gels which will serve as an important basis for researches aiming to understand the properties of the final gels (where both proteins are gelled). In the case of mixed WPI gels, microstructural changes due to the presence of gelatin during the gelation of globular proteins were directly related to a reduction in storage modulus G' of the WPI gels. The mechanism leading to these changes was suggested to be an enhanced segregative phase separation at a late stage of WPI gelation between WPI gel building blocks and the solvent phase containing gelatin which only occurred when gelatin molecules had an effective diameter above that of the globular proteins.

Acknowledgements

We would like to thank Chris P. Duif, Delft University, for his help and expertise in performing the SESANS measurements and Irene ter Laak for her help with the experiments including soy protein isolate.

References

1. Axelos, M.A.V. and M. Kolb, *Crosslinked biopolymers: Experimental evidence for scalar percolation theory.* Physical Review Letters, 1990. **64**(12): p. 1457-1460.
2. Bremer, L.G.B., *Fractal aggregation in relation to formation and properties of particle gels*. 1992, PhD Thesis Wageningen University.
3. Dickinson, E., *On gelation kinetics in a system of particles with both weak and strong interactions.* Journal of the Chemical Society, Faraday Transactions, 1997. **93**(1): p. 111-114.
4. Gabriele, D., B. De Cindio, and P. D'Antona, *A weak gel model for foods.* Rheologica Acta, 2001. **40**(2): p. 120-127.
5. Linden, E.v.d. and E.A. Foegeding, *CHAPTER 2 - Gelation: Principles, Models and Applications to Proteins*, in *Modern Biopolymer Science*. 2009, Academic Press: San Diego. p. 29-91.
6. Çakır, E., C.R. Daubert, M.A. Drake, C.J. Vinyard, G. Essick, and E.A. Foegeding, *The effect of microstructure on the sensory perception and textural characteristics of whey protein/κ-carrageenan mixed gels.* Food Hydrocolloids, 2012. **26**(1): p. 33-43.
7. Çakir, E. and E.A. Foegeding, *Combining protein micro-phase separation and protein-polysaccharide segregative phase separation to produce gel structures.* Food Hydrocolloids, 2011. **25**(6): p. 1538-1546.
8. Çakır, E., S.A. Khan, and E.A. Foegeding, *The effect of pH on gel structures produced using protein–polysaccharide phase separation and network inversion.* International Dairy Journal, 2012. **27**(1–2): p. 99-102.
9. Altay, F. and S. Gunasekaran, *Gelling properties of gelatin–xanthan gum systems with high levels of co-solutes.* Journal of Food Engineering, 2013. **118**(3): p. 289-295.
10. Anderson, V.J. and R.A.L. Jones, *The influence of gelation on the mechanism of phase separation of a biopolymer mixture.* Polymer, 2001. **42**(23): p. 9601-9610.
11. Cavallieri, A.L.F., N.A.V. Fialho, and R.L. Cunha, *Sodium caseinate and κ-carrageenan interactions in acid gels: Effect of polysaccharide dissolution temperature and sucrose addition.* International Journal of Food Properties, 2011. **14**(2): p. 251-263.
12. Gaaloul, S., S.L. Turgeon, and M. Corredig, *Phase behavior of whey protein aggregates/κ-carrageenan mixtures: Experiment and theory.* Food Biophysics, 2010. **5**(2): p. 103-113.
13. Haug, I.J., A.M.H. Carlsen, G.E. Vegarud, T. Langsrud, and K.I. Draget, *Textural Properties of Beta-lactoglobulin – Sodium Alginate Mixed Gels at Large Scale Deformation.* Journal of Texture Studies, 2013. **44**(1): p. 56-65.

14. Lorén, N. and A.-M. Hermansson, *Phase separation and gel formation in kinetically trapped gelatin/maltodextrin gels.* International Journal of Biological Macromolecules, 2000. **27**(4): p. 249-262.
15. Nono, M., T. Nicolai, and D. Durand, *Gel formation of mixtures of κ-carrageenan and sodium caseinate.* Food Hydrocolloids, 2011. **25**(4): p. 750-757.
16. Ould Eleya, M.M. and S.L. Turgeon, *Rheology of κ-carrageenan and β-lactoglobulin mixed gels.* Food Hydrocolloids, 2000. **14**(1): p. 29-40.
17. Picone, C.S.F. and R.L. da Cunha, *Interactions between milk proteins and gellan gum in acidified gels.* Food Hydrocolloids, 2010. **24**(5): p. 502-511.
18. Pires Vilela, J.A., Â.L.F. Cavallieri, and R. Lopes da Cunha, *The influence of gelation rate on the physical properties/structure of salt-induced gels of soy protein isolate-gellan gum.* Food Hydrocolloids, 2011. **25**(7): p. 1710-1718.
19. Ribeiro, K.O., M.I. Rodrigues, E. Sabadini, and R.L. Cunha, *Mechanical properties of acid sodium caseinate-κ-carrageenan gels: Effect of co-solute addition.* Food Hydrocolloids, 2004. **18**(1): p. 71-79.
20. Shrinivas, P., S. Kasapis, and T. Tongdang, *Morphology and mechanical properties of bicontinuous gels of agarose and gelatin and the effect of added lipid phase.* Langmuir, 2009. **25**(15): p. 8763-8773.
21. Spotti, M.J., M.J. Perduca, A. Piagentini, L.G. Santiago, A.C. Rubiolo, and C.R. Carrara, *Does dextran molecular weight affect the mechanical properties of whey protein/dextran conjugate gels?* Food Hydrocolloids, 2013. **32**(1): p. 204-210.
22. Brink, J., M. Langton, M. Stading, and A.-M. Hermansson, *Simultaneous analysis of the structural and mechanical changes during large deformation of whey protein isolate/gelatin gels at the macro and micro levels.* Food Hydrocolloids, 2007. **21**(3): p. 409-419.
23. Chronakis, I.S. and S. Kasapis, *Structural properties of single and mixed milk/soya protein systems.* Food Hydrocolloids, 1993. **7**(6): p. 459-478.
24. Comfort, S. and N.K. Howell, *Gelation properties of soya and whey protein isolate mixtures.* Food Hydrocolloids, 2002. **16**(6): p. 661-672.
25. Donato, L., E. Kolodziejcyk, and M. Rouvet, *Mixtures of whey protein microgels and soluble aggregates as building blocks to control rheology and structure of acid induced cold-set gels.* Food Hydrocolloids, 2011. **25**(4): p. 734-742.
26. Fitzsimons, S.M., D.M. Mulvihill, and E.R. Morris, *Segregative interactions between gelatin and polymerised whey protein.* Food Hydrocolloids, 2008. **22**(3): p. 485-491.
27. Onwulata, C.I., A.E. Thomas-Gahring, and J.G. Phillips, *Physical properties of mixed dairy food proteins.* International Journal of Food Properties, 2014. **17**(10): p. 2241-2262.

28. Pang, Z., H. Deeth, P. Sopade, R. Sharma, and N. Bansal, *Rheology, texture and microstructure of gelatin gels with and without milk proteins.* Food Hydrocolloids, 2014. **35**: p. 483-493.
29. Picone, C., K. Takeuchi, and R. Cunha, *Heat-Induced Whey Protein Gels: Effects of pH and the Addition of Sodium Caseinate.* Food Biophysics, 2011. **6**(1): p. 77-83.
30. Polyakov, V.I., V.Y. Grinberg, and V.B. Tolstoguzov, *Thermodynamic incompatibility of proteins.* Food Hydrocolloids, 1997. **11**(2): p. 171-180.
31. Polyakov, V.I., O.K. Kireyeva, V. Grinberg, and V.B. Tolstoguzov, *Thermodynamic compatibility of proteins in aqueous media. Part. I. Phase diagrams of some water--protein A--protein B systems.* Die Nahrung, 1985. **29**(2): p. 153-160.
32. Polyakov, V.I., I.A. Popello, V. Grinberg, and V.B. Tolstoguzov, *Thermodynamic compatibility of proteins in aqueous media. Part 2. The effect of some physicochemical factors on thermodynamic compatibility of casein and soybean globulin fraction.* Die Nahrung, 1985. **29**(4): p. 323-333.
33. Walkenström, P. and A.-M. Hermansson, *Mixed gels of fine-stranded and particulate networks of gelatin and whey proteins.* Food Hydrocolloids, 1994. **8**(6): p. 589-607.
34. Walkenström, P. and A.-M. Hermansson, *Fine-stranded mixed gels of whey proteins and gelatin.* Food Hydrocolloids, 1996. **10**(1): p. 51-62.
35. Walkenström, P. and A.-M. Hermansson, *High-pressure treated mixed gels of gelatin and whey proteins.* Food Hydrocolloids, 1997. **11**(2): p. 195-208.
36. Ziegler, G.R., *Microstructure of mixed gelatin-egg white gels: Impact on rheology and application to microparticulation.* Biotechnology Progress, 1991. **7**(3): p. 283-287.
37. Ziegler, G.R. and S.S.H. Rizvi, *Predicting the Dynamic Elastic Modulus of Mixed Gelatin-Egg White Gels.* Journal of Food Science, 1989. **54**(2): p. 430-436.
38. van den Berg, L., A.L. Carolas, T. van Vliet, E. van der Linden, M.A.J.S. van Boekel, and F. van de Velde, *Energy storage controls crumbly perception in whey proteins/polysaccharide mixed gels.* Food Hydrocolloids, 2008. **22**(7): p. 1404-1417.
39. van den Berg, L., T. van Vliet, E. van der Linden, M.A.J.S. van Boekel, and F. van de Velde, *Breakdown properties and sensory perception of whey proteins/polysaccharide mixed gels as a function of microstructure.* Food Hydrocolloids, 2007. **21**(5–6): p. 961-976.
40. van den Berg, L., T. van Vliet, E. van der Linden, M.A.J.S. van Boekel, and F. van de Velde, *Serum release: The hidden quality in fracturing composites.* Food Hydrocolloids, 2007. **21**(3): p. 420-432.
41. van den Berg, L., *Texture of food gels explained by combining structure and large deformation properties*. Physics and Physical Chemistry of Foods. 2008: PhD Thesis - Wageningen University.

42. Mosca, A.C., *Designing food structures to enhance sensory responses*, in *Product Design and Quality Management*. 2012, Wageningen University.
43. Mosca, A.C., J.A. Rocha, G. Sala, F. van de Velde, and M. Stieger, *Inhomogeneous distribution of fat enhances the perception of fat-related sensory attributes in gelled foods.* Food Hydrocolloids, 2012. **27**(2): p. 448-455.
44. Mosca, A.C., F. van de Velde, J.H.F. Bult, M.A.J.S. van Boekel, and M. Stieger, *Effect of gel texture and sucrose spatial distribution on sweetness perception.* LWT - Food Science and Technology, 2012. **46**(1): p. 183-188.
45. Mosca, A.C., F.v.d. Velde, J.H.F. Bult, M.A.J.S. van Boekel, and M. Stieger, *Enhancement of sweetness intensity in gels by inhomogeneous distribution of sucrose.* Food Quality and Preference, 2010. **21**(7): p. 837-842.
46. Devi, A.F., R. Buckow, Y. Hemar, and S. Kasapis, *Modification of the structural and rheological properties of whey protein/gelatin mixtures through high pressure processing.* Food Chemistry, 2014. **156**(0): p. 243-249.
47. Renkema, J.M.S., *Formation, Structure and Rheological Properites of Soy Protein Gels*. Physics and Physical Chemistry of Foods. 2001: PhD Thesis - Wageningen University.
48. Urbonaite, V., H.H.J. de Jongh, E.v.d. Linden, and L. Pouvreau, *The origin of water loss from soy protein gels.* Journal of Agriculture and Food Chemistry, 2014. **62**(30): p. 7550-7558.
49. Rekveldt, M.T., W.G. Bouwman, W.H. Kraan, and J. Plomp, *Neutron refraction and transmission studied by SESANS.* Physica B: Condensed Matter, 2004. **350**(1-3 SUPPL. 1): p. e791-e794.
50. Andersson, R., L.F. van Heijkamp, I.M. de Schepper, and W.G. Bouwman, *Analysis of spin-echo small-angle neutron scattering measurements.* Journal of Applied Crystallography, 2008. **41**(5): p. 868-885.
51. Efimova, Y.M., A.A. van Well, U. Hanefeld, B. Wierczinski, and W.G. Bouwman, *On the neutron scattering length density of proteins in H2O/D2O.* Physica B: Condensed Matter, 2004. **350**(1–3, Supplement): p. E877-E880.
52. Robertson, C. and S.C. George, *Theory and practical recommendations for autocorrelation-based image correlation spectroscopy.* Journal of Biomedical Optics, 2012. **17**(8): p. 0808011-0808017.
53. Petersen, N.O., P.L. Höddelius, P.W. Wiseman, O. Seger, and K.E. Magnusson, *Quantitation of membrane receptor distributions by image correlation spectroscopy: concept and application.* Biophysical Journal, 1993. **65**(3): p. 1135-1146.
54. Ako, K., D. Durand, T. Nicolai, and L. Becu, *Quantitative analysis of confocal laser scanning microscopy images of heat-set globular protein gels.* Food Hydrocolloids, 2009. **23**(4): p. 1111-1119.

55. Bos, M.T.A., *The structure of particle gels as studied with confocal microscopy and computer simulations*. 1997, Bos: [S.l.].
56. Urbonaite, V., H.H.J. de Jongh, E. van der Linden, and L. Pouvreau, *Water holding of soy protein gels is set by coarseness, modulated by calcium binding, rather than gel stiffness.* Food Hydrocolloids, 2015. **46**(0): p. 103-111.
57. van der Linden, E. and L.M.C. Sagis, *Isotropic Force Percolation in Protein Gels.* Langmuir, 2001. **17**(19): p. 5821-5824.
58. Ako, K., T. Nicolai, D. Durand, and G. Brotons, *Micro-phase separation explains the abrupt structural change of denatured globular protein gels on varying the ionic strength or the pH.* Soft Matter, 2009. **5**(20): p. 4033-4041.
59. Bremer, L.G.B., B.H. Bijsterbosch, P. Walstra, and T. van Vliet, *Formation, properties and fractal structure of particle gels.* 1993. **46**(C): p. 117-128.
60. Berryman, J.G. and S.C. Blair, *Use of digital image analysis to estimate fluid permeability of porous materials: Application of two-point correlation functions.* Journal of Applied Physics, 1986. **60**(6): p. 1930-1938.
61. Bartasun, P., H. Cieśliński, A. Bujacz, A. Wierzbicka-Woś, and J. Kur, *A Study on the Interaction of Rhodamine B with Methylthioadenosine Phosphorylase Protein Sourced from an Antarctic Soil Metagenomic Library.* PLoS ONE, 2013. **8**(1): p. e55697.
62. Parker, N.G. and M.J.W. Povey, *Ultrasonic study of the gelation of gelatin: Phase diagram, hysteresis and kinetics.* Food Hydrocolloids, 2012. **26**(1): p. 99-107.
63. Donato, L., C. Schmitt, L. Bovetto, and M. Rouvet, *Mechanism of formation of stable heat-induced β-lactoglobulin microgels.* International Dairy Journal, 2009. **19**(5): p. 295-306.
64. Baussay, K., C.L. Bon, T. Nicolai, D. Durand, and J.-P. Busnel, *Influence of the ionic strength on the heat-induced aggregation of the globular protein β-lactoglobulin at pH 7.* International Journal of Biological Macromolecules, 2004. **34**(1–2): p. 21-28.
65. Alting, A.C., M. Weijers, E.H.A. de Hoog, A.M. van de Pijpekamp, M.A. Cohen Stuart, R.J. Hamer, C.G. de Kruif, and R.W. Visschers, *Acid-Induced Cold Gelation of Globular Proteins: Effects of Protein Aggregate Characteristics and Disulfide Bonding on Rheological Properties.* Journal of Agricultural and Food Chemistry, 2004. **52**(3): p. 623-631.
66. Carpineti, M. and M. Giglio, *Spinodal-type dynamics in fractal aggregation of colloidal clusters.* Physical Review Letters, 1992. **68**(22): p. 3327-3330.

CHAPTER 6

Modulating fracture properties of mixed protein systems[7]

ABSTRACT

To design foods with desired textures it is important to understand structure build-up and breakdown. One can obtain a wide range of structures using mixtures of different structuring ingredients such as for example protein mixtures. Mixed soy protein isolate (SPI) / gelatin gels were analyzed for their linear rheological properties, fracture properties and microstructure. The two ingredients were found to form independent networks despite changes in the SPI microstructure, which were attributed to enhanced micro phase separation. It is shown that mixing of SPI and gelatin allows to arrive at a large variety of fracture properties. This provides opportunities for tailoring textures in foods using mixed independent gel networks. The fracture stress of mixed gels corresponded to the fracture stress of the strongest of the two gels. At constant fracture stress, increasing Young's modulus of the mixed independent gels resulted in reduced fracture strain.

[7] This chapter is based on: Ersch, C., ter Laak, I., van der Linden, E., Venema, P., & Martin, A. H. (2015). Modulating fracture properties of mixed protein systems. Food Hydrocolloids, 44, 59-65.

GRAPHICAL ABSTRACT

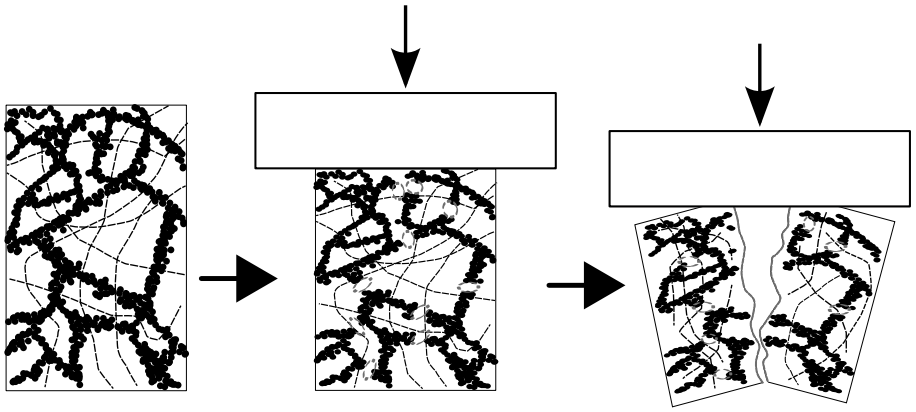

KEYWORDS

fracture, soy protein, gelatin, texture, protein mixture, formulation flexibility

Introduction

The demand for a sustainable production of protein containing products leads to an increased interest in the use of alternative (mostly plant) proteins. This leads to challenges like employing these proteins in existing foods without changing texture, taste and appearance. Because simple replacement of one protein with another usually leads to different properties one needs to resort to mixtures. Studying the fracture properties of mixed protein systems in which one is of plant origin is therefore essential to gain insight on how textural properties can be modulated when introducing new proteins.

To employ biopolymer mixtures in foods, a basic understanding of their interactions and phase behaviour is important. Thermodynamic (in)compatibility of macro constituents is one of the most important and mostly researched topics in mixed systems. Polysaccharide (PS) / protein mixtures as the most commonly researched biopolymer mixture [1-8] usually show phase separation at relatively low (total) polymer concentration [7]. Protein mixtures, on the other hand, are thermodynamically compatible over a wide concentration range dependent on their Osbourne classification, hydrophobicity and surface charges [9] and their similar size (see chapter 3). However, changes such as denaturation, aggregation and/or coil-helix transitions reduce their compatibility with other polymers and interaction with water (i.e. solubility) drastically. This can induce phase separation and therefore structural changes in single and mixed systems [10-12].

The rheological properties and microstructure has been described in detail for several polysaccharide / protein [1-8] and protein / fat [13, 14] mixtures. Van den Berg et al. (2008) and Sala (2007) have linked large deformation properties for two examples of the above mentioned mixtures to sensory attributes by mixing whey protein with different polysaccharides [2] or using different types of proteins in emulsion filled gels [13]. For mixed protein systems, however, these relationships have not yet been established. First steps towards understanding the structure formation and breakdown properties have been undertaken for mixed protein systems containing gelatin and a globular protein. Here, gelatin was shown to gel inside existing networks (gels) of globular proteins whereas the reverse situation is more challenging [15]. Rheological properties of mixed gels ranged from gelatin-like to whey protein [15-18] or egg white-like [19]. Rheological changes were attributed to segregative phase separation driven by polymerization of one of the two proteins (e.g. aggregation or coil to helix transition [12]). However, these results were only obtained for a limited number of proteins (not including plant proteins), protein concentrations and mixing ratios. Therefore, using plant proteins and at the same time mapping rheological properties at all possible concentrations and mixing ratios provides new insight and opportunities for tailoring mixed gelatin / globular protein systems.

Soy protein is one of the most researched and readily available plant storage proteins and therefore, of high interest for research and industrial applications. Only few related studies on mixed gels including soy protein isolate (SPI) have been published [20, 21]. Moreover, the interpretation thereof is often difficult since SPI itself can be considered a mixed system [22-24]. Gelatin, on the other hand, is frequently studied in mixed systems [12, 15, 17-19, 25-34]. Gelatin is thermo-reversible and rheologically well distinguishable from heat induced, globular protein gels such as the brittle and weak (tofu-like) SPI gel. Due to its lack of tertiary structure it compares well to many polysaccharides, when in the coil conformation [7]. Nevertheless, it is thermodynamically compatible with most proteins over a wider range of concentrations other than most polysaccharides [35].

The objective of this study is to map and understand the origin of the fracture properties of mixed gelatin / SPI gels. Differential scanning calorimetry, small deformation measurements and microscopy are combined to gain better understanding of the structure build-up of mixed gelatin / soy protein gels and its relation with fracture properties. These results will help one to employ protein mixtures of plant origin in designing foods.

Material and Methods

Material

Defatted soybean flour was obtained from Cargill having ~50% w/w protein. Pork skin gelatin type A was generously provided by Rousselot BVBA (Ghent, Belgium) having a nominal bloom strength of 150 (determined by manufacturer following a standardized procedure), a protein content of 89.6% (Kjeldahl, N-factor 5.5), an isoelectric point around 8 (Isoelectric focusing and QC-RLT) and negligible amounts of salts (ICP-AES). Chemicals were obtained from Sigma Aldrich (St Louis, MO, USA) and were of analytical grade. They were used without any further purification using demineralized water (conductivity 1.5 µS/cm).

Soy protein isolate and gelatin stock solution preparation

Soy protein isolate (SPI) was prepared by isoelectric precipitation and subsequent washing steps as described in literature [36]. The extracted SPI was kept as solution (pH 7) and had a protein content of 11% (Kjeldahl, N-factor 6.38). For microbiological stability 0.02% sodium-azide was added. Solutions were stored at 4 °C and used within 4 weeks after protein extraction. Within this time no physical changes were observed. Gelatin solutions were prepared by dispersing gelatin granules in demineralized water. For samples with 10% SPI, gelatin was dissolved directly in the SPI solution. Gelatin solutions were heated at 60 °C for 1 hour in a water bath and stored at 4 °C overnight.

Sample Preparation

All solutions (including demineralized water) were degassed before usage and handling was done at a sample temperature of 40 °C to avoid gelling of the gelatin. Protein stock solutions (12% SPI, 20% gelatin) were mixed with demineralized water, NaCl and Na-azide stock solutions to obtain desired protein concentrations (0 - 10% SPI, 0 - 14% gelatin) and constant concentrations of 300 millimolal NaCl and 20 millimolal Na-Azide. MOPS buffer stock solution (1 M, pH 6.8) was added to reach a final buffer concentration of 20 millimolal.

Large deformation rheological characterization

Samples were placed in pre-lubricated (paraffin oil) sealed plastic tubes, tempered for 1 hour at 40 °C, heated at 95 °C for 30 min and afterwards stored in an acclimatized room overnight at 25 °C. Gels were cut into cylindrical pieces (2 cm x 2 cm) using a steel wire. For each sample 4 cylindrical pieces were measured and average values are shown. A 90% strain compression test was performed using a texture analyzer (TA-XT plus, Stable Micro

Systems ltd., Godalming U.K.) equipped with a 500 N load cell. The probe had a much larger diameter than the cylinders and paraffin oil was applied to all surfaces allowing sufficient lubrication. Samples were compressed in a single compression test to 90% of their initial height at a compression speed of 1 mm/s. True stress, true strain and Young's modulus were calculated as described elsewhere [37].

Small deformation rheological measurement

After preparation, samples were stored in the freezer (-20 °C) and thawed in a water bath prior to analysis at 40 °C for 30 min before rheological measurements (Anton Paar MC502 rheometer Graz, Austria). Gelling behavior was compared with non-frozen samples and their behavior did not change significantly upon freezing and thawing. A sand-blasted cup-bob geometry (CC17), a strain of 0.5% and a frequency of 1 Hz were used throughout the experiment. Samples were covered with a thin layer of paraffin oil to prevent evaporation and heated from 40 °C to 95 °C. They were kept at 95 °C for 1 h before cooling back to 15 °C. The temperature was then kept at 15 °C for 1 h before re-heating again to 95 °C. Heating and cooling rates were set at 5 °C/min.

Differential Scanning Calorimetry (DSC)

Samples were placed in aluminum pans, equilibrated at 40 °C inside the equipment (TA Instruments DSC Q1000 New Castle, USA) and then cooled to 15 °C before starting the measurements. The samples were heated at 1 °C/min to 110 °C and subsequently cooled again to 15 °C. Samples were kept at both 15 and 110 °C for 5 min. Analysis was performed using the manufacturer software (TA Universal Analysis). Data smoothing was done at 2 °C/min and baseline rotation was done between 40 °C and 60 °C.

Confocal Laser Scanning Microscopy (CLSM)

For CLSM analysis, 0.05% (w/w) Rhodamine B was added to the samples and gels were made by heating at 95 °C for 30 min inside sealed cuvettes (Product Name: Gene Frame® 125 µl, obtained from Thermo Scientific) in a water bath. Afterwards, cuvettes were cooled down to room temperature and samples analyzed using a Leica DMI6000 (Wetzlar, Germany) equipment. Several pictures at different location in the samples were scanned and shown structures were found throughout the sample.

Results and discussion

Transition and denaturation temperatures of single and mixed systems

The thermogram for single SPI, single gelatin and their mixtures is given in Figure 6.1. The two endothermic peaks in single SPI represent the denaturation temperatures of the two main soy protein fractions β-conglycinin (77 °C) and glycinin (97 °C) [38-40]. When reheated these peaks are absent in all curves, pointing to the irreversible nature of SPI denaturation.

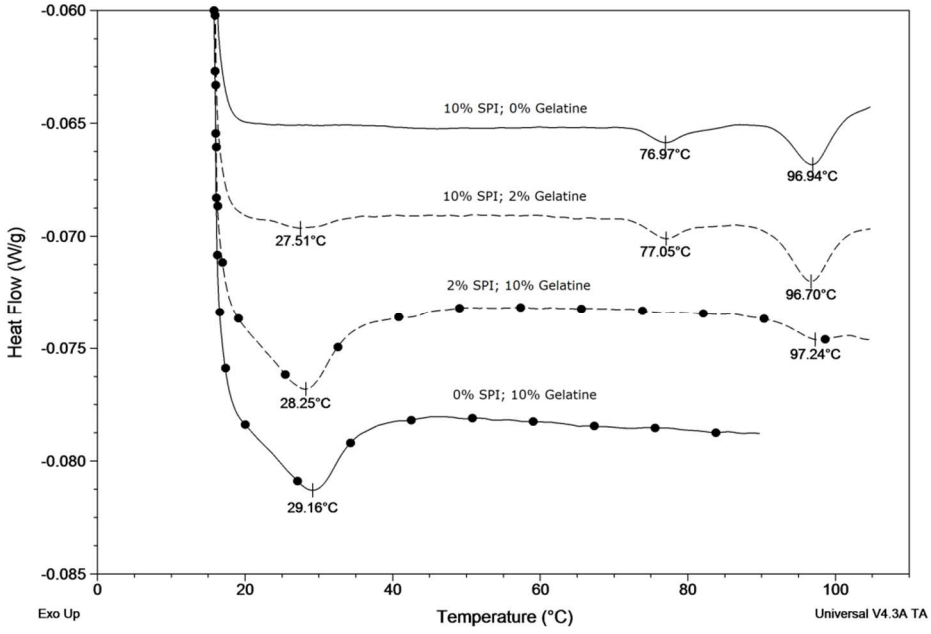

Figure 6.1 Thermogram (heating) for single SPI (10% w/w, solid line), single gelatin (10% w/w, solid line with dots) and mixed SPI / gelatin having 10% gelatin and 2% SPI (dashed line with dots) and 10% SPI and 2% gelatin (dashed line)

For single gelatin, the endothermic peak around 28 °C corresponds to the helix to coil transition (melting). During cooling helix to coil formation of gelatin resulted in one exothermic peak. Results for the cooling ramps are not shown since they show the same trends as the heating ramps. Gelling and melting peaks are present upon re-measuring the samples indicating the reversibility of the coil helix transition. Transition temperature values agree with literature for gelatin [38, 41, 42].

When gelatin and SPI are mixed, all the peaks belonging to the single proteins were observed. The SPI denaturation temperatures were not influenced by the presence of

gelatin. On the other hand the melting (and also gelling) temperature of gelatin increased with increasing gelatin ratio. This is most likely due to increasing total gelatin concentration when changing polymer ratios. This presumably kinetic effect is in line with earlier reported DSC measurements on gelatin at different gelatin concentrations [43].

Since no significant changes in the enthalpic peaks were found upon mixing, it is generally accepted [8, 44, 45] that no specific interactions between SPI and gelatin are to be expected.

Structure build-up in single and mixed systems

Gel formation was analyzed by measuring the storage modulus (G') while applying a thermal treatment as presented in Figure 6.2. For single SPI, a sharp increase in G' occurred at a gelling time of 30 min which for ease of wording, will be referred to as gelling time. For all tested samples, tan(δ) was < 0.5 independent of the gelatin concentration at the end of the heating time. Upon cooling (Figure 6.2, 70-90 min), non-covalent bonds such as hydrogen bonds strengthen the network further leading to an additional increase in G' [46, 47]. On the other hand, single gelatin forms a gel once cooled below the coil to helix transition after ~90 min in Figure 6.2. Re-heating this gel leads to melting of the gelatin network (at ~150 min) indicated by a sharp drop in G'.

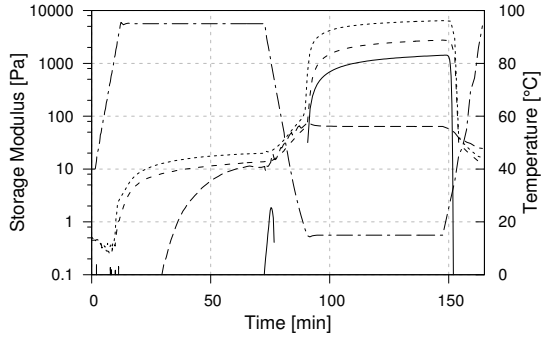

Figure 6.2 Storage modulus during heating and cooling for 4% single SPI (long dashes) and mixed systems containing 4% SPI plus 5% gelatin (short dashes) and 4% SPI with 10% gelatin (dotted line). As a reference 5% single gelatin (solid line) is added. Also shown is the temperature profile (dash dot) with heating / cooling performed at 5 °C/min.

In mixed systems of SPI and gelatin, addition of gelatin to SPI leads to a significant reduction in gelling time for the SPI network accompanied by an increase in the plateau value of G' at 95 °C (70 min). This reduction in gelling time can be caused by a decrease in repulsive forces between proteins [48] but it can also be caused by an increase in overall protein concentration [49]. Since 300 millimolal NaCl was added, electrostatic interactions

are strongly screened. It is therefore unlikely that addition of gelatin has an effect on electrostatic interactions between soy proteins. This suggests that the cause for the reduced gelling time is based on a concentration effect based on the choice of definition of protein concentration which will be discussed in chapter 8. Higher effective SPI concentrations are also in line with the increased G' plateau values compared to single SPI gels observed at 95 °C (72 min). A similar effect is observed for gelatin gels (~140min) where increasing G' values upon SPI addition are observed.

When comparing G' values of the mixed systems before gelatin gelation (corresponding to 75 min in Figure 6.2) and after gelatin melting (corresponding to 150 min in Figure 6.2) they are comparable. This suggests that the gelation of gelatin in the presence of a continuous SPI gel does not affect the continuity of the SPI network. Together with the DSC results this suggests that both proteins form independent gels.

The microstructure of single and mixed systems was probed by CLSM (Figure 6.3). Single SPI gels as well as gelatin gels (results not shown) do not show any structures above the resolution of the CLSM independent of protein concentrations. However, mixed gels do show structures with an increase in coarseness (typical distance between areas with higher and lower intensity) upon addition of gelatin at a given initial SPI concentration in line with results from chapter 5.

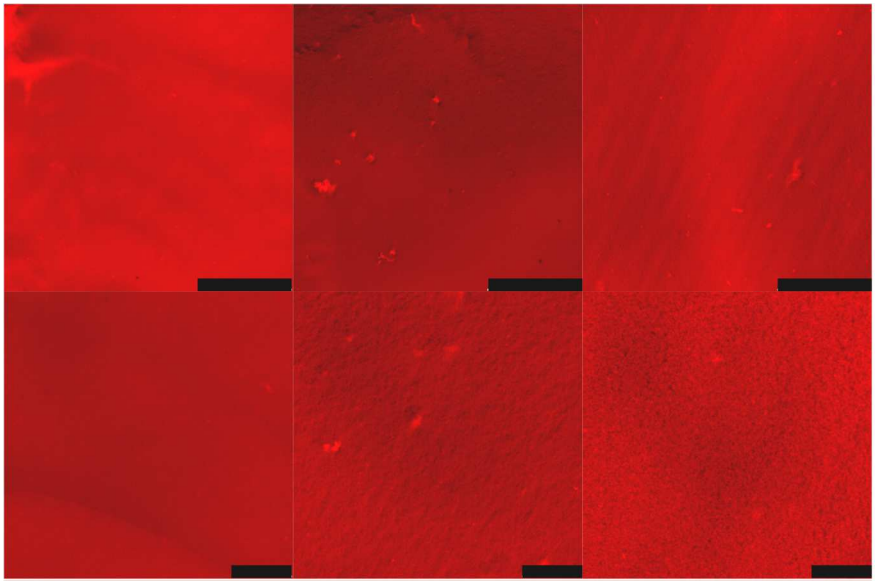

Figure 6.3 CLSM pictures (at different magnification top/bottom) of 10% SPI (left) and mixed systems containing 7.5% SPI plus 2% (middle) and 4.5% (right) gelatin. Samples were heated to 95 °C and cooled to room temperature before analysis (both proteins are in the gel state). Scale bars are 250 µm (top) and 50µm (bottom)

Fracture properties of mixed protein gels

Large deformation tests were performed on single and mixed SPI / gelatin samples. Figure 6.4 shows fracture stress, fracture strain and Young's modulus as a function of gelatin concentration at different SPI concentrations. For single SPI, only a concentration of 10% gave a self-supporting gel and therefore no values for lower concentrations could be measured. For single gelatin, gels above 8% were strong enough to be measured. Their fracture stress and Young's modulus increased with protein concentration while the fracture strain is concentration independent.

The fracture stress (Figure 6.4A) of mixed gels closely follows the behavior of the single gelatin gels deviating only at low gelatin (< 5 %) and high SPI concentration. At these deviating conditions, gelatin alone forms a weak gel with lower fracture stress than the (in this case stronger) SPI gel. Nevertheless, in most samples gelatin forms stronger gels and dominates the fracture stress of the mixed gels. Knowing that in mixed gels SPI and gelatin networks co-exist leads to the hypothesis that during compression both networks are able to break independently. The measured fracture stress corresponds to the fracture stress of the stronger network implying that the other network has already been broken at a lower stress. Unfortunately, due to limited sensitivity in large deformation experiments the fracturing of the weaker network stays undetected as was also reported earlier by Brink et al. (2007).

The Young's modulus (G_E) is defined by the initial slope of the stress versus strain relationship during compression. In mixed gels, G_E increases with increasing gelatin and increasing SPI concentration (Figure 6.4C). The general shape of the G_E versus gelatin concentration curve, however, is not significantly altered by the presence of SPI. Higher G_E values lead to a "faster" increase in stress over strain. Samples reach their fracture stress at a lower deformation (strain). This effect is represented in the reduced fracture strain values upon SPI addition at constant gelatin concentration as presented in Figure 6.4B.

Fracture properties of mixed SPI / gelatin gels (and possibly other globular protein / gelatin gels) were found to be dependent on only two factors, the fracture stress of the stronger of the two networks (as known for single systems) and the Young's modulus of the system. To enable one to modulate the fracture properties of a mixed system, the main question that remains is the mechanism underlying the increase in G_E upon addition of either one of the proteins which will be discussed in detail in chapter 7.

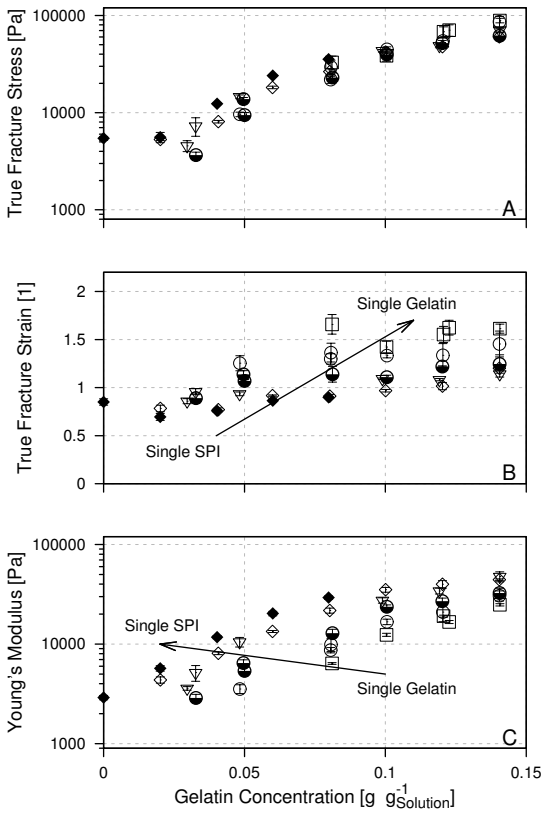

Figure 6.4 True fracture stress (A), true fracture strain (B) and Young's modulus (C) of mixed gelatin / SPI gels as a function of gelatin concentration with SPI concentrations of 0 (□), 0.02 (○), 0.04 (◒), 0.06 (▽), 0.08% (◊) and 0.1 (⧫) $g_{protein}$ / $g_{Solution}$. Gels were measured at room temperature after heat treatment to allow both proteins to form a gel.

Opportunities for mixed protein systems

A wide range in breakdown properties of mixed gels can be obtained using a combination of SPI and gelatin. In Figure 6.5 a texture map as commonly used for food systems is presented.

SPI gels are commonly brittle and soft whereas gelatin gels are deformable and hard (for definition of terms please refer to Figure 6.5). By combining SPI and gelatin, gels with intermediate values in hardness and deformability can be prepared. Increasing the SPI concentration at fixed gelatin concentration leads to a reduced fracture strain making the gels more brittle. Gelatin on the other hand increases fracture strain and fracture stress making the gels harder and more deformable. This allows one to modulate the fracture properties and obtain combinations of fracture properties which are not possible with just SPI or gelatin. Especially being able to increase or decrease fracture stress and strain partially independently in these type of gels is of high importance in developing novel foods or food ingredients.

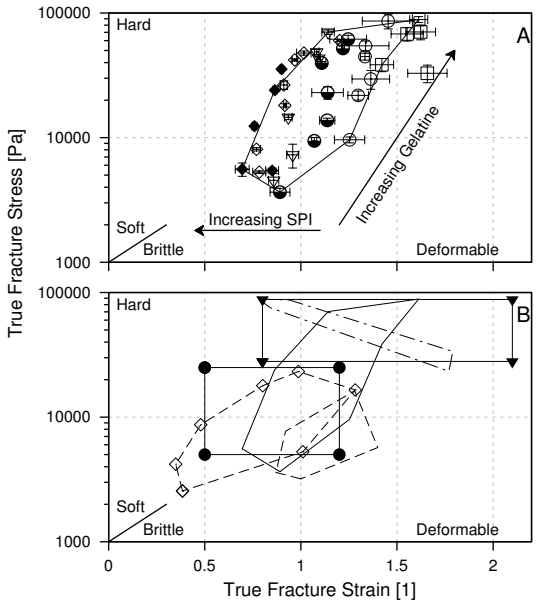

Figure 6.5 Texture map of mixed gels as analyzed in this research (A) and an overlay of the texture maps of different literature values with the current research (B); details graph A: Samples contain 0 – 0.14 $g_{protein}$ / $g_{solution}$ gelatin and 0 (□), 0.02 (○), 0.04 (⬬), 0.06 (▽), 0.08% (◊) and 0.1 (⧫) $g_{protein}$ / $g_{Solution}$ SPI, line shows outline as used in graph B; details graph B: outline from this research (solid line) together with WPI / kappa-carrageenan cold set gels [2] (dashed line), different tofu model systems (dashed line with ◊) [36], gelatin / xanthan mixed gels (interrupted dashes) [28] and WPI / kappa-carrageenan [1] with the continuous phase being kappa-carrageenan (●) or WPI (▼)

Mixed SPI / gelatin samples cover a wide range of fracture stress (10 to 100 kPa) and fracture strain (0.7 to 1.6). To compare this range in fracture properties to other type of mixed systems, the outlined area from Figure 6.5A is displayed in Figure 6.5B together with data from other studies. Harder, elastic SPI / gelatin samples are in the same region as different tofu model system [36] and the whey protein continuous part of a whey protein / k-carrageenan study [1]. Weaker more brittle samples show overlap with the phase inverted (k-carrageenan continuous) part of the same study [1]. Also within the range of SPI / gelatin are studies on the textural properties of a system with polysaccharide addition to whey protein aggregate gels [2] as well as mixed gelatin/xanthan gum gels [54].

The wide range in fracture properties of mixed SPI / gelatin gels and the overlap with other (mixed) biopolymer systems indicate the application possibilities that this system offers. Selectively mixing of proteins may lead to design of new textures with controllable sensory properties. However, the physical aspects of sensory perception is not limited to location in the texture map only. In fact, the texture map mainly relates to sensory perception “first bite” and neglects all other oral processing steps [55]. For a more detailed description of sensory, factors such as water release, recoverable energy, microstructure and rheological properties after fracture [54] but also the balance between energy going into fracture and dissipation [2] are of importance.

Conclusions

SPI and gelatin formed mixed gels upon applying an appropriate heating and cooling profile, in which both proteins are able to form independent gel network structures. Interactions between proteins are non-specific and lead to enhanced micro-phase separation during heat induced gelation of SPI. Mixed gels had increased moduli (G' and G_E) while the fracture stress was determined by whichever single gel formed a stronger gel. Gelatin tends to dominate rheological properties of mixed protein / gelatin systems as reported in literature [15, 17, 18, 34]. However, the fact that gelatin is able to dominate mixed gel fracture properties is mainly based on the fact that gelatin is able to form strong gels already at low total polymer concentration. Using the SPI / gelatin gels as an example, these results suggest that for any mixed gel with two independent networks the fracture behavior will always be dominated by the stronger of the two gels. However, the relationship between the modulus of single and mixed gels still requires more attention to be able to entirely predict the fracture properties of mixed gels based on the properties of the single gels which will be dealt with in more detail in chapter 7.

Fracture properties of SPI / gelatin mixed gels were found to overlap with existing studies having significant differences in sensorial properties. This proves the system to be interesting for future textural studies and developments of new foods. Mixing SPI / gelatin allows one to modulate the breakdown properties (and possibly textures) and increases the formulation flexibility during the development of foods as ingredients can be chosen partially independent of the products fracture properties.

References

1. Çakir, E. and E.A. Foegeding, Combining protein micro-phase separation and protein-polysaccharide segregative phase separation to produce gel structures. Food Hydrocolloids, 2011. **25**(6): p. 1538-1546.
2. van den Berg, L., Texture of food gels explained by combining structure and large deformation properties. Physics and Physical Chemistry of Foods. 2008: PhD Thesis - Wageningen University.
3. Martínez, K.D. and A.M.R. Pilosof, Relative viscoelasticity of soy protein hydrolysate and polysaccharides mixtures at cooling conditions analyzed by response surface methodology. Food Hydrocolloids, 2012. **26**(1): p. 318-322.
4. Pires Vilela, J.A., Â.L.F. Cavallieri, and R. Lopes da Cunha, The influence of gelation rate on the physical properties/structure of salt-induced gels of soy protein isolate-gellan gum. Food Hydrocolloids, 2011. **25**(7): p. 1710-1718.
5. Turgeon, S.L. and M. Beaulieu, Improvement and modification of whey protein gel texture using polysaccharides. Food Hydrocolloids, 2001. **15**(4–6): p. 583-591.
6. Tolstoguzov, V.B., Functional properties of food proteins and role of protein-polysaccharide interaction. Food Hydrocolloids, 1991. **4**(6): p. 429-468.
7. Doublier, J.L., C. Garnier, D. Renard, and C. Sanchez, Protein-polysaccharide interactions. Current Opinion in Colloid and Interface Science, 2000. **5**(3-4): p. 202-214.
8. Ould Eleya, M.M. and S.L. Turgeon, Rheology of κ-carrageenan and β-lactoglobulin mixed gels. Food Hydrocolloids, 2000. **14**(1): p. 29-40.
9. Polyakov, V.I., O.K. Kireyeva, V. Grinberg, and V.B. Tolstoguzov, Thermodynamic compatibility of proteins in aqueous media. Part. I. Phase diagrams of some water--protein A--protein B systems. Die Nahrung, 1985. **29**(2): p. 153-160.
10. Ako, K., T. Nicolai, D. Durand, and G. Brotons, Micro-phase separation explains the abrupt structural change of denatured globular protein gels on varying the ionic strength or the pH. Soft Matter, 2009. **5**(20): p. 4033-4041.
11. Polyakov, V.I., V.Y. Grinberg, and V.B. Tolstoguzov, Thermodynamic incompatibility of proteins. Food Hydrocolloids, 1997. **11**(2): p. 171-180.
12. Fitzsimons, S.M., D.M. Mulvihill, and E.R. Morris, Segregative interactions between gelatin and polymerised whey protein. Food Hydrocolloids, 2008. **22**(3): p. 485-491.
13. Sala, G., Food gels filled with emulsion droplets : linking large deformation properties to sensory perception. 2007: PhD Thesis - Wageningen University.
14. Kim, K.H., J.M.S. Renkema, and T. Van Vliet, Rheological properties of soybean protein isolate gels containing emulsion droplets. Food Hydrocolloids, 2001. **15**(3): p. 295-302.

15. Walkenström, P. and A.-M. Hermansson, High-pressure treated mixed gels of gelatin and whey proteins. Food Hydrocolloids, 1997. **11**(2): p. 195-208.
16. Brink, J., M. Langton, M. Stading, and A.-M. Hermansson, Simultaneous analysis of the structural and mechanical changes during large deformation of whey protein isolate/gelatin gels at the macro and micro levels. Food Hydrocolloids, 2007. **21**(3): p. 409-419.
17. Walkenström, P. and A.-M. Hermansson, Mixed gels of fine-stranded and particulate networks of gelatin and whey proteins. Food Hydrocolloids, 1994. **8**(6): p. 589-607.
18. Walkenström, P. and A.-M. Hermansson, Fine-stranded mixed gels of whey proteins and gelatin. Food Hydrocolloids, 1996. **10**(1): p. 51-62.
19. Ziegler, G.R., Microstructure of mixed gelatin-egg white gels: Impact on rheology and application to microparticulation. Biotechnology Progress, 1991. **7**(3): p. 283-287.
20. Chronakis, I.S. and S. Kasapis, Structural properties of single and mixed milk/soya protein systems. Food Hydrocolloids, 1993. **7**(6): p. 459-478.
21. Comfort, S. and N.K. Howell, Gelation properties of soya and whey protein isolate mixtures. Food Hydrocolloids, 2002. **16**(6): p. 661-672.
22. Kasapis, S. and S.L. Tay, Morphology of Molecular Soy Protein Fractions in Binary Composite Gels†. Langmuir, 2009. **25**(15): p. 8538-8547.
23. Renkema, J.M.S., J.H.M. Knabben, and T. van Vliet, Gel formation by β-conglycinin and glycinin and their mixtures. Food Hydrocolloids, 2001. **15**(4–6): p. 407-414.
24. Sok, L.T., S. Kasapis, and A.T.K. Han, Phase model interpretation of the structural properties of two molecular soy protein fractions. Journal of Agricultural and Food Chemistry, 2008. **56**(7): p. 2490-2497.
25. Alevisopoulos, S., S. Kasapis, and R. Abeysekera, Formation of kinetically trapped gels in the maltodextrin—gelatin system. Carbohydrate Research, 1996. **293**(1): p. 79-99.
26. Almrhag, O., P. George, A. Bannikova, L. Katopo, D. Chaudhary, and S. Kasapis, Phase behaviour of gelatin/polydextrose mixtures at high levels of solids. Food Chemistry, 2012. **134**(4): p. 1938-1946.
27. Almrhag, O., P. George, A. Bannikova, L. Katopo, D. Chaudhary, and S. Kasapis, Investigation on the phase behaviour of gelatin/agarose mixture in an environment of reduced solvent quality. Food Chemistry, 2013. **136**(2): p. 835-842.
28. Altay, F. and S. Gunasekaran, Gelling properties of gelatin–xanthan gum systems with high levels of co-solutes. Journal of Food Engineering, 2013. **118**(3): p. 289-295.
29. Ares, G., D. Gonçalvez, C. PÉrez, G. Reolón, N. Segura, P. Lema, and A. Gámbaro, Influence of gelatin and starch on the instrumental and sensory texture of stirred yogurt. International Journal of Dairy Technology, 2007. **60**(4): p. 263-269.

30. Fiszman, S.M., M.A. Lluch, and A. Salvador, Effect of addition of gelatin on microstructure of acidic milk gels and yoghurt and on their rheological properties. International Dairy Journal, 1999. **9**(12): p. 895-901.
31. Fiszman, S.M. and A. Salvador, Effect of gelatine on the texture of yoghurt and of acid-heat-induced milk gels. Zeitschrift fur Lebensmittel -Untersuchung und -Forschung, 1999. **208**(2): p. 100-105.
32. Salvador, A. and S.M. Fiszman, Textural Characteristics and Dynamic Oscillatory Rheology of Maturation of Milk Gelatin Gels with Low Acidity. Journal of Dairy Science, 1998. **81**(6): p. 1525-1531.
33. Shrinivas, P., S. Kasapis, and T. Tongdang, Morphology and mechanical properties of bicontinuous gels of agarose and gelatin and the effect of added lipid phase. Langmuir, 2009. **25**(15): p. 8763-8773.
34. Ziegler, G.R. and S.S.H. Rizvi, Predicting the Dynamic Elastic Modulus of Mixed Gelatin-Egg White Gels. Journal of Food Science, 1989. **54**(2): p. 430-436.
35. Tolstoguzov, V.B., Concentration and purification of proteins by means of two-phase systems: membraneless osmosis process. Food Hydrocolloids, 1988. **2**(3): p. 195-207.
36. Urbonaite, V., H.H.J. de Jongh, E.v.d. Linden, and L. Pouvreau, The origin of water loss from soy protein gels. Journal of Agriculture and Food Chemistry, 2014. **62**(30): p. 7550-7558.
37. de Jong, S. and F. van de Velde, Charge density of polysaccharide controls microstructure and large deformation properties of mixed gels. Food Hydrocolloids, 2007. **21**(7): p. 1172-1187.
38. Bainy, E., S. Tosh, M. Corredig, L. Woodrow, and V. Poysa, Protein Subunit Composition Effects on the Thermal Denaturation at Different Stages During the Soy Protein Isolate Processing and Gelation Profiles of Soy Protein Isolates. 2008. **85**(6): p. 581-590.
39. Margatan, W., K. Ruud, Q. Wang, T. Markowski, and B. Ismail, Angiotensin Converting Enzyme Inhibitory Activity of Soy Protein Subjected to Selective Hydrolysis and Thermal Processing. Journal of Agricultural and Food Chemistry, 2013. **61**(14): p. 3460-3467.
40. Tseng, Y.C., Y.L. Xiong, and W.L. Boatright, Effects of Inulin/Oligofructose on the Thermal Stability and Acid-Induced Gelation of Soy Proteins. Journal of Food Science, 2008. **73**(2): p. E44-E50.
41. Dranca, I. and S. Vyazovkin, Thermal stability of gelatin gels: Effect of preparation conditions on the activation energy barrier to melting. Polymer, 2009. **50**(20): p. 4859-4867.

42. Soeda, T., T. Kaneko, A. Hokazono, K. Tujimoto, and H. Murakami, Effects of microbial transglutaminase on melting point and gel property of gelatins. Nippon Shokuhin Kagaku Kogaku Kaishi, 2005. **52**(6): p. 251-256.
43. Koh, M.W.W., L. Matia Merino, and E. Dickinson, Rheology of acid-induced sodium caseinate gels containing added gelatin. Food Hydrocolloids, 2002. **16**(6): p. 619-623.
44. Kasapis, S., E.R. Morris, I.T. Norton, and C.R.T. Brown, Phase equilibria and gelation in gelatin/maltodextrin systems — Part III: phase separation in mixed gels. Carbohydrate Polymers, 1993. **21**(4): p. 261-268.
45. Kasapis, S., Phase separation in biopolymer gels: A low- to high-solid exploration of structural morphology and functionality. Critical Reviews in Food Science and Nutrition, 2008. **48**(4): p. 341-359.
46. Beliciu, C.M. and C.I. Moraru, Physico-chemical changes in heat treated micellar casein – Soy protein mixtures. LWT - Food Science and Technology, 2013. **54**(2): p. 469-476.
47. Renkema, J.M.S., Formation, Structure and Rheological Properites of Soy Protein Gels. Physics and Physical Chemistry of Foods. 2001: PhD Thesis - Wageningen University.
48. Verheul, M. and S.P.F.M. Roefs, Structure of Particulate Whey Protein Gels: Effect of NaCl Concentration, pH, Heating Temperature, and Protein Composition. Journal of Agricultural and Food Chemistry, 1998. **46**(12): p. 4909-4916.
49. Fernandes, P.B., Viscoelastic characteristics of whey protein systems at neutral pH. Food Hydrocolloids, 1994. **8**(3–4): p. 277-285.
50. Tobin, J.T., S.M. Fitzsimons, V. Chaurin, A.L. Kelly, and M.A. Fenelon, Thermodynamic incompatibility between denatured whey protein and konjac glucomannan. Food Hydrocolloids, 2012. **27**(1): p. 201-207.
51. Ako, K., D. Durand, T. Nicolai, and L. Becu, Quantitative analysis of confocal laser scanning microscopy images of heat-set globular protein gels. Food Hydrocolloids, 2009. **23**(4): p. 1111-1119.
52. Verheul, M., S.P.F.M. Roefs, J. Mellema, and K.G. de Kruif, Power Law Behavior of Structural Properties of Protein Gels. Langmuir, 1998. **14**(9): p. 2263-2268.
53. Campbell, L.J., X. Gu, S.J. Dewar, and S.R. Euston, Effects of heat treatment and glucono-δ-lactone-induced acidification on characteristics of soy protein isolate. Food Hydrocolloids, 2009. **23**(2): p. 344-351.
54. Çakır, E., C.R. Daubert, M.A. Drake, C.J. Vinyard, G. Essick, and E.A. Foegeding, The effect of microstructure on the sensory perception and textural characteristics of whey protein/κ-carrageenan mixed gels. Food Hydrocolloids, 2012. **26**(1): p. 33-43.
55. Stokes, J.R., M.W. Boehm, and S.K. Baier, Oral processing, texture and mouthfeel: From rheology to tribology and beyond. Current Opinion in Colloid and Interface Science, 2013. **18**(4): p. 349-359.

CHAPTER 7

Predicting the mechanical response of mixed gels

ABSTRACT

Measured storage modulus data for three mixed protein systems (WPI / gelatin type A, WPI / gelatin type B and SPI / gelatin type A) were compared to predictions from a number of different theories relating mixed gel moduli to microstructure and single gel moduli. Discrepancies in the application of these theories suggested that their applicability is limited in mixed gels where globular proteins formed a gel in the presence of gelatin. Discrepancies were attributed to gelatin induced changes in the gel structure (and gel modulus) of the globular protein gels, which cannot be accounted for using the available models.

GRAPHICAL ABSTRACT

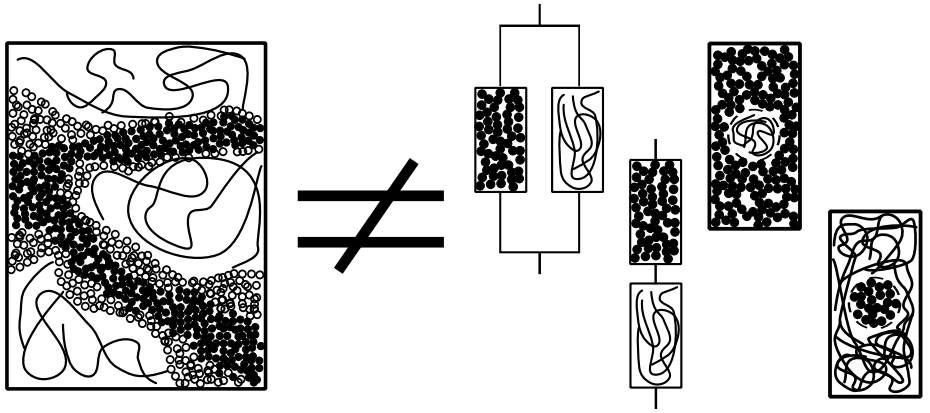

KEYWORDS

Mixed gels, composites, rheological response, modulus, applicability theories

Introduction

Describing quantitatively the rheological properties of gel composites (mixed gels) has been under investigation for several decades in the field of material science [1-6]. Developed theories require knowledge of rheological properties for the separate single gel systems and their structural arrangement of phases and phase volumes in the mixed gel. In material science relevant composites like alloys or inorganic polymer blends, the phase volumes and rheological properties of the separate phases are often known and theories are straightforwardly applicable [6, 7].

More recently these approaches have also been adopted by several researchers to describe phase separated biopolymer mixtures [8-10]. Unfortunately, biopolymers often share the same solvent (typically water) and the rheological properties as well as the volume fraction of the phases both depend on the distribution of water over the phases [11, 12]. Clark et al. (1983) [9] were first to include this biopolymer specific solvent distribution behavior in theories on composite moduli using a relative water affinity parameter (*p*). The assumption was that during gelation each biopolymer phase would attract a constant amount of water dependent on the interaction of the polymer with water (related to Flory Huggins polymer – solvent interaction parameter $\Delta\chi$) [9]. This assumption was later re-evaluated by Kasapis et al. in a series of publications where it was argued that the relative water affinity *p* also depends on which biopolymer occupies the continuous phase. In their approach they identified two populations of *p*-values in mixed systems which was explained by phase inversion, defined as the inversion of biopolymer arrangement in the discontinuous and continuous phase upon changes in polymer concentration (biopolymer formerly in continuous phase forms the discontinuous phase and the other way around) [13-18].

Despite these difficulties in determining the exact solvent partitioning several researchers have applied the available models to predict the moduli of mixed biopolymer gels. For systems where biopolymers phase separated into a continuous and discontinuous phase this led to a good agreement between experimental and predicted storage modulus G' of mixed gels for e.g. mixtures of maltodextrin with gelatin, non-gelled milk protein or caseinate [14-16]. For mixtures containing globular proteins the results are less clear. For globular protein / gelatin gels similar to those presented in chapter 6, Walkenström and Hermansson (1994) [19] reported, based on the rheological data, a transition from whey protein continuous to gelatin continuous mixed gels with increasing gelatin concentration. Ziegler and Rizvi (1989) [20] and Ziegler (1991) [21] obtained similar results on the egg white / gelatin mixed system. This transition pointed towards a microstructure where one protein forms the continuous and the other the discontinuous

phase. The microstructure of egg white / gelatin or whey protein / gelatin gels, however, was reported to be bi-continuous which was contradictory to the underlying assumptions of the rheological theories used in these studies. Recently, also Katopo, Kasapis et al. (2012) [22] used similar theories in systems where globular proteins form a gel. Also in their example no phase inversion could be detected which was reported as a mixed system with a single *p*-value regime. Still, a relationship of these rheological results with the changes in gel microstructure could not be obtained.

In this chapter we will discuss the discrepancies we have observed when applying the different models to mixed gels where globular proteins formed a gel. We performed this investigation on a large set of measurement points for three different mixed systems in parallel (whey protein isolate (WPI) / gelatin A, WPI / gelatin B and soy protein isolate (SPI) / gelatin A) and at two different conditions where either one or both proteins formed a gel. Our initial goal was that an appropriate model should not only describe experimental values in a limited range of protein concentrations, as typically reported in literature, but needs to be valid over the whole range of experimentally accessible protein concentrations. Additionally, the model should be able to predict the systems independent of whether only one phase (one biopolymer) or both biopolymers formed a gel as long as one accounts for the appropriate gel modulus of each phase. Using this approach, Takayanagi et al. (1963) [6] were able to predict the complete melting profile for inorganic polymer blends over a large temperature range. We performed our analysis at 95 °C where only the globular proteins (WPI and SPI) formed a gel and at 15 °C (after being heated to 95 °C) where globular proteins and gelatin formed a gel.

In this chapter we have chosen to only include theories based on Hooke's law. Alternatively, especially in the research on emulsion filled gels, various extensions of the famous Einstein equation have been successfully applied to describe the rheology of mixed gels [23, 24]. We have also applied these theories to our systems and despite numerical differences have arrived at similar results as those presented here which led to the decision not to present them here.

Theory

In chapter 1 different ways to categorize mixed gels were presented. For the rheological response of a mixed system the final microstructural arrangements of the phases is more relevant than the events leading to this arrangement. Figure 1.2 shows three idealized microstructures that one may expect in mixed gels. The bi-continuous microstructure (Figure 1.2.1) is typical for systems where gelation arrests phase separation (occurring via spinodal decomposition) at an early stage and has been observed in several studies involving polysaccharides and proteins [19, 25-27]. Spherical enclosures of one phase in a continuous matrix of another phase (Figure 1.2.2) are typically found for gels where gelation occurred at a later stage of phase separation or where phase separation occurs via a nucleation and growth mechanism (see also chapter 1). This microstructure is frequently reported especially for mixed polysaccharide and mixed gelatin / polysaccharide systems [28-30]. The third possible, yet often practically not observed microstructure, is a completely mixed situation (Figure 1.2.3). Here molecules are assumed to stay mixed on a molecular scale throughout the gelation process.

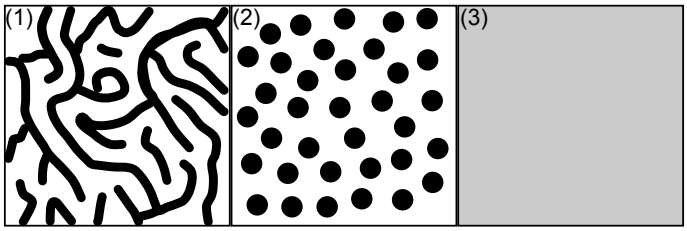

Figure 7.1 Schematic 2D representation of typical gel microstructures in phase separated mixed gels. (1) bi-continuous, (2) spherical enclosures in a continuous gel matrix and (3) completely mixed

Here we will discuss the relationship between the microstructure, the phase volumes (relative amount of area of white and black phases in Figure 1.2) and the rheological properties of mixed gels on the example of the mixed globular protein / gelatin gels. This approach, however, is applicable to any polymer A / polymer B system. Gelatin will be referred to with the subscript *G* and globular proteins with the subscript *GP*. To distinguish between the different microstructures, the subscripts *PS* for the phase separated gels and *M* for gels mixed on a molecular scale will be used. In addition, the subscript *PS-B* is used for a bi-continuous micro-structure and the subscript *PS-SE* is used for a micro-structure with spherical enclosures of one phase in the other.

Water distribution and phase volumes in phase separated gels

During segregative phase separation of proteins each protein is concentrated in one phase and depleted from the other phase. In gels where phases cannot be experimentally separated and analyzed the protein concentration inside each phase is unknown and depends on the distribution of solvent between the two phases. Knowledge of the protein concentrations in each phase, however, is crucial in order to describe the rheological properties of the mixed gel in terms of the properties of the individual phases.

To describe the partitioning of solvent between the phases the simplest, and often applied route, is the assumption of complete phase separation relative to the proteins. In this case each phase only contains solvent and one of the proteins. One way to model the water distribution in this way is by introducing the so called *p*-value (equation 7.1) which reflects the relative affinity of water to the proteins (and more generally biopolymers) [9]. The *p*-values have been shown to be constant for a given biopolymer pair at constant solvent and gelation conditions [22]. A *p*-value of 1 indicates equal affinity of water to both proteins, $p > 1$ corresponds to the situation where water has a higher affinity to globular proteins compared to gelatin and $p < 1$ to the opposite situation. Here *p* is given by

$$p \equiv \frac{\frac{w_{GP;PS}}{m_{GP}}}{\frac{w_{G;PS}}{m_{G}}} \qquad 7.1$$

where *w* denotes the mass of water in the corresponding phase and *m* the mass of the protein in the sample (globular proteins or gelatin). The total amount of water (m_{Water}) in a mixture is known and constant

$$m_{Water} = w_{GP;PS} + w_{G;PS} \qquad 7.2$$

Using equation 7.1 and 7.2 it is possible to calculate the water distribution for any given polymer mixture. Knowing the water distribution and assuming equal densities of the two phases also allows one to calculate the volume fraction using

$$1 = \phi_{G;PS} + \phi_{GP;PS} \equiv \frac{w_{G;PS}}{m_{Water}} + \frac{w_{GP;PS}}{m_{Water}} \qquad 7.3$$

with Φ being the volume fraction for the two phases indicated by their subscript. Using the above relationships, it is possible to calculate phase volumes and concentrations of both polymers in a phase separated system as a function of the *p*-value. This will be subsequently used for predicting the storage modulus of mixed gels.

Storage modulus of phase separated gels with spherical enclosures

Over the years, multiple models to describe the storage modulus of phase separated composites in terms of the properties of the individual phases have been developed [1, 2, 4-6, 31-34]. In order to find a relationship between the modulus of the single phases and the mixture, equations for the lowest upper and greatest lower bound of composite moduli were derived using a variational approach (equations 7.4) [1, 2]. Any phase separated mixture, independent of the microstructural arrangement, must have an effective modulus between the two bounds given by:

$$G'_{C\ Lower,PS-SE(HA)} = G'_{G;PS} + \frac{\phi_{GP;PS}}{\frac{1}{G'_{GP;PS} - G'_{G;PS}} + \frac{6\left(K_{G;PS} + 2G'_{G;PS}\right)\phi_{G;PS}}{5G'_{G;PS}\left(3K_{G;PS} + 4G'_{G;PS}\right)}} \qquad 7.4\,a$$

$$G'_{C\ Upper,PS-SE(HA)} = G'_{GP;PS} + \frac{\phi_{G;PS}}{\frac{1}{G'_{G;PS} - G'_{GP;PS}} + \frac{6(K_{GP;PS} + 2G'_{GP;PS})\phi_{GP;PS}}{5G'_{GP;PS}(3K_{GP;PS} + 4K_{GP;PS})}} \qquad 7.4\,b$$

Here G'_C is the storage modulus of the composite or mixed gels (also: effective storage modulus), Φ the volume fraction, K the bulk modulus and G' the storage modulus of single systems at the corresponding concentrations being a function of Φ. The subscript *(HA)* will from now on be used to refer to these expressions derived originally by Hashin and Shtrikman (1963) [35]. Equations 7.4 are only valid when $G'_{GP;PS} > G'_{G;PS}$ and $K_{GP;PS} > K_{G;PS}$. For the situation $G'_{GP;PS} < G'_{G;PS}$ the upper and lower bounds have to be reversed. At a later stage, these expressions were extended so that they are also valid for materials where $G'_{GP;PS} > G'_{G;PS}$ and $K_{GP;PS} < K_{G;PS}$ [32]. Nevertheless, water based gels are typically incompressible (with a Poisson ratio equal to ½), leading to an infinite bulk modulus K for both phases which makes it unnecessary to use the extended expressions. It is emphasized here that lowest upper and greatest lower bounds do under normal circumstances not lead to an exact result for the modulus of a composite. However, for spherical enclosures of one phase being dispersed in the second phase in a specific way and for single droplets at low volume fractions, the variational principle leads to an exact expression for the composite bulk modulus. It has been argued that in this specific case, the expression for the storage modulus is also exact [35]. In the following, the Hashin approach will therefore be used to determine the upper and lower boundaries of the effective storage modulus. In addition, under the assumption of a specific arrangement of

spherical enclosures of one phase in a matrix of the other phase, an exact result for the storage modulus is calculated.

To our knowledge the Hashin approach has not been used in mixed biopolymer gels. Therefore, the more frequently used theory referred to as Takayanagi approach (also called 'blending laws') [10, 13, 15, 19, 20] will also be considered here. Even though the corresponding expressions have also been derived by Hashin as the worst possible bounds within his variational approach [35], the Takayanagi approach has been experimentally determined and shown to be an exact result for parallel or serial stacked gel pieces [6]. Assuming its validity for spherical enclosures with an isotropic arrangement, this theory has been used in several studies on aqueous biopolymer mixtures [8, 9, 13, 36]. The Takayanagi approach distinguishes between the isostrain (parallel stacking) situation (equation 7.5a) where the storage modulus of the continuous phase is larger than the one of the discontinuous phase and the inverse situation called isostress (serial stacking, equation 7.5b) [8]. The isostress situation is related to the lower bound of the Hashin approach and the isostrain situation to the upper bound (equations 7.4).

$$G'_{C\ Isostrain;PS-SE(T)} = \phi_{GP;PS} G'_{GP;PS} + \phi_{G;PS} G'_{G;PS} \qquad 7.5a$$

$$\frac{1}{G'_{C\ Isostress;PS-SE(T)}} = \frac{\phi_{GP;PS}}{G'_{GP;PS}} + \frac{\phi_{G;PS}}{G'_{G;PS}} \qquad 7.5b$$

Being able to predict lowest upper and greatest lower bounds for the effective storage modulus is an important step to narrow down the range of expected G'_C values for mixed gels. This unfortunately does not give additional information on the microstructure of the gels. When mixing two polymers, either one of the two phases can be continuous or discontinuous as well as stronger or weaker than the other phase which dependent on the used theory needs to be taken into account to calculate the modulus of composites with certain microstructures. For the Takayanagi approach, the isostrain and isostress situations can be combined dependent on the storage modulus ratio of the two phases to calculate the modulus of a composite where either gelatin or globular protein is in the continuous phase according to

$$G'_{C_{G;PS-SE(T)}} \begin{cases} G'_{C\ Isostrain;PS(T)}, & G'_{G;PS} \geq G'_{GP;PS} \\ G'_{C\ Isostress;PS(T)}, & G'_{G;PS} < G'_{GP;PS} \end{cases} \qquad 7.6a$$

$$G'_{C_{GP;PS-SE(T)}} \begin{cases} G'_{C\ Isostrain;PS(T)}, & G'_{GP;PS} \geq G'_{G;PS} \\ G'_{C\ Isostress;PS(T)}, & G'_{GP;PS} < G'_{G;PS} \end{cases} \qquad 7.6b$$

where $G'_{C_{GP;PS-SE}}$ is a composite in which by definition the globular protein forms the continuous phase having spherical enclosures of a gelatin rich phase and $G'_{C_{G;PS-SE}}$ the

reverse situation with gelatin in the continuous phase. For the Hashin approach equations 7.4 can be simplified by assuming infinite bulk moduli and, using the same arguments as for the Takayanagi approach, the upper lower and lower upper bounds can be expressed for gelatin and globular protein continuous system given by:

$$G'_{C_{G;PS-SE(HA)}} = G'_{G;PS} + \frac{(G'_{GP;PS} - G'_{G;PS})\phi_{GP;PS}}{1 + \frac{6\phi_{G;PS}}{15G'_{G;PS}}(G'_{GP;PS} - G'_{G;PS})} \qquad 7.7a$$

$$G'_{C_{GP;PS-SE(HA)}} = G'_{GP;PS} + \frac{(G'_{G;PS} - G'_{GP;PS})\phi_{G;PS}}{1 + \frac{6\phi_{GP;PS}}{15G'_{GP;PS}}(G'_{G;PS} - G'_{GP;PS})} \qquad 7.7b$$

Using relationships 7.6 and 7.7, it is possible to calculate the storage modulus of phase separated gels having spherical enclosures of one phase in a continuous matrix of the second phase. In this way, a micro-structural characteristic is added to the numerical results (keeping in mind the limitations thereof) which allows an easier interpretation of the results.

Storage modulus of phase separated bi-continuous gels

The effective storage modulus of a bi-continuous gel will also fall between the upper and lower bounds as given by the Hashin approach. Nevertheless, for this specific situation the modulus of the composite can be directly described [3, 4] via

$$G'^{\frac{1}{5}}_{C;PS-B} = \phi_{GP;PS}G'^{\frac{1}{5}}_{GP;PS} + \phi_{G;PS}G'^{\frac{1}{5}}_{G;PS} \qquad 7.8$$

Storage modulus of completely mixed gels

Despite the fact that most research has focused on phase separated systems when addressing composite rheology, the importance of miscibility of polymers has also been addressed early on [6]. While at low polymer miscibility, earlier described theories on phase separated systems can still describe the composite modulus reasonably well, they fail at higher polymer miscibility [6]. Since protein blends are known to mix up to high total protein content [11] the possibility that they form completely mixed gels should not be excluded for the gelatin / globular protein mixed gels. The ideal case of a mixed gel is represented by a situation where both proteins (or polymers in general) stay mixed on a molecular level throughout the gelation [37]. If polymers do not phase separate, the composite modulus of an ideally mixed gel should be additive (each polymer has a phase volume of 1 in equation 7.5a) which in case of the mixed globular protein / gelatin gel would read as:

$$G'_{C;M} = G'_{GP;M} + G'_{G;M} \qquad 7.9$$

This simple addition, even though it is not part of the above theories on composite moduli, is typically used to determine whether experimental results are “simply additive” [19, 38]. Even though in practice it is probably impossible to obtain a gel with molecules mixed on a molecular level equation 7.9 will be included in the subsequent considerations as an idealized form of a mixed gel.

Experimental

The experimental results presented in this chapter were taken from chapters 5 where the sample preparation and the rheological methods are described. All protein concentrations are given relative to the amount of available water (in $g_{protein}$ / g_{water}) which is important when dealing with mixed systems which has been addressed shortly in chapter 4 and chapter 5 and will be discussed in more detail in chapter 8.

Storage modulus of single protein gels

The first step in the analysis of composite moduli is the determination of the relationship between storage modulus and the protein concentration in single component systems. Figure 5.1 (taken from chapter 5) shows an example of such an analysis on WPI, SPI and gelatin type A and type B. Samples were kept at 95 °C for 1 hour and the final storage modulus is shown as a function of protein concentration. Globular proteins (WPI and SPI) formed a gel and the storage modulus G' of WPI and SPI was fitted using

$$G' = C\left(c_p - c_0\right)^t \qquad \textbf{7.10}$$

where *C* and *t* are constants, c_p is the protein concentration and c_0 a minimum gelling concentration. We have performed the same analysis also at 15 °C for gelatin gels which is shown in chapter 4. In all cases the storage modulus was well described by the percolation model (equation 7.10). This allows for the calculation of the storage moduli for both phases in a mixed gel if the protein concentration inside the phases is known or estimated via water distribution factor *p*.

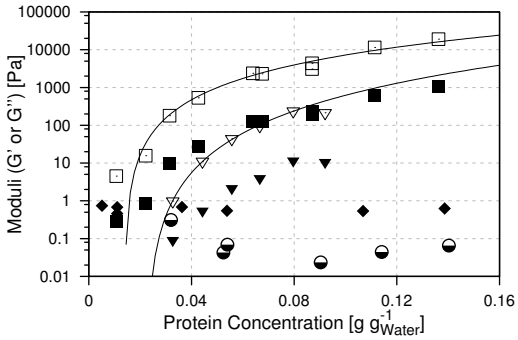

Figure 7.2 Storage modulus G' (open symbols) and loss modulus (closed symbols) for single SPI (▽,▼) and single WPI (□,■) gels after 1 hour at 95 °C. Lines were fitted using equation 7.10. Gelatin type A (◒) and type B (◆) did not show an elastic response and only loss modulus values are shown. (from chapter 5)

Storage modulus of globular protein gels with a liquid gelatin phase

Figure 7.3 shows the measured and calculated storage modulus G'_C for a series of mixed gels at constant SPI concentration and varying gelatin type A concentration. The measurements were performed at 95 °C where SPI formed a heat induced gel and gelatin behaves like a viscous liquid without an elastic response (G'_G = 0). To calculate the G'_C of mixed gels with a phase separated microstructure p = 1 (equal water distribution) was used which is within the range of p-values typically observed for protein mixtures [13, 14, 19].

The measured storage modulus of the composites (G'_c) as well as the calculated values for the completely mixed ($G'_{c;M}$) and the bi-continuous gels ($G'_{c;PS\text{-}B}$) are between the upper and lower bounds as given by the Hashin and Takayanagi approach. In agreement with theory, the bounds given by the Hashin approach are more stringent compared to the Takayanagi approach and the therefore closer to the experimental values [35]. The SPI continuous gels show an increasing G'_C value with increasing gelatin concentration. In the model, the addition of gelatin at constant SPI concentration leads to an increased concentration of SPI in its phase (relatively more water moves to the gelatin phase) thereby increasing G'_{GP} and simultaneously G'_C. For the situation where (liquid) gelatin forms the continuous phase, low G'_C values are predicted once sufficient gelatin is present to form a continuous gelatin phase (above 0.02 $g_{protein}$ / g_{water} gelatin). Addition of gelatin above this concentration does not lead to further reduction in predicted G'_C values which reflects the large dependency of mixed gels on the continuous phase as found earlier for model systems [6].

While the theoretical models for phase separated gels with spherical enclosures fail to predict the behavior of the SPI / gelatin A system (cf. Figure 7.3), models for bi-continuous and completely mixed gels are close to the measured ones. In case of the completely mixed gel, a line is obtained in Figure 7.3 since in this special case SPI is not concentrated in its phase but assumed to form a continuous network independent of the gelatin concentration. The bi-continuous model shows initially an increase in G'_C due to the concentration effect of SPI upon gelatin addition. Above a certain gelatin concentration this is counteracted by the fact that the gelatin phase increases in volume fraction which weakens the composite indicated by a decrease in G'_C.

Figure 7.3 suggests that the microstructure of mixed SPI / gelatin gels is likely completely mixed or bi-continuous. However, this is only a snapshot of the system at one specific temperature and one single SPI concentration. In order to generalize this finding all mixing ratios and all total protein concentrations of gelatin and SPI should be similarly well described by these theories. As the moduli of the composites depend on the protein

concentration of gelatin and globular protein we have introduced in chapters 4 and 5 the storage modulus ratio *s* to quantify the effect of gelatin on the modulus of globular protein gels independent of the globular protein concentration ($s = G'_{measured} / G'_{GP;M}$ where $G'_{GP;M}$ is the storage modulus expected for a pure globular protein gel). Using this scaling, increasing concentrations of gelatin type A were shown to decrease the storage modulus of WPI and SPI gels in chapter 5.

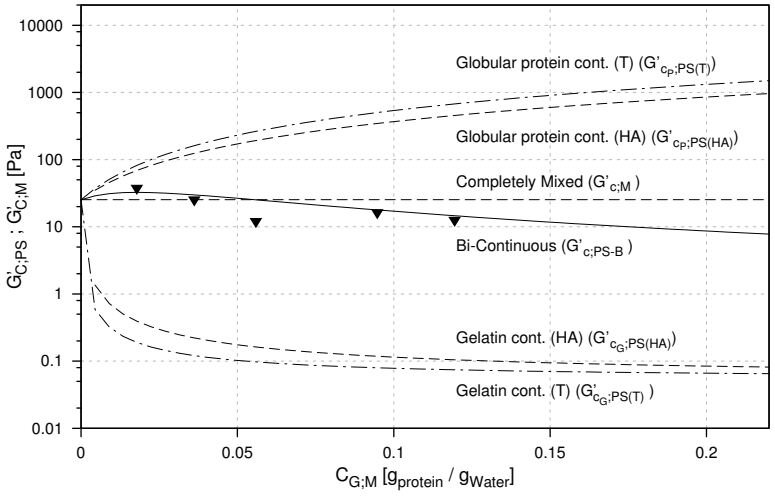

Figure 7.3 Storage modulus G'_C of mixed gels at 95 °C for samples containing 0.045 $g_{Protein}$ / g_{Water} SPI at different gelatin concentrations. Experimental data are shown as symbols (▼) and lines are obtained from calculations using equations 7.7 to 7.8 using p = 1.

The measured ratio *s* for SPI / gelatin A mixtures from chapter 5 is shown in Figure 7.4. Lines in the same graph present the expected ratio *s* calculated using the bi-continuous model (Figure 7.4A, equation 7.8) or models with one protein in the continuous phase with the other protein located in spherical enclosures by the Takayanagi approach (Figure 7.4B, equations 7.6). The results for the Hashin approach are close to the Takayanagi approach and are not shown. The measured ratio *s* decreases with increasing gelatin concentration from slightly above 1 to approximately 0.2 at 0.15 $g_{protein}$ / g_{water} gelatin type A. Figure 7.4A shows the expected behavior of bi-continuous gels at five different SPI concentrations. At low SPI concentration and increasing gelatin concentrations an increase in *s* at low gelatin concentration followed by a decrease in *s* at higher gelatin concentrations is predicted. At increasing SPI concentrations the initially increase is not observed anymore and *s* decreases with increasing gelatin concentration. Measured *s*

values are within the range of predicted values which will be discussed in more detail later on.

The predicted *s* values for the microstructures with either one of the proteins (SPI or gelatin) in the continuous phase and the other in the dispersed phase are shown in Figure 7.4B. Calculated *s* values for gelatin continuous systems decrease with increasing gelatin concentration and are much lower than the measured values. For SPI continuous systems an increase in *s* with increasing gelatin concentration is predicted which is opposite to the decreasing trend of *s* as observed experimentally. Both of these theoretical descriptions thus fail to describe the experimental results.

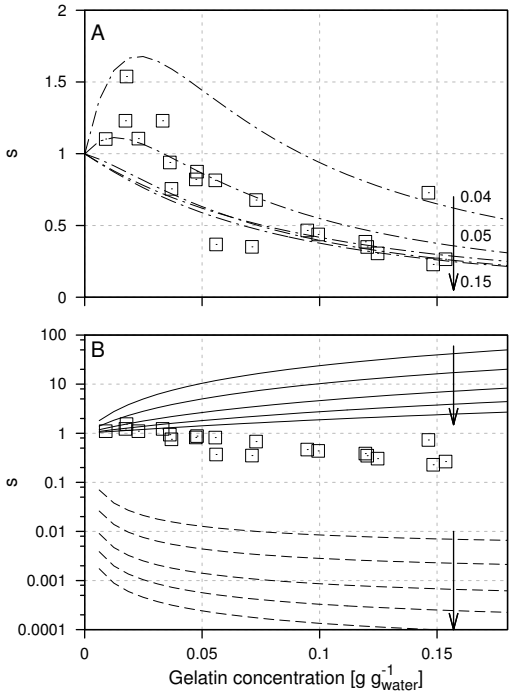

Figure 7.4 Ratio *s* ($G'_{measured}$ / $G'_{GP;M}$) for SPI / gelatin type A mixtures at 95 °C as a function of gelatin concentration at different SPI concentrations. SPI values for calculations were 0.04, 0.05, 0.07, 0.1 and 0.15 $g_{protein}$ / g_{water}. Increasing SPI concentrations are indicated by an arrow in the graphs. Graph A: Experimental results (□) together with theoretical values obtained from the bi-continuous model (equation 7.8). Graph B: Experimental results (□) together with theoretical values for spherical enclosure of one phase in a second phase (equations 7.6). SPI continuous systems are shown as solid lines and gelatin continuous as dashed line. Note that the vertical axis in graph B is on a logarithmic scale. The *p* - value was set to *p* = 1.

These experimental results suggest that the SPI / gelatin A system forms mixed gels with a bi-continuous microstructure something in line with the results from chapter 5 and

chapter 6. Using the experimental results from chapter 5 we were able to analyze the mixed WPI / gelatin A and WPI / gelatin B gels in the same way as outlined here for SPI / gelatin A gels. Results revealed that also for the WPI / gelatin (type A or B) mixed gels the bi-continuous model gives the best description of the experimental results.

For all three globular protein / gelatin mixed gels we were able to fit the measured data using the bi-continuous model (equation 7.8) by varying the *p*-value (relative affinity of proteins towards water). Using one *p*-value per protein pair (SPI / gelatin A, WPI / gelatin A or WPI / gelatin B) resulted in good fits between the experimental and predicted data. The measured versus predicted *s* values (predicted via bi-continuous model using the obtained *p*-value) for the three mixed systems are shown in Figure 7.5. For all three systems the values scatter around the diagonal line where the predicted *s* is equal to the measured *s*. In fact, WPI / gelatin A or gelatin B mixed systems show a lower degree of scatter in Figure 7.5 indicating an even better fit than obtained for the earlier presented SPI / gelatin A mixture.

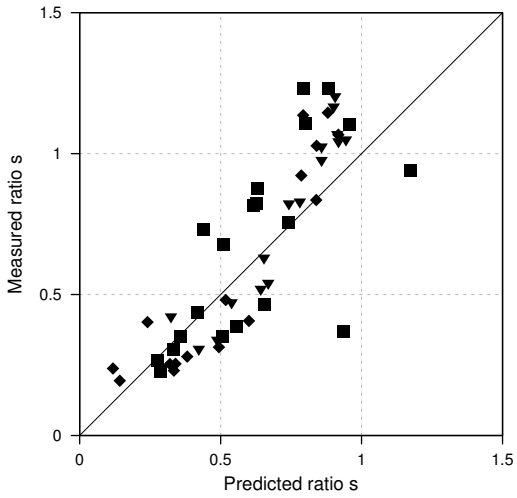

Figure 7.5 Measured storage modulus ratio *s* versus predicted storage modulus ratio *s* for WPI / gelatin type A (*p* = 1.95, ▼), WPI / gelatin type B (*p* = 0.77, ◆) and SPI / gelatin type A (*p* = 1.08, ■) gels at 95 °C using the bi-continuous model

Best fits were obtained for $p = 1.95$ for the WPI / gelatin type A mixed gels, $p = 1.08$ for the SPI / gelatin type A mixed gels and $p = 0.77$ for the WPI / gelatin type B mixed gels. These *p*-values are within the expected range for mixed protein gels [8, 22]. However, to

our knowledge these p-values are the first ones obtained assuming a bi-continuous microstructure.

Storage modulus of mixed globular protein / gelatin gels

Figure 7.6 shows the proposed mechanism leading to the phase separated microstructure of globular protein gels prepared in the presence of gelatin as proposed in chapter 5. The presence of gelatin was suggested to alter the structure of the bi-continuous globular protein gel leading to a coarsening of the globular gel microstructure. Gelatin was proposed to be present in the gel pores of the globular protein gel which are by definition continuous throughout the whole system (i.e. form a second continuous phase). This bi-continuous structure was shown in chapter 6 to allow gelatin to form a space spanning gel inside the globular protein gel pores which, dependent on the gelatin concentration, can dominate the rheological behavior of the mixed gels.

In the experiments used in chapters 5 and 6 globular proteins were gelled first and afterwards gelatin gelled inside the existing globular protein gels. Globular protein gels are not expected to be altered in structure or rheological response by the gelatin gelation. We verified this hypothesis by measuring storage modulus (results not shown), by analyzing the microstructure (using CLSM), and by measuring the globular protein gel structure using SESANS (chapter 5) before and after gelling and melting of gelatin inside globular protein gels. No significant changes in the structure and rheological response of the globular protein gels were found which suggests that gelatin only gels inside its phase without altering the globular protein gels. It is therefore a reasonable assumption that the phase volumes (areas of globular protein gel and gelatin occupied areas in Figure 7.6B4) of the two protein phases do not change during gelatin gelation inside the globular protein gel pores.

The composite modulus at 15°C should thus be predictable using the same water distribution as obtained at 95 °C where only globular proteins formed a gel by accounting for an increase in the storage modulus (gelation) of the gelatin phase upon cooling.

Figure 7.7A1 and Figure 7.7B1 show measured and predicted G'_c after 1 hour at 15 °C for mixed systems at one constant globular protein concentration (0.065 $g_{protein}$ / g_{water} WPI or SPI) at varying gelatin concentration. Here gelatin has formed a gel which was accounted for in the models by assigning the gelatin phase a storage modulus dependent on the gelatin concentration in its own phase. Additionally, an increase in the storage modulus of the globular proteins was measured upon cooling to 15 °C which was also included in the models. Even though it has already been found that the bi-continuous model gives the

best description the modulus of the systems also the predictions for the other earlier presented microstructures are shown.

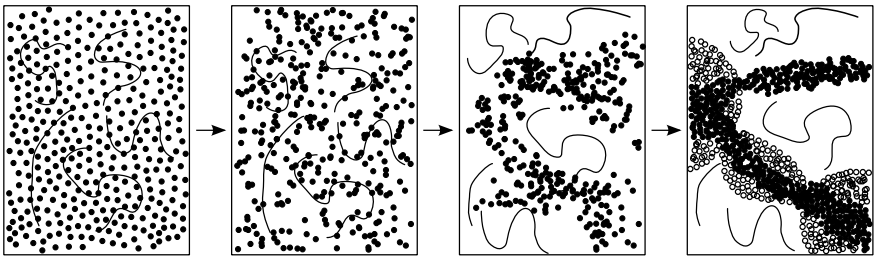

Figure 7.6 Schematic presentation of gel formation of globular protein / gelatin systems from chapter 5. Globular proteins are represented as spheres and gelatin as curves. B.1: mixed solution of globular proteins and gelatin. B.2: Primary aggregation of globular proteins in the presence of gelatin. B.3: Phase separation of globular protein aggregates and solvent phase (containing gelatin). B.4: Microstructure of mixed globular protein gels where gelatin is in the continuous solvent phase (= gel pores).

For SPI / gelatin A mixtures (Figure 7.7A1) all models (except the completely mixed one) describe the measured values well. The storage modulus increases strongly with increasing gelatin concentration. Figure 7.7A2 shows the plot of measured versus predicted G'_c values using the bi-continuous model and the water distribution that best described the SPI / gelatin A system at 95 °C (p = 1.08). This plot includes all measured samples prepared over the whole range of experimentally possible protein concentrations with gelatin concentrations between 0.01 and 0.14 $g_{protein}$ / g_{water} and SPI concentrations between 0.04 and 0.10 $g_{protein}$ / g_{water}. For all samples the bi-continuous model describes G'_c of the mixed gels well without a large scatter of the data around the diagonal line where the predicted G'_c is equal to the measured G'_c.

Following the same route for the WPI / gelatin type B mixture (results shown in Figure 7.7B1 and Figure 7.7B2), Figure 7.7B1 shows the measured and predicted G'_c at one constant WPI concentration with increasing gelatin concentration. Calculations were performed using p = 0.77 which was the water distribution that described the WPI / gelatin B mixed systems best at 95 °C. One pre-requisite to apply the above theories is that the measured data lies between the upper and lower bounds of the Hashin approach (or isostrain and isostress from Takayanagi). For p = 0.77 our experimental data is below these bounds suggesting that the storage modulus of one or even both phases is over-estimated in the models. As shown in Figure 7.7B2 this over estimation was found for most experimentally accessible samples containing 0.01 to 0.12 $g_{protein}$ / g_{water} gelatin and WPI concentrations between 0.06 and 0.17 $g_{protein}$ / g_{water} .

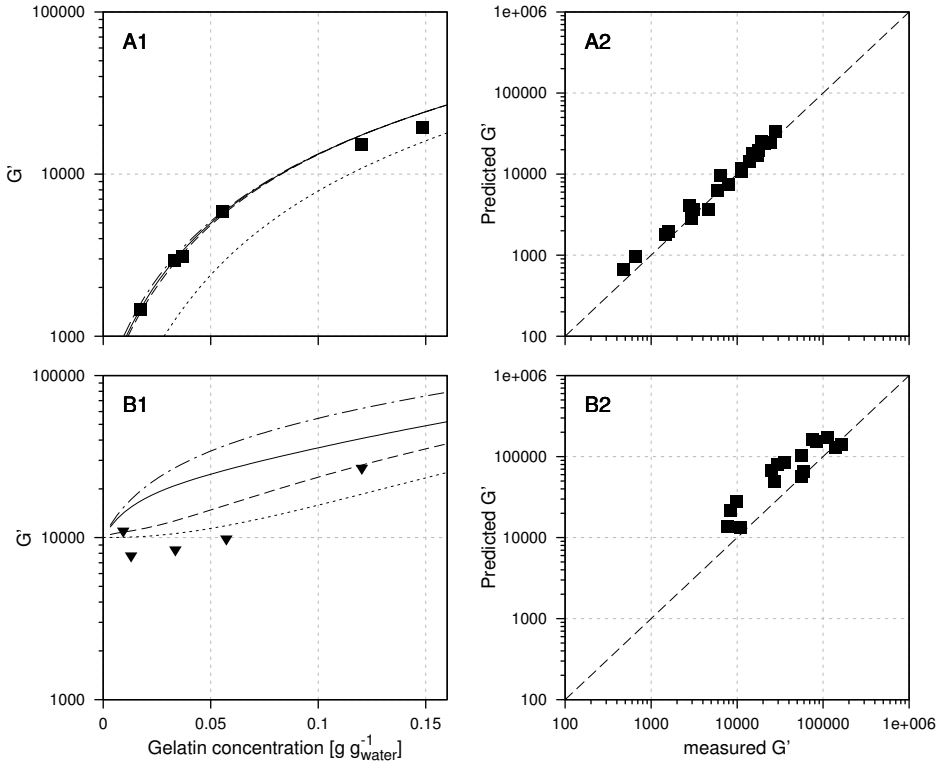

Figure 7.7 GraphA1: Measured storage modulus for mixed gels containing 0.065 $g_{protein}$ / g_{water} SPI and varying gelatin A concentration (■). Graph B1: Measured storage modulus values for mixed gels containing 0.065 $g_{protein}$ / g_{water} WPI and varying gelatin type B concentration (▼). Lines in graphs A1 and B1 are the theoretical G' values for the completely mixed (short dashed line), gelatin continuous (dashed line), WPI or SPI continuous (interrupted line) or bi-continuous (solid line) microstructural arrangement of globular proteins and gelatins at 15 °C (both proteins formed a gel). Graphs A2 and B2 show predicted versus measured G' values for SPI / gelatin type A mixtures (graph A2) or WPI / gelatin type B mixtures (graph B2) for the bi-continuous system using the p-values as obtained from fitting at 95 °C (p = 1.08 for SPI / gelatin A and p = 0.77 for WPI / gelatin B) over the whole experimentally accessible concentration ranges for both proteins.

To fit the experimental data to the models it is possible to use *p* as a fitting parameter. For $p \approx 0.15$ most experimental data points were found to be within the bounds of the Takayanagi approach. The physical picture behind this fitting procedure, however, is questionable. A change in *p*-value between 95 °C and 15 °C would imply that the water

distribution and phase volumes of the gelatin phase and globular protein phase change upon gelatin gelation. It also implies that the globular protein gel (WPI) increases in internal protein concentration and correspondingly storage modulus during gelling of gelatin inside the existing globular protein gel which is something not expected to occur. Results for WPI / gelatin type A were similar to those obtained for WPI / gelatin type B and are not shown separately. We observed a systematic over-estimation of G'_c for all WPI / gelatin mixed gels at conditions where both proteins gelled. We conclude that it is not possible to describe the composite modulus of all three mixed systems using the same water distribution factor *p* at conditions where initially only globular protein gelled and subsequently gelatin was gelled.

Discussion

The gelation of three mixed systems (WPI / gelatin A, WPI / gelatin B and SPI / gelatin A) at two conditions was modeled by different theories. At 95 °C where only globular proteins formed a gel the bi-continuous model described the measurement data best using reasonable *p*-values (water distribution) for all three systems. The results were in line with microstructural analysis showing bi-continuous gels (chapter 5).

The assumption that the *p*-values do not change during gelatin gelation (phase volumes stay constant) did not lead to a good description for two of the three systems studied. In fact, closer analysis of the SPI / gelatin A mixtures indicate that the good description of this system is probably coincidental. Namely, at the *p*-value we obtained from fitting the data to the bi-continuous model at 95 °C (p = 1.08) the two phases were predicted to have comparable G' values at all protein concentrations which makes the prediction insensitive for microstructure (see proximity of predictions from different models in Figure 7.7A1).

The discrepancy between predictions and measured values seems to be specific for the globular protein / gelatin mixed gels, as some of the used theories have been successfully applied in other systems. One reason might be the description of the water distribution by using only one *p*-value [16, 17]. Other reasons might be that complete phase separation is assumed. Proteins have been shown to have a high co-solubility (chapter 3, [11]) which might significantly change their concentrations in each phase or possibly enable them to form a gel in both phases (at different concentrations). Also, phase separation usually leads to a fractionation especially in the case of poly-disperse biopolymer mixtures which impacts on the biopolymer concentration and consequently the modulus of the individual gels in each phase. This effect has been shown to lead to large errors in predicting the storage modulus of the gels [39]. In addition, gelation does not necessarily lead to a complete arrest of phase separation. As shown for the whey protein aggregate /

carrageenan systems, gelation can lead to an increased tendency of the non-gelled biopolymer to distribute evenly throughout the systems after the gelation of the other biopolymer [40]. This observation could also serve as an explanation for the over-estimation of the G'_c in mixtures of WPI / gelatin type A and type B. Finally, as shown in chapter 5 the assumption that in phase separated mixtures WPI (and most probable also SPI) gels at an increased concentration is only valid to a limited extent for the globular protein / gelatin systems. The structure of gel building blocks of WPI in phase separated mixed gels was similar to the gel building block structure of single WPI systems on a low length scale (< approx. 300 nm) and differed at a larger length scale (mainly > 1 µm). The assumption that this gel has the rheological properties of a gel which was formed at a higher WPI concentration, is questionable and might be another reason why the currently available theories fail to explain the behavior of mixed globular protein / gelatin gels.

Conclusion

The application of material science approaches for mixed gels (composites) is not able to account for the changes that occur in the mixed globular protein / gelatin gels. Despite the feasibility to model the experimental results using the different models, the physical picture behind the necessary adjustments of the fit parameter *s* is questionable. This was concluded after analyzing several mixed systems at two conditions where proteins were selectively gelled. Results do not imply that this approaches are per se wrong for mixed biopolymer gels. For mixed gels where biopolymers are well separated in their own phase and where their gel properties inside the phase are comparable to those observed in bulk these models are expected to be reasonably successful. Nonetheless, one should be careful to apply the models to mixed systems in particular in systems where no phase inversion is observed or where the presence of a secondary biopolymer alters the gel microstructure of the other gelling biopolymer.

References

1. Hashin, Z. and S. Shtrikman, *Note on the effective constants of composite materials.* Journal of the Franklin Institute, 1961. **271**(5): p. 423-426.
2. Hashin, Z. and S. Shtrikman, *Note on a variational approach to the theory of composite elastic materials.* Journal of the Franklin Institute, 1961. **271**(4): p. 336-341.
3. Davies, W.E.A., *The theory of elastic composite materials.* Journal of Physics D: Applied Physics, 1971. **4**(9): p. 1325.
4. Davies, W.E.A., *The elastic constants of a two-phase composite material.* Journal of Physics D: Applied Physics, 1971. **4**(8): p. 1176.
5. Wang, M. and N. Pan, *Elastic property of multiphase composites with random microstructures.* Journal of Computational Physics, 2009. **228**(16): p. 5978-5988.
6. Takayanagi, M., H. Harima, and Y. Iwata, *Viscoelastic behavior of polymer blends and its comparison with model experiments.* The Society of Material Science, 1963.
7. Zhou, Z.M., J. Gao, F. Li, Y.P. Wang, and M. Kolbe, *Experimental determination and thermodynamic modeling of phase equilibria in the Cu-Cr system.* Journal of Materials Science, 2011. **46**(21): p. 7039-7045.
8. Kasapis, S., *Phase separation in biopolymer gels: A low- to high-solid exploration of structural morphology and functionality.* Critical Reviews in Food Science and Nutrition, 2008. **48**(4): p. 341-359.
9. Clark, A.H., R.K. Richardson, S.B. Ross-Murphy, and J.M. Stubbs, *Structural and mechanical properties of agar/gelatin co-gels. Small-deformation studies.* Macromolecules, 1983. **16**(8): p. 1367-1374.
10. Morris, E.R., *The effect of solvent partition on the mechanical properties of biphasic biopolymer gels: an approximate theoretical treatment.* Carbohydrate Polymers, 1992. **17**(1): p. 65-70.
11. Polyakov, V.I., O.K. Kireyeva, V. Grinberg, and V.B. Tolstoguzov, *Thermodynamic compatibility of proteins in aqueous media. Part. I. Phase diagrams of some water--protein A--protein B systems.* Die Nahrung, 1985. **29**(2): p. 153-160.
12. Tolstoguzov, V., *Some thermodynamic considerations in food formulation.* Food Hydrocolloids, 2003. **17**(1): p. 1-23.
13. Chronakis, I.S. and S. Kasapis, *Structural properties of single and mixed milk/soya protein systems.* Food Hydrocolloids, 1993. **7**(6): p. 459-478.
14. Alevisopoulos, S., S. Kasapis, and R. Abeysekera, *Formation of kinetically trapped gels in the maltodextrin—gelatin system.* Carbohydrate Research, 1996. **293**(1): p. 79-99.
15. Chronakis, I.S., S. Kasapis, and R.K. Richardson, *Small deformation rheological properties of maltodextrin—milk protein systems.* Carbohydrate Polymers, 1996. **29**(2): p. 137-148.

16. Manoj, P., S. Kasapis, and I.S. Chronakis, *Gelation and phase separation in maltodextrin-caseinate systems.* Food Hydrocolloids, 1996. **10**(4): p. 407-420.
17. Manoj, P., S. Kasapis, and M.W.N. Hember, *Sequence-dependent kinetic trapping of biphasic structures in maltodextrin-whey protein gels.* Carbohydrate Polymers, 1997. **32**(2): p. 141-153.
18. Richardson, R.K. and S. Kasapis, *Rheological methods in the characterisation of food biopolymers*, in *Developments in Food Science*. 1998. p. 1-48.
19. Walkenström, P. and A.-M. Hermansson, *Mixed gels of fine-stranded and particulate networks of gelatin and whey proteins.* Food Hydrocolloids, 1994. **8**(6): p. 589-607.
20. Ziegler, G.R. and S.S.H. Rizvi, *Predicting the Dynamic Elastic Modulus of Mixed Gelatin-Egg White Gels.* Journal of Food Science, 1989. **54**(2): p. 430-436.
21. Ziegler, G.R., *Microstructure of mixed gelatin-egg white gels: Impact on rheology and application to microparticulation.* Biotechnology Progress, 1991. **7**(3): p. 283-287.
22. Katopo, L., S. Kasapis, and Y. Hemar, *Segregative phase separation in agarose/whey protein systems induced by sequence-dependent trapping and change in pH.* Carbohydrate Polymers, 2012. **87**(3): p. 2100-2108.
23. Dickinson, E., *Emulsion gels: The structuring of soft solids with protein-stabilized oil droplets.* Food Hydrocolloids, 2012. **28**(1): p. 224-241.
24. van Vliet, T., *Rheological properties of filled gels. Influence of filler matrix interaction.* Colloid & Polymer Science, 1988. **266**(6): p. 518-524.
25. Çakir, E. and E.A. Foegeding, *Combining protein micro-phase separation and protein-polysaccharide segregative phase separation to produce gel structures.* Food Hydrocolloids, 2011. **25**(6): p. 1538-1546.
26. Herzig, E.M., K.A. White, A.B. Schofield, W.C.K. Poon, and P.S. Clegg, *Bicontinuous emulsions stabilized solely by colloidal particles.* Nature Materials, 2007. **6**(12): p. 966-971.
27. Shrinivas, P., S. Kasapis, and T. Tongdang, *Morphology and mechanical properties of bicontinuous gels of agarose and gelatin and the effect of added lipid phase.* Langmuir, 2009. **25**(15): p. 8763-8773.
28. Anderson, V.J. and R.A.L. Jones, *The influence of gelation on the mechanism of phase separation of a biopolymer mixture.* Polymer, 2001. **42**(23): p. 9601-9610.
29. de Jong, S. and F. van de Velde, *Charge density of polysaccharide controls microstructure and large deformation properties of mixed gels.* Food Hydrocolloids, 2007. **21**(7): p. 1172-1187.
30. Van De Velde, F., F. Weinbreck, M.W. Edelman, E. Van Der Linden, and R.H. Tromp, *Visualisation of biopolymer mixtures using confocal scanning laser microscopy (CSLM)*

and covalent labelling techniques. Colloids and Surfaces B: Biointerfaces, 2003. **31**(1-4): p. 159-168.
31. Hashin, Z., *The Elastic Moduli of Heterogeneous Materials.* Journal of Applied Mechanics, 1962. **29**(1): p. 143-150.
32. Hsiao-Sheng, C. and A. Acrivos, *The effective elastic moduli of composite materials containing spherical inclusions at non-dilute concentrations.* International Journal of Solids and Structures, 1978. **14**(5): p. 349-364.
33. Watt, J.P., G.F. Davies, and R.J. O'Connell, *The elastic properties of composite materials.* Reviews of Geophysics, 1976. **14**(4): p. 541-563.
34. Yang, X.I.N., N.R. Rogers, T.K. Berry, and E.A. Foegeding, *MODELING THE RHEOLOGICAL PROPERTIES OF CHEDDAR CHEESE WITH DIFFERENT FAT CONTENTS AT VARIOUS TEMPERATURES.* Journal of Texture Studies, 2011. **42**(5): p. 331-348.
35. Hashin, Z. and S. Shtrikman, *A variational approach to the theory of the elastic behaviour of multiphase materials.* Journal of the Mechanics and Physics of Solids, 1963. **11**(2): p. 127-140.
36. Sok, L.T., S. Kasapis, and A.T.K. Han, *Phase model interpretation of the structural properties of two molecular soy protein fractions.* Journal of Agricultural and Food Chemistry, 2008. **56**(7): p. 2490-2497.
37. Lipatov, Y. and T. Alekseeva, *Phase-Separated Interpenetrating Polymer Networks*. 2007, Springer Berlin Heidelberg. p. 1-227.
38. Walkenström, P. and A.-M. Hermansson, *Fine-stranded mixed gels of whey proteins and gelatin.* Food Hydrocolloids, 1996. **10**(1): p. 51-62.
39. Edelman, M.W., R.H. Tromp, and E. van der Linden, *Phase-separation-induced fractionation in molar mass in aqueous mixtures of gelatin and dextran.* Physical Review E - Statistical, Nonlinear, and Soft Matter Physics, 2003. **67**(2 1): p. 214041-2140411.
40. Baussay, K., D. Durand, and T. Nicolai, *Coupling between polysaccharide gelation and micro-phase separation of globular protein clusters.* Journal of Colloid and Interface Science, 2006. **304**(2): p. 335-341.

CHAPTER 8

General Discussion

Most foods are mixtures of a large number of ingredients. Selective mixing of ingredients together with the appropriate processing happens every day in millions of kitchens worldwide. The main reason to apply a variety of ingredients is to create foods with improved texture and taste compared to the single ingredients. Linking textural aspects of foods to their structure, and first of all, linking the ingredients and processing steps to their structure forms a constant challenge in food science. This thesis presented a general approach towards understanding the relationships between food ingredients and food structure in mixed systems, which is a first step towards linking ingredient properties and processing steps to textural properties of foods. We focused on the gel microstructure and its relationship to the rheological properties of the mixed protein gels. Characterization of the proteins, their mutual interactions, and changes thereof throughout the gelation process was proven to be a valuable approach towards identifying the relevant parameters that influence the gel formation and concomitant gel network structure in mixed systems.

In this chapter we discuss some of the important aspects of gelation and molecular interactions in mixed systems that were not in detail dealt with in the separate chapters. We will start with the importance of molecular interactions in gelation processes which, despite being outside the scope of chapter 2, is an important aspect in understanding gelation in protein and mixed protein solutions.

Molecular interactions and gelation

In chapter 2, membrane osmometry was presented as a valuable tool for the characterization of molecular size and molecular interactions (in terms of the second virial coefficient B') of proteins in solutions. Most scientists nowadays use scattering techniques (light, x-ray or even neutron scattering) to characterize molecular size [1-4] and in some cases also molecular interactions [5-9]. However, especially the insensitivity of osmometry towards impurities and the number-averaged results make it an important complementary technique to scattering techniques. In some cases, osmometry in fact has specific advantages over other techniques, especially when the results are used in (number based) theories like the virial approach presented in chapter 3. Besides proving the relevance of osmometry measurements in the molecular characterization of biopolymers, chapters 2 and 3 also showed the practical applicability of membrane osmometry which has been sparsely used as an experimental technique over the last decades.

For mixed protein gels, the second virial coefficients B' were crucial in describing the phase behavior of mixed biopolymer solutions using the virial theory presented in chapter 3. Yet, second virial coefficients are essential in many thermodynamic descriptions where they can often only be estimated due to the lack of experimental results [10-12]. Additionally, second virial coefficients are interesting in understanding the behavior of e.g. proteins as shown on the example of protein crystallization [13, 14].

In a preliminary study we have used measured second virial coefficients to investigate the relationship between electrostatic repulsion and gel microstructures of protein gels. For proteins that form heat-set gels the reduction in electrostatic repulsion (via e.g. changes in pH or ionic strength) has been used to explain a transition from fine stranded, transparent, gel to coarse, turbid (micro-phase separated) gels [15]. Figure 8.1 shows the second virial coefficient B' for pea protein as a function of pH. A characterization of the gel microstructures and the small and large deformation properties of these gels has been published elsewhere [16]. Below pH 3.4 at conditions where a strongly positive second virial coefficient B' represents repulsive interactions between pea protein molecules fine stranded gels were formed when heating pea protein solutions. At pH values above pH ≈ 3.5 where B' is negative (attraction between pea protein molecules) coarse protein gels were obtained which was correlated to changes in rheological properties of these gels.

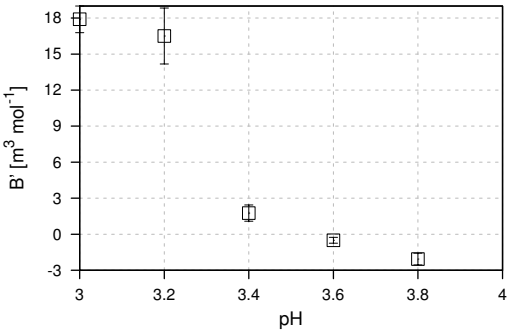

Figure 8.1 Second virial coefficient B' of pea protein as a function of pH

Similar relationships between measured molecular interactions and gel microstructure also hold for other proteins. In chapter 2 we demonstrated that the repulsion between β-lactoglobulin, BSA and WPI molecules below an ionic strength of 20 mM were dominated by electrostatic repulsion. At increasing ionic strength BSA and WPI could be well approximated as hard spheres and β-lactoglobulin molecules as adhesive hard spheres. For β-lactoglobulin, Ako,Nicolai et al. (2009) [17] and Baussay et al. (2004) [1] observed a transition from fine to coarse, micro – phase separated gels and correlated changes in the gel building blocks at 20 mM ionic strength which is consistent with the B' results from chapter 2. Similarly, the minimum gelling concentration of WPI gels [18] and the macroscopic appearance and storage modulus of BSA gels [19] show a transition from fine stranded to coarse gel structures at the point where we reported in chapter 2 a transition from electrostatic repulsion dominated to hard body interactions.

Molecular interactions and phase behavior

Using the second virial coefficients from chapter 2 for single protein systems it was possible in chapter 3 to quantify the molecular interactions between different proteins (e.g. WPI / gelatin) in terms of the second cross virial coefficient $B'_{1,2}$. Besides these experimental results, chapter 3 also presented a virial approach to predict liquid – liquid phase separation of binary biopolymer or colloidal mixtures. This theory is directly applicable to systems where second virial coefficients and second cross virial coefficients were experimentally determined or where second virial coefficients can be obtained analytically, as is the case for i.e. binary hard sphere mixtures. In literature, similar approaches successfully described the phase behavior of PEG mixtures [20], dextran / PEG mixtures [21] and several protein / polysaccharide mixtures [5]. In these systems, polymers are well approximated as spherical particles whose phase behavior was well described taking into account only the two particle interaction (second virial coefficients

and second cross virial coefficient). For dextran / β-lactoglobulin [22] and PEG / lysozyme mixtures [23], however, the virial approach failed to predict their phase behavior, which is most likely a result of the large size ratio of polymers to globular proteins. In the virial approach polymers are characterized by their excluded volume. In mixtures of polymers (e.g. dextran or PEG) with much smaller colloids (such as globular proteins) the colloids are able to enter the radius of gyration of the polymers, and the second virial theory breaks down [10, 23, 24].

Other shortcomings, which in return make the virial approach simple and easily applicable to many systems, are that the theory omits the possible formation of a solid phase (crystals) as found in some colloidal or protein solutions [24]. Nor does the virial approach account for the disproportionation of salts between different phases in systems containing charged macromolecules (e.g. proteins) which can have effects on the phase behavior of biopolymer mixtures [25, 26]. The behavior of the solvent, in fact, is integrated out which simplifies the theory but in return disregards any changes in the chemical potential of the solvent. On the other hand, in the prediction of liquid – liquid phase separation the virial approach accounts for the excluded volume of the depletant. Most theories dealing with depletion typically model the depletant as inter-penetrating or ghost particles and the osmotic pressure is typically based on Van 't Hoff's law discarding non-ideal behavior [24]. Whether in a specific case the virial theory has advantages or disadvantages over other theories should be carefully considered before its application. One example where we have observed inconsistencies in results obtained via the virial approach are situations where virial coefficients become strongly negative which most probably is caused by excluding a possible solid phase.

Independent of the limitations of the virial approach compared to other theories, an advantage is that using membrane osmometry one can experimentally directly obtain all relevant parameters (molecular size and second virial coefficients B' and $B'_{1,2}$) to predict the (liquid – liquid) phase behavior of mixed biopolymer solutions.

In chapter 3 we used a combination of measured virial coefficients and the virial approach to investigate the difference in phase behavior between mixtures including polysaccharide, which typically phase separate at relatively low concentrations [27], and protein mixtures, which typically show high compatibility [28-30]. Using the measured second virial (and second cross virial) coefficients it was possible to successfully predict the phase diagram of the mixed dextran / gelatin system. This not only proved the applicability of the virial approach towards predicting phase separation but also verified that using osmometry the relevant parameters (number averaged molecular weight and second virial coefficients) can be obtained experimentally. For mixed protein systems the

measured second virial (and second cross virial) coefficients were important in explaining the absence of phase separation in solutions of globular proteins and gelatin (chapter 3). Gelatins and globular proteins (and also globular protein aggregates) were similar in their effective molecular sizes which excluded the possibility of phase separation by depletion interaction. Together with the relatively low additional attraction (at a pH between the isoelectric points (pI) of the proteins) or repulsion (at a pH above the pI of both proteins) via electrostatic interactions between gelatin and globular proteins, this small difference in molecular size of the proteins was used to explain the high co-solubility of proteins.

In chapters 2 and 3 a quantitative description of molecular interactions and relevant molecular sizes in mixed protein solutions up to the moment before gelation was given. This is an important pre-requisite for the preparation of mixed gels. Only in this case the observed changes in gel structures of mixed protein systems can be directly attributed to the gelation process. For solutions where phase separation already occurs in solution before gelation, the sample handling (mixing times, shear, time between sample preparation and measurement) becomes important in determining the rheological properties and microstructure of the mixed gels [31-34], a situation which was purposely avoided.

Concentrations in Protein Mixtures

Regarding the molecular interactions of proteins (chapter 2 and 3) we observed that it was crucial to carefully determine the protein concentration as described in detail in the Material and Methods section of chapter 2. Here we address the importance of protein concentration and ion concentration (ionic strength) as we have used it throughout the chapters dealing with gelation of proteins.

Solvent conditions and protein concentration have large effects on properties such as elastic modulus, fracture properties and visual appearance (e.g. turbidity or sense of touch) of protein gels. For proteins solvent conditions (we here only consider water as a solvent) like pH and the ionic strength are important. All results presented in this thesis were obtained at neutral pH and the main difference in solvent conditions was the variation in ionic strength. The concentration of small molecules, such as ions, is commonly expressed in molarity [$mol_A\ l^{-1}$]. For solutions containing low total solid contents which also can be prepared volumetrically such as e.g. buffer solutions this is a convenient and well-established measure. For non-dilute solutions or those prepared on a weight basis (density unknown) the concentration of a solute is better expressed by the molality [$mol_A\ kg^{-1}_{water}$] [25, 35]. In this way one not just avoids having to estimate the

solution density, but also accounts for the amount of total available water in the system which decreases with increasing dry matter content (protein in our case).

In the same line of thought, also the concentration of proteins in mixed systems must be corrected for the amount of water in a solution. The most commonly used definition for concentration of e.g. a protein A in solution is in terms of the mass concentration $c_{p(total)}$ as commonly expressed by the weight fraction

$$c_{p(total)} = \frac{m_A}{m_{Total}} = w_A \qquad 8.1$$

with w_A the weight fraction of protein A, m_A the mass of the protein *A* and m_{Total} the total mass of all components in the mixture. For a mixture of two proteins m_{total} is given by

$$m_{Total} = m_A + m_B + m_w + m_o \qquad 8.2$$

where m_B is the weight of protein B, m_w the weight of the water and m_o the weight of all other components such as e.g. salts or other solutes. For the simplicity of the following examples we will assume that $m_o = 0$. Following the route of expressing the concentration of constituents relatively to the amount of available water (molality), we can also define the protein A concentration (c_p) as

$$c_p = \frac{m_A}{m_w} \qquad 8.3$$

The difference between these two approaches is illustrated in Figure 8.2 which also contains the concentration of protein A as calculated via equations 8.1 or 8.3. For a mixture with m_w = 0.8, m_A = 0.2, m_B = 0 (Figure 8.2.1) a protein weight fraction of 0.2 (20%) is obtained using the commonly used definition of protein concentration given by equation 8.1. Expressed based on the water (equation 8.3) we obtain 0.25 $g_{protein}$ / g_{water}. When adding protein B to the systems (m_w = 0.6, m_A = 0.2, m_B = 0.2, Figure 8.2.2) the weight fractions of protein A defined by equation 8.1 stays at 0.2. However, as shown in Figure 8.2.2 the mixed system contains less water than the systems that only contains protein A which effectively concentrates protein A. Calculating the protein concentration via equation 8.3, accounts for this concentration effect where we find an increase from 0.25 to 0.33 $g_{protein}$ / g_{water}.

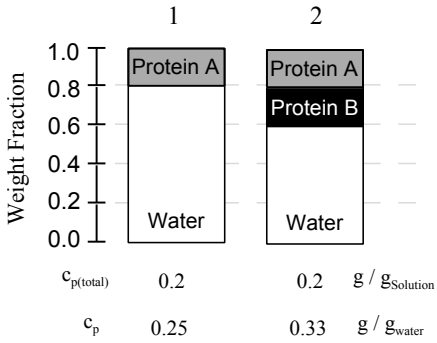

Figure 8.2 Schematic representation of protein concentration in a binary protein system using different definitions of mass concentration. Bottom two rows show concentration of protein A calculated via equations 8.1 (traditional calculation of concentration) and 8.3 (calculation based on available water) respectively

To demonstrate the difference between the two definitions we will further discuss the storage modulus as measured for single and mixed gelatin gels. In chapter 4 the effect of added globular protein on the storage modulus was investigated using the ratio between the measured storage modulus $G'_{measured}$ of a mixture scaled by the storage modulus expected for a single gelatin gel $G'_{Gelatin}$ given by the parameter *s*:

$$s = \frac{G'_{measured}}{G'_{Gelatin}} \qquad 8.4$$

Here *s* = 1 indicates that the storage modulus of a mixed gel is equal to that of a pure gelatin gel, *s* > 1 indicates an increased modulus. In chapter 4 we used this approach to show that the addition of WPI to gelatin type A or type B gels did not change their rheological properties which was in line with microstructural observations. The original graph is shown in Figure 8.3A where the ratio *s* of WPI / gelatin mixtures is close to 1 independent of the WPI concentration (given in $g_{protein}$ / g_{water}). For the addition of whey protein aggregates (WPA) *s* > 1 correlated to microstructural changes in the mixed gels.

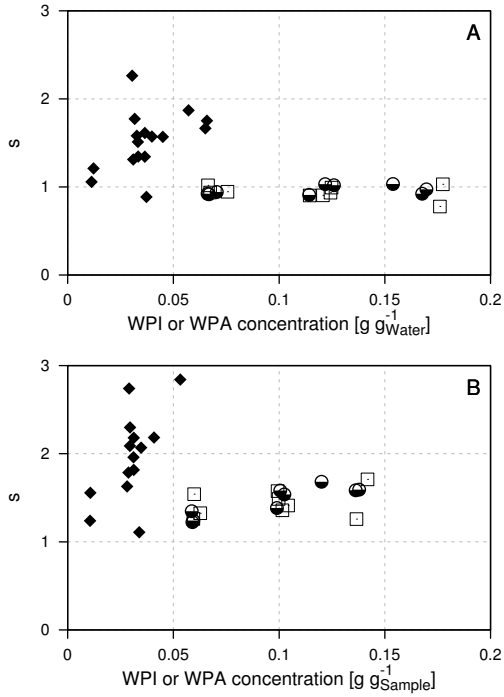

Figure 8.3 Storage modulus ratio *s* for gelatin gels at 15 °C with added globular protein for mixtures of gelatin A / WPI (◒), gelatin B / WPI (□) and gelatin A / WPA (◆). Graph A: calculations performed by defining protein concentrations via equation 8.3. graph B: Calculations performed using the definition of protein concentration given by equation 8.1

Figure 8.3B shows the same data re-calculated when expressing the concentration based on the total sample weight instead of the available water. For the gelatin / WPI mixed gels the ratio *s* is > 1 for all measured samples, with an increase for increasing WPI concentration (in $g_{protein}$ / $g_{Solution}$). This significantly changes the interpretation of the (same) rheological data. Based on Figure 8.3B one would conclude that the addition of WPI has a synergistic effect on the gelatin gel stiffness (G'). This effect, however, would also observed when adding inert glass beads that do not influence the gelatin gel network, and is only based on the lower amount of water in the system at constant total weight.

The above example points out the importance of the choice of concentration measure in mixed protein systems. The choice should be considered carefully, in contrast to the fact that it is typically considered to be a trivial matter.

The rheological response of mixed gels

Having illustrated the importance for the appropriate choice for a concentration measure on the example of the rheological response of mixed gelatin gels we now discuss the rheological response of mixed protein gels in more detail. For food relevant mixed systems an increasing number of relationships between the rheological responses and the corresponding microstructural changes in protein / polysaccharide [12, 36-50] or mixed protein [51-64] gels are published. Research on mixed systems, such as mixed protein gels, typically aims to create systems with properties, i.e. rheological properties, which are not possible using either one of the single systems.

For example, Brink et al. (2007) [51], Walkenström et al. (1994) [60], Walkenström et al. (1996) [61], and Walkenström et al. (1997) [62] showed that a large variety of rheological responses can be obtained by varying the order of gelation or protein ratios in mixed WPI / gelatin gels. Non-additivity of elastic moduli and fracture stress in mixed gels were attributed to segregative phase separation between gelatin and whey protein during gelation. In chapter 6 we were able to show that the fracture stress of the similar soy protein isolate (SPI) / gelatin gels was simply determined by the stronger of the two networks in the bi-continuous mixed gels. However, also in our research we were not able to explain the modulus of the mixed gels by simply adding the modulus of the individual SPI and gelatin gels. This non-additivity has also been reported for the egg white / gelatin [63, 64] and whey protein / agarose [65] mixed gels and in literature has been modelled using the so-called blending laws (see chapter 7) as initially introduced to biopolymer mixtures by Clark, Richardson et al. (1983) [66]. The applicability of the blending laws or similar theoretical approaches, however, is problematic as discussed in chapter 7. They only lead to exact results for ideal bi-continuous systems [67, 68], systems with spherical enclosures of one phase in a second phase arranged in a specific way [69] or mixed gels consisting of parallel or serial gel pieces [70]. In any other case they are only able to predict the range of expected moduli via the prediction of upper and lower bounds and cannot be used to describe the modulus of experimental data.

Furthermore, in the case of globular protein gels results in chapter 7 showed that besides difficulties of the solvent partitioning between phases in mixed biopolymer gels [65, 71-75] also the assumption that each protein forms a gel inside its own phase as it would in bulk is questionable. This difficulty is schematically summarized in Figure 8.4. Figure 8.4A is a representation of a coarse globular protein gel as typically obtained at conditions where electrostatic interactions are screened. The assumption that in a phase separated, bi-continuous mixed gel the globular protein forms a gel with the same gel structure as in bulk (Figure 8.4A) would lead to a microstructure as depicted in Figure

8.4B. Here the structure of the globular protein network (and therefore also the rheology) is not altered compared to Figure 8.4A, but the globular protein network is simply confined in its phase. The remaining volume fraction (second phase) is occupied by the secondary ingredient, here shown for the case of gelatin, which leads to a bi-continuous arrangement of the two gels. In chapter 5, however, we discussed that for the case for globular protein gels formed in the presence of secondary (non-gelling) gelatin with a molecular size above that of the gelling globular protein the microstructural arrangement is most probably not as depicted in Figure 8.4B. Results indicated that the microstructure of the globular protein gel was altered rather than the gel solely confined in one phase. In chapter 5 we proposed that the microstructure of these mixed gels is more likely as depicted in Figure 8.4C. The presence of gelatin during the globular protein gelation led to an increasing coarseness (size of the black gel domains in Figure 8.4C compared to Figure 8.4A). In chapter 7 we discussed that this has an significant impact on the ability to model the rheological behavior of these gels which we propose here to be due to the difference in the assumed arrangement of gels (Figure 8.4B) versus the arrangement we propose based on the results from our results in this thesis (Figure 8.4C).

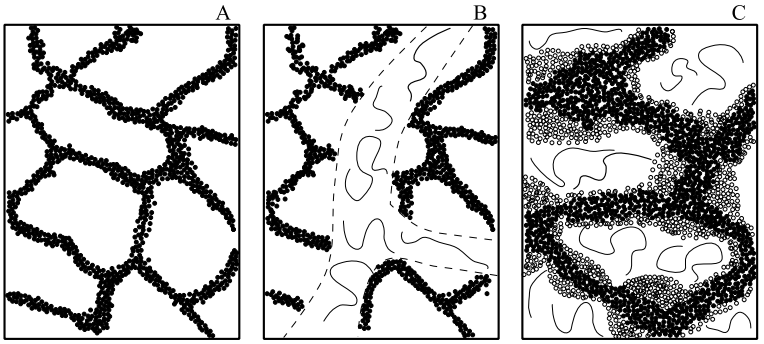

Figure 8.4 Schematic representation of gel microstructures. A: Microstructure of a single globular protein gel prepared at conditions where electrostatic repulsion is minimized. B: Idealized bi-continuous globular protein / gelatin gel expected for application of rheological models. C: Representation of the proposed structure of mixed globular protein / gelatin gels from this thesis. Black spheres represent WPI molecules, lines represent gelatin. Open circles in scheme C indicate changes upon increasing globular protein concentration.

Importance of molecular size in mixed protein gels

Alongside the reported changes in gel rheology and gel microstructure we also presented certain mixed systems where the presence of secondary proteins did not alter the rheological and microstructural properties of the initially formed gel. In chapter 4 this was the case for gelatin gels with added globular proteins. In chapter 5 the presence of hydrolyzed gelatin did not induce the changes that we observed when using non-hydrolyzed gelatin. In both chapters the molecular sizes (defined by the radius of spherical equivalent of the excluded volume) of proteins as obtained in chapter 2 and chapter 3 were used to explain the presence or absence of (enhanced) phase separation during gelation leading to rheological changes in mixed systems.

By interpreting gelation as an increase in size from the single protein to a space spanning network (with accordingly an infinite size) we concluded that mixtures that during gelation initially pass a region with high miscibility (where the molecular size ratio q = 1) and subsequently a region of reduced miscibility are prone to (increased) phase separation during gelation (alteration in gel microstructure). The underlying mechanisms leading to this phase separation are, however, still unknown. As suggested in chapters 4 and 5 and proposed earlier in other mixed systems [37, 58, 76-78], depletion interactions between the differently sized proteins and intermediate aggregates formed during gelation forms a defendable explanation. However, changes in the shape of the intermediate aggregates, the stiffness of e.g. gelatin molecules due to helix formation or changes in the two particle interactions upon e.g. protein denaturation cannot be ruled out.

The generality of the proposed relationship between molecular size changes and the occurrence of phase separation during gelation still has to be proven by studying other systems and conditions. If applicable to mixed systems in general this relationship can be translated into simple guidelines for the development of gelled foods containing more than one type of biopolymers. By tuning the molecular sizes of the non-gelling biopolymer via e.g. hydrolysis or pre-aggregation one can purposefully induce or prevent microstructural and rheological changes in mixed gels. In this way, together with an improved generalized relationship between mixed gel properties (e.g. microstructure, rheological properties but also e.g. tribological properties) and sensorial perception [36-38, 79-84] careful considerations of molecular sizes can facilitate the development of foods with targeted sensorial properties, one increasingly important challenge in food industry.

Concluding remarks

The number of food-relevant mixed gels is countless considering the large number of possible biopolymers (mainly proteins and polysaccharides), solvent conditions (pH, ionic strength, divalent ions, other solutes) and gelation conditions (kinetics of gelation, gelation mechanisms). To use mixed gels in obtaining desired gel properties such as the rheological and microstructural characteristics considered in this thesis, but also others such as for instance macroscopic appearance, texture or even taste, it is thus not efficient to investigate all combinations of biopolymers, conditions and gelation kinetics.

In the effort towards generally applicable mechanisms describing the formation and final properties of mixed gel systems this thesis focused on the effect of size. The molecular size ratio was proposed to be the most important parameter in determining whether phase separation during gelation can (or cannot) occur in systems where molecular interactions are mainly due to hard body interactions (excluded volume interactions). The validity of this approach still has to be proven in future studies while its importance at conditions where increased repulsion or attraction between molecules exists is also still to be evaluated.

In preliminary studies we have observed that when electrostatic repulsion dominates the protein interaction ($B'_{1,2}$) the presence of gelatin can almost completely inhibit the formation of a space spanning whey protein network (at pH 2 without added salt). In a second example, we observed that the phase separation between whey protein aggregates and gelatin during gelatin gelation at pH 7 and ionic strengths around 20 mM could be inhibited as electrostatic repulsion dominate the interactions. In both cases mixed systems with new properties were formed. The whey protein / gelatin A mixed gel at pH 2 showed yielding behavior comparable to spreadable cheese and the non-phase separated gelatin gels with added WPA were transparent in contrast to the typically opaque mixed WPA / gelatin gels. Thus, it seems that at these conditions the molecular interactions rather than the changes in molecular size are the relevant parameters in determining the microstructural and rheological properties in mixed gels. Quantification of the relevant molecular interactions by measuring the second virial coefficients B' and $B'_{1,2}$, is believed to be the next important step towards a better understanding of generally applicable mechanisms and their targeted applications to mixed biopolymer gels.

References

1. Baussay, K., C.L. Bon, T. Nicolai, D. Durand, and J.-P. Busnel, *Influence of the ionic strength on the heat-induced aggregation of the globular protein β-lactoglobulin at pH 7.* International Journal of Biological Macromolecules, 2004. **34**(1–2): p. 21-28.
2. Harnsilawat, T., R. Pongsawatmanit, and D.J. McClements, *Characterization of β-lactoglobulin-sodium alginate interactions in aqueous solutions: A calorimetry, light scattering, electrophoretic mobility and solubility study.* Food Hydrocolloids, 2006. **20**(5): p. 577-585.
3. Phan-Xuan, T., D. Durand, T. Nicolai, L. Donato, C. Schmitt, and L. Bovetto, *On the crucial importance of the ph for the formation and self-stabilization of protein microgels and strands.* Langmuir, 2011. **27**(24): p. 15092-15101.
4. Wang, T. and J.A. Lucey, *Use of Multi-Angle Laser Light Scattering and Size-Exclusion Chromatography to Characterize the Molecular Weight and Types of Aggregates Present in Commercial Whey Protein Products.* Journal of Dairy Science, 2003. **86**(10): p. 3090-3101.
5. Semenova, M.G. and L.B. Savilova, *The role of biopolymer structure in interactions between unlike biopolymers in aqueous medium.* Food Hydrocolloids, 1998. **12**(1): p. 65-75.
6. Wanka, J. and W. Peukert, *Optimized Production of Protein Crystals: From 1D Crystallization Slot towards 2D Supersaturation B22 Diagram.* Chemical Engineering & Technology, 2011. **34**(4): p. 510-516.
7. Rosenbaum, D.F., A. Kulkarni, S. Ramakrishnan, and C.F. Zukoski, *Protein interactions and phase behavior: Sensitivity to the form of the pair potential.* The Journal of Chemical Physics, 1999. **111**(21): p. 9882-9890.
8. Hasse, H., H.P. Kany, R. Tintinger, and G. Maurer, *Osmotic Virial Coefficients of Aqueous Poly(ethylene glycol) from Laser-Light Scattering and Isopiestic Measurements.* Macromolecules, 1995. **28**(10): p. 3540-3552.
9. Velev, O.D., E.W. Kaler, and A.M. Lenhoff, *Protein Interactions in Solution Characterized by Light and Neutron Scattering: Comparison of Lysozyme and Chymotrypsinogen.* Biophysical Journal, 1998. **75**(6): p. 2682-2697.
10. Mutch, K.J., J.S. van Duijneveldt, and J. Eastoe, *Colloid-polymer mixtures in the protein limit.* Soft Matter, 2007. **3**(2): p. 155-167.
11. Quemada, D. and C. Berli, *Energy of interaction in colloids and its implications in rheological modeling.* Advances in Colloid and Interface Science, 2002. **98**(1): p. 51-85.
12. Gaaloul, S., S.L. Turgeon, and M. Corredig, *Phase behavior of whey protein aggregates/κ-carrageenan mixtures: Experiment and theory.* Food Biophysics, 2010. **5**(2): p. 103-113.

13. Bonneté, F., S. Finet, and A. Tardieu, *Second virial coefficient: Variations with lysozyme crystallization conditions.* Journal of Crystal Growth 1999. **196**(2-4): p. 403-414.
14. Lu, Y., D.-J. Chen, G.-K. Wang, and C.-L. Yan, *Study of Interactions of Bovine Serum Albumin in Aqueous (NH4)2SO4 Solution at 25 °C by Osmotic Pressure Measurements.* Journal of Chemical & Engineering Data, 2009. **54**(7): p. 1975-1980.
15. Linden, E.v.d. and E.A. Foegeding, *CHAPTER 2 - Gelation: Principles, Models and Applications to Proteins*, in *Modern Biopolymer Science*. 2009, Academic Press: San Diego. p. 29-91.
16. Munialo, C.D., E. van der Linden, K. Ako, and H.H.J. de Jongh, *Quantitative analysis of the network structure that underlines the transitioning in mechanical responses of pea protein gels.* Food Hydrocolloids, 2015. **49**(0): p. 104-117.
17. Ako, K., T. Nicolai, D. Durand, and G. Brotons, *Micro-phase separation explains the abrupt structural change of denatured globular protein gels on varying the ionic strength or the pH.* Soft Matter, 2009. **5**(20): p. 4033-4041.
18. Mahmoudi, N., S. Mehalebi, T. Nicolai, D. Durand, and A. Riaublanc, *Light-scattering study of the structure of aggregates and gels formed by heat-denatured whey protein isolate and β-lactoglobulin at neutral pH.* Journal of Agricultural and Food Chemistry, 2007. **55**(8): p. 3104-3111.
19. Richardson, R.K. and S.B. Ross-Murphy, *Mechanical properties of globular protein gels: II concentration, pH concentration, ph and ionic strength dependence.* British Polymer Journal, 1981. **13**(1): p. 11-16.
20. Edmond, E. and A.G. Ogston, *An approach to the study of phase separation in ternary aqueous systems.* Biochemical Journal, 1968. **109**(4): p. 569-576.
21. Kang, C.H. and S.I. Sandler, *Phase behavior of aqueous two-polymer systems.* Fluid Phase Equilibria, 1987. **38**(3): p. 245-272.
22. Schaink, H.M. and J.A.M. Smit, *Protein–polysaccharide interactions: The determination of the osmotic second virial coefficients in aqueous solutions of β-lactoglobulin and dextran.* Food Hydrocolloids, 2007. **21**(8): p. 1389-1396.
23. Bloustine, J.D., *Experimental Investigations into Interactions and Collective Behavior in Protein/Polymer Mixtures and Granular Rods*, in *The Faculty of the Graduate School of Arts and Sicences*. 2005, Brandeis University. p. 120.
24. Lekkerkerker, H.N.W. and R. Tuinier, *Colloids and the Depletion Interaction*. Lecture Notes in Physics 2011: Springer Science+Business Media B.V.
25. Walstra, P., *Physical Chemistry of Foods*. 2003: Marcel Dekker.
26. Wang, S., J.A.P.P. van Dijk, T. Odijk, and J.A.M. Smit, *Depletion-Induced Demixing in Aqueous Protein−Polysaccharide Solutions.* Biomacromolecules, 2001. **2**(4): p. 1080-1088.

27. Tolstoguzov, V.B., *Concentration and purification of proteins by means of two-phase systems: membraneless osmosis process.* Food Hydrocolloids, 1988. **2**(3): p. 195-207.
28. Polyakov, V.I., V.Y. Grinberg, and V.B. Tolstoguzov, *Thermodynamic incompatibility of proteins.* Food Hydrocolloids, 1997. **11**(2): p. 171-180.
29. Polyakov, V.I., O.K. Kireyeva, V. Grinberg, and V.B. Tolstoguzov, *Thermodynamic compatibility of proteins in aqueous media. Part. I. Phase diagrams of some water--protein A--protein B systems.* Die Nahrung, 1985. **29**(2): p. 153-160.
30. Polyakov, V.I., I.A. Popello, V. Grinberg, and V.B. Tolstoguzov, *Thermodynamic compatibility of proteins in aqueous media. Part 2. The effect of some physicochemical factors on thermodynamic compatibility of casein and soybean globulin fraction.* Die Nahrung, 1985. **29**(4): p. 323-333.
31. Leng, X.J. and S.L. Turgeon, *Study of the shear effects on the mixture of whey protein/polysaccharides—2: Application of flow models in the study of the shear effects on WPI/polysaccharide system.* Food Hydrocolloids, 2007. **21**(7): p. 1014-1021.
32. Ould Eleya, M.M., X.J. Leng, and S.L. Turgeon, *Shear effects on the rheology of β-lactoglobulin/β-carrageenan mixed gels.* Food Hydrocolloids, 2006. **20**(6): p. 946-951.
33. Turgeon, S.L., M. Beaulieu, C. Schmitt, and C. Sanchez, *Protein–polysaccharide interactions: phase-ordering kinetics, thermodynamic and structural aspects.* Current Opinion in Colloid & Interface Science, 2003. **8**(4–5): p. 401-414.
34. Wolf, B., R. Scirocco, W.J. Frith, and I.T. Norton, *Shear-induced anisotropic microstructure in phase-separated biopolymer mixtures.* Food Hydrocolloids, 2000. **14**(3): p. 217-225.
35. Figura, L. and A.A. Teixeira, *Food Physics: Physical Properties - Measurement and Applications*. 2010: Springer.
36. Çakır, E., C.R. Daubert, M.A. Drake, C.J. Vinyard, G. Essick, and E.A. Foegeding, *The effect of microstructure on the sensory perception and textural characteristics of whey protein/κ-carrageenan mixed gels.* Food Hydrocolloids, 2012. **26**(1): p. 33-43.
37. Çakir, E. and E.A. Foegeding, *Combining protein micro-phase separation and protein-polysaccharide segregative phase separation to produce gel structures.* Food Hydrocolloids, 2011. **25**(6): p. 1538-1546.
38. Çakır, E., S.A. Khan, and E.A. Foegeding, *The effect of pH on gel structures produced using protein–polysaccharide phase separation and network inversion.* International Dairy Journal, 2012. **27**(1–2): p. 99-102.
39. Altay, F. and S. Gunasekaran, *Gelling properties of gelatin–xanthan gum systems with high levels of co-solutes.* Journal of Food Engineering, 2013. **118**(3): p. 289-295.
40. Anderson, V.J. and R.A.L. Jones, *The influence of gelation on the mechanism of phase separation of a biopolymer mixture.* Polymer, 2001. **42**(23): p. 9601-9610.

41. Cavallieri, A.L.F., N.A.V. Fialho, and R.L. Cunha, *Sodium caseinate and κ-carrageenan interactions in acid gels: Effect of polysaccharide dissolution temperature and sucrose addition.* International Journal of Food Properties, 2011. **14**(2): p. 251-263.
42. Haug, I.J., A.M.H. Carlsen, G.E. Vegarud, T. Langsrud, and K.I. Draget, *Textural Properties of Beta-lactoglobulin – Sodium Alginate Mixed Gels at Large Scale Deformation.* Journal of Texture Studies, 2013. **44**(1): p. 56-65.
43. Lorén, N. and A.-M. Hermansson, *Phase separation and gel formation in kinetically trapped gelatin/maltodextrin gels.* International Journal of Biological Macromolecules, 2000. **27**(4): p. 249-262.
44. Nono, M., T. Nicolai, and D. Durand, *Gel formation of mixtures of κ-carrageenan and sodium caseinate.* Food Hydrocolloids, 2011. **25**(4): p. 750-757.
45. Ould Eleya, M.M. and S.L. Turgeon, *Rheology of κ-carrageenan and β-lactoglobulin mixed gels.* Food Hydrocolloids, 2000. **14**(1): p. 29-40.
46. Picone, C.S.F. and R.L. da Cunha, *Interactions between milk proteins and gellan gum in acidified gels.* Food Hydrocolloids, 2010. **24**(5): p. 502-511.
47. Pires Vilela, J.A., Â.L.F. Cavallieri, and R. Lopes da Cunha, *The influence of gelation rate on the physical properties/structure of salt-induced gels of soy protein isolate-gellan gum.* Food Hydrocolloids, 2011. **25**(7): p. 1710-1718.
48. Ribeiro, K.O., M.I. Rodrigues, E. Sabadini, and R.L. Cunha, *Mechanical properties of acid sodium caseinate-κ-carrageenan gels: Effect of co-solute addition.* Food Hydrocolloids, 2004. **18**(1): p. 71-79.
49. Shrinivas, P., S. Kasapis, and T. Tongdang, *Morphology and mechanical properties of bicontinuous gels of agarose and gelatin and the effect of added lipid phase.* Langmuir, 2009. **25**(15): p. 8763-8773.
50. Spotti, M.J., M.J. Perduca, A. Piagentini, L.G. Santiago, A.C. Rubiolo, and C.R. Carrara, *Does dextran molecular weight affect the mechanical properties of whey protein/dextran conjugate gels?* Food Hydrocolloids, 2013. **32**(1): p. 204-210.
51. Brink, J., M. Langton, M. Stading, and A.-M. Hermansson, *Simultaneous analysis of the structural and mechanical changes during large deformation of whey protein isolate/gelatin gels at the macro and micro levels.* Food Hydrocolloids, 2007. **21**(3): p. 409-419.
52. Chronakis, I.S. and S. Kasapis, *Structural properties of single and mixed milk/soya protein systems.* Food Hydrocolloids, 1993. **7**(6): p. 459-478.
53. Comfort, S. and N.K. Howell, *Gelation properties of soya and whey protein isolate mixtures.* Food Hydrocolloids, 2002. **16**(6): p. 661-672.

54. Devi, A.F., R. Buckow, Y. Hemar, and S. Kasapis, *Modification of the structural and rheological properties of whey protein/gelatin mixtures through high pressure processing.* Food Chemistry, 2014. **156**(0): p. 243-249.
55. Donato, L., E. Kolodziejcyk, and M. Rouvet, *Mixtures of whey protein microgels and soluble aggregates as building blocks to control rheology and structure of acid induced cold-set gels.* Food Hydrocolloids, 2011. **25**(4): p. 734-742.
56. Fitzsimons, S.M., D.M. Mulvihill, and E.R. Morris, *Segregative interactions between gelatin and polymerised whey protein.* Food Hydrocolloids, 2008. **22**(3): p. 485-491.
57. Onwulata, C.I., A.E. Thomas-Gahring, and J.G. Phillips, *Physical properties of mixed dairy food proteins.* International Journal of Food Properties, 2014. **17**(10): p. 2241-2262.
58. Pang, Z., H. Deeth, P. Sopade, R. Sharma, and N. Bansal, *Rheology, texture and microstructure of gelatin gels with and without milk proteins.* Food Hydrocolloids, 2014. **35**: p. 483-493.
59. Picone, C., K. Takeuchi, and R. Cunha, *Heat-Induced Whey Protein Gels: Effects of pH and the Addition of Sodium Caseinate.* Food Biophysics, 2011. **6**(1): p. 77-83.
60. Walkenström, P. and A.-M. Hermansson, *Mixed gels of fine-stranded and particulate networks of gelatin and whey proteins.* Food Hydrocolloids, 1994. **8**(6): p. 589-607.
61. Walkenström, P. and A.-M. Hermansson, *Fine-stranded mixed gels of whey proteins and gelatin.* Food Hydrocolloids, 1996. **10**(1): p. 51-62.
62. Walkenström, P. and A.-M. Hermansson, *High-pressure treated mixed gels of gelatin and whey proteins.* Food Hydrocolloids, 1997. **11**(2): p. 195-208.
63. Ziegler, G.R., *Microstructure of mixed gelatin-egg white gels: Impact on rheology and application to microparticulation.* Biotechnology Progress, 1991. **7**(3): p. 283-287.
64. Ziegler, G.R. and S.S.H. Rizvi, *Predicting the Dynamic Elastic Modulus of Mixed Gelatin-Egg White Gels.* Journal of Food Science, 1989. **54**(2): p. 430-436.
65. Katopo, L., S. Kasapis, and Y. Hemar, *Segregative phase separation in agarose/whey protein systems induced by sequence-dependent trapping and change in pH.* Carbohydrate Polymers, 2012. **87**(3): p. 2100-2108.
66. Clark, A.H., R.K. Richardson, S.B. Ross-Murphy, and J.M. Stubbs, *Structural and mechanical properties of agar/gelatin co-gels. Small-deformation studies.* Macromolecules, 1983. **16**(8): p. 1367-1374.
67. Davies, W.E.A., *The theory of elastic composite materials.* Journal of Physics D: Applied Physics, 1971. **4**(9): p. 1325.
68. Davies, W.E.A., *The elastic constants of a two-phase composite material.* Journal of Physics D: Applied Physics, 1971. **4**(8): p. 1176.

69. Hashin, Z. and S. Shtrikman, *A variational approach to the theory of the elastic behaviour of multiphase materials.* Journal of the Mechanics and Physics of Solids, 1963. **11**(2): p. 127-140.
70. Takayanagi, M., H. Harima, and Y. Iwata, *Viscoelastic behavior of polymer blends and its comparison with model experiments.* The Society of Material Science, 1963.
71. Alevisopoulos, S., S. Kasapis, and R. Abeysekera, *Formation of kinetically trapped gels in the maltodextrin—gelatin system.* Carbohydrate Research, 1996. **293**(1): p. 79-99.
72. Chronakis, I.S., S. Kasapis, and R.K. Richardson, *Small deformation rheological properties of maltodextrin—milk protein systems.* Carbohydrate Polymers, 1996. **29**(2): p. 137-148.
73. Manoj, P., S. Kasapis, and I.S. Chronakis, *Gelation and phase separation in maltodextrin-caseinate systems.* Food Hydrocolloids, 1996. **10**(4): p. 407-420.
74. Manoj, P., S. Kasapis, and M.W.N. Hember, *Sequence-dependent kinetic trapping of biphasic structures in maltodextrin-whey protein gels.* Carbohydrate Polymers, 1997. **32**(2): p. 141-153.
75. S, K., *The elastic moduli of the microcrystalline cellulose–gelatin blends.* Food Hydrocolloids, 1999. **13**(6): p. 543-546.
76. de la Fuente, M.A., Y. Hemar, and H. Singh, *Influence of κ-carrageenan on the aggregation behaviour of proteins in heated whey protein isolate solutions.* Food Chemistry, 2004. **86**(1): p. 1-9.
77. Gaaloul, S., M. Corredig, and S.L. Turgeon, *Rheological study of the effect of shearing process and κ-carrageenan concentration on the formation of whey protein microgels at pH 7.* Journal of Food Engineering, 2009. **95**(2): p. 254-263.
78. Tuinier, R., J.K.G. Dhont, and C.G. De Kruif, *Depletion-induced phase separation of aggregated whey protein colloids by an exocellular polysaccharide.* Langmuir, 2000. **16**(4): p. 1497-1507.
79. Mosca, A.C., J.A. Rocha, G. Sala, F. van de Velde, and M. Stieger, *Inhomogeneous distribution of fat enhances the perception of fat-related sensory attributes in gelled foods.* Food Hydrocolloids, 2012. **27**(2): p. 448-455.
80. Mosca, A.C., F. van de Velde, J.H.F. Bult, M.A.J.S. van Boekel, and M. Stieger, *Effect of gel texture and sucrose spatial distribution on sweetness perception.* LWT - Food Science and Technology, 2012. **46**(1): p. 183-188.
81. Mosca, A.C., F.v.d. Velde, J.H.F. Bult, M.A.J.S. van Boekel, and M. Stieger, *Enhancement of sweetness intensity in gels by inhomogeneous distribution of sucrose.* Food Quality and Preference, 2010. **21**(7): p. 837-842.
82. Renkema, J.M.S., *Formation, Structure and Rheological Properites of Soy Protein Gels*. Physics and Physical Chemistry of Foods. 2001: PhD Thesis - Wageningen University.

83. Renkema, J.M.S., J.H.M. Knabben, and T. van Vliet, *Gel formation by β-conglycinin and glycinin and their mixtures.* Food Hydrocolloids, 2001. **15**(4–6): p. 407-414.
84. Renkema, J.M.S. and T. van Vliet, *Concentration dependence of dynamic moduli of heat-induced soy protein gels.* Food Hydrocolloids, 2004. **18**(3): p. 483-487.

Summary

In this thesis we presented a systematic bottom-up approach to investigate gelation in protein mixtures. Throughout the thesis the molecular interactions and molecular dimensions of proteins and their changes during gelation were first quantified and subsequently used to explain phase separation during gelation which could be coupled to changes in the rheological behavior of the mixed gels.

Chapter 1 presented a short overview of the available literature on mixed protein gels. Different classifications of mixed gels were given and their relation to phase separation processes during gelation processes outlined.

Chapter 2 dealt with the quantification of molecular size and molecular interactions via the second virial coefficient in pure and single protein (and dextran) solutions. This allowed the identification of solvent conditions where proteins behaved as hard spheres and solvent conditions where electrostatic interactions dominated the interactions. This thorough characterization of the biopolymers was essential for the discussions in the subsequent chapters.

Chapter 3 was divided in a theoretical and an experimental section. In the theoretical section we presented a virial approach to predict the liquid – liquid phase behavior of binary mixtures. The properties of this approach were outlined for binary hard sphere mixtures. In the experimental section of chapter 3 we then used the virial approach to predict the phase diagram for the gelatin / dextran mixture based on the measured second virial coefficients (molecular interactions). For mixed protein systems, being the focus of this thesis, chapter 3 presented evidence that the absence of phase separation in these systems is mainly due to the similar molecular size and molecular interactions comparable to those expected for hard spheres.

Chapter 4 took the first step towards mixed gels by investigating microstructure and rheological properties of mixed gels where gelatin gelled in the presence of globular proteins. Here a correlation between phase separated microstructures and increased storage modulus values of the mixed gels was found. The occurrence of phase separation was explained by the changes in molecular size of gelatin molecules during gelation relative to the molecular size of globular proteins. It was observed that only systems that during gelatin gelation passed a region of high compatibility (similar molecular size) and afterwards a region of reducing compatibility phase separated.

Chapter 5 applied the same experimental techniques (microstructural analysis and rheology) to globular protein gels which were prepared in the presence of non-gelling gelatin. Also here microstructural changes were observed in mixtures passing a region of high compatibility before entering a region of reducing compatibility during gelation. For globular protein gels, however, these microstructural changes resulted in a decreased storage modulus in contrast to the increase in storage modulus presented in chapter 4. This difference was attributed to the different gelling mechanisms of gelatin (chapter 4) and globular proteins (chapter 5). Upon phase separation, gelatin was concentrated in its phase where it formed a gel as it would in bulk. However, this occurred at an increased concentration compared to the situation when gelatin is distributed over the whole sample leading to an increased gel modulus. Globular protein gels in mixed gels, on the other hand, were mainly altered in their microstructure and did not gel at an increased protein concentration.

Chapter 6 dealt with fracture properties of mixed globular protein / gelatin gels using the example of soy protein isolate (SPI) / gelatin mixed gels where both proteins were in their gelled state. The coexisting, bi-continuous microstructure of the two gels was connected to a gradual change of gel fracture properties from single SPI to single gelatin gels. While the fracture stress was dominated by the stronger of the two protein gels, the non-additivity of the gel modulus could at this point not be explained.

Chapter 7 was dedicated to the applicability of several theoretical models towards explaining the earlier observed changes in the rheological response of globular protein gels and non-additivity of the modulus for mixed gels. Using rheological data from chapters 5 and 6 several problems regarding the applicability of the available theories to globular protein gels were identified and discussed based on the other results from this thesis. Especially the change in gel microstructure of globular protein gels, when prepared in the presence of gelatin, was suggested to be the reason for the limited applicability of the available theories to mixed protein gels where globular proteins formed a space spanning network.

Chapter 8 discussed the results from the preceding chapters in the context of the currently available literature. Second virial coefficients were shown to not only be useful in determining phase behavior in solutions, but also to determine solvent conditions where proteins form fine stranded or coarse stranded gels. Furthermore, the importance of how to calculate the (protein) concentration in mixed systems was stressed. Using the rheological properties of gelatin gels from chapter 4 the importance of this sometimes as too trivial seen subject was shown to change the interpretation of results if not considered carefully. Finally, the limitations of available theories to explain the non-additivity of the

storage modulus from chapter 7 was discussed in a wider perspective and some concluding remarks on the outlook in mixed biopolymer research given.

In conclusion, this thesis contributed to a better understanding of the gel formation in mixed gelatin / globular protein gels. However, more importantly, it presented an approach towards research in mixed biopolymer systems, in solution or in the gelled state, which can be applied straightforward to other mixed systems.

LIST OF PUBLICATIONS

PEER REVIEWED PUBLICATIONS

Ersch, C., ter Laak, I., van der Linden, E., Venema, P., & Martin, A. H. (2015). Modulating fracture properties of mixed protein systems. *Food Hydrocolloids*, 44, 59-65.

Ersch, C., Meijvogel, L. M., van der Linden, E., Martin, A. H., & Venema, P. (2015). Interactions in protein Mixtures. Part I: Second Virial Coefficients from Osmometry. *Food Hydrocolloids* (Accepted)

Ersch, C., van der Linden, E., Martin, A. H., & Venema, P. (2015). Interactions in Protein Mixtures. Part II: A Virial Approach to Predict Phase Behaviour. *Food Hydrocolloids* (Accepted).

Ersch, C., Linden, E. v. d., Venema, P., & Martin, A. H. (2015). The microstructure and rheology of homogeneous and phase separated gelatine gels. (Submitted).

Ersch, C., Meinders, M. B. J., Bouwman, W. G., Nieuwland, M., Linden, E. v. d., Venema, P., & Martin, A. H. (2015). Microstructure and rheology of globular protein gels in the presence of gelatin. (Submitted).

Rijgersberg, H., Wigham, M., Ersch, C., Keijsers, J., Meinders, M.B.J., Damjanovic, S., Broekstra, J., Top, J. (2015). Integration of scientific spreadsheet data in a Semantic Web approach (To be Submitted)

PATENTS

Ersch, C. and Olijve, J.H.; Gelatin hydrolysates in protein systems. (2015) European patent Application No. 15166825.8

ACKNOWLEDGEMENTS

Above all I would like to express my appreciation to Paul Venema without whom I could not have finished this thesis at the scientific level it has. Thank you for always having an open door and ear for me and for answering each and every question patiently no matter how trivial it seemed to you.

Furthermore, I would like to express my gratitude towards TIFN and the Food Physics Group for giving me the chance and time to develop myself personally and professionally over the last years. Thank you particularly to the people represented in the pictures below that have helped and supported me during the last four years.

Finally I would like to thank my family for their support and for continuously showing me that for everything there are alternative points of views.

In picture:

Supervisors: Erik van der Linden, Paul Venema, Anneke Martin

Colleagues: Vaida Urbonaite, Miranda de Beus, Elke Scholten, Marcel Meinders, Anika Oppermann, Jinfeng Peng, Laura Oliver, Leonard Sagis, Claire Munialo, Laurice Pouvreau, Eefjan Timmerman, Pauline van Leusden, Jacob Bouman, Min Chen, Harry Baptist, Els Jansen, Maaike Nieuwland, Tijs Rovers, Alev Ince, Lenka Tonneijck-Srpova, Kun Liu, Saskia de Jong, Harmen de Jongh

Students: Anja Schröder, Patrick Wilms, Lennart Meijvogel, Irene ter Laak, Yvonne Ringelspacher, Eline Bakhuizen, Maaike Renssen

Others: Marielle Timmer, Jan Top, Wim Bouwman, Hajo Rijgersberg, Surender Dhayal

AUTHOR INFORMATION

COMPLETED TRAINING ACTIVITIES

Discipline specific activities

- Basic rheology for food sciences (Ede, The Netherlands, 2011)
- Reaction Kinetics in Food Sciences (Wageningen, The Netherlands, 2012)
- Combining rheology with microscopy and scattering techniques (Rotterdam, The Netherlands, 2012)
- Tenth one day symposium on protein folding and stability (Liège, Belgium, 2012)
- Food Symposium (Valencia, Spain, 2013)[9]
- Biopolymers (Nantes, France 2013)[8]
- Food Structure and Functionality Forum (Amsterdam, The Netherlands, 2014)[9]
- Food Hydrocolloids (Karlsruhe, Germany, 2014)[9]
- TIFN Annual Conference (Arnhem, The Netherlands, 2012)[9]
- TIFN Annual Conference (Amsterdam, The Netherlands, 2013)
- TIFN Annual Conference (Utrecht, The Netherlands, 2014)[9]

General courses

- Basic IP knowledge for TIFN researchers (Wageningen, The Netherlands, 2012)
- Ethics and Philosophy in Food Science (Wageningen, The Netherlands, 2012)
- VLAG PhD week (Baarlo, The Netherlands, 2012)[9]
- Career perspectives (Wageningen, The Netherlands, 2014)
- Entrepreneurship in and outside science (Wageningen, The Netherlands, 2014)

Optional Activities

- Preparation research proposal (2011)
- Master Course Datamanagement (2011)
- PhD Trip USA and Canada (2014)[9]

Teaching

- Advanced Food Physics (2011, 2012)
- Food Physics (2012, 2015)
- Advanced Molecular Gastronomy (2013)
- Mathematical concepts of foods (2012, 2014)

[8] Poster Presentation

[9] Oral Presentation

The studies presented in this thesis were performed within the framework of TI Food and Nutrition

Financial Support from Wageningen University and the Top Institute Food and Nutrition is gratefully acknowledged.

Cover Design: Carsten Ersch

Printed by Ridderprint B.V.